EVALUATION OF ALKALI-SURFACTANT-POLYMER FLOODING IN OIL-WET RESERVOIR CONTAINING HIGH PERMEABILITY CHANNEL

Mr. Charat Thamcharoen

A Thesis Submitted in Partial Fulfillment of the Requirements
for the Degree of Master of Engineering Program in Petroleum Engineering
Department of Mining and Petroleum Engineering
Faculty of Engineering
Chulalongkorn University
Academic Year 2013

การประเมินกระบวนการฉีดอัดสารละลายผสม อัลคาไลน์ สารลดแรงตึงผิว และโพลีเมอร์ในแหล่งเก็บกักน้ำมันที่มีสภาพความเปียกด้วยน้ำมันและมีช่องหินที่มีค่าความสามารถในการซึมผ่านสูง

นายชรัช ธรรมเจริญ

วิทยานิพนธ์นี้เป็นส่วนหนึ่งของการศึกษาตามหลักสูตรปริญญาวิศวกรรมศาสตรมหาบัณฑิต
สาขาวิชาวิศวกรรมปิโตรเลียม ภาควิชาวิศวกรรมเหมืองแร่และปิโตรเลียม
คณะวิศวกรรมศาสตร์ จุฬาลงกรณ์มหาวิทยาลัย
ปีการศึกษา 2556

Thesis Title	EVALUATION OF ALKALI-SURFACTANT-POLYMER FLOODING IN OIL-WET RESERVOIR CONTAINING HIGH PERMEABILITY CHANNEL
By	Mr. Charat Thamcharoen
Field of Study	Petroleum Engineering
Thesis Advisor	Falan Srisuriyachai, Ph.D.

Accepted by the Faculty of Engineering, Chulalongkorn University in Partial Fulfillment of the Requirements for the Master's Degree

.....Dean of the Faculty of Engineering

(Professor Bundhit Eua-arporn, Ph.D.)

THESIS COMMITTEE

.....Chairman

(Associate Professor Sarithdej Pathanasethpong)

.....Thesis Advisor

(Falan Srisuriyachai, Ph.D.)

.....Examiner

(Assistant Professor Suwat Athichanagorn, Ph.D.)

.....External Examiner

(Dalad Nuttwongasem, Ph.D.)

ชรัช ธรรมเจริญ : การประเมินกระบวนการฉีดอัดสารละลายผสม อัลคาไลน์ สารลดแรงตึงผิว และโพลีเมอร์ในแหล่งเก็บกักน้ำมันที่มีสภาพความเปียกด้วยน้ำมันและมีช่องหินที่มีค่าความสามารถในการซึมผ่านสูง. (EVALUATION OF ALKALI-SURFACTANT-POLYMER FLOODING IN OIL-WET RESERVOIR CONTAINING HIGH PERMEABILITY CHANNEL) อ.ที่ปรึกษาวิทยานิพนธ์หลัก: อ. ดร. ฟ้าลั่น ศรีสุริยชัย, 219 หน้า.

กระบวนการฉีดอัดสารละลายผสม อัลคาไลน์ สารลดแรงตึงผิว และโพลีเมอร์เป็นเทคนิคที่รวมข้อดีของสารทั้งสามชนิดเพื่อลดแรงตึงผิวของน้ำมันและน้ำให้เข้าสู่สภาวะแรงตึงผิวต่ำพิเศษ และลดอัตราส่วนการเคลื่อนที่ระหว่างน้ำกับน้ำมันเพื่อปรับปรุงประสิทธิภาพการกวาดน้ำมัน

ผลการศึกษาด้วยแบบจำลองแหล่งกักเก็บแสดงให้เห็นว่าประสิทธิภาพของการผลิตน้ำมันสูงสุดเกิดจากการฉีดอัดโพลีเมอร์ขนาด 0.25 เท่าของรูพรุนทั้งหมด ตามด้วยสารละลายผสมระหว่างอัลคาไลน์และสารลดแรงตึงผิวขนาด 0.10 เท่าของรูพรุนทั้งหมด และตามด้วยโพลีเมอร์ขนาด 0.55 เท่าของรูพรุนทั้งหมด ตามความเข้มข้นของสารที่ได้เลือกไว้

การเพิ่มขึ้นของปัจจัยความต้านทานโพลีเมอร์สามารถลดปริมาณโพลีเมอร์ที่จำเป็นต้องใช้ แต่อย่างไรก็ดียังคงมีค่าขอบเขตสูงสุดของปัจจัยความต้านทานที่สามารถเพิ่มได้

ผลกระทบจากช่องหินที่มีค่าความสามารถในการซึมผ่านสูงกับการเพิ่มขึ้นของประสิทธิภาพการผลิตน้ำมันจากการฉีดอัดน้ำ และความแตกต่างสัมพัทธ์ของการผลิตน้ำมันระหว่างมีกับไม่มีการฉีดอัดโพลีเมอร์ช่วงต้นของการผลิตน้ำมันสามารถคาดการณ์ได้จากอัตราส่วนระหว่างความกว้างกับความลึกของช่องหินที่มีค่าความสามารถในการซึมผ่านสูง

การศึกษาตัวแปรที่มีผลกระทบอย่างมีนัยสำคัญแสดงให้เห็นว่าตัวแปรที่มีความสัมพันธ์อย่างใกล้ชิดกับความสามารถในการซึมผ่านสัมพัทธ์ระหว่างน้ำกับน้ำมันส่งผลกระทบต่อกระบวนการฉีดอัดสารละลายผสม อัลคาไลน์ สารลดแรงตึงผิว และโพลีเมอร์ อย่างเห็นได้ชัด อันได้แก่ เลขยกกำลังคอรีย์ และสภาพความเปียก สภาพความเปียกสามารถเปลี่ยนแปลงประสิทธิภาพของการผลิตน้ำมันจาก 53.73 ถึง 60.62% และ 60.19 ถึง 68.74% สำหรับกรณีไม่มีและมีการฉีดอัดโพลีเมอร์ช่วงต้นการผลิตน้ำมันตามลำดับ ถึงแม้ว่าการฉีดอัดโพลีเมอร์ช่วงต้นจะช่วยเพิ่มประสิทธิภาพของการผลิตน้ำมันแต่การฉีดอัดโพลีเมอร์ช่วงต้นมีความแปรปรวนสูงกับตัวแปรที่ทำการศึกษา ซึ่งส่งผลในด้านลบกับวิธีการนี้

ภาควิชา วิศวกรรมเหมืองแร่และปิโตรเลียม ลายมือชื่อนิสิต .....

สาขาวิชา วิศวกรรมปิโตรเลียม ลายมือชื่อ อ.ที่ปรึกษาวิทยานิพนธ์หลัก .....

ปีการศึกษา 2556

5571202021 : MAJOR PETROLEUM ENGINEERING
KEYWORDS: ASP FLOODING / OIL-WET RESERVOIR / HIGH PERMEABILITY CHANNEL

CHARAT THAMCHAROEN: EVALUATION OF ALKALI-SURFACTANT-POLYMER FLOODING IN OIL-WET RESERVOIR CONTAINING HIGH PERMEABILITY CHANNEL. ADVISOR: FALAN SRISURIYACHAI, Ph.D., 219 pp.

Alkali-Surfactant-Polymer (ASP) flooding is a technique combining benefits of alkaline, surfactant and polymer substances to decrease interfacial tension (IFT) to an ultra-low IFT condition and to reduce mobility ratio to improve sweep efficiency.

Simulation results obtained from STAR® commercial simulator showed that the highest oil recovery is obtained from P+AS+P flooding composes of injecting 0.25PV of pre-flushed polymer followed by 0.10PV of alkali-surfactant slug and chased by 0.55PV of post-flushed polymer at chosen chemical concentrations.

Incremental of resistance factor can reduce the amount of polymer required. However, upper limit of resistance factor exists.

Impact of high permeability channel to incremental of recovery factor compared to waterflooding and relative recovery difference between P+AS+P and AS+P can be predicted from width/height ratio of high permeability channel.

Sensitivity analysis shows that parameters which are closely related to relative permeability curves impact the most to ASP flooding such as Corey's exponent and wettability. Wetting condition can vary recovery factor from 53.73 to 60.62% in AS+P flooding and 60.19 to 68.74% in P+AS+P flooding. Although incremental of recovery factor from P+AS+P flooding compared to waterflooding is higher than that of AS+P flooding in all cases, high sensitivity to variation of parameters could result in negative image of this technique.

Department:	Mining and Petroleum Engineering	Student's Signature	.....
		Advisor's Signature	.....
Field of Study:	Petroleum Engineering		
Academic Year:	2013		

ACKNOWLEDGEMENTS

First of all, I would like to express the deepest appreciation to my thesis advisor, Dr. Falan Srisuriyachai, who conveys the invaluable guidance, assistance and inspiration during my study. His wisdom and trustworthy knowledge has helped me a lot throughout this study.

I would like to thank all professors and faculty members in Department of Mining and Petroleum Engineering who have provided the petroleum engineering knowledge and advices. I sincerely appreciate the opportunity to study in petroleum engineering field. I also would like to thank the thesis committee members for their recommendations on my thesis.

I would like to thank Mr. Natchapon Muchalintamolee and Ms. Kunwadee Teerakijpaiboon for guiding me basic knowledge of using CMG software. I also appreciate the valuable discussion to find the solution. I am so grateful to Mr. Liam Barry, Customer Support Engineer from S3GRAF who expressed the ability of S3GRAF program.

I acknowledge Chevron Thailand Exploration and Production, Ltd. for financial support for this study.

I appreciate all of my petroleum engineering classmates who offer me sincere friendship. I also thank to my colleagues who always support me all the time. I am grateful to this group of people. I would like to thank Mr. Wisarut Satitkanitkul who turned me into petroleum field.

At the end, my biggest thank must go to my family, for their patience, understanding and support.

CONTENTS

Page

Page

Page

List of Tables

Page

List of Figures

Page

List of Abbreviations

µg/g	Microgram per gram
°API	American Petroleum Institute gravity
AS	Alkali-Surfactant
ASP	Alkali-Surfactant-Polymer
bbl/day	Barrel per day
bbl oil/polymer	Additional oil produced per mass of polymer used
bbl oil/surfactant	Additional oil produced per mass of surfactant used
BHP	Bottomhole pressure
Ca^{2+}	Calcium ion
°C/km	Degree Celsius per kilometer
CMC	Critical micelle concentration
cP	Centipoise
dyne/cm	Dyne per centimeter
DTWELL	First time step size after well change
DWOC	Water-oil contact depth
EOR	Enhance oil recovery
°F	Degree Fahrenheit
GOR	Gas-oil ratio
H^+	Hydrogen ion
H_2O	Water
HPAM	Hydrolyzed Polyacrylamides
IFT	Interfacial tension
IOIP	Initially oil in place
ISOTHERM	Isothermal option
ITERMAX	Linear solver iterations
kg/cm^2	Kilogram per square centimeter

KRGCL	Relative permeability to gas at connate liquid saturation
KROCW	Relative permeability to oil at connate water saturation
KROGCG	Relative permeability to oil at connate gas saturation
KRWIRO	Relative permeability to water at irreducible oil saturation
kv/kh	Ratio of vertical to horizontal permeability
lb/lbmole	Pound per pound-mole
m	Month
MMbbl	Million barrels
mN/m	Millinewton per meter
mD	Millidarcy
Mg^{2+}	Magnesium ion
mg/L	Milligram per liter
mg/m^2	Milligram per square meter
MW	Molecular weight
Na_2CO_3	Sodium carbonate
NaOH	Sodium hydroxide
OOIP	Original oil in place
P	Polymer slug
PAC	Polyacrylate copolymer
PAM	Polyacrylamides
pH	Potential hydrogen
psia	Pound per square inch absolute
PV	Pore volume
PV/gm	Pore volume per gram
ppm	Part per million
PVT	Pressure-Volume-Temperature
p.z.c	Point of zero charge
REFDEPTH	Reference depth

REFPW or REFPRES	Reference pressure
ROIP	Remaining oil in place
ROS	Residual oil saturation
SGCON	Connate gas saturation
SGCRIT	Critical gas saturation
SOIRG	Irreducible oil saturation for Gas-Liquid table
SOIRW	Irreducible oil saturation for Water-Oil table
SORG	Residual oil saturation for Gas-Liquid table
SORW	Residual oil saturation for Water-Oil table
SWCON	Connate water saturation
SWCRIT	Critical water saturation
scf/stb	Standard cubic feet per stock-tank barrel
STL	Surface liquid rate
STO	Surface oil rate
STW	Surface water rate
TRES	Reservoir temperature
WCUT	Water-cut
WOC	Water-oil contact
w/h ratio	width per height ratio
w/w	Weight by weight
XG	Xanthan gum
y	Year

Nomenclatures

α_d	Dip angle
$\Delta\rho$	Water-oil density difference
$\frac{\partial P_c}{\partial L}$	Capillary pressure
$\frac{\partial P}{\partial L}$	Pressure gradient in flow direction
λ_p	Mobility of polymer slug
λ_o	Mobility of residual oil
λ_w	Mobility of water
σ	Interfacial tension between two phase
$\gamma_{o/w}$	Interfacial tension between oil and water
ϕ	Porosity
ϕ_{ma}	Matrix porosity
θ	Contact angle
μ	Fluid viscosity
μ_o	Oil viscosity
μ_p	Polymer viscosity
μ_w	Water viscosity
A_{gr}	Grain size coefficient
A_{mcp}	Cementation-compaction coefficient
B_g	Formation volume factor of gas
B_o	Formation volume factor of oil
C_o	Corey oil exponent
C_w	Corey water exponent
d_{gr}	Average particle diameter
E_A	Areal sweep efficiency
E_D	Displacement efficiency
E_I	Vertical sweep efficiency

E_R	Oil recovery efficiency
E_v	Volumetric sweep efficiency
f_w	Fractional flow of water
g	Acceleration term due to gravity
k	Absolute permeability
k_{ma}	Matrix permeability
k_{rg}	Relative permeability to gas
k_{ro}	Relative permeability to oil for Water-Oil system
$k_{ro}(S_w)$	Relative permeability to oil at any water saturation
$k_{ro@}S_{wmin}$	Relative permeability to oil at minimum water saturation
k_{rog}	Relative permeability to oil for Gas-Liquid system
kr_p	Relative permeability to polymer for Water-Oil system
k_{rw}	Relative permeability to water for Water-Oil system
$k_{rw}(S_w)$	Relative permeability to water at any water saturation
$k_{rw@}S_{orw}$	Relative permeability to water at residual oil saturation
M	Mobility ratio
N_c	Capillary number
P_c or P_{cow}	Capillary pressure for Water-Oil system
P_{NW}	Pressure in the non-wetting phase
P_{WET}	Pressure in the wetting phase
q	Flow rate per unit cross-sectional area of water
r_c	Radius of measured tube
R	Resistance factor
R_s	Solution gas-oil ratio
S_l	Liquid saturation
S_{or} or S_{orw}	Residual oil saturation to water
S_w	Water saturation
S_{wc} or S_{wcr}	Critical water saturation

S_{wi}	Initial water saturation
S_{wmin}	Minimum water saturation (irreducible water saturation)
S_{wmax}	Maximum water saturation
u_t or v	Total fluid velocity

CHAPTER 1
INTRODUCTION

1.1 Background

Primary recovery is performed to extract oil from reservoir by exploiting natural stored force as a drive mechanism. After certain period of production by means of primary recovery, previously mentioned force is substantially declined and this results in requirement of additional force, turning production into secondary recovery phase. Secondary recovery is generally performed to maintain reservoir pressure in order to prolong production life. Waterflooding is a technique that is widely implemented due to its simplicity and availability of injectant which is water. However, many oil fields encounter a problem of severe heterogeneity. After performing waterflooding, high amount of oil saturation is still remained in those fields due to inaccessibility and attraction force by rock. For example, carbonate reservoir is a good example. This type of reservoir usually contains both inaccessibility (irregularity of permeability, natural fractures) and attraction force (oil-wet surface). Sandstone reservoir seldom contains both unfavorable conditions as well. Tertiary recovery is therefore implemented to minimize these adverse effects and to improve oil recovery.

Nowadays, improving oil recovery techniques are still under development to recover more additional crude oil remained in the reservoir. Alkali-Surfactant-Polymer (ASP) flooding is relatively new technology compared to others. ASP flooding was firstly studied in 1980's. The technique combines benefits of alkaline, surfactant and polymer substances. Surfactants contain both polar and non-polar segments in each single molecule. This type of chemical has a potential to decrease interfacial tension (IFT) between oil and water. At certain surfactant concentration, ultra-low IFT condition is achieved and oil is liberated in an emulsion form. Although surfactant seems to yield great effect in oil recovery process, surfactant depletion by adsorption onto rock surface generally causes an extra cost and hence required quantity is hardly predicted. Alkaline substance which is relatively cheap compared to surfactant is added into injected solution to prevent depletion of surfactant. Alkali reacts with fatty acid in crude oil, creating in-situ surfactant through saponification reaction. Together with surfactant, alkali assists to lower IFT value. Hence, ultra-low

IFT can be achieved at lower surfactant concentration. Alkali can also reverse wettability of rock surface to a more favorable condition for oil production. This function is more pronounced in carbonate reservoir where it is originally found as strongly oil-wet. Polymer is co-injected to decrease mobility ratio of displacement mechanism by increasing viscosity of injectant. At proper mobility ratio, oil can be well volumetrically swept.

Carbonate reservoir is generally found in nature to have complex structure in both microscopic and macroscopic points of view. This complexity results in very low recovery factor by means of natural drive mechanisms and also secondary recovery. Rock matrix of carbonate rock is often found oil-wet that is a result from adsorption of organic acid compounds. This condition is well known as unfavorable condition for oil production. Moreover, an appearance of reservoir heterogeneity such as high permeability streaks, natural fractures and vugs also causes several problems such as thief zone, channeling flow and consecutively a tremendous early breakthrough.

According to oil mechanisms provided by alkaline, surfactant and polymer substance, unfavorable condition of oil-wet reservoir containing high permeability channels can be mitigated. Alkali and surfactant collaborate to liberate oil that is captured by capillary pressure and in the same time, polymer decreases permeability contrast and controls mobility ratio. Nevertheless, combining these substances does not always yield the highest benefit. Incompatibility of substances and ineffective mechanisms are the main reasons to perform ASP flooding in certain sequences and details. Therefore, optimization of process is necessary to perform especially with complex reservoir.

Not only optimization is required for ASP flooding for a specific reservoir, sensitivity analysis of such properties should be investigated since reservoirs are not homogeneous and some properties cannot be precisely achieved.

In this study, reservoir simulation is performed to evaluate effects of various parameters on effectiveness of ASP flooding in oil-wet reservoir containing high permeability channel. The reservoir models are constructed by using the commercialized **STAR**: Advanced Processes & Thermal Reservoir Simulator commercialized by **Computer Modeling Group Ltd. (CMG®)**. In this study, two ASP flooding sequences are selected which are AS+P and P+AS+P. Base case reservoir model is selected and constructed to contain high permeability channels. Optimization of both ASP flooding sequence is performed in order to determine the best flooding strategy. Several operational parameters are optimized including

presence of pre-flushed water, slug size and resistance factor of polymer solution. After best flooding strategies are identified, they are applied on reservoir models constructed to have certain types of high permeability channels including vertical channels, horizontal channels and presence of both. Direction of high permeability channels of both along and across to displacement mechanism is also included. Cases showing best improvement compared to waterflooding process are taken for sensitivity analysis. In this study chosen uncertain parameters are exponents of relative permeability curve between oil and water, wettability, permeability contrast between channel and matrix, ratio of vertical permeability to horizontal permeability and porosity of matrix in high permeability channel.

1.2 Objectives

1. To determine optimal conditions and effects of various operational parameters including sequence of slug and slug size on alkali-surfactant-polymer flooding in oil-wet reservoir containing high permeability channel
2. To evaluate effects of several reservoir properties including exponent of relative permeability curve, wetting condition, permeability contrast between channel and matrix, ratio of vertical to horizontal permeability and porosity in high permeability channel on alkali-surfactant-polymer flooding in oil-wet reservoir containing high permeability channel

1.3 Outline of Methodology

The methodology is summarized by a flow chart shown in Figure 1.1. The details of thesis methodology are described in Chapter 4.

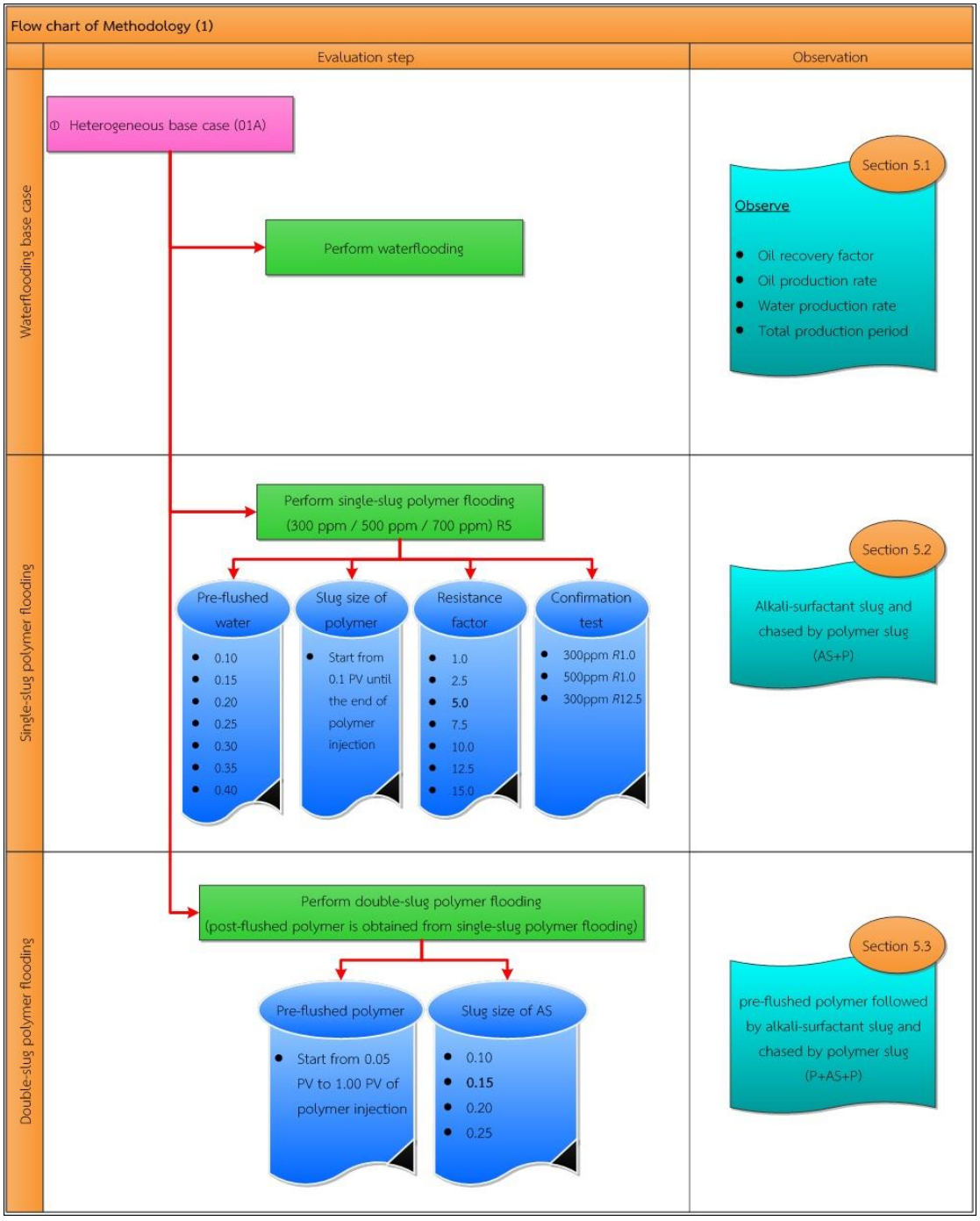

Figure 1.1 Outline methodology in flow chart

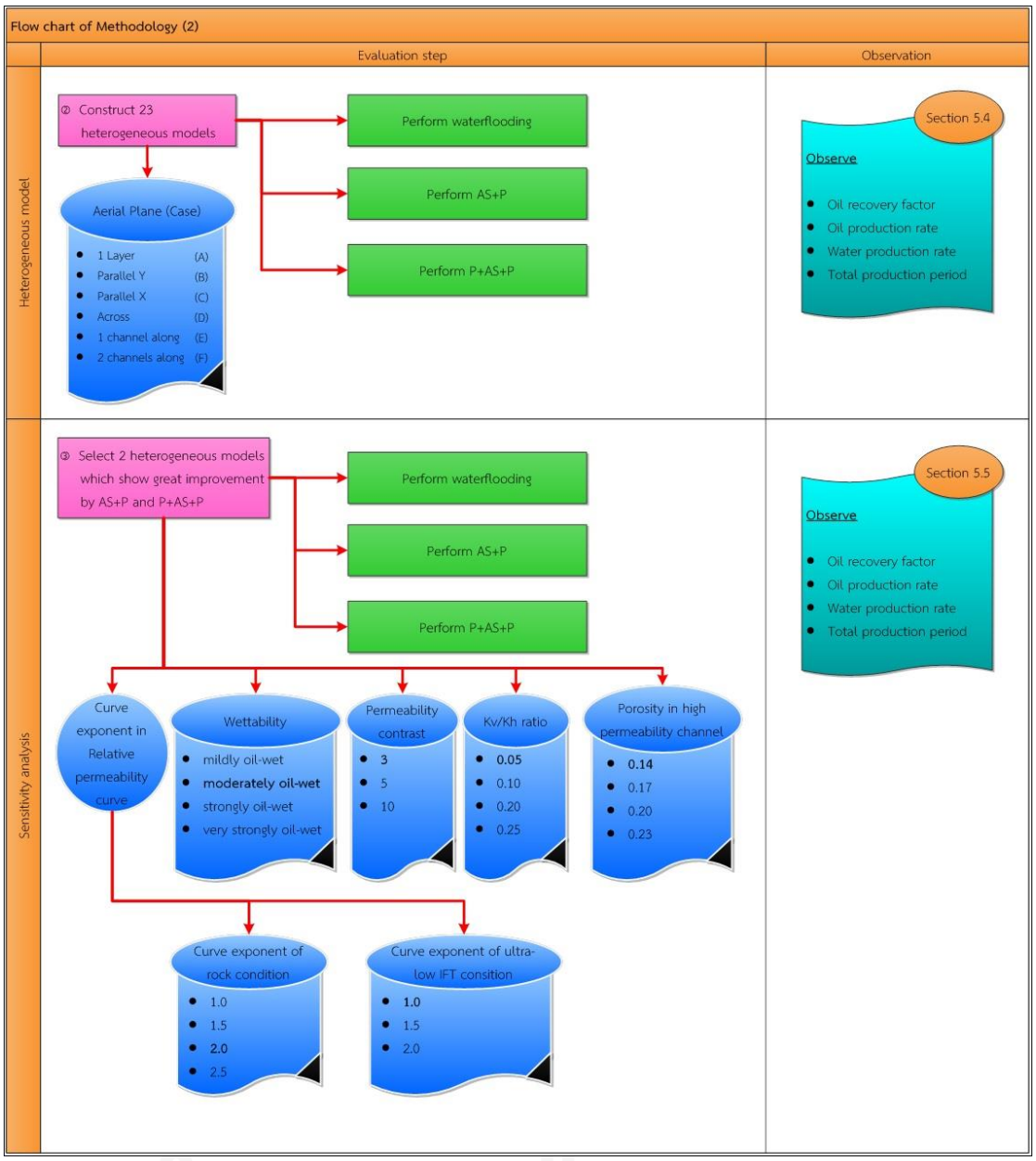

Figure 1.1 Outline methodology in flow chart (continued)

1.4 Outline of Thesis

The thesis is composed of six chapters as following

Chapter I, this chapter, introduces background of ASP flooding and indicates the objectives as well as methodology outline of this study.

Chapter II introduces various literatures related to the study ASP flooding and heterogeneity.

Chapter III presents important concepts related to each chemical properties and concepts of high permeability channel.

Chapter IV provides details of reservoir simulation models construction in CMG® STARS. This chapter consists of the detail of reservoir properties and chemical properties. At the end of this chapter, thesis methodology in detail is described.

Chapter V presents results and discussions from simulation study for each studied parameters. Results are mainly investigated by using oil recovery factor from each technique compared to waterflooding base case.

Chapter VI provides conclusions and recommendations of this study.

CHAPTER 2
LITURATURE REVIEW

This chapter summarizes previous studies of oil recovery process by ASP flooding, effect of heterogeneity on ASP flooding and application of ASP flooding in oil field.

2.1 Study of Oil Recovery Process by ASP Flooding

ASP flooding is a combination of chemical flooding process that provides several oil recovery mechanisms from alkaline, surfactant and polymer substances. One of these mechanisms that favor oil production is wettability reversal. Wettability directly controls petrophysical properties in which one of the most important properties controlling flow ability is relative permeability. Not only wettability and relative permeability that are petrophysical properties important for determining effectiveness of ASP flooding, slug size and sequence of injected chemicals are often considered in ASP flooding in terms of operational parameters. Several study publications showed effects of ASP flooding on relative permeability curves as well as wettability. Determination of optimal slug size and sequence of chemicals in ASP flooding was also performed and is reviewed in this section.

Bo [1] studied behavior of relative permeability curves during ASP flooding in water-wet surface. Relative permeability of a fluid is not only a function of its saturation in a pore space, but it is also a function of IFT existed between bounding fluids, viscosity and residual saturation. Surfactant in ASP flooding increases capillary number by reducing IFT. This study showed that relative permeability to oil and water increased when IFT was decreased below 10^{-2} mN/m. Especially when IFT was lower than 10^{-4} mN/m, both relative permeability to oil and water tend to be linear function with water saturation as shown in Figure 2.1. Viscosity ratio of injected slug to displaced slug was also found to have significant effect on relative permeability curves when IFT is low. From Figure 2.2 it was found that relative permeability curves turned into straight line when IFT is below 10^{-3} mN/m.

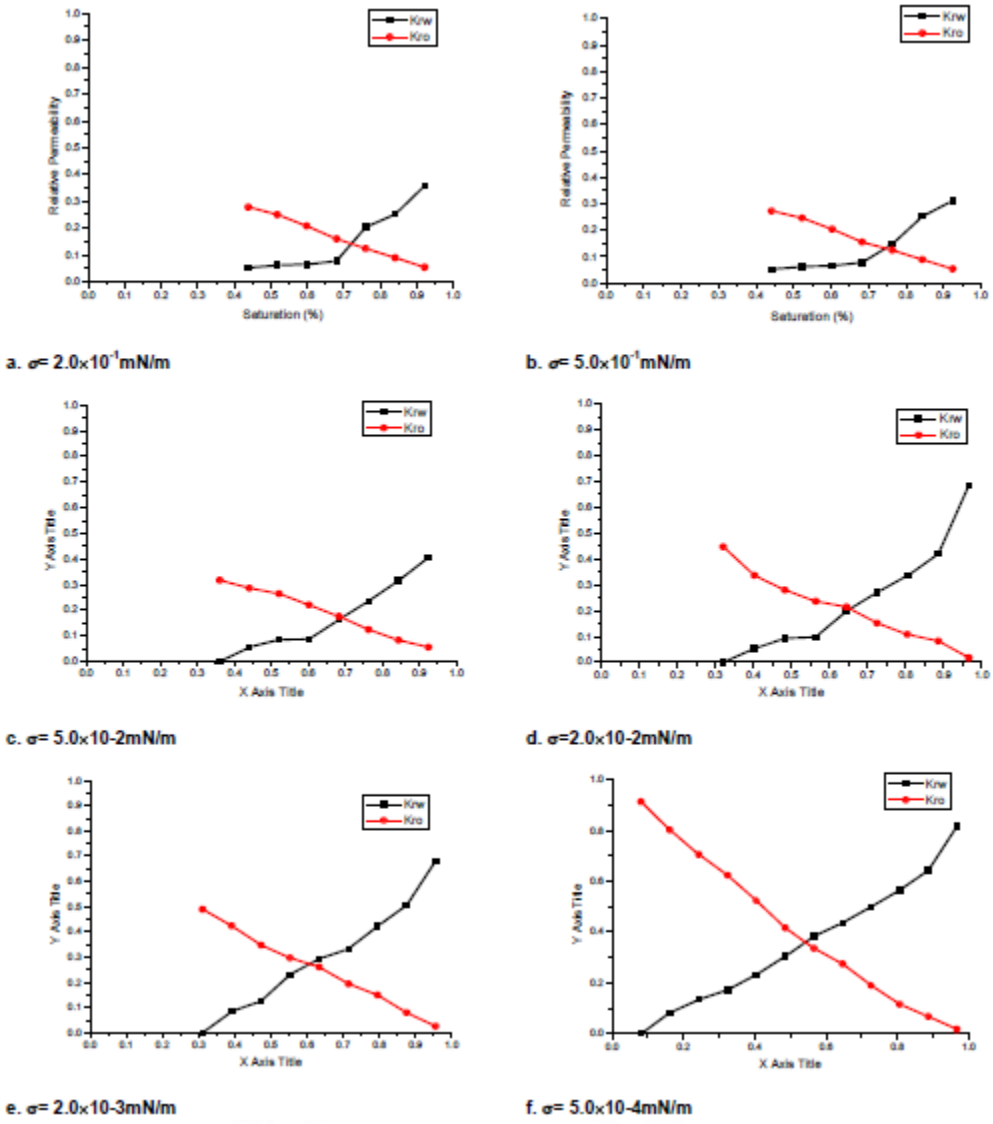

Figure 2.1 Relative permeability curves at different IFT values [1]

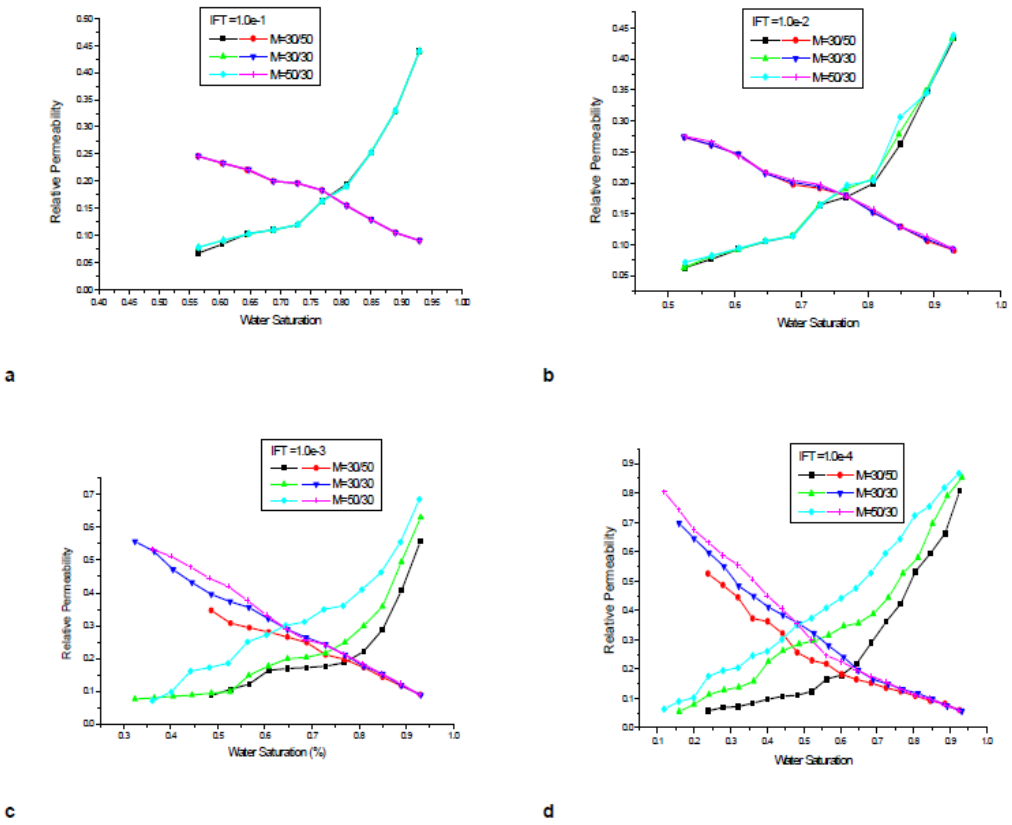

Figure 2.2 Effect of viscosity on relative permeability curves with vary IFT values [1]

Han et al. [2] evaluated effect of wettability on oil recovery of ASP flooding. In this study, Berea sandstone was used in experiment in three different wettability conditions. Wettability condition was altered by the use of organic reactant. Chemical slug composed of Sodium alkyl benzene sulfonate 0.2%wt (SY) as surfactant, Sodium hydroxide NaOH 1.0%wt (AR) as alkali and hydrolyzed polyacrylamide 0.1%wt (KY-26) as polymer was used. ASP slug was injected after waterflooding process reached 98% watercut. At first stage of experiment, the highest result of oil recovery during waterflooding stage occurred in neutral-wet condition. When ASP flooding was utilized, order from the highest oil recovery percent to the lowest oil recovery percent was found to be water-wet, oil-wet and neutral-wet condition, respectively. Result indicated that water-wet and oil-wet reservoirs are best candidates for ASP flooding as they could yield high oil recovery compared to neutral-wet condition. On the other hand, oil recovery percent by solely polymer flooding did not show much different for all three wetting conditions, meaning that polymer flooding was not sensitive to wettability of reservoir.

Zhang et al. [3] experimented on several studied parameters in ASP flooding that affect oil recovery such as concentration of surfactant, slug size and chasing fluid. This study used Instow coreflood as sample, flooded by a combination of 0.15%wt of Polyacrylamide (AN923 PG0) as polymer, 1.0%wt of Sodium hydroxide as alkali and Petroleum sulfonate (ORS-62HF) as surfactant at different surfactant concentrations. They found that surfactant concentration of 0.15%wt was an optimal concentration to form oil bank to obtain the highest oil recovery. Moreover, significant change in oil recovery when concentration of surfactant was slightly changed was obtained in this condition. They determined the smallest slug size with minimal chemical consumption by using cumulative oil recovery (%IOIP) and tertiary oil recovery (%ROIP) compared to amount of injected fluid. From experiment, slug size of 0.5 PV yielded the highest oil recovery as it could maintain high displacement efficiency ratio. Residual oil saturation also showed different effectiveness of ASP flooding. Higher residual oil saturation facilitated ASP slug to form bigger oil bank and as a consequence, higher oil recovery could be obtained. Thus, ASP flooding should be applied as early as possible. Last, experiment of injection scheme was tested to observe effect on oil recovery. Polymer solution acting as mobility buffer was additionally flooded after ASP slug. Results showed that this additional chasing polymer did not help the system to form second oil bank effectively. An increment about 6% compared to case without chasing polymer slug was obtained.

French [4] studied injection strategy of ASP flooding by coreflood test with Berea sandstone cores. When alkaline substance and surfactant were flooded together and chased by polymer slug (AS+P), the highest oil recovery was achieved. In contrast, combination of alkaline substance, surfactant and polymer together in one slug (ASP) yielded slightly lower oil recovery compared to the previous case. Oil recovery was significantly reduced when surfactant was followed by alkaline substance and polymer (S+AP) or surfactant slug was followed by polymer (S+P). Adding alkali in pre-flushed water before injecting chemical slug was observed to increase oil production. Injecting small slug of alkali preceding surfactant slug yielded the highest oil recovery compared to injecting surfactant before alkali or injecting both simultaneously. Moreover, injecting small alkali and surfactant slugs during polymer flood (P+0.05 PV of AS+P) greatly improved oil recovery compared to traditional polymer flood.

2.2 Effect of Heterogeneity on ASP Flooding

Naturally, most carbonate reservoirs contain induced voids so-called secondary porosity. Similar to porosity, secondary or induced permeability can be termed as well. One type of secondary porosity that is responsible for major storage capacity is fracture. This makes carbonate reservoirs to possess high degree of heterogeneity. Oil production of these carbonate reservoirs is therefore complicated and difficult to predict. In general, oil production is high at the beginning due to presence of oil storage in fracture. Afterwards oil production sharply decreases due to insufficient flow from matrix to fracture. In order to improve oil recovery from highly heterogeneous carbonate reservoirs, these following papers showed attempts by the use of ASP flooding.

Anderson et al. [5] simulated and presented result of surfactant and polymer (SP) flooding in a mixed-wet dolomite reservoir with high permeability layer. This study used a three-dimensional, multi-component chemical flooding simulator called UTCHEM as reservoir simulator and properties of Grayburg dolomite reservoir in Permian Basin to represent model. Reservoir model was built at 4,700 feet deep with a thickness of 100 feet. Watercut from undergoing waterflooding process was 98% from five-spot 40 acres pattern. Permeability distribution was two high permeability layers surrounded by lower permeability layers. Simulation results showed that additional oil recovery percent by SP flooding was 28%. However, early surfactant breakthrough occurred due to severe channeling through high permeability layers. This result from high permeability layers caused a significant amount of residual oil remained in location far away from injector due to fast displacement of SP through high permeability layers. They studied parameters that affect oil recovery factor such as rock wettability, surfactant slug size and polymer adsorption by sensitivity analysis. Result of wettability study showed that slow surfactant breakthrough was obtained in water-wet reservoir according to relative permeability that affects fractional flow behavior. Increasing in polymer adsorption showed higher oil recovery and better chemical efficiency than that of base case. This occurrence was obtained from permeability reduction in high permeability channel. This showed that polymer could displace oil in low permeability zone, resulting in higher sweep efficiency.

Tabary et al. [6] investigated chemical flooding in carbonate formation. They studied main factors to increase oil recovery from oil-wet fractured reservoirs. Study factors included reducing IFT and changing rock wettability. In experiment they used Sodium carbonate (Na_2CO_3) as alkaline substance and Sasol Alfoterra sulfated propoxylatedalcols as surfactant. Crude oil was obtained from the south-west province in France and Lavoux limestone from Paris basin in France represented reservoir rock. From experiment results, they recommended to use nonionic and mixed anionic-nonionic as surfactant for carbonate reservoir in order to reduce amount of surfactant adsorption onto rock surface although performance of IFT reduction of the nonionic and mixed anionic-nonionic is less effective than anionic sulfonates. Alkaline substance was found to improve oil recovery through wettability alteration to a more water-wet condition and also to decrease IFT value between water-oil interfaces.

Teklu et al. [7] constructed numerical model to investigate effect of polymer-augment waterflooding in heterogeneous reservoir. Waterflooding showed less effectiveness in heterogeneous reservoir especially when channels are present, causing early breakthrough of water and leaving most of oil behind in un-swept zones. Therefore, injection of polymer-augment water aimed to enhance oil recovery in by-passing channel reservoir to reduce conductivity dominated along channel. Two dimensional models were constructed, composing of eleven grid blocks in both x and y directions. High permeability channel with a value of 10,000 mD permeability was located along and across location of injector and producer in the model. Polymer-augment waterflooding process was started at 50% of watercut, after that polymer-augment waterflooding was performed for four years before switching back to conventional waterflooding until watercut reaches economic limit of 98%. Results indicated that production performance significantly dropped in case of high permeability channel along injector and producer, causing early water breakthrough. When polymer was injected into the system, water production was significantly reduced. However, changing from polymer injection to conventional waterflooding caused a raise of water production again. Therefore, polymer injection can divert fluid away from high permeability channel. On the other hand, result of polymer injection with high permeability channel across injector and producer showed maximum oil recovery factor when compared to high permeability channel along injector and producer.

2.3 Application of ASP Flooding in Oil Fields

Historical fields exploited by ASP flooding in pilot scale are summarized in this section.

In 1998, Zhijian et al. [8] reported a successful case of ASP flooding in Gudong oil field. Result showed that an increment of 13.4% of original oil in place as additional oil recovery was obtained by ASP flooding. Reservoir was unconsolidated sandstone with thickness of eleven meter. Five-spot pattern with well spacing of 50 meter was used in this project.

Li et al. [9], [10], Shutang and Qiang [11] showed successful recent progress of ASP flooding in Daqing Oil Field. This field has been applied ASP flooding since 1980s. In 1993, three pilot tests of ASP flooding have been carried out in the western part of central Saertu, central part of Xing5 areas. Result from ASP pilot test showed an increase of oil recovery in percentage of original oil in place compared to conventional waterflooding of 21.4%, 25.0% and 23.24%, respectively. After that two extended ASP flooding tests have been implemented in west Xing2 area and west part of North 1 zone in 1996. Incremental of oil recovery obtained from these two projects compared to conventional waterflooding were 19.6% and 21.04%, respectively. Afterwards, an extended ASP flooding in West Xing2 area showed improving of 19.6% compared to conventional waterflooding. This result indicated that ASP flooding does not only improve oil recovery, but also expands sweep volume.

For a purpose of studying ASP flooding in condition such as long well spacing, multi-layers and low concentration with large chemical slug, the first commercial field test was established in the Central Xing2 in 1998. They obtained oil recovery about 19% of original oil in place higher than waterflooding, although injection capacity was less than that of small pilot test field. From 1987 - 2010, twelve pilot tests were conducted for studying proper surfactant type, slug design and size. In summary, incremental recovery was around 20% of original oil in place volume over conventional waterflooding.

According to previous studies, it is obvious that ASP flooding is nowadays considered as one of the techniques chosen to improve oil recovery in complex reservoirs especially for those possess oil-wet condition and high permeability channels. This study is therefore performed to provide insight idea of ASP flooding in both optimization of operational parameters and sensitivity analysis of petrophysical and reservoir properties points of view.

CHAPTER 3
THEORY AND CONCEPT

In this chapter, detailed mechanisms of each chemical substance composed in ASP flooding are described. Principal of ASP flooding reflects the major criteria of reservoir and fluid properties in order to prevent the undesirable effects. Moreover, explanation of occurrence of high permeability channel is stated later in this chapter.

3.1 Principal of ASP Flooding

According to certain strictly requirements of ASP flooding, oil-wet reservoir does not seem to be good candidate formation for ASP flooding. High depletion rate can occur especially when anionic surfactant is used, causing higher requirement of injectant amount. Due to the fact that alkali is relatively cheap compared to surfactant, adding this low-cost chemical into surfactant can lower injectant cost due to several effects such as reducing of surfactant amount in order to achieve ultra-low IFT condition, and preventing of surfactant depletion. In certain conditions where depletion of chemical can be managed, combination of ASP flooding can be one of candidates in oil-wet reservoir. Basically, ASP flooding technique requires certain criteria for both reservoir and oil properties. For reservoir properties, temperature is one of the most concerned properties because surfactant and polymer are quickly degraded at elevated temperature. Moreover, alkali consumption by rock is also accelerated. Typically, formation temperature is limited below 200°F for ASP flooding. As reservoir depth is inter-related with temperature, reservoir depth should be less than 9,000 feet in corresponding with reservoir temperature. Average permeability and reservoir thickness are not critically concerned [12]. Presence of clays can deplete alkali through ion exchange mechanism, whereas divalent ions such as Ca^{2+} and Mg^{2+} decrease effectiveness of all substances by precipitation mechanism and this could turn the process to a severe damage [13]. Nevertheless, sequential injection of soften pre-flushed water can mitigate effects of divalent ion by avoiding direct contact between injected chemicals and formation brine. For oil properties, light to medium oil reflects good benefit by ASP flooding technique.

Criterion for oil gravity is generally higher than 20°API, and viscosity should be lower than 35 cP [14].

3.2 Surfactant Flooding

Surfactant improves oil recovery mainly through reduction of interfacial tension (IFT) between oil and aqueous phases. At certain IFT value, oil is liberated from rock surface as small droplets or emulsion form. A single molecule of surfactant is literally called monomer. Structure of surfactant monomer contains 2 parts: polar part (head portion) which is water-soluble and non-polar part (tail portion) which is oil-soluble. This structure is illustrated in Figure 3.1 [15].

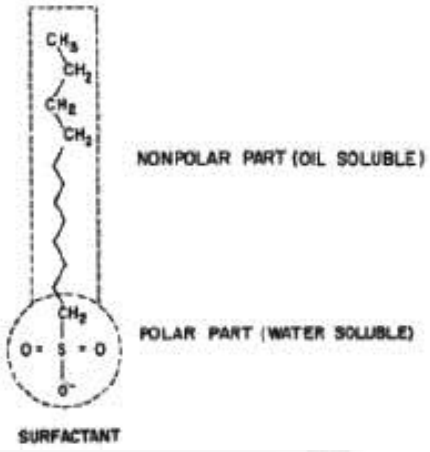

Figure 3.1 Structure of surfactant monomer [13]

Interfacial tension (IFT) is defined as a force per unit length that is parallel to interface of two immiscible fluids. Within the immiscible fluid and far away from the wall, molecules attach each other in all directions, while molecules at surface of two immiscible fluids have just only one inward-directed force that attempts to reduce the surface by pulling themselves into spherical form [16].

Using charge property of polar part, surfactant can be classified into four different groups: anionic, cationic, nonionic and amphoteric as shown in Figure 3.2. Anionic and cationic surfactants are theoretically used in sandstone and carbonate formations, respectively. Anionic surfactant possesses negative charge at polar part; therefore, anionic surfactant tends to be adsorbed onto the surface of carbonate

reservoirs since these rocks are positively charged at normal reservoir conditions. On the contrary, cationic surfactant possesses positive charge at polar part; hence, cationic surfactant is highly adsorbed onto sandstone surface [15]. However, cost of anionic surfactant is relatively cheaper than cationic one, making anionic surfactants as the most widely used surfactant in petroleum production industry. Surfactant depletion problem from adsorption can be reduced by adding several chemicals for instance alkaline and nonionic surfactant.

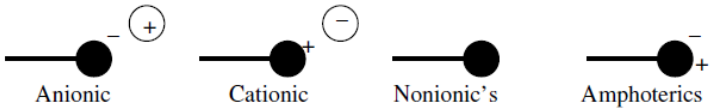

Figure 3.2 Classification of surfactant by using charge property [15]

Surfactant adsorption is defined as amount of absorbed surfactant per unit weight [17]. Most of surfactant adsorption is generally consumed by rock surface. Surfactant adsorption depends on many factors such as type of surfactant, charge of rock surface, pH of reservoir and salinity. For example, anionic surfactant is directly adsorbed onto positively charged rock surface due to attraction force between different charges. Charge of rock surface can be explained by the term called Point of Zero Charge (p.z.c.) [15] which is the pH value where surface charge density is changed from negative to positive charges vice versa. Typical p.z.c. value of sandstone is about 2.5 (representing by quartz), whereas carbonate possesses much higher value of 9.0 (representing by calcite). This makes sandstones having negatively charge at typical reservoir condition (pH around 6-8). In contrast, carbonate has positive charge at reservoir condition. However, anionic adsorption onto carbonate rock surface can be substantially reduced by using alkali to alter surface charge by raising pH value above 9.0.

Surfactant greatly reduces IFT between oil and aqueous phase by sticking polar part into aqueous phase and non-polar part into oil phase. Therefore, molecule remains at interface between oil and aqueous phases, taking an action as a linking bridge. At very low surfactant concentration, monomers freely move and they stick themselves at interface, reducing effectively IFT. Increasing concentration of surfactant results in drastic reduction of IFT until the Critical Micelle Concentration (CMC) [13] is reached. When surfactant concentration is higher than CMC, monomers

start to form micelles and IFT is raised again due to less effective monomer at interface. Change of IFT related with surfactant concentration is shown in Figure 3.3. At certain surfactant concentration, IFT starts to reduce again as surfactant concentration is increased. New created phase as a film layer linked between oil and aqueous phase is formed. Effect of surfactant concentration on IFT value is depicted in Figure 3.4.

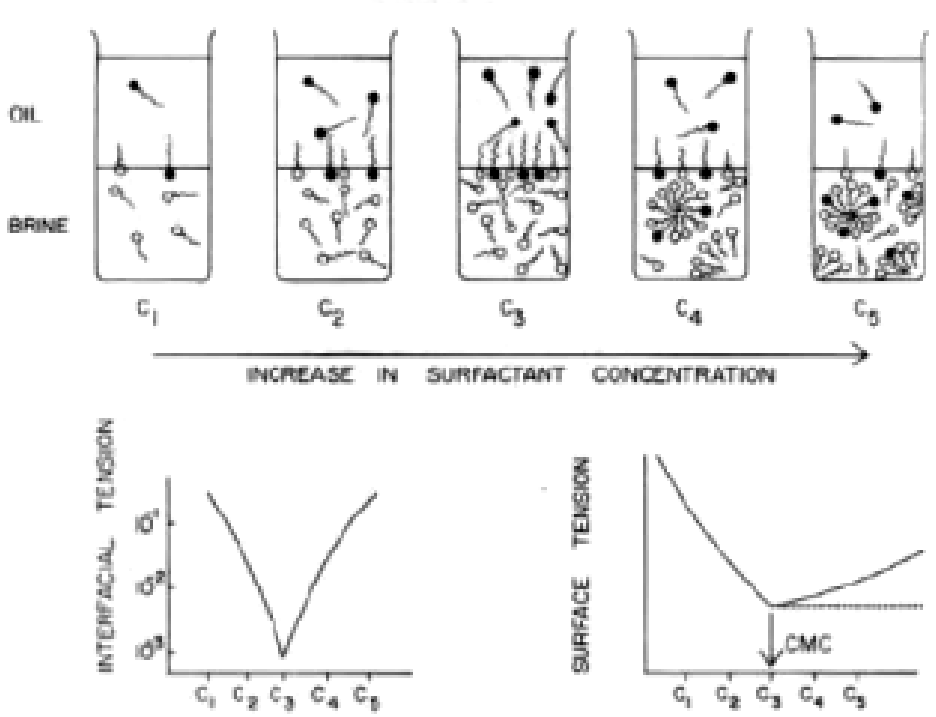

Figure 3.3 Changes of monomers into micelles related to surfactant concentration, interfacial tension and surface tension [13]

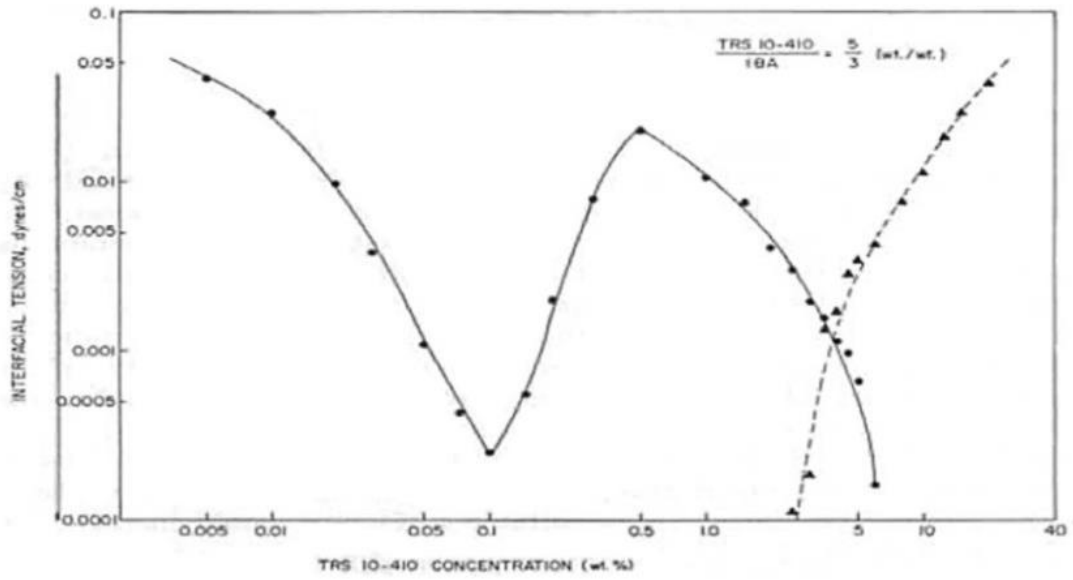

Figure 3.4 Effect of surfactant concentration on interfacial tension [13]

Not only surfactant monomers that effectively reduce IFT, but also micro-emulsion phase behavior [18] causes reduction of IFT at a distinctly high surfactant concentration. Salinity is a major key that controls appearance of micro-emulsion. Ternary phase diagram is generally used to explain effect of surfactant concentration on IFT at different salinity as shown in Figure 3.5. At low salinity, surfactant is mostly soluble in aqueous phase but poorly soluble in oil phase. This phase behavior is called Winsor type I or type II (-) based on the tie line with negative slope. At very high salinity, solubility of surfactant in aqueous phase shifts to oil phase instead due to abundant of electrostatic force. This phase behavior is called Winsor type II (+) due to positive slope of the tie lines. At moderate value of salinity, surfactant generates a micro-emulsion phase and this phase behavior is called Winsor type III. At the moderate salinity, number of surfactant molecule in oil and aqueous is theoretically equivalent. As a result, water-in-oil as well as oil-in-water emulsion are equally formed, resulting in an appearance of middle phase micro-emulsion. Phase diagrams of Winsor type I, II and III are illustrated in Figure 3.6 and consecutively in Figure 3.7, effect of salinity change on IFT covering regions of three phase behaviors is shown. From Figure 3.7, ultra-low IFT occurs when salinity is at optimal value (Winsor type III). Ultra-low IFT increases displacement efficiency (E_D) by allowing oil droplets to entrain through small pore throats as shown in Figure 3.8.

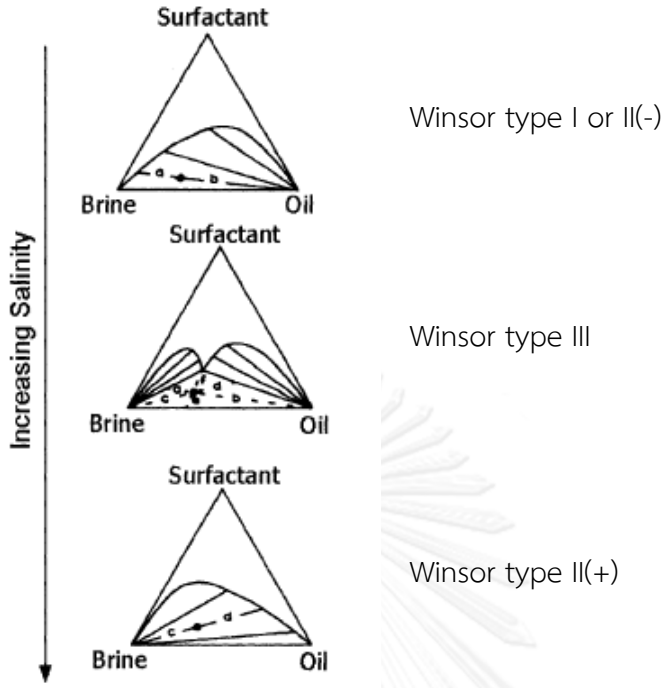

Figure 3.5 Micro-emulsion ternary phase diagram at different salinity [17]

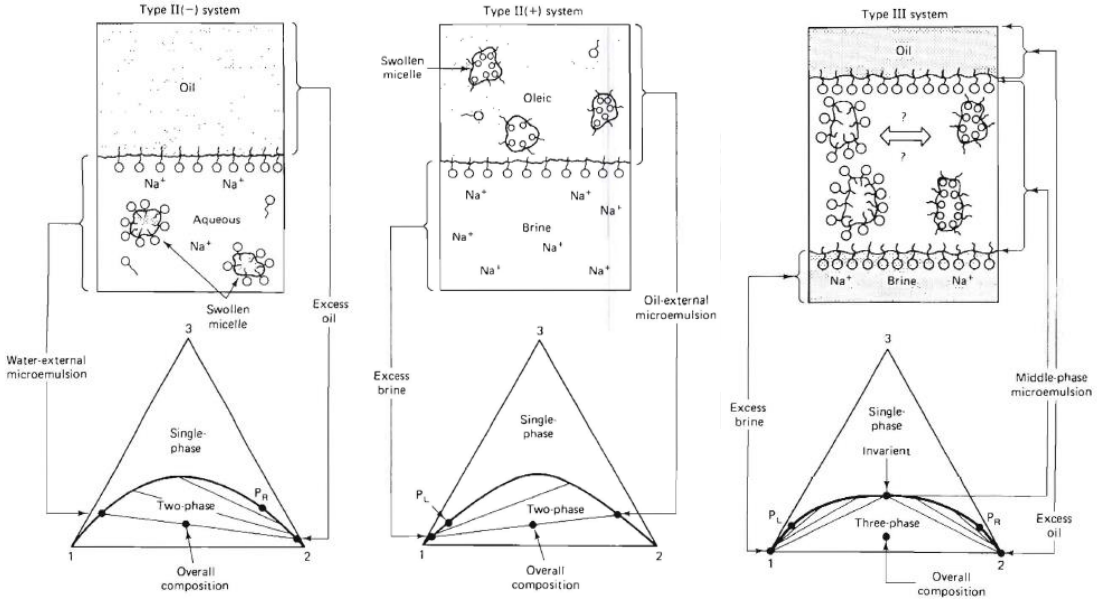

Figure 3.6 Micro-emulsion ternary phase diagram of Winsor type I, II and III [18]

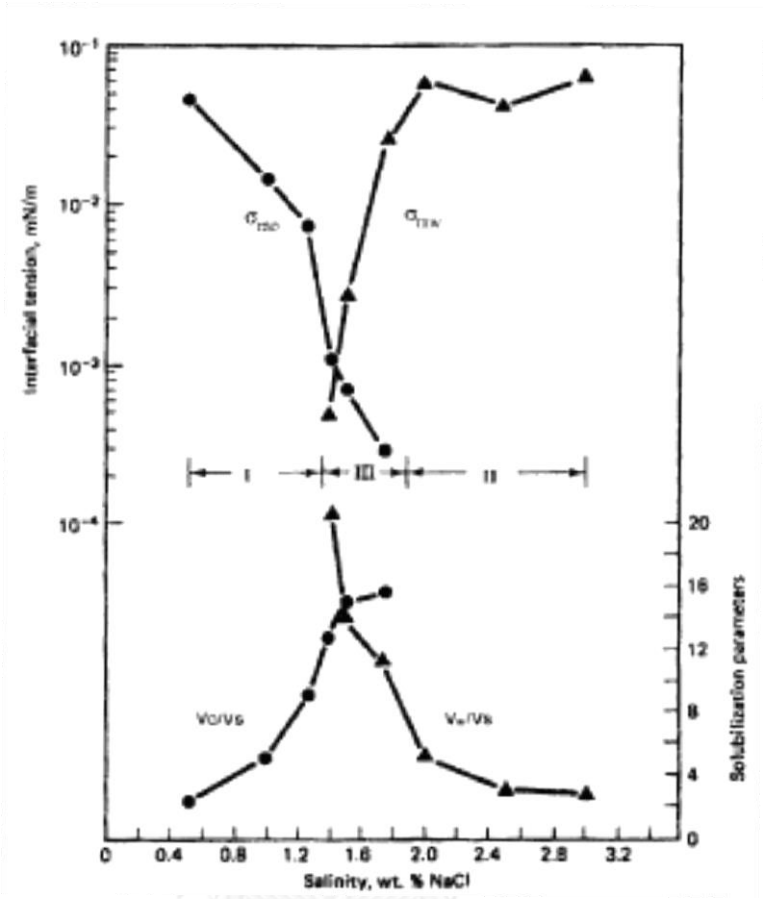

Figure 3.7 Effect of interfacial tension as a function of salinity [18]

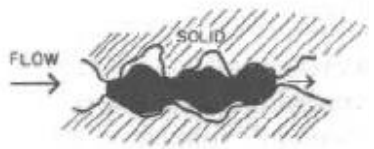

FOR THE MOVEMENT OF OIL THROUGH NARROW NECK OF PORES, A VERY LOW OIL/WATER INTERFACIAL TENSION IS DESIRABLE≈ 0.001 DYNE/CM

Figure 3.8 Role of IFT in surfactant flooding [13]

Emulsification occurred from IFT reduction directly affects relative permeability functions. Effects can be divided into two major groups of improving in terms of microscopic and macroscopic levels. Emulsification and entrainment [13] improve in terms of microscopic point of view. Generated fine emulsion can flow with water flow line through pore throats at the same velocity. This occurs when concentration of surfactant increases, lowering IFT until ultra-low condition is achieved (about 10^{-3} dyne/cm). At low IFT condition, oil which is liberated from

remaining residual oil forms an oil bank in front of the chemical front. This liberation of oil in emulsion form occurs until there is no residual oil left in pore body. Meanwhile, flow ability of water is improved compared to the previously higher IFT condition because of increasing of relative permeability to water. Increment of relative permeability to water stimulates chemical shock front to flow at the same velocity as oil shock front by displacing irreducible water saturation in reservoir. In case where concentration of surfactant is high enough to reach an ultra-low IFT condition, relative permeability curves to both oil and water are in linear function with saturation. Therefore, water and oil can flow without interference and trapped phase by rock preference disappears. At this condition, injected chemical displaces all the fluids, creating pseudo oil bank as shown in Figure 3.9(a).

For macroscopic aspect, emulsification and entrapment [13] occurs. Generated emulsion is re-trapped at small pore throats. Although residual oil does not decrease in Figure 3.9(b), result from this mechanism generally increases volumetric efficiency by diverting flow to difficultly accessible area.

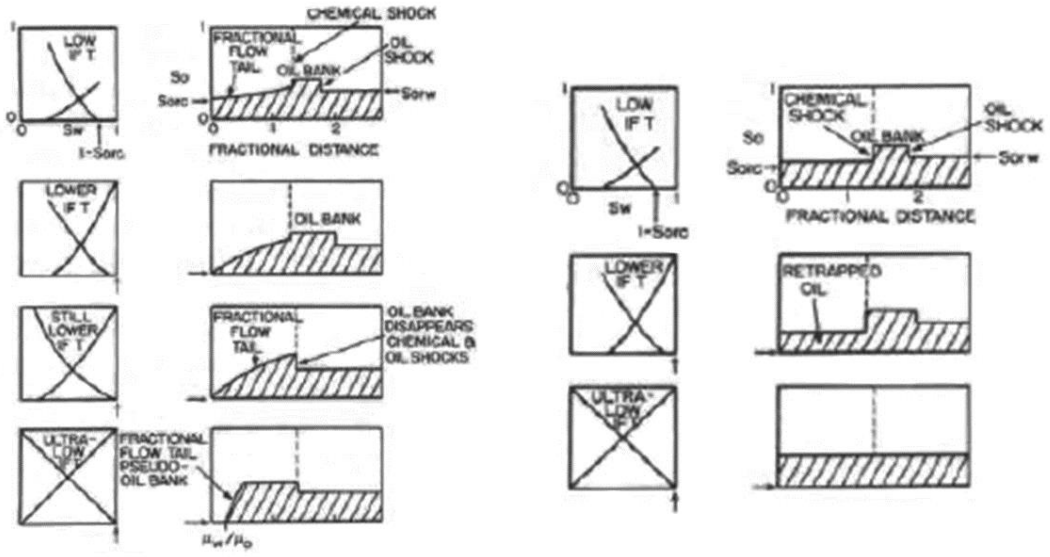

(a) (b)

Figure 3.9 Displacement profile and relative permeability at different IFT (a) emulsification and entrainment (b) emulsification and entrapment [13]

Not only relative permeability curves that are altered by the use of chemical flooding, but also capillary pressure which acts against flow through small pore throats is also reduced. This results in displacement mechanism in smaller pores. Capillary pressure (*Pc*) is defined as a difference in pressure existing across interface of two immiscible fluids. This term can be also related to curvature of interface as shown in Figure 3.10. Capillary force is also one of the three important forces controlling flow of injected fluid. [16]

$$P_C = P_{NW} - P_{WET} \text{ and } P_c = \frac{2\sigma Cos\theta}{r_c} \quad (3.1)$$

where P_C = capillary pressure,

P_{NW} = pressure in the non-wetting phase,

P_{WET} = pressure in the wetting phase,

σ = interfacial tension between two phases,

θ = contact angle,

r_c = radius of measured tube.

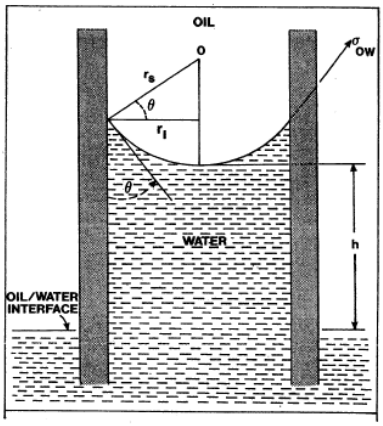

Figure 3.10 Capillary rise of water in a water-wet capillary tube [16]

Efficiency of displacement mechanism in reservoirs is generally determined from fraction flow equation. This equation describes flooding behavior in porous medium. The term fractional water [19] is calculated by including three important forces; capillary, gravity and viscous forces as illustrated in equation (3.2).

$$f_w = \frac{1+\frac{kk_{ro}}{u_t\mu_o}[\left(\frac{\partial P_c}{\partial L}\right)-g\Delta\rho sin\alpha_d]}{1+\frac{\mu_w k_o}{\mu_o k_w}} \qquad (3.2)$$

where f_w = fractional flow of water,

k = absolute permeability,

k_{ro} = relative permeability to oil,

k_{rw} = relative permeability to water,

u_t = total fluid velocity,

μ_o = viscosity of oil,

μ_w = viscosity of water,

$\frac{\partial \mathrm{P_c}}{\partial \mathrm{L}}$ = capillary pressure,

g = acceleration term due to gravity,

$\Delta\rho$ = water-oil density difference,

α_d = dip angle.

Capillary number (N_c) [16] is termed to compare effect of capillary force to viscous force as in equation (3.3). In general, conventional waterflooding is performed at capillary number ranging from values of 10^{-6} to 10^{-7}. When IFT is reduced for a few magnitudes, capillary number can be raised up to 10^{-2} which is adequate to increase displacement efficiency [13].

$$N_c = \frac{\mu_w \phi q}{\gamma_{o/w}} \tag{3.3}$$

where N_c = capillary number,

μ_w = viscosity of water,

ϕ = porosity,

q = flow rate per unit cross-sectional area of water,

$\gamma_{o/w}$ = interfacial tension between oil and water.

In general, relationship between capillary number and residual oil in percentage is illustrated in Figure 3.11 showing that the higher the capillary number the lesser the residual oil saturation.

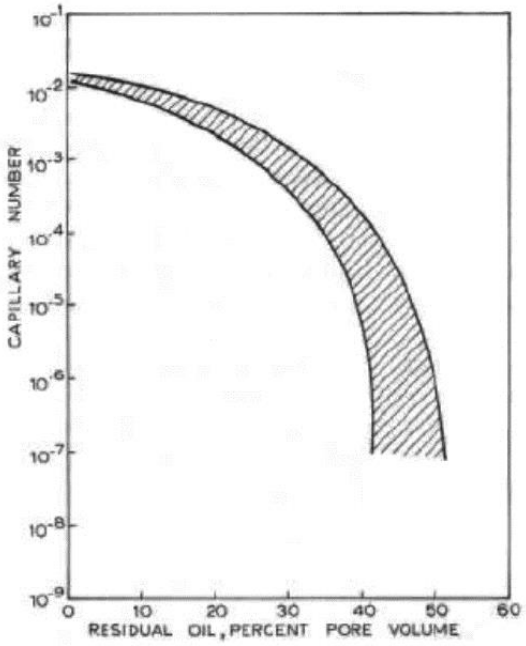

Figure 3.11 Capillary number as a function of residual oil saturation [13]

3.3 Alkali Flooding

Alkali is a group of an inexpensive base compound that has an ability to generate high pH value. Common alkaline substances used in chemical flooding are sodium hydroxide, sodium carbonate and sodium orthosilicate. Alkali substance reacts with saponifiable acid compounds in oil phase to generate in-situ soap through saponification reaction. Similar to surfactant discussed in section 3.2, in-situ soap produced from alkaline substance and acid compounds in oil phase leads to IFT reduction [13]. IFT reduction from produced soap from saponification can be lower than 10^{-3} mN/m that is enough to activate spontaneous emulsification. Moreover, in-situ surfactant from alkali also dissolves insoluble film at oil-water interface which is a product from water washing process. Solubilization of this film results in restoration of original permeability and hence, injectivity of fluid into porous medium is increased.

Moreover, alkaline substance also reacts with rock formation, resulting in wettability alteration [13]. Wettability of rock is changed from oil-wet to a more water-wet direction by the use of alkaline substance. This results in a more favorable condition for oil production. Wettability alteration mechanism by alkali occurs in carbonate reservoirs. When pH value of surrounding system is raised over the value of 9 which is p.z.c. of carbonate rock, surface switches to be negative charge by removing hydrogen ion (H^+) to H_2O. According to this mechanism, previously adsorbed material causing oil-wet surface is liberated due to repulsion force, leaving surface cleaned. Nevertheless, result from wettability alteration also causes extra alkali consumption. Sequence of wettability alteration can be explained by Figures 3.12 a-d. Prior to oil migration mechanism into pore body of reservoir rock, wettability of reservoir is water-wet (a). After oil migration, non-polar compound in crude oil precipitates onto rock surface and changes the wettability to oil-wet condition. Performing waterflooding in this state will displace part of mobile oil. However, most of immobile oil still remains on the rock surface in pore body (b). During this process, alkali leads to reduction of capillary resistance. Therefore, oil can be removed from rock surface (c and d).

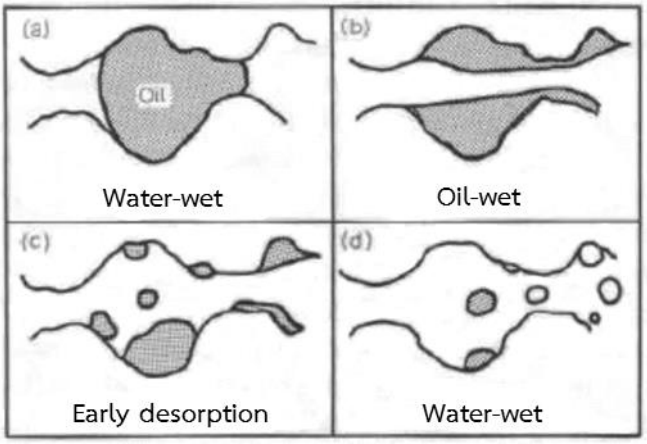

Figure 3.12 Mechanism of trapped oil removal by wettability alteration [13]

Wettability is a tendency of fluids to spread or adhere onto solid surface in a presence of other immiscible fluids [16]. Wettability is considered as an important factor that controls flow and fluids distribution in reservoir. Wettability affects most of the petrophysical properties including capillary pressure, relative permeability and displacement mechanism. Immiscible fluids in this study are water and oil. From these two phases, wettability can be mainly classified into three types which are water-wet, oil-wet and neutral-wet. Water-wet is a condition where rock surface prefers to be adhered by water; whereas, oil-wet reservoir is in the opposite condition where rock surface prefers to stick with oil. Rock surface that has preference of both water and oil evenly is called neutral-wet. Both carbonate and sandstone rocks are believed to be strongly water-wet at their origin since they are both originated in aqueous environment deposition. Due to oil migration and oil trapping in reservoir rocks, wettability of the rocks can be altered to oil-wet by means of four wettability alteration mechanisms which are polar interaction, surface precipitation, acid/base interaction and ion binding [15]. Wettability can be quantitatively measured by three methods which are contact angle, Amott method and USMB method.

Relative permeability is one of petrophysical properties that are majorly affected from wettability. This term describes relative flow ability of fluids in porous media when the others fluid are presented. Relative permeabilities of oil and water are plotted on y-axis as a function of water saturation on x-axis. The flow of fluid is found in the range between connate water saturation and residual oil saturation. That means under connate water saturation and beyond residual oil saturation, one fluid will remain immobile whereas another phase is still moving. The crossover of

relative permeability curves could imply wetting condition of rock. As the crossover saturation shifts to the right, that means relative permeability to water or flow ability water is less dependent on its saturation. In other word, water tends to be adhered on rock surface and hence flow ability is low. Crossover saturation over 50% is therefore, referred to water-wet condition. Wettability of rock can be indicated from relative permeability curves as shown in Figure 3.13 (a) and (b) for strongly water-wet and oil-wet, respectively. Generally, the rule of thumb of relative permeability [19] can be roughly used to classify wetting condition from physical aspects of relative permeability curves as shown in Table 3.1. In practice, relative permeability curves are constructed from multi-phase flow ability in laboratory. This technique is time consuming to complete and in order to simplify this, construction of relative permeability curves can be performed by method using Corey's correlation. The relative permeability of oil and water at different water saturation are calculated from end-point relative permeability to as illustrate in equation (3.4) and (3.5). The curvature of relative permeability curves is so called Corey's exponent which are applied to both oil and water. The Corey's exponent of 2.0 is used as base value for oil and water in this study.

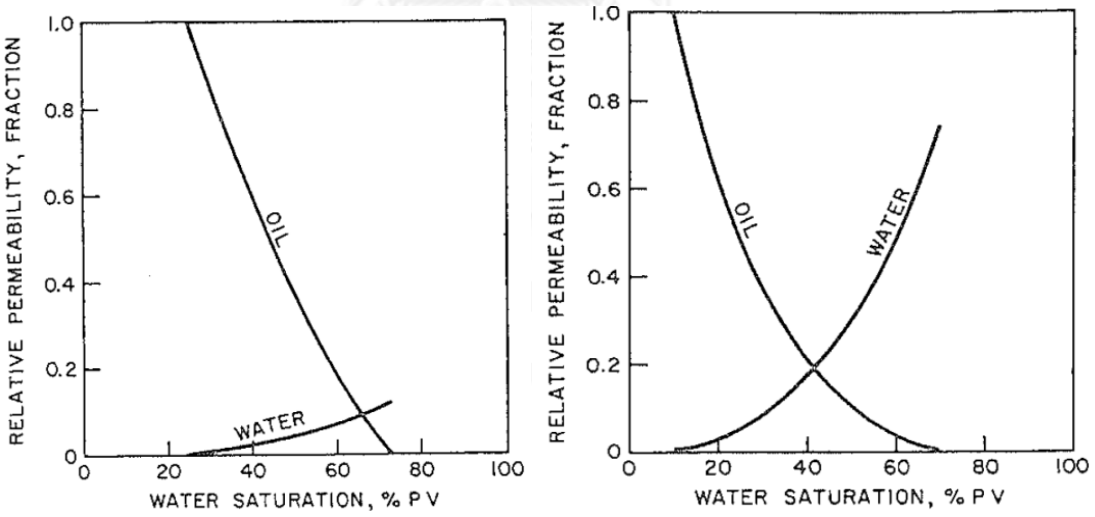

(a) (b)

Figure 3.13 Typical relative permeability curves (a) Strongly water-wet (b) Strongly oil-wet [19]

Table 3.1 Rule of thumb of relative permeability for classifying wetting condition [19]

Properties	Water wet	Oil wet
Connate water saturation (S_{wc})	Greater than 20-25%	Frequently less than 10%
Crossover saturation	Greater than 50%	Less than 50%
krw at residual oil saturation ($k_{rw}(S_{orw})$)	Generally less than 30%	Greater than 50%

$$k_{ro}(S_w) = k_{ro@S_{wmin}} \left[\frac{1 - S_{orw} - S_w}{1 - S_{orw} - S_{wc}}\right]^{C_o} \quad (3.4)$$

$$k_{rw}(S_w) = k_{rw@S_{orw}} \left[\frac{S_w - S_{wc}}{1 - S_{orw} - S_{wc}}\right]^{C_w} \quad (3.5)$$

where S_w = water saturation,

S_{orw} = residual oil saturation to water,

S_{wc} = critical water saturation,

$k_{ro}(S_w)$ = relative permeability to oil at any water saturation,

$k_{rw}(S_w)$ = relative permeability to water at any water saturation,

$k_{ro@Swmin}$ = relative permeability to oil at minimum water saturation,

$k_{rw@}S_{orw}$ = relative permeability to water at residual oil saturation,

C_o = Corey oil exponent,

C_w = Corey water exponent.

3.4 Polymer Flooding

Polymer flooding is an EOR technique where soluble polymer is mixed with injected water to improve volumetric sweep efficiency. This improvement is accomplished through the incremental of viscosity of injected slug which results in more favorable mobility ratio. Polymer is formed from linking of individual molecules in the same pattern. These individual molecules are so-called monomer. To achieve favorable condition, molecular weight of polymer molecule is generally greater than 200 and one molecule normally composes of at least 8 repeating units. Structurally, polymer composes of backbone which is a main part of molecule structure and side chains rooting out from main backbone. Common polymer used in flooding can be grouped in four types which are Polyacrylamides (PAM), Xanthan gum (XG), Cellulosic compounds and Polyacrylate copolymer (PAC). The most widely used polymer is hydrolyzed Polyacrylamides (HPAM). In the reservoir, HPAM is severely adsorbed onto rock surface especially carbonate rocks because of an interaction between negatively charged polymer and positively charged carbonate surface. Adsorption of polymer (in general refer to only PAM) can be related to the Resistance factor (*R*) [13] which is a term to represent relative pressure drop caused by polymer solutions in porous media as showed in equation (3.6). For polymer flooding, this number should be minimized to decrease pressure loss from the polymer. However, moderate polymer adsorption yields benefit to stabilize flow through high permeability channel by diverting flow to lower permeability zone [20].

$$R = \frac{\lambda_w}{\lambda_p} = \frac{k_{rw}}{\mu_w}\frac{\mu_p}{k_{rp}} \tag{3.6}$$

where, R = resistance factor,

λ_w = mobility of water,

λ_p = mobility of polymer slug,

k_{rw} = relative permeability to water,

k_{rp} = relative permeability to polymer,

μ_w = viscosity of water,

μ_p = viscosity of polymer solution.

Mobility ratio defined in equation (3.7), is a ratio of mobility of displacing phase (injected fluid) to mobility of displaced phase (remaining oil). Since polymer molecule has higher molecular weight compared to water, viscosity of polymer solution is therefore higher than water or produced water that is commonly used in conventional waterflooding. Increasing of viscosity by polymer substantially plays an important role in decreasing mobility ratio of polymer flooding process. Decreasing mobility ratio dominates viscous force term in the fractional flow equation over others [15]. This results in smooth flood front and hence volumetric efficiency is improved as shown in Figure 3.14.

$$M = \frac{\lambda_p}{\lambda_o} = \frac{k_{rp}}{\mu_p}\frac{\mu_o}{k_{ro}} \tag{3.7}$$

where M = mobility ratio,

λ_p = mobility of polymer slug,

λ_o = mobility of residual oil,

k_{rp} = relative permeability to polymer slug,

k_{ro} = relative permeability to residual oil,

μ_p = viscosity of polymer slug,

μ_o = viscosity of residual oil.

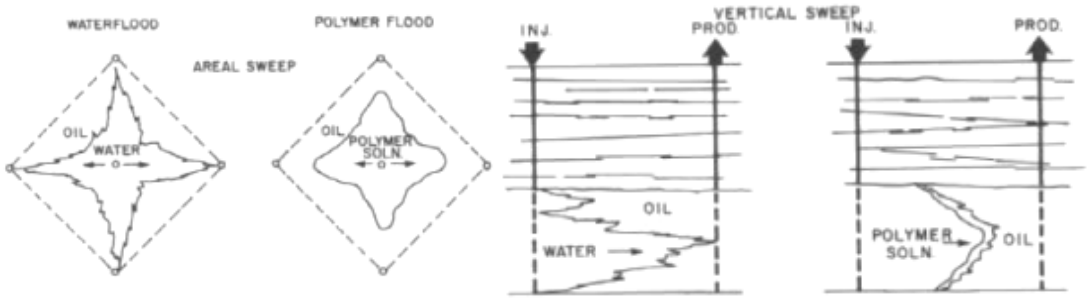

Figure 3.14 Areal and vertical sweep efficiency in waterflooding and polymer flooding cases [13]

Polymer flooding is mainly functioned to improve volumetric sweep efficiency. This term is a product of two important terms which are areal sweep efficiency (E_A) and vertical sweep efficiency (E_I). Areal sweep efficiency is defined as area contact by injected fluid divided by total area, representing coverage area that displacing phase can reach. Areal sweep efficiency depends on several factors such as flood pattern, elapsed time and mobility ratio. Vertical sweep efficiency is defined as a cross-sectional area of injected fluid over total cross-sectional area. This value reveals efficiency of injected fluid in vertical direction. Factor affecting vertical sweep efficiency is variation of permeability in stratified layers. A presence of high permeability channel could results in poor vertical sweep efficiency for most injectant. Product of areal and vertical sweep efficiency is called volumetric sweep efficiency (E_v) which exhibits efficiency of displacement mechanism in terms of volume. Besides volumetric sweep efficiency, injected fluid should have also an ability to displace hydrocarbon in place when they are in contact. This ability is defined as displacement efficiency (E_D) representing by an amount of displaced oil by amount of oil contacted by injected fluid. Polymer flooding also increases displacement efficiency since adsorption of polymer onto rock surface slightly changes relative permeability curves. Nevertheless, displacement efficiency is much higher in case of alkali-surfactant flooding compared to polymer flooding.

Oil recovery efficiency (E_R) [19] is eventually a multiplication of volumetric sweep efficiency and displacement efficiency. Relationship of all terms is expressed in equation (3.8).

$$E_R = E_D \times E_A \times E_I \tag{3.8}$$

where E_R = oil recovery efficiency,

E_D = displacement efficiency,

E_A = areal sweep efficiency,

E_I = vertical sweep efficiency.

3.5 High Permeability Channel

Rock which is formed from depositional process is called sedimentary rock. Sandstone, carbonate, and shale are examples of sedimentary rocks that are involved in petroleum reservoirs. Sedimentation is a process that particles are accumulated in basin and are lithified by compaction and cementation. Sediments can be classified as detrital sediment and chemical sediment. Detrital sediments are discrete particles occurred by mechanical weathering. Among this type of sediments, sand grains is a major source of sandstone rock which is one of examples of rock formed by detrital sediment. Chemical sediments are previously soluble and eventually precipitated to form rock such as carbonate. Sedimentation usually results in void space that is a result from packing of particles. This void space is so-called porosity representing ability of fluid storage. Primary porosity comes directly with depositional and burial environment [21]. Primary porosity of carbonate rock is quite small compared to that of sandstone due to sedimentation process of chemical sediment. Nevertheless, porosity can be formed after deposition and this is called secondary porosity or induced porosity. For carbonate reservoirs, secondary porosity is much more important than primary porosity. Several examples of secondary porosity are porosity from dolomitization, fracture porosity and solution porosity. Dolomitization creates voids by transforming limestone into dolomite. Fracture porosity creates wide space due to anisotropic stress. And finally solution porosity increases primary porosity by flowing of acidic water, dissolving calcium carbonate and creating cavernous space.

Related to porosity, permeability is an ability of rock to allow fluids to flow through interconnected pore throats. Once rock developed secondary porosity, secondary permeability is also found. Higher permeability can be found for those three mechanisms in carbonate rocks. Solution porosity which is caused by water channeling can result in difference in permeability where certain location possesses higher permeability compared to the rest that has not been passed by other dissolving solutions. An example of high permeability channel in horizontal layer is shown in Figure 3.15.

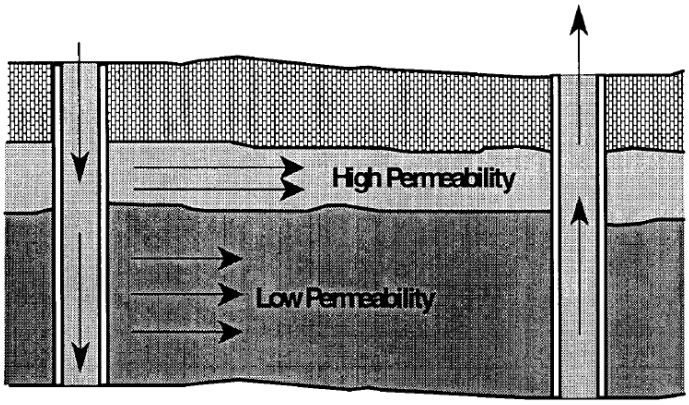

Figure 3.15 Schematic of high permeability channel in horizontal direction [22]

Permeability can be expressed by Darcy's equation as equation (3.9). There are many parameters affecting permeability value [16].

$$v = \frac{-k}{\mu}\frac{dP}{dl} \tag{3.9}$$

where v = fluid velocity,

k = permeability,

μ = fluid viscosity,

$\frac{dP}{dl}$ = pressure gradient in flow direction.

Porosity is found to be one of those that control magnitude of permeability. However, relationship between permeability and porosity in carbonate reservoir is quite complicated compared to clastic rock, depending on many factors such as rock matrix, inter-connected vug and un-connected vug. Empirical relationships between permeability and porosity in carbonate reservoir are documented. An example is shown in Figure 3.16, illustrating log-log plot of permeability-porosity relationship [16]. Nevertheless, permeability of carbonate rock can be calculated, using parameters related to grain size as illustrated in equation (3.10). Normally, the value of grain size coefficient and cementation coefficient are related to the average particle diameter (d_{gr}) as shown in Table 3.2. Nevertheless, it is found that this relationship is only valid for matrix part of rock. Induced porosity and permeability

from secondary process are not included. Although, this relationship cannot use to estimate permeability value of high permeability channel effectively, relationship can be used to estimate permeability value in the matrix reasonably.

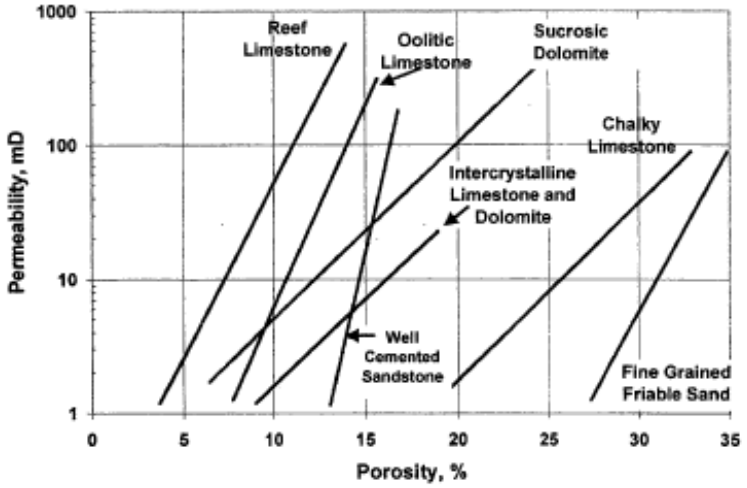

Figure 3.16 Permeability and porosity relationship in various rock types [16]

$$k_{ma} = A_{gr}\phi_{ma}^{A_{mcp}} \tag{3.10}$$

where k_{ma} = matrix permeability,

A_{gr} = grain size coefficient,

ϕ_{ma} = matrix porosity,

A_{mcp} = cementation-compaction coeffieient.

Table 3.2 Value of grain size coefficient and cementation coefficient [16]

Range of d_{gr} (μm)	A_{gr}	A_{mcp}
d_{gr}< 20	1.50×10^{3}	4.18
20 <d_{gr}< 200	2.60×10^{5}	5.68
d_{gr}> 20	8.25×10^{8}	8.18

CHAPTER 4
RESERVOIR SIMULATION MODEL

The reservoir simulation called STAR® commercialized by Computer Modeling Group Ltd. (CMG) is chosen as a tool to studying the effect of ASP flooding in oil-wet reservoir containing high permeability channel. Details of properties of each component in this study are described in this chapter. The chapter is divided into three main parts which are reservoir physical properties, chemical properties and lastly, details of thesis methodology. All keywords used to construct this model are included in Appendices A and B.

4.1 Reservoir Properties

The reservoir properties are contributed from several specific characters of rock and fluid properties such as basic reservoir physical properties, Pressure-Volume-Temperature (PVT) properties, rock-fluid properties and well & recurrent. The keywords used to construct the reservoir model are summarized in Appendix A.

4.1.1 Reservoir Properties and Initial Conditions

The size of reservoir model is 990 × 990 × 108 ft in x, y and z directions. The model is constructed in Cartesian coordinate to have a rectangular shape with 33 × 33 × 9 grid blocks in x, y and z directions, respectively. The total number of grid blocks is 9,801 grid blocks which is lower than limitation of academic license of CMG program (10,000 grid blocks).

The reservoir physical properties are summarized in Table 4.1. Total volume of this reservoir is 18.8MMbbl. According to 14% of effective porosity in this reservoir, the total effective pore volume of this reservoir model is 2.64 MMbbl. Original Oil In Place (OOIP) is 2.24 MMbbl based on 15% of connate water saturation. The reef limestone is used to represent an oil-wet reservoir in this study with a relationship between porosity and matrix permeability as shown in chapter 3 in Figure 3.16. The location of Water-Oil Contact (WOC) is set at the bottom of reservoir at 3,308 ft, and

datum depth is located at the top of reservoir at the depth of 3,200 ft with an initial pressure of 1,440 psia. This reservoir pressure is referred from relationship between typical hydrostatic pressure values vs. depth as shown in Figure 4.1.

The initial base case is represented by heterogeneous reservoir pattern 01A. The high permeability channel possesses three times of absolute permeability values in x and y directions compared to matrix permeability. The channel has a form of planar layer located at the 5^{th} layer from the top. Top and right side views of the 01A heterogeneous reservoir model are shown in Figure 4.2.

Table 4.1 Basic reservoir physical properties of base case heterogeneous model

Parameters	Values	Unit
Grid number	33 × 33 × 9	blocks
Grid size	30 × 30 × 12	ft
Top of reservoir (datum depth)	3,200	ft
Water-Oil Contact depth	3,308	ft
Effective porosity	0.14	fraction
Horizontal permeability (x,y)	500	mD
Vertical permeability (z)	$0.1 \times k_h$	mD
Permeability of channel	$3 \times k_h$	mD
Connate water saturation	0.15	fraction
Water mole fraction	1.0	fraction
Reference pressure at datum depth	1,440	psia

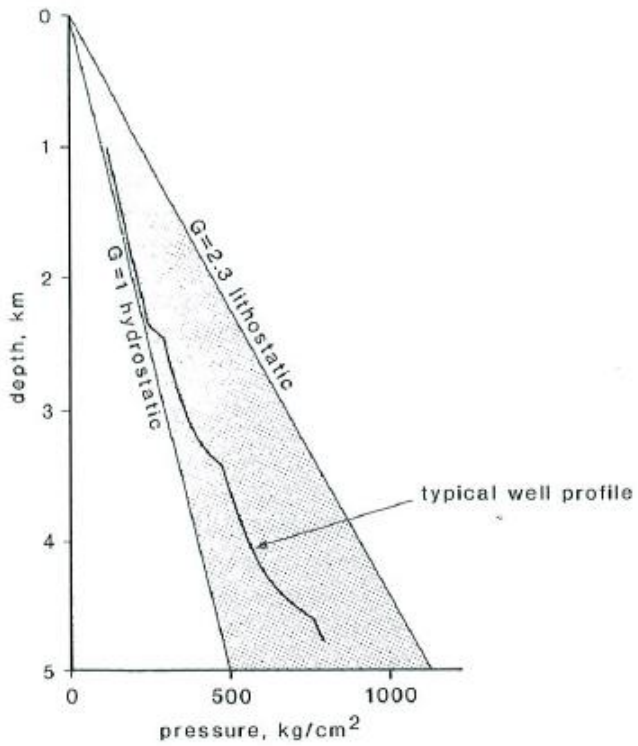

Figure 4.1 Reservoir pressure varying in between hydrostatic and lithostatic gradient as a function of depth [23]

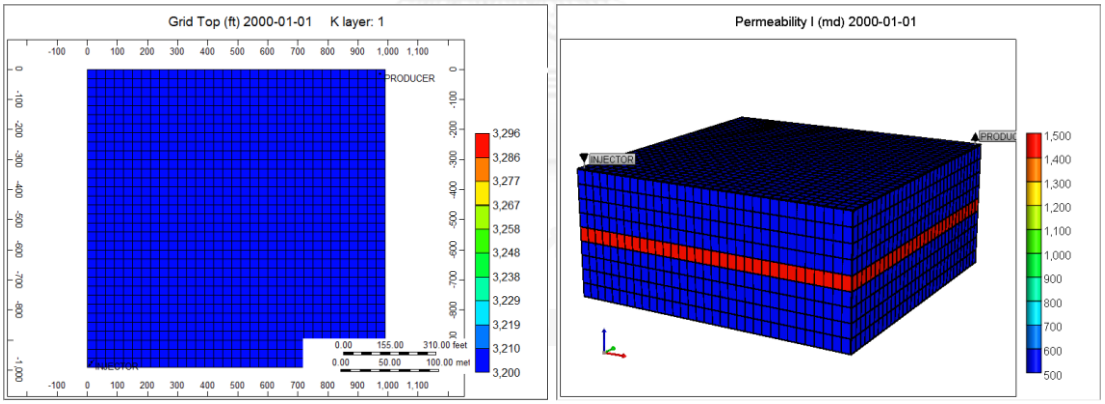

Figure 4.2 Top and right side views of 01A heterogeneous reservoir model

4.1.2 Pressure-Volume-Temperature (PVT) Properties

This PVT section composes of properties of all fluids presented in the reservoir which are solution gas, oil, water and injected chemical. However, properties of chemicals which are alkali, surfactant and polymer in will be illustrated in the chemical section. PVT data of solution gas, oil and water are generated from the correlations which are shown in the Appendix A. Properties of oil and gas which are dry gas formation volume factor (B_g), dry gas viscosity (μ_g), oil formation volume factor (B_o), oil viscosity (μ_o), and gas-oil ratio (R_s) are demonstrated in Figures 4.3 to 4.7, respectively. Essential information used to generate PVT data is shown in Table 4.2. Solution Gas-Oil Ratio (GOR) values are achieved relatively to bubble point pressure by using correlation chart illustrated Figure 4.8.Therefore, bubble point pressure is at 660 psi when GOR is about 78 scf/stb. Reservoir temperature is related to geothermal gradient. A value of 20°C/km geothermal gradient is used in this study. Figure 4.9 illustrates values of geothermal gradients compared to the typical oil field value. Based on this chosen geothermal gradient and reservoir depth, reservoir temperature at datum is at 140°F. Reservoir temperature is very important in this study because it could cause ineffectiveness of process by degradation of chemical. However, the limitation of most chemical flooding is fixed at 200°F to prevent degradation of surfactant and polymer as well as too decrease the rate of alkali depletion. Hence, reservoir temperature of 140°F is suited for the study of ASP.

Table 4.2 Basic properties important for PVT data

Parameters	Values	Unit
Oil gravity	20	°API
Gas gravity	0.7	fraction
GOR	78	scf/stb
Reservoir temperature	140	°F

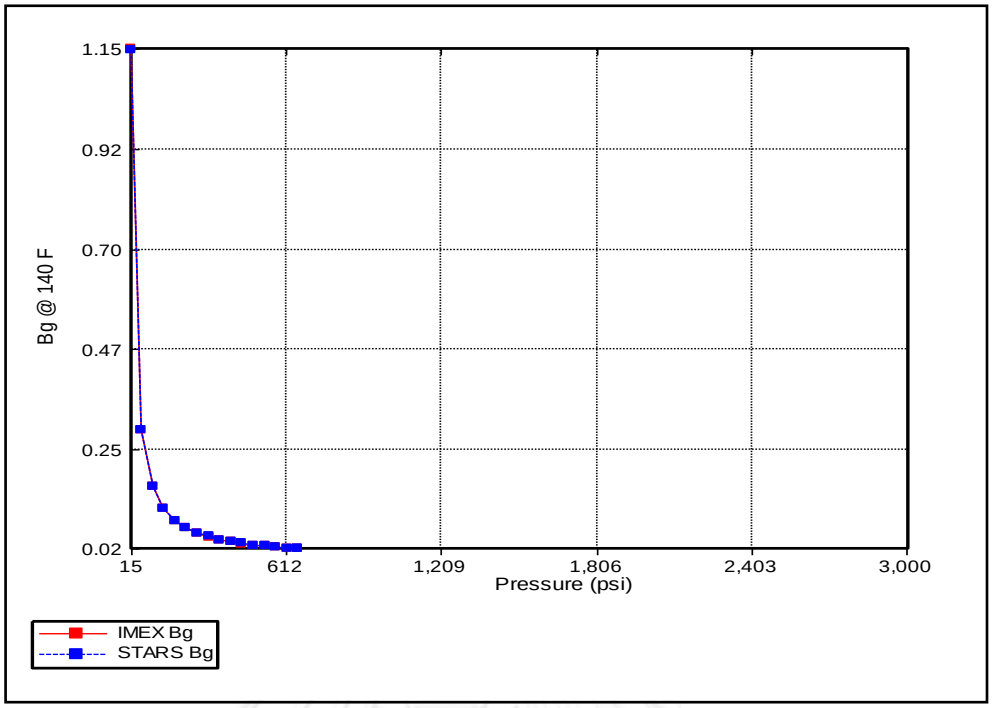

Figure 4.3 Dry gas formation volume factor as a function of pressure

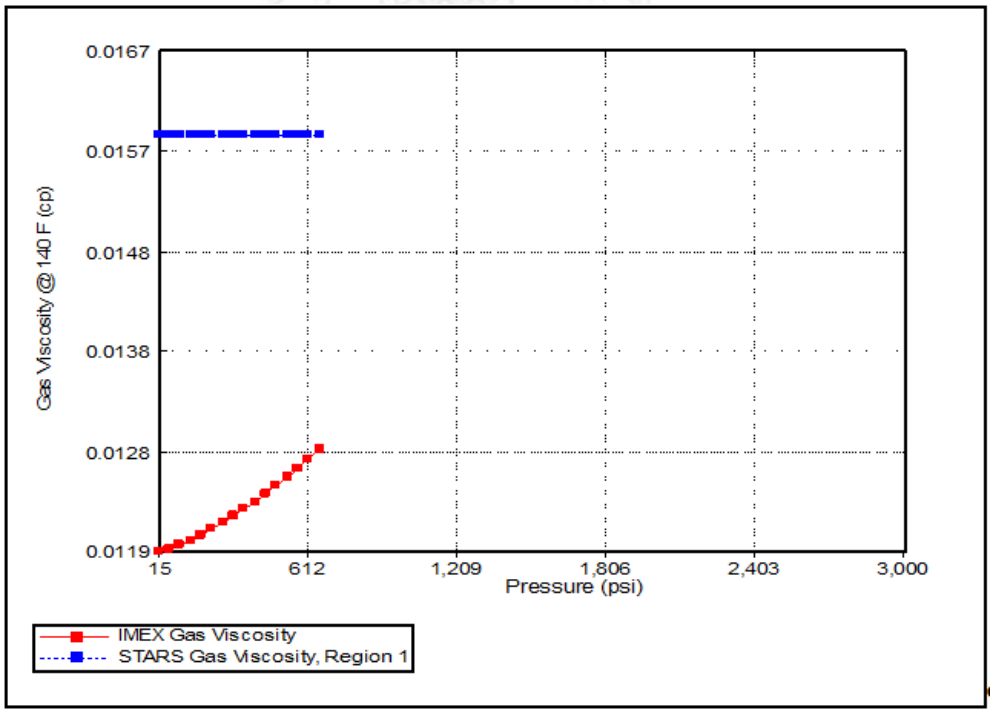

Figure 4.4 Dry gas viscosity as a function of pressure

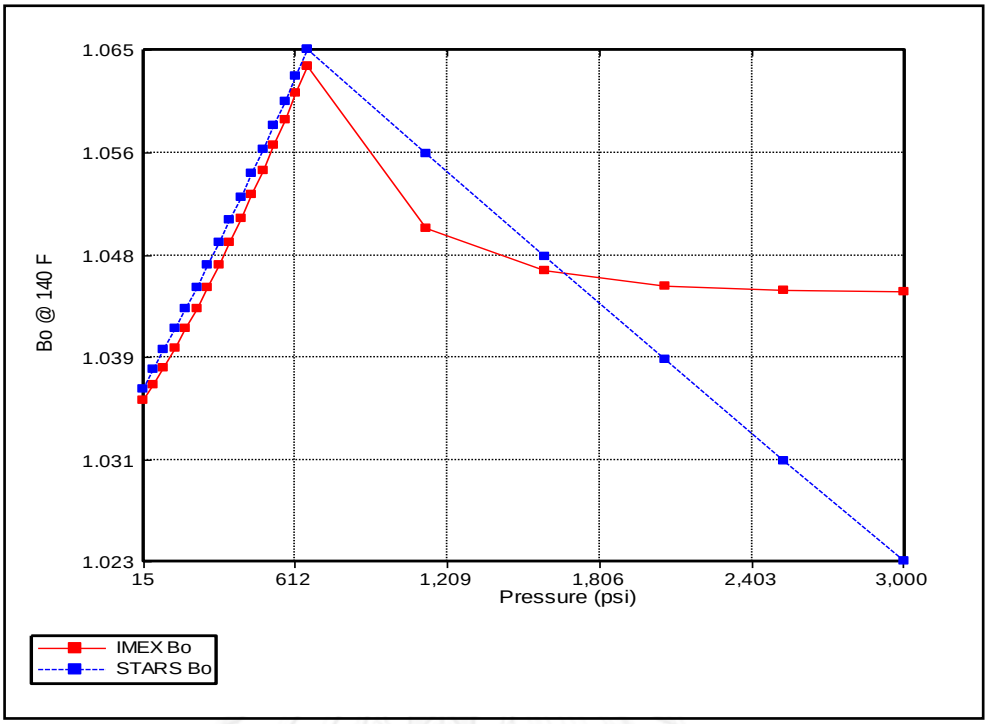

Figure 4.5 Oil formation volume factor as a function of pressure

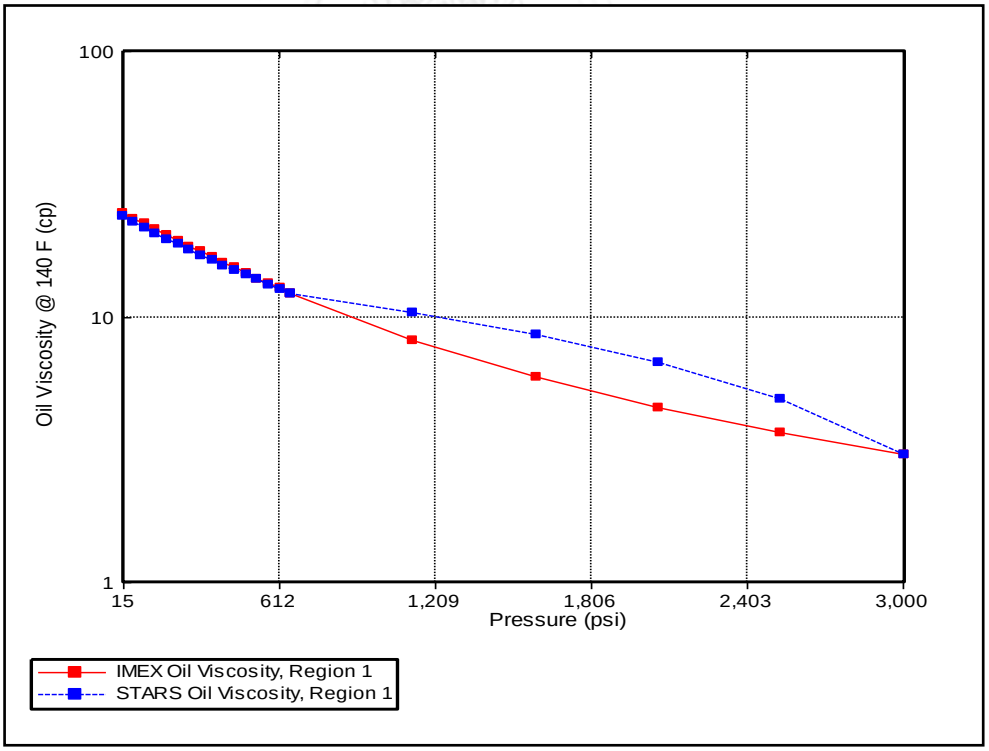

Figure 4.6 Oil viscosity as a function of pressure

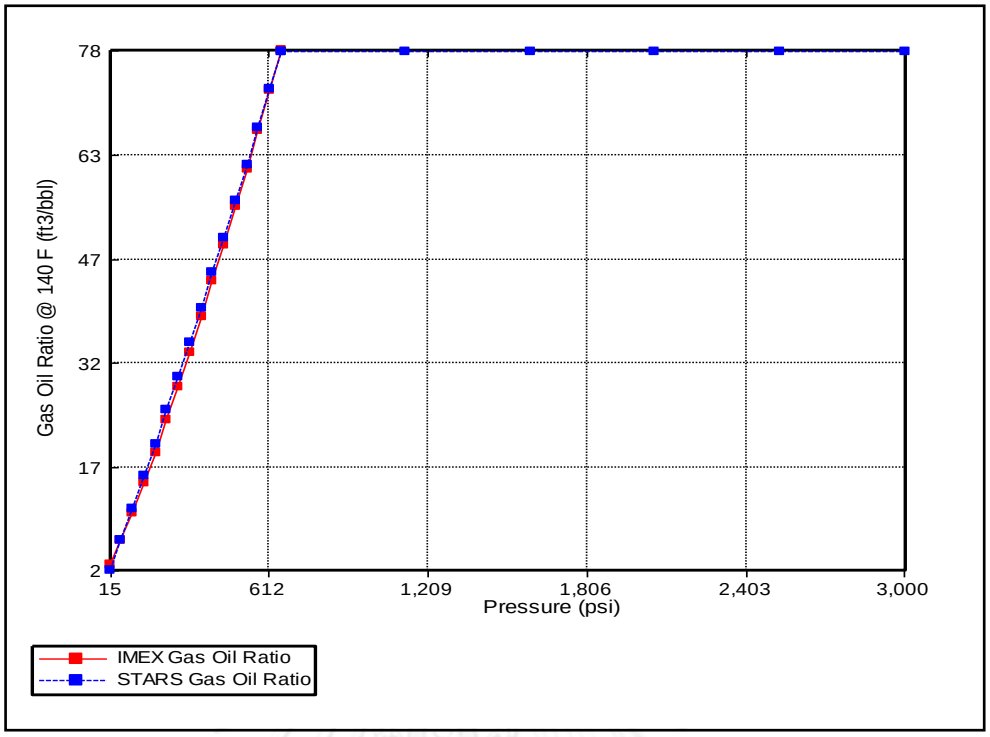

Figure 4.7 Solution gas-oil ratio as a function of pressure

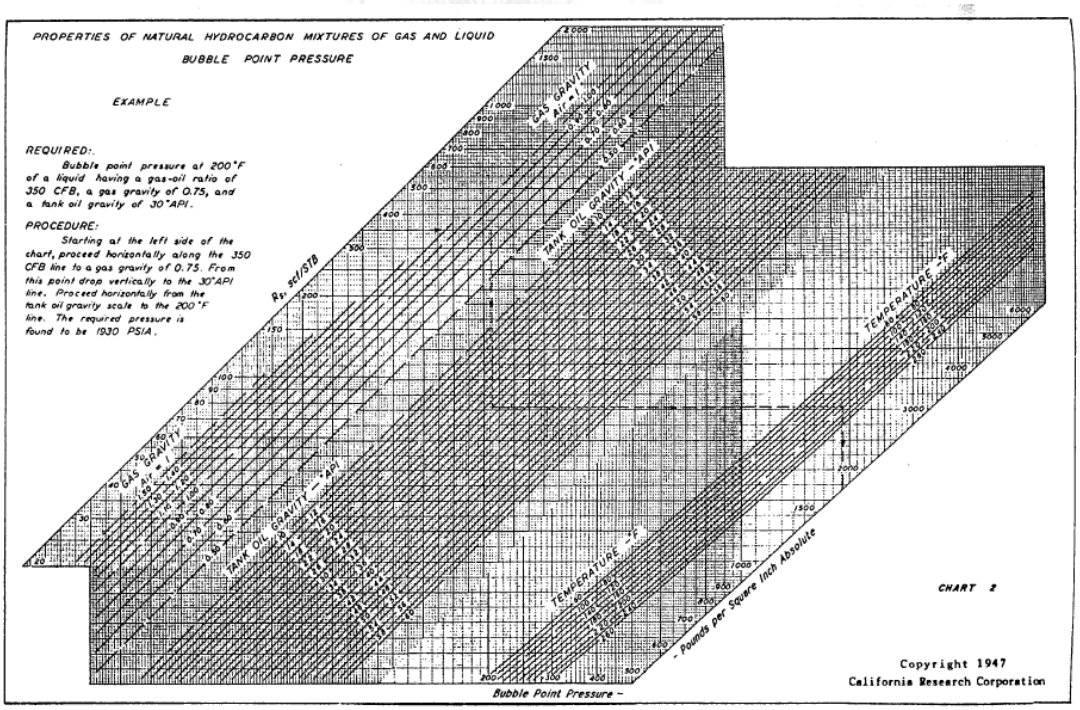

Figure 4.8 Relationship between bubble point pressure and solution gas-oil ratio [24]

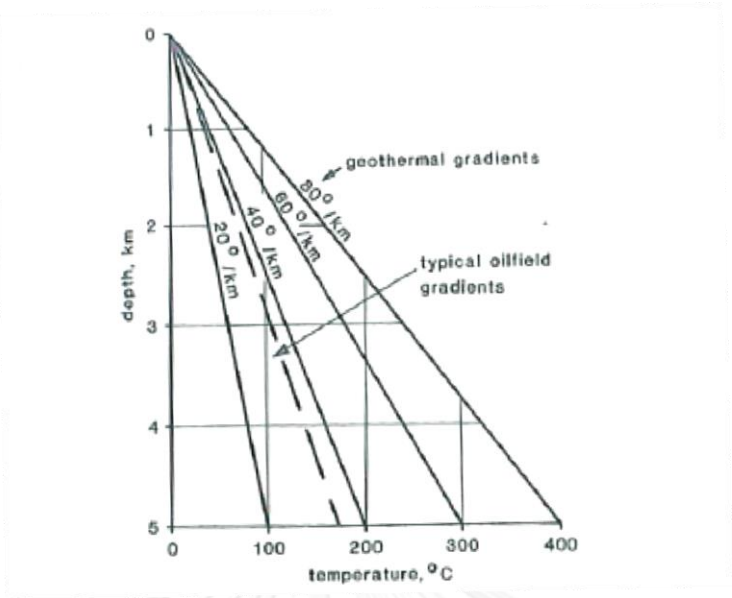

Figure 4.9 Several geothermal gradients compared to typical oil field value as a function of depth [23]

4.1.3 Rock-Fluid properties

For rock-fluid properties, it is usually emphasized on relative permeability curves and adsorption function of each component onto rock surface. This section also describes wettability of rock that is related to relative permeability, of which oil-wet condition is considered in this study. The rule of thumb is a quick look to determine wettability of rock as shown in Table 3.1. Moderately oil-wet reservoir is constructed as initial wettability condition by specifying relative permeability curves shown in Figures 4.10 and 4.11. Relative permeability curves are generated from the Corey's correlation and aligned with oil-wet condition validation in STAR program. Important parameters required to construct relative permeability curves are illustrated in Table 4.3. The output tables which are calculated from Corey's correlation are demonstrated in the Appendix A. Besides, connate water saturation, cross over saturation and relative permeability to water at residual oil saturation are in concordance with the rule of thumb for oil-wet surface. The water-oil capillary pressure is fixed at the maximum value of -2 in the reservoir model as shown in Figure 4.12.

Alteration of relative permeability by reduction of IFT by means of alkali and surfactant in this study is illustrated in the chemical section.

Table 4.3 Parameters required construct relative permeability curve for base case model

Parameters	Values	Unit
Connate water saturation (SWCON)	0.15	fraction
Critical water saturation (SWCRIT)	0.2	fraction
Irreducible oil saturation for Water-Oil table (SOIRW)	0.4	fraction
Residual oil saturation for Water-Oil table (SORW)	0.4	fraction
Irreducible oil saturation for Gas-Liquid table(SOIRG)	0.25	fraction
Residual oil saturation for Gas-Liquid table (SORG)	0.3	fraction
Connate gas saturation (SGCON)	0	fraction
Critical gas saturation (SGCRIT)	0.15	fraction
Relative permeability to oil at connate water saturation (KROCW)	0.6	fraction
Relative permeability to water at irreducible oil saturation (KRWIRO)	0.3	fraction
Relative permeability to gas at connate liquid saturation (KRGCL)	0.6	fraction
Relative permeability to oil at connate gas saturation (KROGCG)	0.3	fraction
Exponent of k_{rw} from KRWIRO	2	
Exponent of k_{row} from KROCW	2	
Exponent of k_{rg} from KROGCG	2	
Exponent of k_{rg} from KRGCL	2	

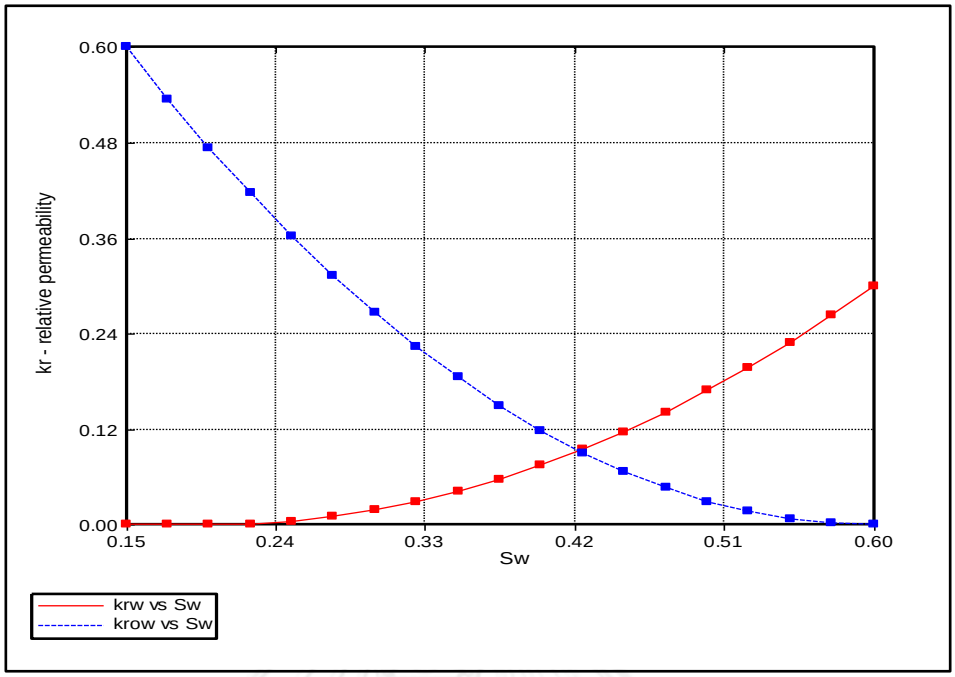

Figure 4.10 Relative permeability curves of oil and water system as a function of water saturation

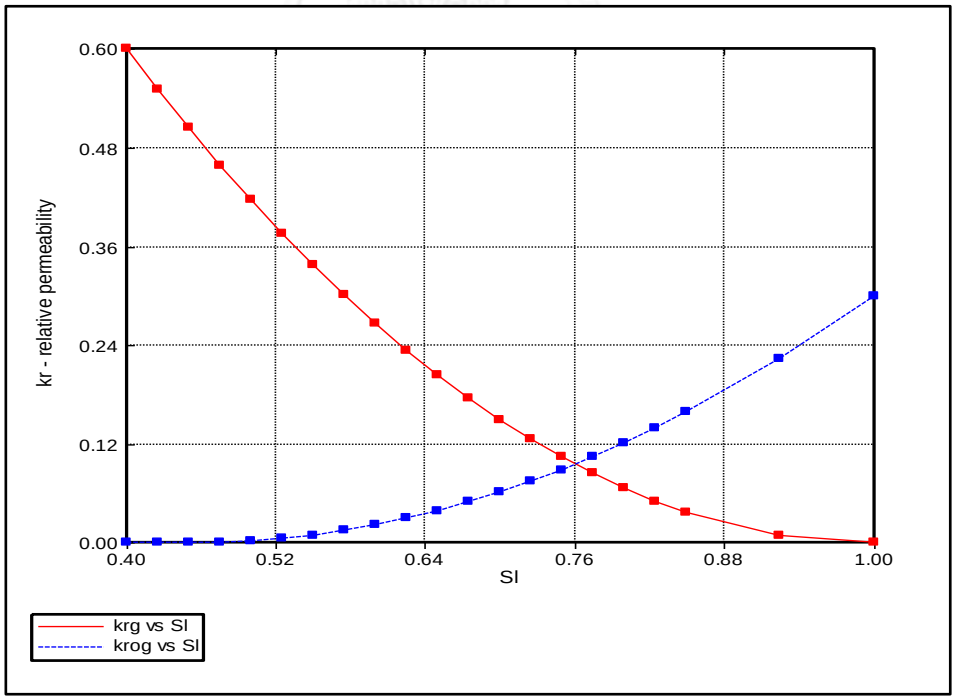

Figure 4.11 Relative permeability curves of liquid and gas system as a function of liquid saturation

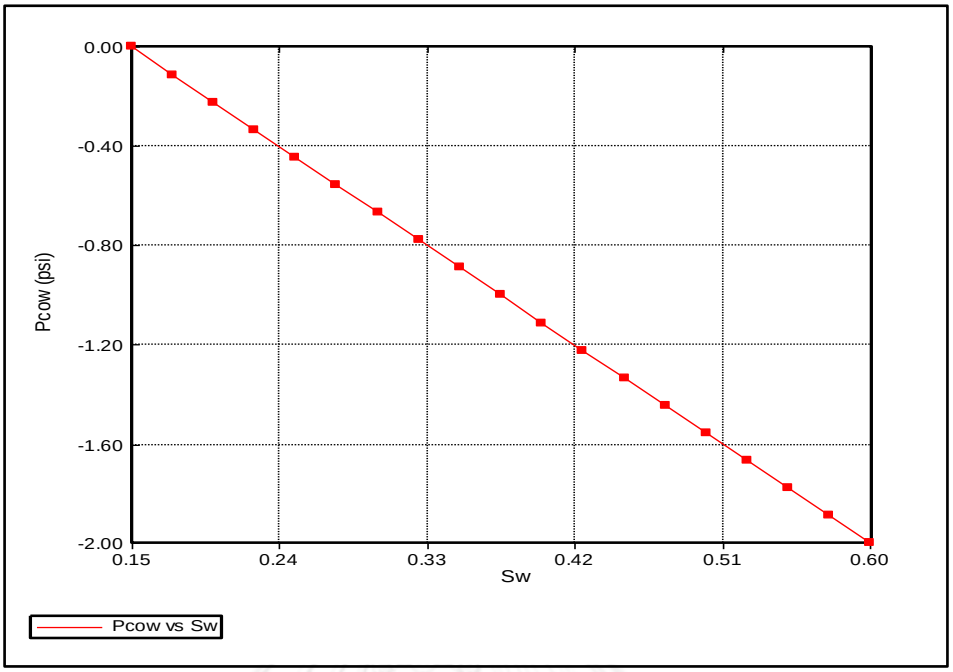

Figure 4.12 Capillary pressure as a function of water saturation

4.1.4 Well and Recurrent

Injection and production wells are placed at the opposite corners of reservoir model as shown in Figure 4.2. Wellbore radius of both wells is 0.51 ft. Skin around wellbore is assumed to be zero for this study. Perforation of both wells is performed through all layers where wells are placed. Constraints and economic limits of injector and producer are summarized in Tables 4.4 and 4.5, respectively. Maximum bottomhole pressure of injector well is fixed below fracture pressure of matrix which is calculated from the fracture gradient equations in order to avoid undesired leakage of injectant. Injected fluid is determined by mole fraction from operation process such as waterflooding and ASP flooding. Total production period is set maximum at 30 years. Termination of production could be reached if one of constrains is approached.

Table 4.4 Constraints of injection well

Parameters	Values	Unit
Maximum bottomhole pressure (BHP)	2,000	psi
Surface injection rate (STW)	1,000	bbl/day

Table 4.5 Constraints and economic limits for producer well

Parameters	Values	Unit
Minimum bottomhole pressure (BHP)	200	psi
Surface production rate (STW)	500	bbl/day
Water-cut (WCUT)	0.95	fraction
Minimum surface oil rate (STO)	50	bbl/day

4.2 Chemical Properties

Chemical properties compose of IFT as a function of concentration, adsorption, viscosity and also properties of alkali, surfactant and polymer. Keywords to construct the reservoir model are summarized in Appendix B.

4.2.1 Alkali and Surfactant Processes

To set up the alkali and surfactant (AS) flooding in simulator, the process wizard is chosen to specify important parameters for AS flooding. Due to a great reduction of IFT by means of Sodium Carbonate (Na_2CO_3) compared to Sodium Hydroxide (NaOH), Sodium Carbonate (Na_2CO_3) is chosen as the alkaline agent in this study. Anionic surfactant which is Sodium Dodecylbenzenesulfonate is chosen as surfactant agent in this study. Necessary parameters to identify AS model are listed in Table 4.6.

Table 4.6 Necessary parameters required for alkali and surfactant flooding model

Parameters	Values	Unit
Number of relative permeability sets for interpolation	3	Sets
Use adsorption for alkaline	No	
Use adsorption for surfactant	Yes	
Make surfactant adsorption dependent on alkaline weight	Yes	
Number of alkaline weight % value	3	Sets
Number of surfactant weight % value	2	Sets
Interfacial tension is also dependent on surfactant weight %	Yes	

Main mechanism of AS flooding is to decrease IFT value to a state called ultra-low condition. At this condition, residual oil saturation is reduced to almost zero. IFT reduction function is divided into IFT reduction by means of solely alkaline and IFT reduction by means of solely surfactant and IFT reduction of a combination of alkali and surfactant. Liu et al. [17] conducted experiments using Sodium Carbonate (Na_2CO_3) and surfactant S4 to observe reduction of IFT value with time as illustrated in Figures 4.13 to 4.15. The solely surfactant has more ability to decreasing IFT more than solely alkaline. The ultra-low IFT condition occurs when alkali and surfactant are mixed together. These data are used as a guideline for the input IFT value in three conditions [17].

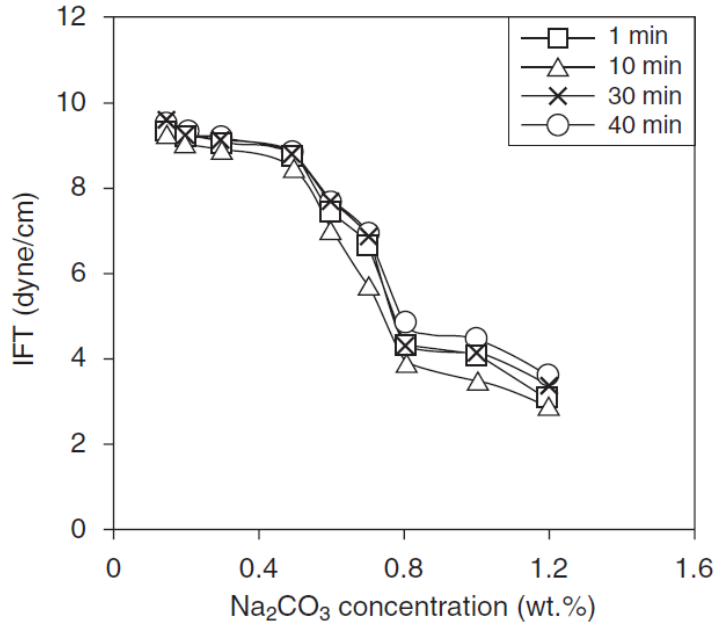

Figure 4.13 IFT values as a function of Sodium Carbonate (Na2CO3) concentration at different measure times [25]

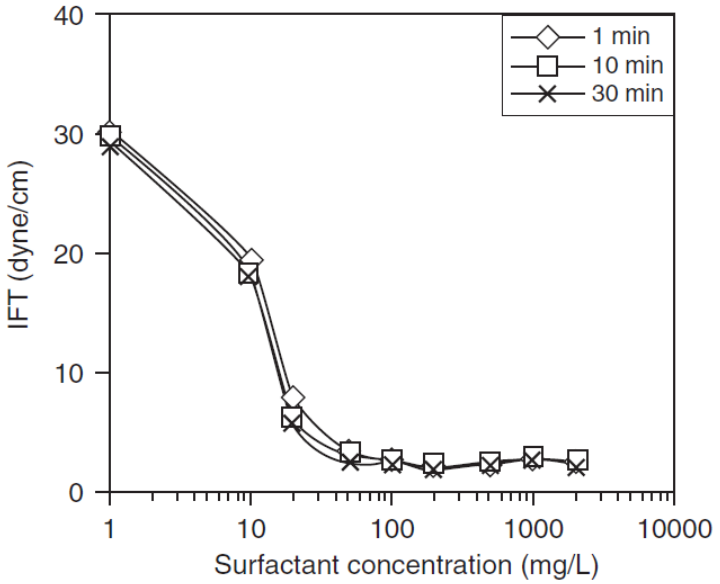

Figure 4.14 IFT values as a function of surfactant concentration at different measure times [25]

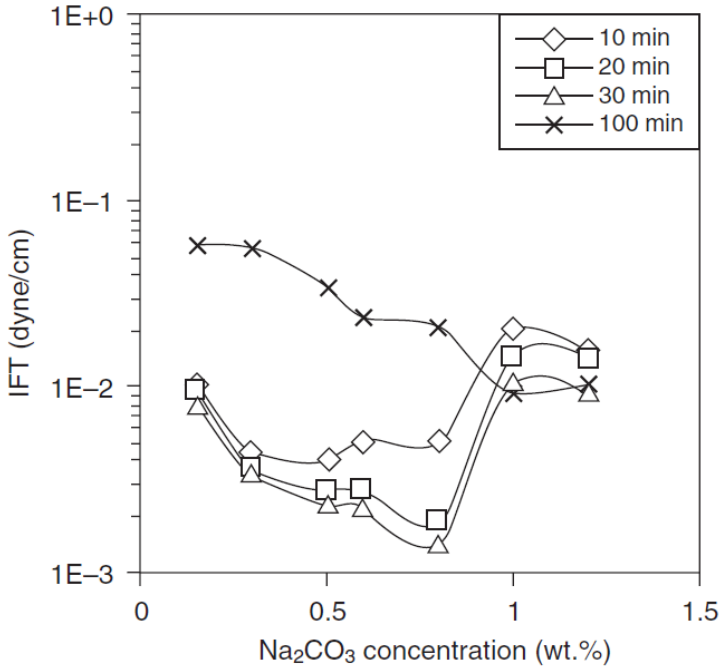

Figure 4.15 IFT values as a function of Sodium Carbonate (Na2CO3) concentration with a presence of 50 mg/L surfactant at different measure times [25]

Adsorption of alkali and surfactant is one of important parameters controlling effectiveness of the whole process. Adsorption value is divided into two types; adsorption of surfactant with and without the presence of alkali. Based on the experiment of caustic consumption in calcium sulfate, result showed the alkaline is significantly less consumed compared to surfactant [25]. Therefore, adsorption of alkali is set as "No" as shown in Table 4.6. Liu et al. [17] conducted a static adsorption of anionic surfactant in a presence and absence of Sodium Carbonate (Na_2CO_3) onto dolomitic porous media and results are demonstrated in Figure 4.16. Adsorption of solely surfactant onto dolomitic porous media is approximately 0.87 mg/m^2. When 0.05% w/w alkaline substance is presented, adsorption of surfactant is greatly decreased to 0.1 mg/m^2. Therefore, presence of alkali can decrease adsorption of surfactant on rock surface which could be explained by increasing of surface charge above p.z.c. of carbonate rock.

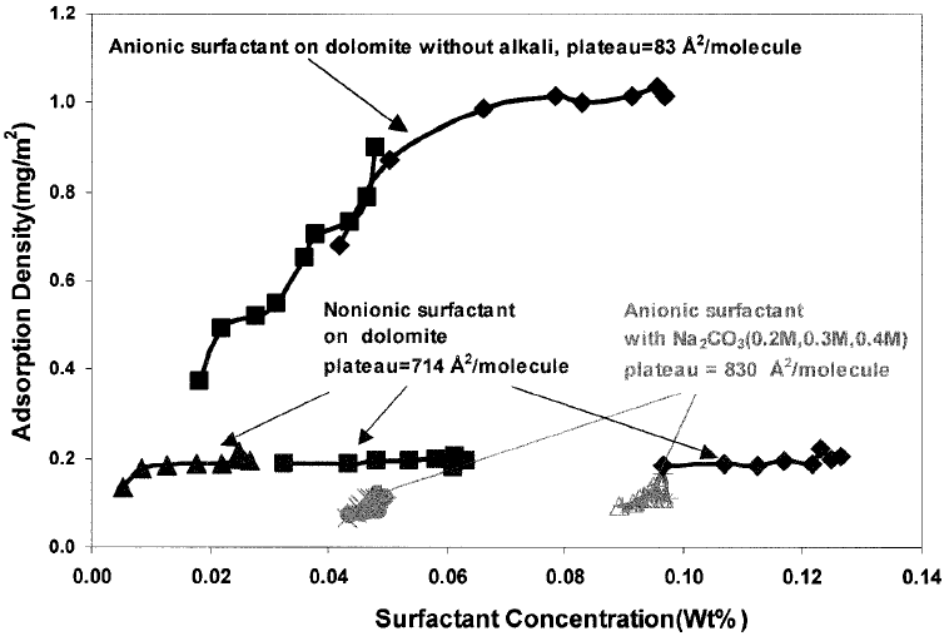

Figure 4.16 Static adsorption of surfactant onto dolomitic porous media [17]

From all input data of alkali and surfactant, additional two sets of relative permeability curves and capillary pressure are generated by means of interpolation and consecutively labeled as set2 and set3. Relative permeability curves and capillary pressure of interpolation set2 and set3 are illustrated in Figures 4.17 to 4.20, respectively. Interpolation set is functioned by capillary number which is principally controlled by changing of IFT when surfactant appears in the system. In other words, two-phase flow ability will switch from one to another based on changing capillary number or concentration of surfactant. These capillary numbers related to interpolation set are summarized in Table 4.7. According to the change of relative permeability curves, residual oil is liberated when capillary number is raised to 10^{-5} (relative permeability curves set2 is used). Eventually, ultra-low IFT condition (set3 relative permeability curves) occurs when capillary number is increased to 10^{-4}. The capillary pressure at the end point of residual oil saturation is increased from -2, -1 and 0 when the interpolation set is altered from set1 to set3.

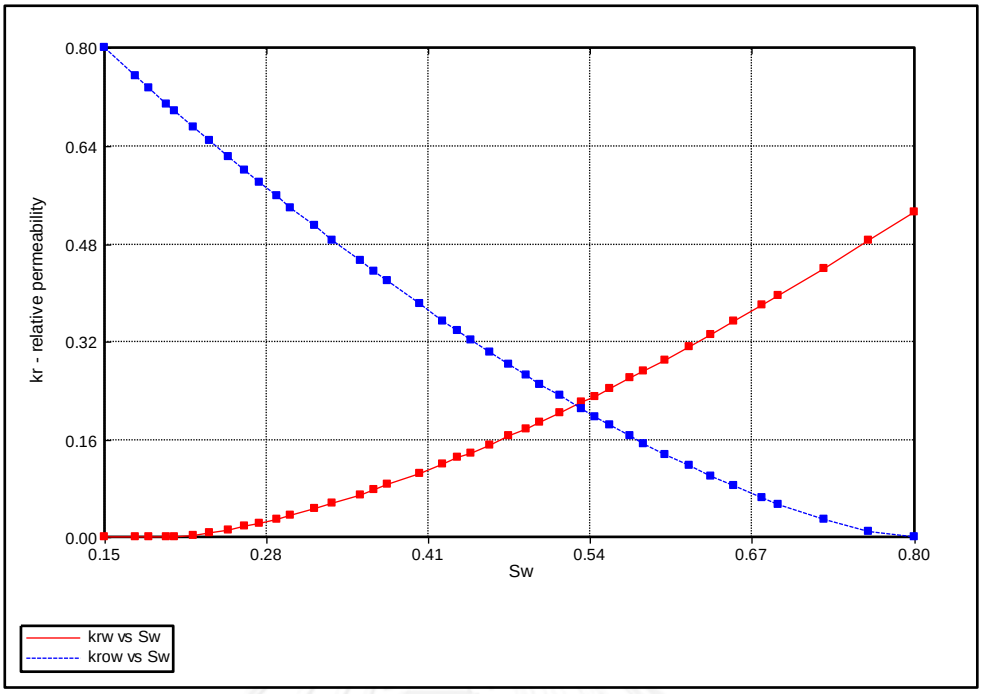

Figure 4.17 Relative permeability curves of oil and water system of interpolation set2 as a function of water saturation

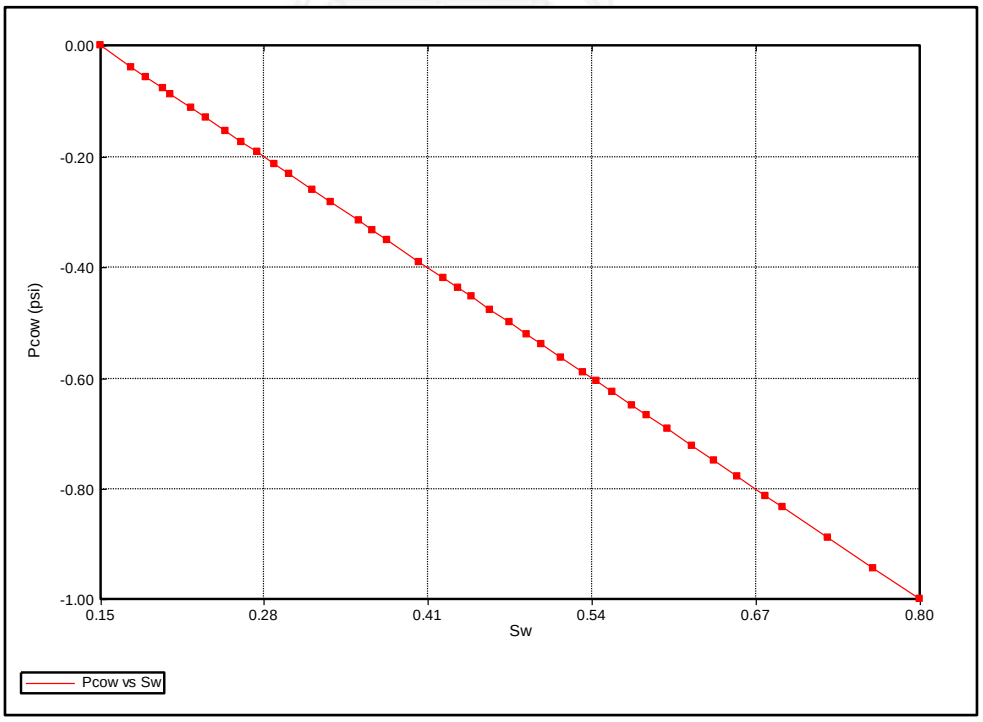

Figure 4.18 Capillary pressure of interpolation set2 as a function of water saturation

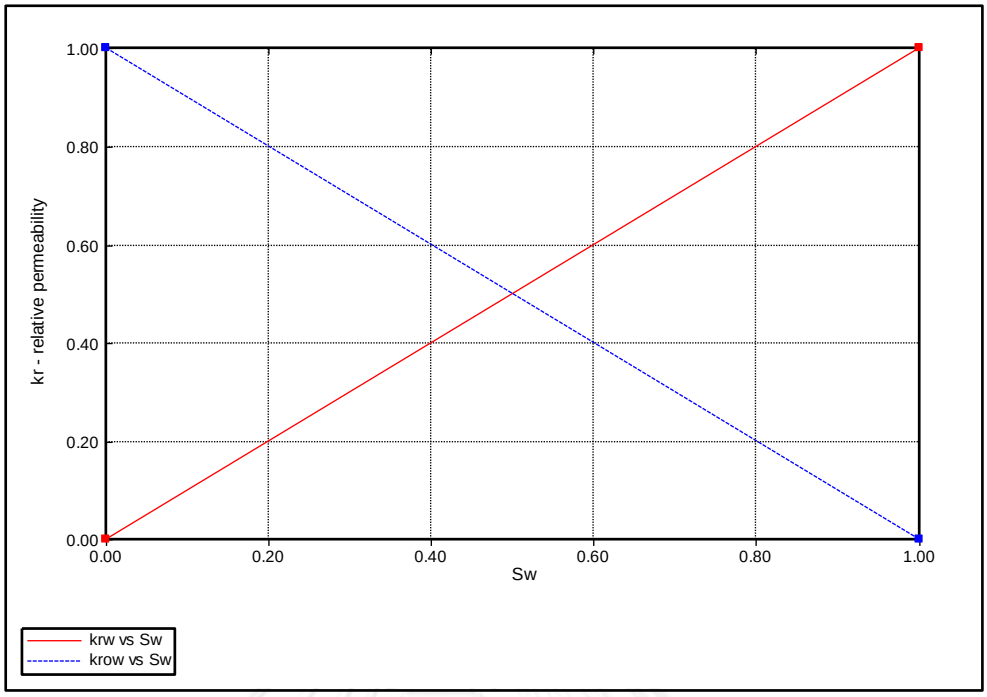

Figure 4.19 Relative permeability curves of oil and water system of interpolation set3 as a function of water saturation

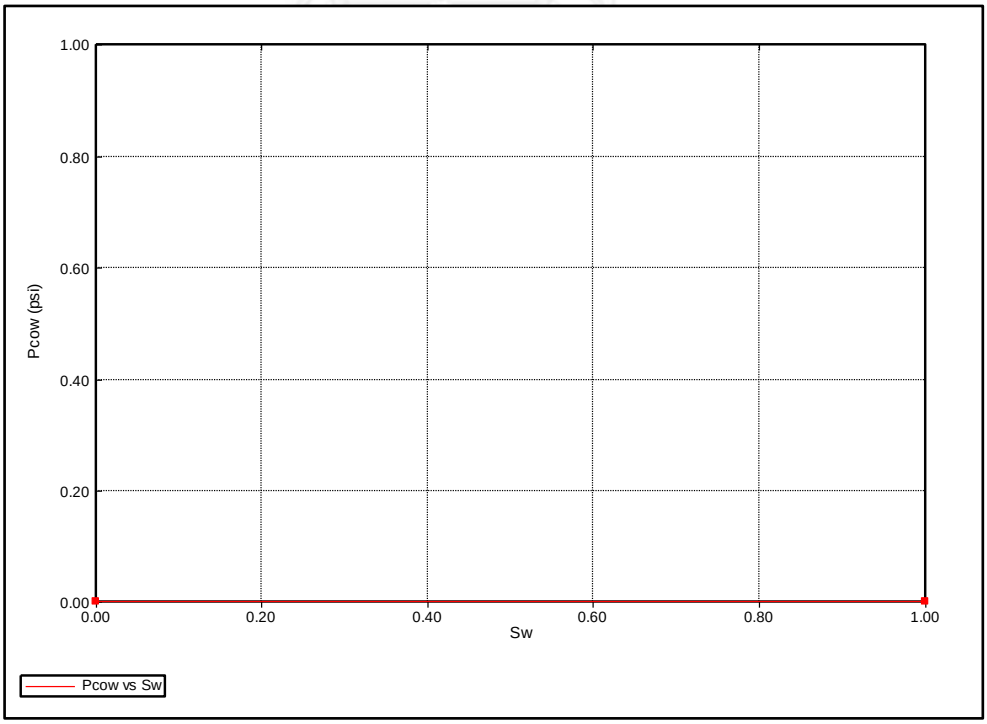

Figure 4.20 Capillary pressure of interpolation set3 as a function of water saturation

Table 4.7 Log Capillary number for interpolation set

Interpolation set	Phase	Values
set 1	Wetting phase	-7<n<-5
	Non-Wetting phase	-7<n<-5
set 2	Wetting phase	-5<n<-4
	Non-Wetting phase	-5<n<-4
set 3	Wetting phase	n>-4
	Non-Wetting phase	n>-4

In the pilot test fields in China, amount of alkali and surfactant used are summarized in Figures 4.21 and 4.22, respectively, and locations of each field are summarized in Table 4.8. Concentration of alkali and surfactant used in this study is therefore based on the average concentration of pilot test fields. Concentrations of alkali and surfactant in this study are shown in Table 4.9.

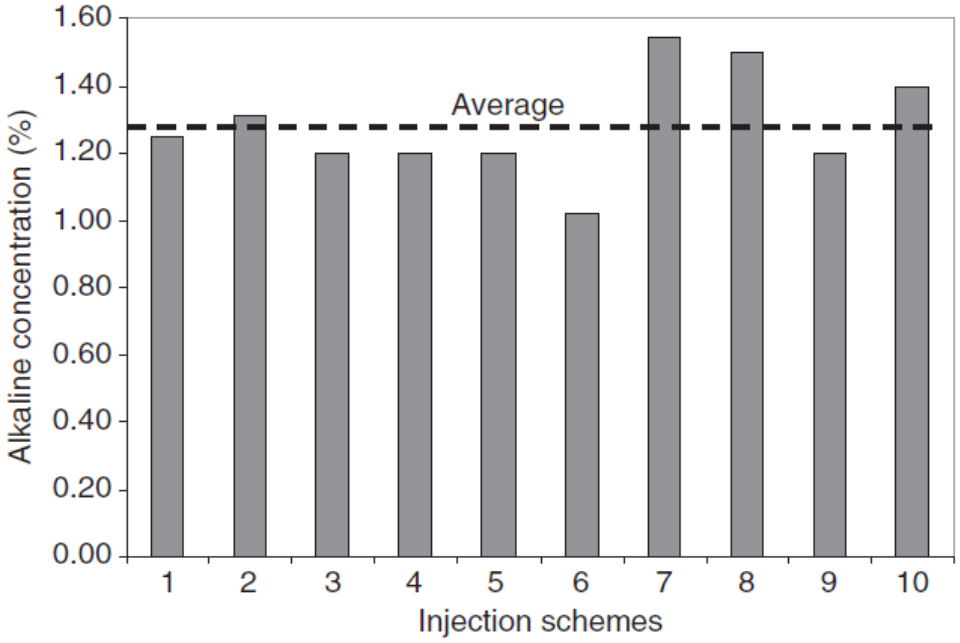

Figure 4.21 Alkali concentrations used in pilot test fields in China [25]

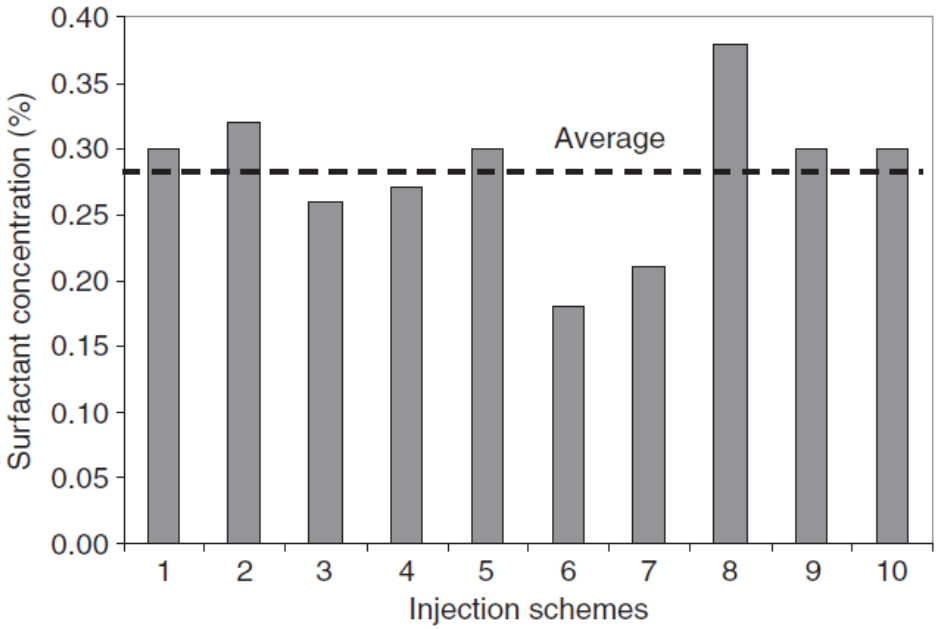

Figure 4.22 Surfactant concentrations used in pilot test fields in China [25]

Table 4.8 Location of pilot test field in China [25]

Location	Field name
1	Sa-Zhong-Xi, Daqing
2	Xing-5, Daqing
3	Xing-2-Xi, Daqing
4	Bei-1-Xi, Daqing
5	Bei-2-Dong, Daqing
6	Xing-2-Zhong, Daqing
7	Bei-2-Dong, Daqing
8	Gudong, Shengli
9	Gudao, Shengli
10	Er-Zhong-Bei, Karamy

Table 4.9 Concentration of alkali and surfactant used in this study

Chemical	% weight
Alkali	1.3
Surfactant	0.28

4.2.2 Polymer Process

In order to set up polymer flooding in the simulator, process wizard is chosen to specify important parameters for polymer flooding. The synthetic polymer is chosen as polymer model in this study. Mechanisms of polymer are expressed in reservoir model by improving the mobility ratio, stabilizing travelling flood front and increasing displacement efficiency. Propagation of injected fluid is affected by increasing viscosity and decreasing effective permeability. The necessary parameters to identify polymer model are listed in Table 4.10.

Resistance factor is defined as a pressure drop from a presence of polymer compared to conventional waterflooding. Resistance factor controls reduction of permeability by means of polymer adsorption onto the rock surface [25]. However, precise resistance factor has to be measured in the laboratory to match specific values of permeability, porosity and salinity. Resistance factor value is commonly less than 10, but it can be higher than 10 in case of low permeability formations. In this study, the resistance factor is initially fixed at 5 as a default resistance factor of polymer.

Table 4.10 Important parameters of polymer flooding

Parameters	Values	Unit
Polymer resistance factor	5	
Accessible pore volume for polymer adsorption	0.8	PV
Rock type for conversion of adsorption values	Limestone (2.71)	PV/gm

Polymer degradation is assumed to omit the half-life of polymer due to stability of synthetic polymer. Polymer adsorption is the most important parameter to settle the phenomena from polymer, depending on lithology of formation. Szabo recorded adsorption data of polymer experimented with a variation of surface materials and these data are summarized in Table 4.11 [25]. This experiment reveals static bulk adsorption of 0.06% concentration synthetic polymer on carbonate material that is 100 µg/g of carbonate. Consecutively these data are used as input of adsorption data in the simulator.

Table 4.11 Adsorption data of synthetic polymer on several of surface material [25]

Rock	Adsorption type	Adsorption value	Unit
Silica flour	Static bulk adsorption	55	µg/g
Sand pack	Dynamic flow test	3.3	µg/g
Carbonate	Static bulk adsorption	100	µg/g

Viscosity of mixing synthetic polymer in water is set based on default values of STAR as shown in Table 4.12. The non-linear viscosity of polymer solution is calculated from the initial input data in the simulator. Concentration of polymer in part per million (ppm) is converted at injection well to a unit of mole fraction [25].

Table 4.12 Viscosity of polymer solution at different concentration

Weight % of polymer in water	Viscosity	Unit
0 %	0.507059	cP
0.03 %	3.5	cP
0.05 %	5.2	cP
0.075%	10.8	cP

4.3 Thesis Methodology

The details of thesis methodology are described in this section as following;

Step 1. Construct base case reservoir model with high permeability channel at the middle layer along the x-y plane (model 01A). Perform waterflooding to obtain reference oil recovery factor from this model.

Step 2. Perform single-slug polymer flooding on the model 01A to optimize important parameters for three chosen polymer concentrations including 300, 500 and 700 ppm. As polymer flooding might lower injectivity of injection well, optimization of polymer slug is therefore performed before alkali and surfactant slug. The chosen parameters are as followed: (bold value represents the base value of each parameter)

- pre-flushed water slug size; 0.10, 0.15, 0.20, 0.25, 0.30, 0.35 and 0.40 PV,
- slug size of polymer; start from 0.10 PV until the end of polymer injection,
- resistance factor (*R*); 1.0, 2.5, **5.0**, 7.5, 10, 12.5 and 15.0,
- confirmation test; 300 ppm *R*=1.0, 500 ppm *R*=1.0 and 300 ppm *R*=12.5.

Step 3. Perform double-slug polymer flooding by using the slug size of post-flushed polymer obtained in Step 2. The slug size of pre-flushed polymer and alkali-surfactant are considered. At the end of this step, operational parameters of pre-flushed polymer slug followed by alkali-surfactant slug and chased by polymer slug (P+AS+P) are determined, and the alkali-surfactant slug and chased by polymer slug (AS+P) are selected at the same total volume of P+AS+P. The chosen parameters are as followed: (bold value represents the base value of each parameter)

- slug size of pre-flushed polymer; start from 0.05 to 1.0 PV of polymer injection,
- slug size of alkaline-surfactant; 0.10, **0.15**, 0.20 and 0.25 PV.

Step 4. Construct total of 23 models of different heterogeneous models having different directions and planes of high permeability channels as summarized in Figure 4.23. All models are fixed to have equal formation volume of high permeability channel. Perform waterflooding for every case to obtain reference oil recovery factors. Heterogeneity models can be categorized in groups as:

- single-layered high permeability channel (Cases A)
- parallel y-axis of high permeability channel (Cases B)
- parallel x-axis of high permeability channel (Cases C)
- high permeability channel across flow direction (Cases D)
- high permeability channel along flow direction (Cases E)
- double high permeability channels along flow direction (Cases F)

Step 5. Perform AS+P and P+AS+P flooding in heterogeneous models using obtained operational parameters from Step 3. Both P+AS+P and AS+P are performed to observe difference oil recovery results of cases with presence and absence of pre-flushed polymer slug in reservoir containing high permeability channel in different planes and directions.

Step 6. Compare additional oil recovery from every model and choose only two heterogeneous models that yield maximum incremental oil recovery by (one for P+AS+P and one for AS+P) comparing results to those obtained from solely waterflooding to perform sensitivity analysis. The chosen parameters for sensitivity analysis are as followed: (bold value represents the base value of each parameter)

- Corey's exponent of rock at normal condition; 1.0, 1.5, **2.0** and 2.5,
- Corey's exponent of rock at ultra-low IFT condition; **1.0**, 1.5 and 2.0,
- wettability of rock; mildly oil-wet, **moderately oil-wet**, strongly oil-wet and very strongly oil-wet,
- permeability contrast between channel and matrix; **3 times**, 5 times and 10 times,

- ratio of vertical to horizontal permeability; 0.05, **0.10**, 0.20 and 0.25,
- porosity in high permeability channel; **0.14**, 0.17, 0.20 and 0.23.

Step 7. Compare and discuss results from simulation outcomes for each studied parameter.

Step 8. Summarize and indicate the parameters that have impact on effectiveness of AS+P and P+AS+P flooding in oil-wet reservoir containing high permeability channel.

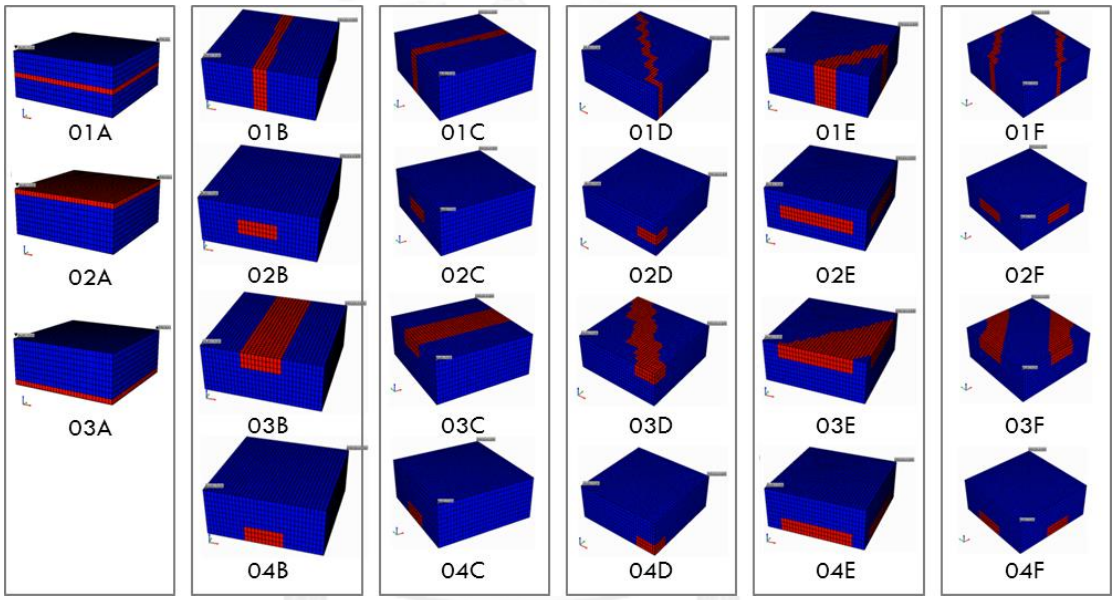

Figure 4.23 Summary of heterogeneous models

CHAPTER 5
SIMULATION RESULT AND DISCUSSION

In this study, evaluation of alkali-surfactant slug, chased by polymer slug (AS+P) and pre-flushed polymer followed by alkali-surfactant slug and chased by polymer slug (P+AS+P) are performed on heterogeneous reservoir model 01A in which waterflooding is previously performed. After that, model 01A is replaced by different 23 heterogeneous models to perform waterflooding, AS+P and P+AS+P in order to evaluate the effects of direction and planar system of high permeability channels. At the end, sensitivity analysis is performed in chosen two heterogeneous models that yield the highest additional oil recovery (one for P+AS+P and one for AS+P) compared to waterflooding to identify the most sensitive reservoir properties for AS+P and P+AS+P techniques. In brief, this chapter contains:

5.1 waterflooding base case in heterogeneous model 01A

5.2 single-slug polymer flooding in heterogeneous model 01A

5.3 double-slug polymer flooding in heterogeneous model 01A

5.4 heterogeneous models

5.5 sensitivity analysis

5.1 Waterflooding Base Case in Heterogeneous Model 01A

Waterflooding in reservoir model with high permeability channel at the middle layer along the x-y plane (model 01A) is performed as the base case for comparing with all simulation cases. Waterflooding is started from the first day of simulation until one of production constraints is reached. Figures 5.1 and 5.2 illustrate recovery factor, oil and water production rates during entire production life. From Figure 5.1, recovery factor obtained by means of waterflooding is 33.92% in nine years and seven months. According to Figure 5.2, oil production rate can be maintained for plateau production for approximately a year due to an early water breakthrough travelling through the high permeability channel at the middle layer as shown in Figure 5.3. After nine years of waterflooding, high amount of residual oil cannot be swept by means of conventional waterflooding as shown in Figure 5.4. It is

a result from co-effect of oil-wet surface condition. This oil-wet surface controls relative permeability curves, capillary pressure and together with high permeability channel, an extreme water channeling is favored. Therefore, a sharp interface of water bank is not occurred in this reservoir. Figure 5.5(a) demonstrates gradual flood front in top layer, whereas the high permeability layer is well swept compared to other layers in Figure 5.5(b). Result from conventional waterflooding is used as the base result to compare with other simulation cases.

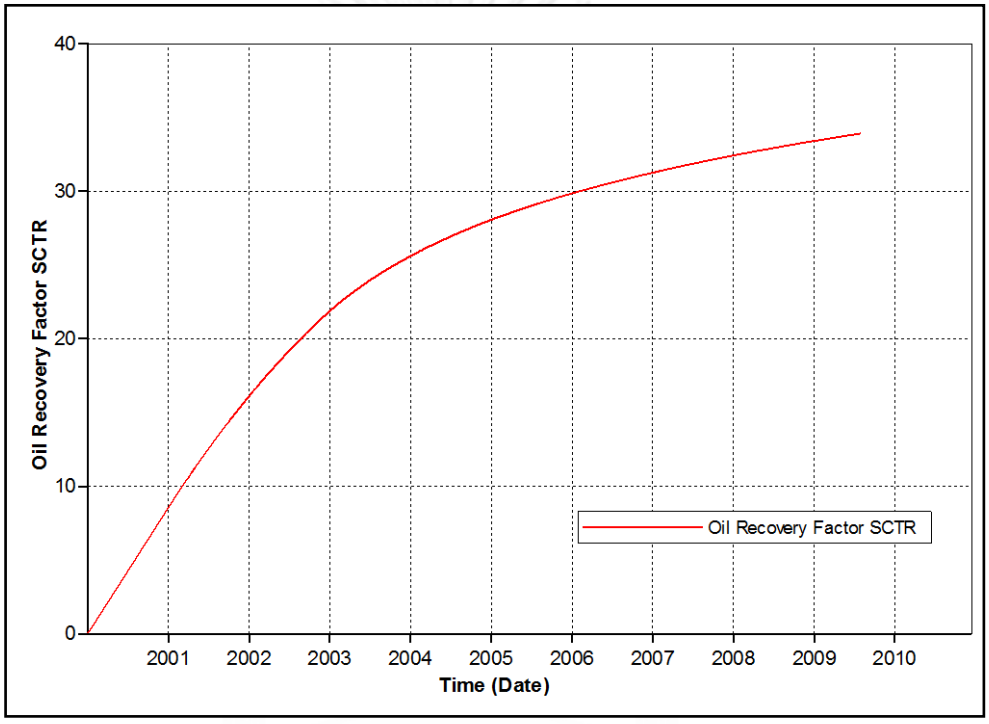

Figure 5.1 Recovery factor of waterflooding base case as a function of time

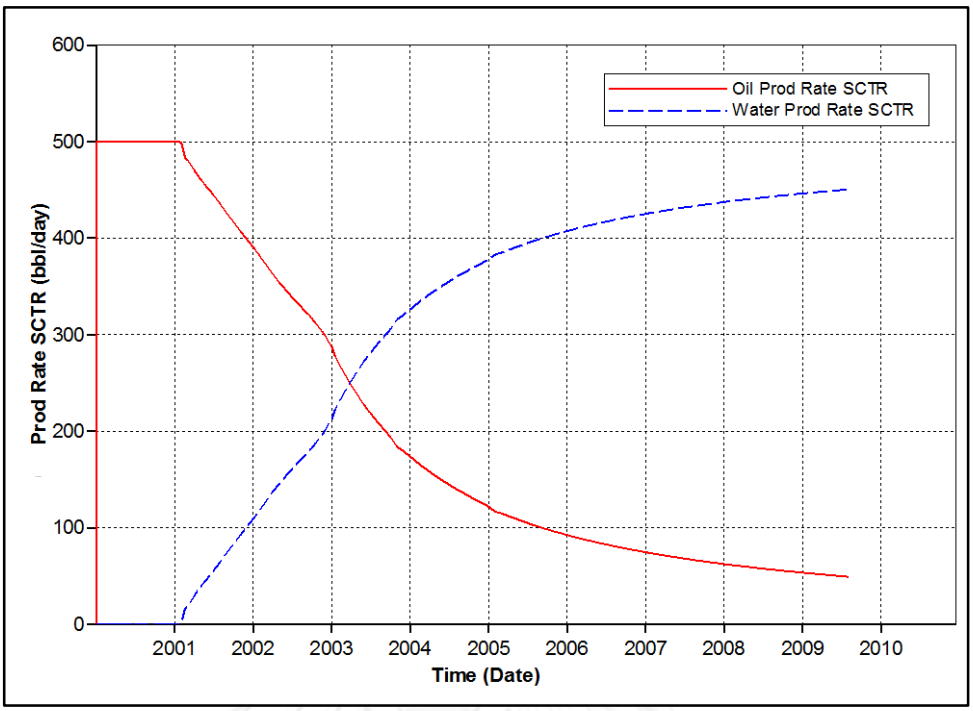

Figure 5.2 Oil and water production rates of waterflooding base case as a function of time

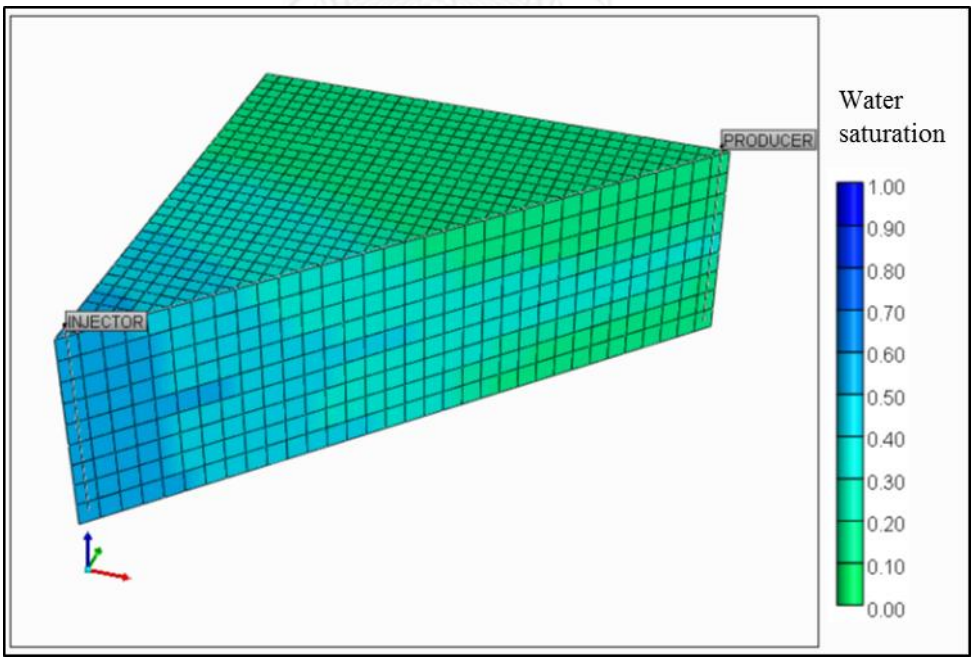

Figure 5.3 Early water breakthrough of waterflooding base case in the middle layer (representing by light blue color) at the 2nd year, 1st month

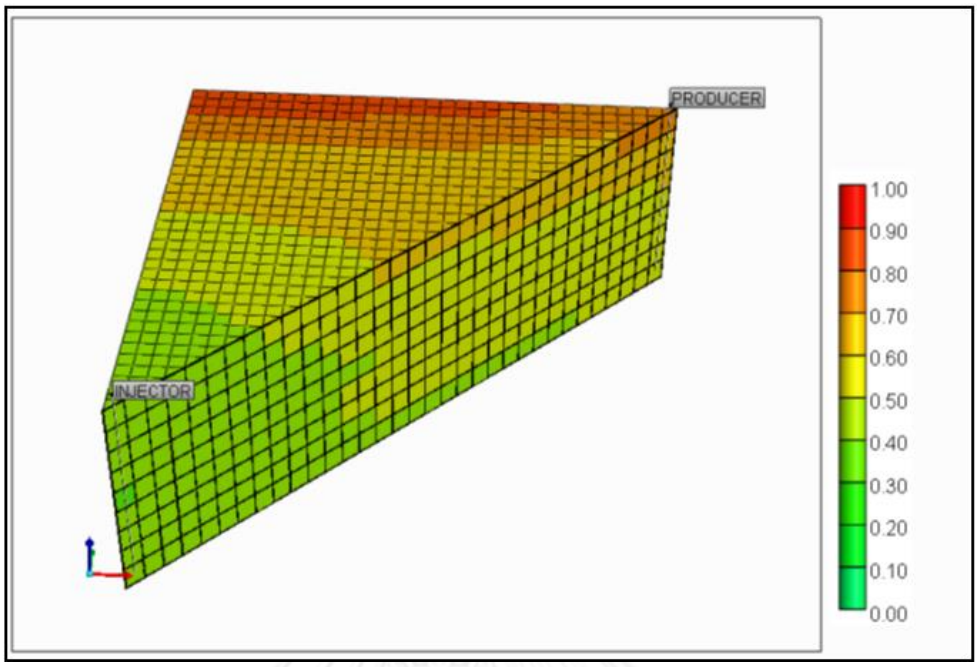

Figure 5.4 Oil saturation profile of waterflooding base case at the end of production showing high amount of oil is left (yellow to red colors)

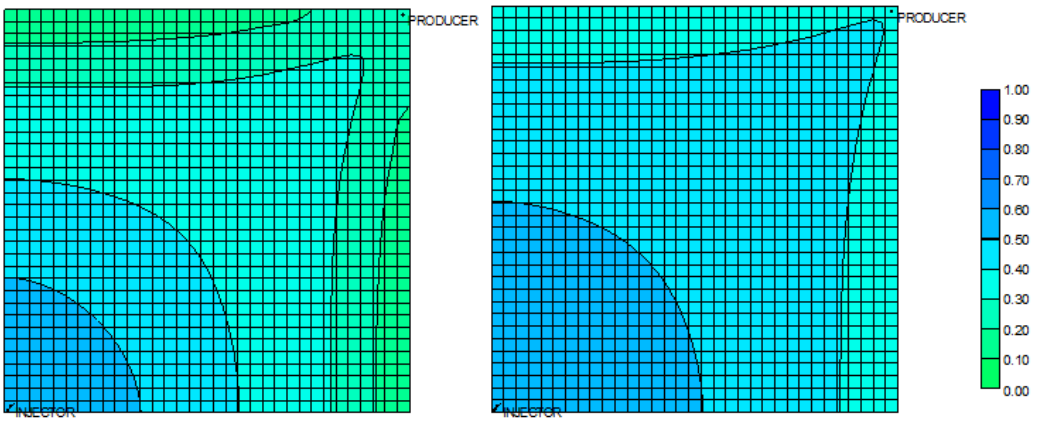

(a) (b)

Figure 5.5 Water saturation profiles of waterflooding at the end of production from different layers of reservoir (a) top layer (b) middle layer (layer5)

5.2 Single-slug Polymer Flooding in Heterogeneous Model 01A

In this study, polymer slug is the first material used to evaluate effectiveness compared to waterflooding base case. The study parameters of polymer are presence of pre-flushed water and its slug size, slug size of polymer and resistance factor of polymer. Polymer flooding is performed on model 01A in order to optimize important parameters of three polymer concentrations including 300ppm, 500ppm and 700 ppm. Polymer flooding in this section is aimed only for polymer post-slug to improve sweep efficiency without presence of alkali and surfactant. Characteristics of polymer are previously explained in Tables 4.10 to 4.12.

Resistance factor which is one of parameters in this study is initially fixed at default value of five (R5) and varied in the study of resistance factor section. The study of polymer flooding contains:

5.2.1 pre-flushed water slug size

5.2.2 slug size of polymer

5.2.3 resistance factor

5.2.4 confirmation test of *R*1.0 and *R*12.5 polymer flooding

5.2.1 Pre-flushed Water Slug Size

Study of pre-flushed water slug size has a main objective to identify an optimal slug of pre-flushed water before starting injection of polymer in different three cases of polymer concentration. Slug size of pre-flushed water is varied from 0.10 PV to 0.40 PV. After that, polymer concentration of 300, 500 and 700 ppm with resistance factor R5 are injected until termination of production. Recovery factor and amount of additional oil produced per mass of polymer used (bbl oil/mass of polymer) are main criteria to select the best conditions. Recovery factor is extracted from the CMG results, whereas amount of additional oil produced per mass of polymer used is calculated from amount of additional oil produced compared to waterflooding base case divided by mass of polymer used. Amount of additional oil produced per mass of polymer used can be used to consider the optimized case with proper amount of injected polymer.

Recovery factors and amount of additional oil produced per mass of polymer used of all cases are summarized in Figures 5.6 to 5.8. From these results, optimal condition for polymer concentration of 300 ppm is 0.20 PV pre-flushed water and polymer concentration of 500 ppm is 0.15 PV pre-flushed water. Recovery factor of polymer concentration of 700 ppm is less than waterflooding base case as shown in Figure 5.9. This adverse result from polymer concentration of 700 ppm is due to propagation of polymer mass that occurs very slowly in reservoir compared to other concentrations as can be seen in Figures 5.10 (a) and (b). Eventually, recovery factor obtained from polymer concentration of 700 ppm is less than other cases even waterflooding base case due to poor sweep efficiency. Thus, 700 ppm polymer is removed from the following test list in Section 5.2.2. Optimal pre-flushed water slugs for polymer concentrations of 300 ppm and 500 ppm are summarized in Table 5.1.

Effect of pre-flushed water is demonstrated by using data of polymer concentration of 300 ppm and illustrated in Figure 5.11(a). In case of pre-flushed water slugs of 0.10 PV, 0.15 PV and 0.20 PV, polymer can prolong production period more than 20th year. On the other hand, the oil production rate when pre-flushed water slug is greater than 0.20 PV drops under economic limit of 50 bbl/day at the 9th year. This is the main reason of low recovery factor and amount of low additional oil produced per mass of polymer used that is switched into minus sign. Oil production rate is significantly dropped because low saturation of oil bank is formed after polymer injection. However, production constraint of oil mainly affects total production period in case of high amount of pre-flushed water. Oil production rate of the case 0.30 PV pre-flushed water slug terminates at the 9th year with this constraint, whereas production can be prolonged when this constraint is removed.

Pre-flushed water slugs of 0.20 and 0.3 PV in 300 ppm polymer are selected to explain decreasing of oil production rate. Oil saturation profile of 0.20 PV pre-flushed water slug in 300 ppm polymer in Figure 5.12 (a) shows that oil bank is clearly formed. Therefore, oil production rate can be maintained at higher rate compared to the case of 0.30 PV of pre-flushed water slug in 300 ppm polymer shown in Figure 5.12 (b). Effect of pre-flushed water will be confirmed in confirmation test of R1 and R12.5 polymer flooding in section 5.2.4.

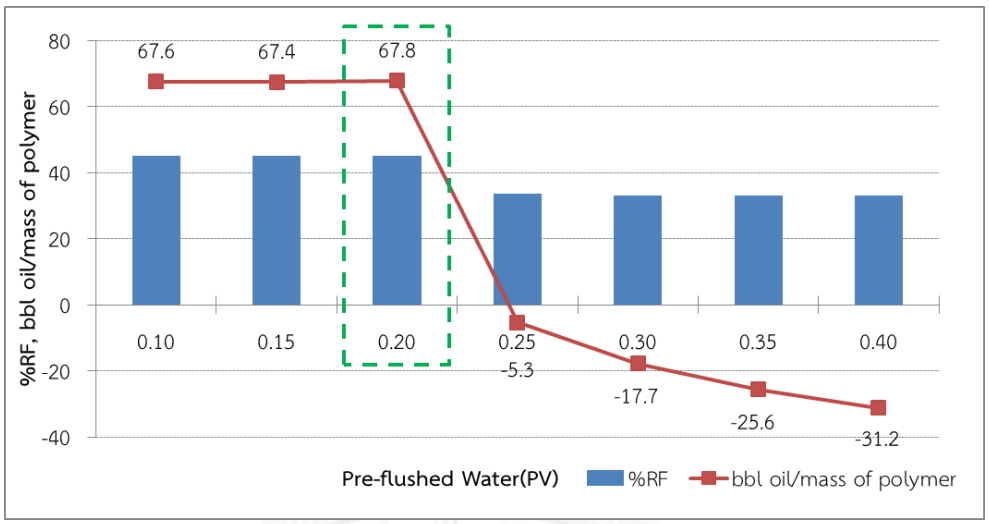

Figure 5.6 Recovery factors and additional oil produced per mass of polymer used of various pre-flushed water slugs of polymer concentration 300 ppm resistance factor 5

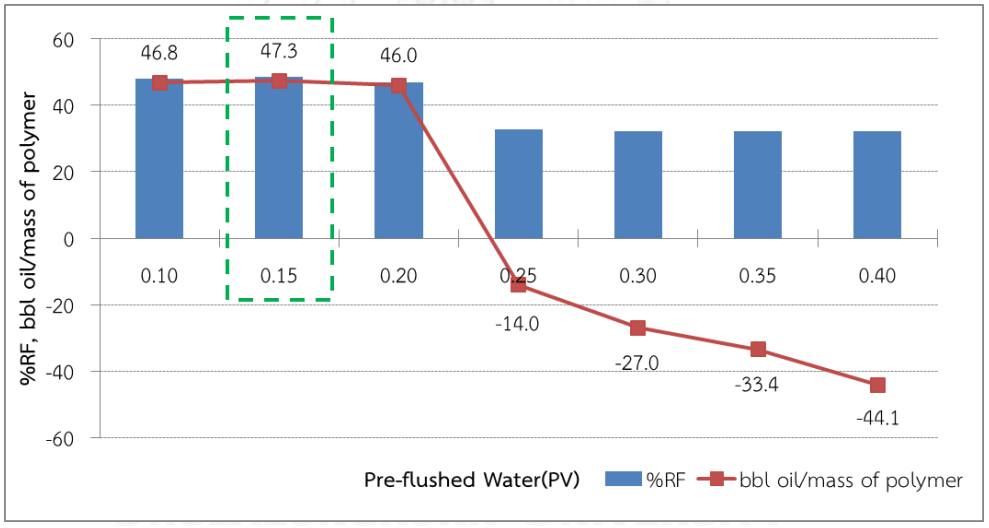

Figure 5.7 Recovery factors and additional oil produced per mass of polymer used of various pre-flushed water slugs of polymer concentration 500 ppm resistance factor 5

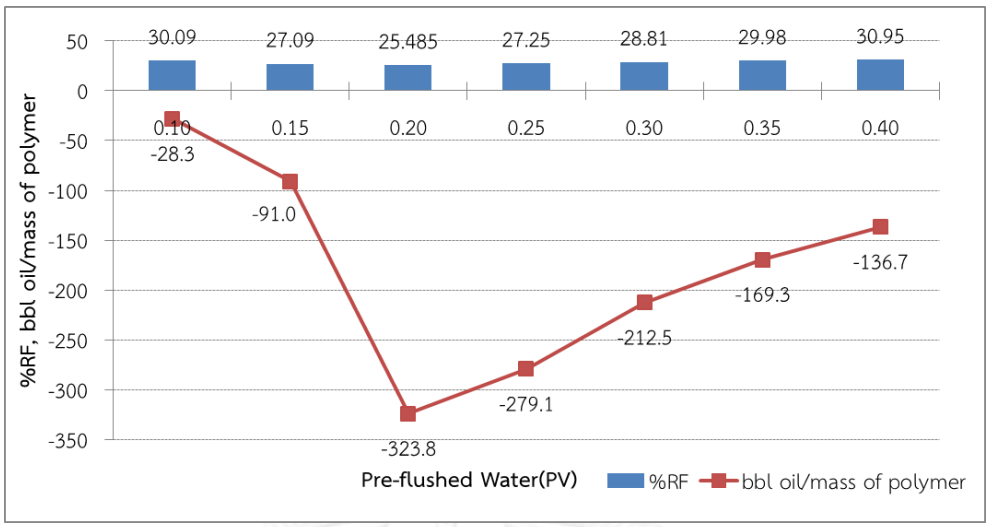

Figure 5.8 Recovery factors and additional oil produced per mass of polymer used of various pre-flushed water slugs of polymer concentration 700 ppm resistance factor 5

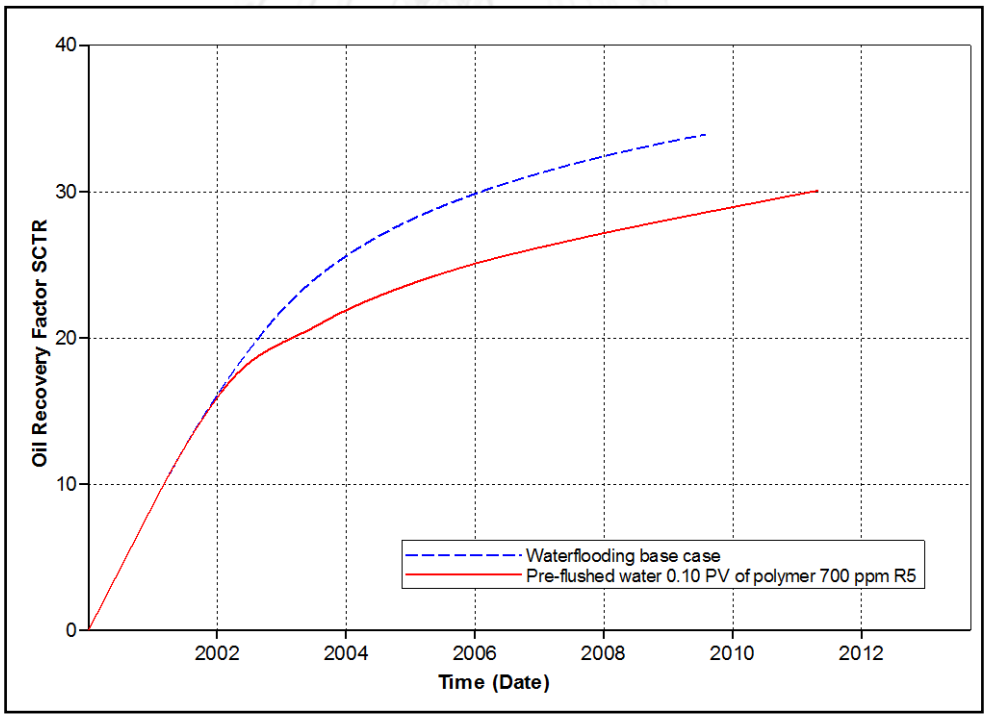

Figure 5.9 Comparison of recovery factor obtained from 0.1 PV pre-flushed water slug of polymer concentration 700 ppm resistance factor 5 to waterflooding base case

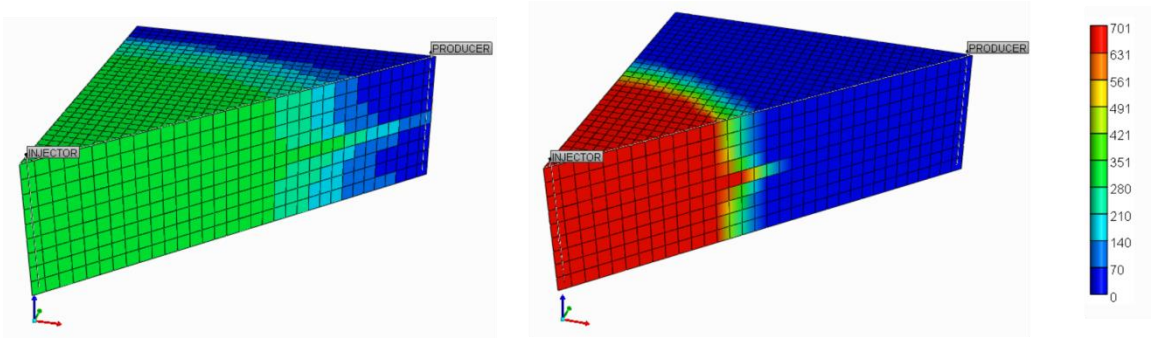

(a) (b)

Figure 5.10 Polymer concentrations profiles of 300 ppm and 700 ppm polymer concentrations at the end of production (a) 300 ppm (b) 700 ppm

Table 5.1 Summary of optimal pre-flushed water slugs of polymer concentration 300, 500 and 700 ppm resistance factor 5

Cases	Optimal Pre-flushed water (PV)
300 ppm R5	0.2
500 ppm R5	0.15
700 ppm R5	-

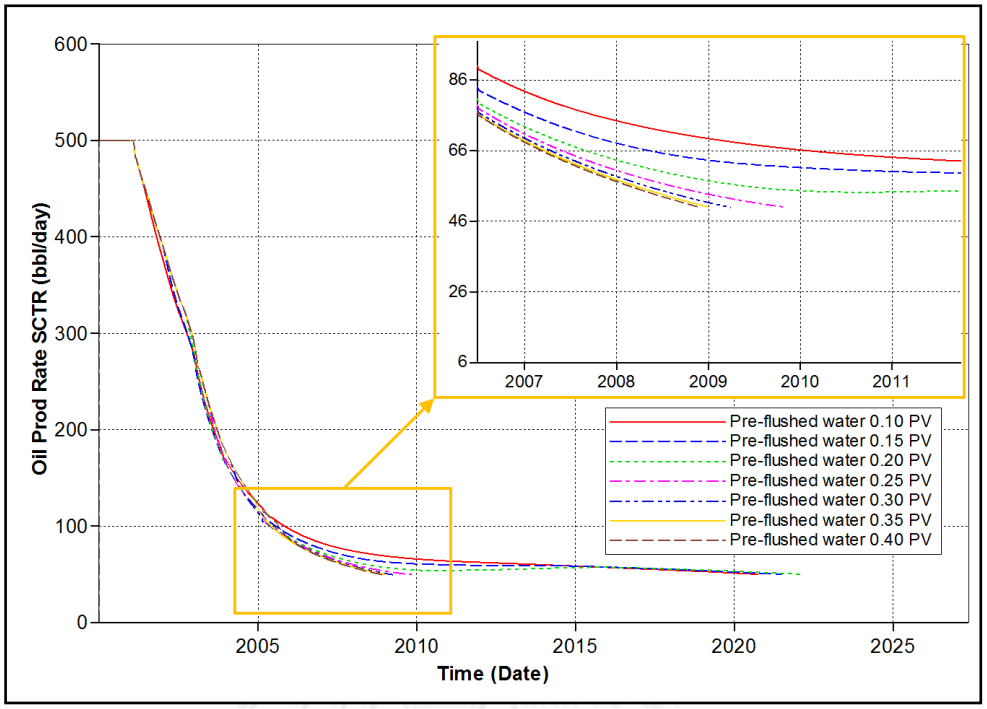

(a)

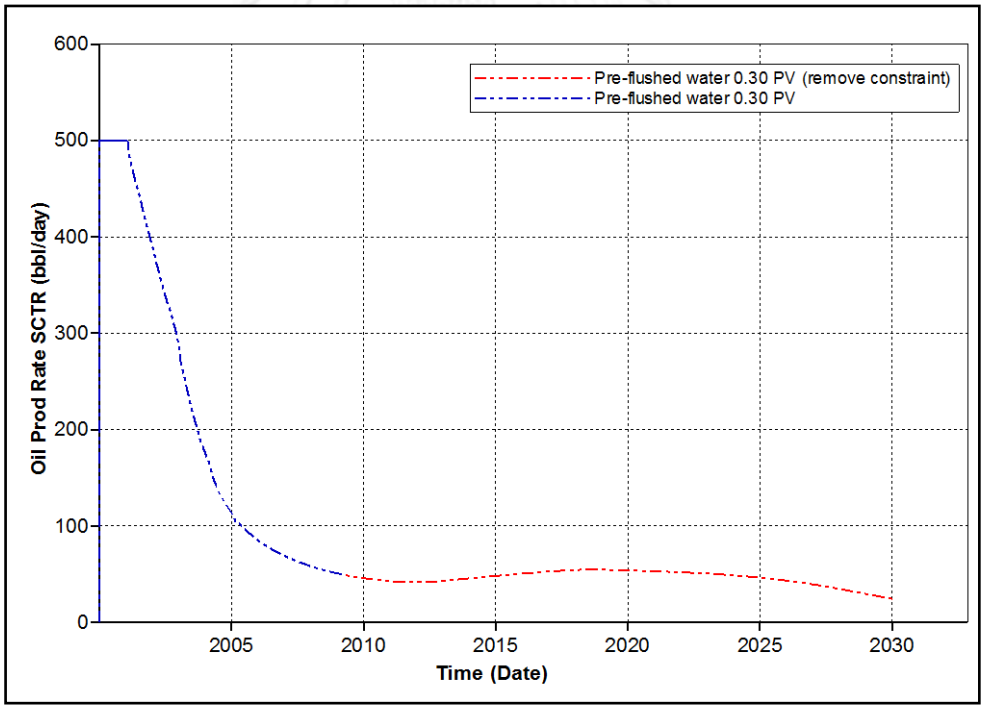

(b)

Figure 5.11Oil production rates of various pre-flushed water slugs of 300 ppm polymer concentration resistance factor 5 (a) normal constraint (b) result of different constraints on 0.30 PV pre-flushed water slug case

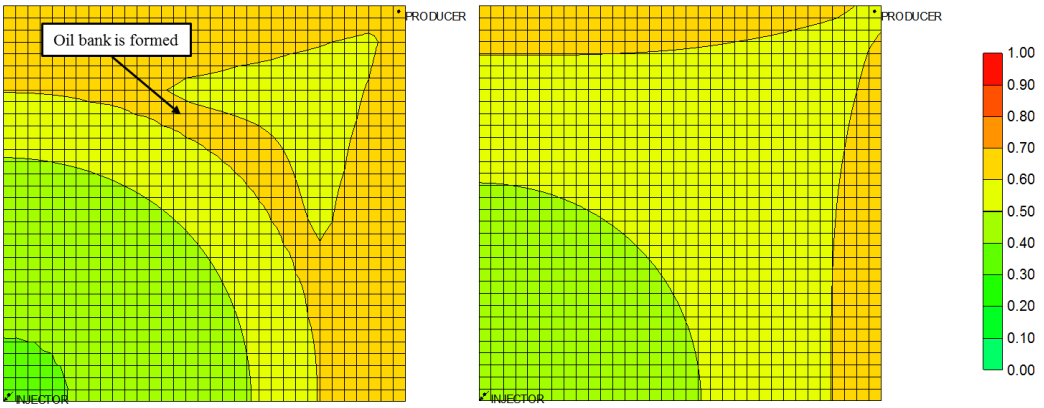

(a) (b)

Figure 5.12 Oil saturation profiles in high permeability layer at 9th year, 2nd month (a) pre-flushed water slug 0.2 PV (b) pre-flushed water of 0.3 PV

5.2.2 Slug Size of Polymer

After optimal slug size of pre-flushed water is determined in previous section, slug size of 300 ppm and 500 ppm polymer slug is varied in this section in order to determine optimal polymer slug sizes. Resistance factor is kept constant at five which is default value. Slug size of polymer is varied from 0.1 PV to reach maximum PV of injected polymer in both 300 ppm and 500 ppm cases. After that, chasing water slug is injected until the end of production. Recovery factor and amount of additional oil produced per mass of polymer used are the main criteria to select the best conditions as same as previous section.

Recovery factors and amount of additional oil produced per mas of polymer used of all cases are summarized in Figures 5.13 and 5.14. From these results, optimal polymer slug for polymer 300 ppm is 0.55 PV and in case of polymer 500 ppm is 0.25 PV. Optimal slug size of polymer in each concentration is summarized in Table 5.2.

Comparing amount of additional oil produced per mass of polymer used between the previous section (5.2.1) and this section (5.2.2) in Table 5.3, result implies that chasing water can increase amount of additional oil produced per mass of polymer used. Starting point of chasing water injection and end of production of optimal slug size 300 and 500 ppm polymer compared to waterflooding are illustrated in Figure 5.15. Chasing water injection can stimulate polymer slug to faster

propagate into reservoir in especially high permeability channel. Therefore, oil production rate is also built up in certain period. End of production occurs when polymer cannot maintain stable front in high permeability channel nearby producer. Figures 5.16 and 5.17 illustrate sequence from starting point of chasing water injection to the end of production of optimal slug size 300 and 500 ppm polymer in two views, respectively. Although chasing water can stimulate polymer propagation into reservoir, chasing water decreases stability of polymer front especially in high permeability channel, causing termination of production due to high water production by polymer slug breakthrough at producer.

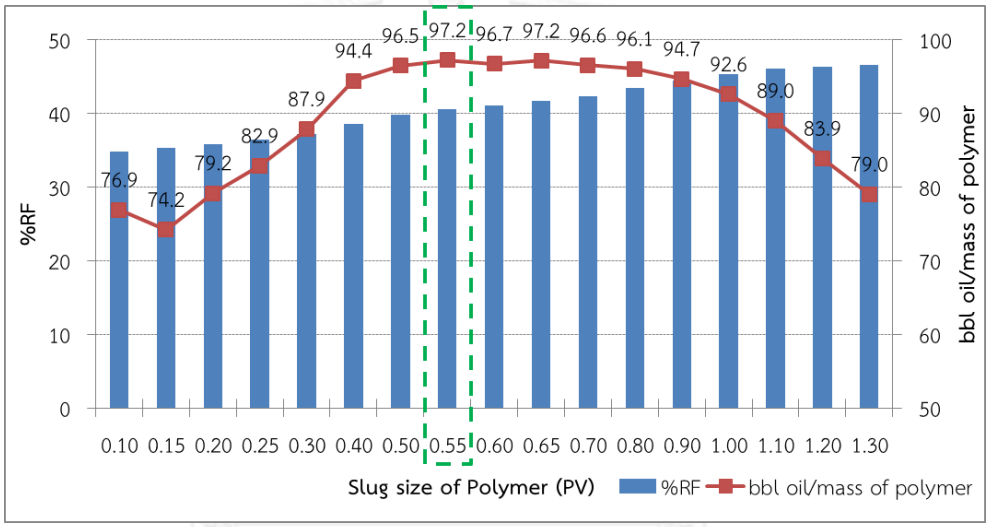

Figure 5.13 Recovery factors and additional oil produced per mass of polymer used of various polymer slug sizes of polymer concentration 300 ppm resistance factor 5

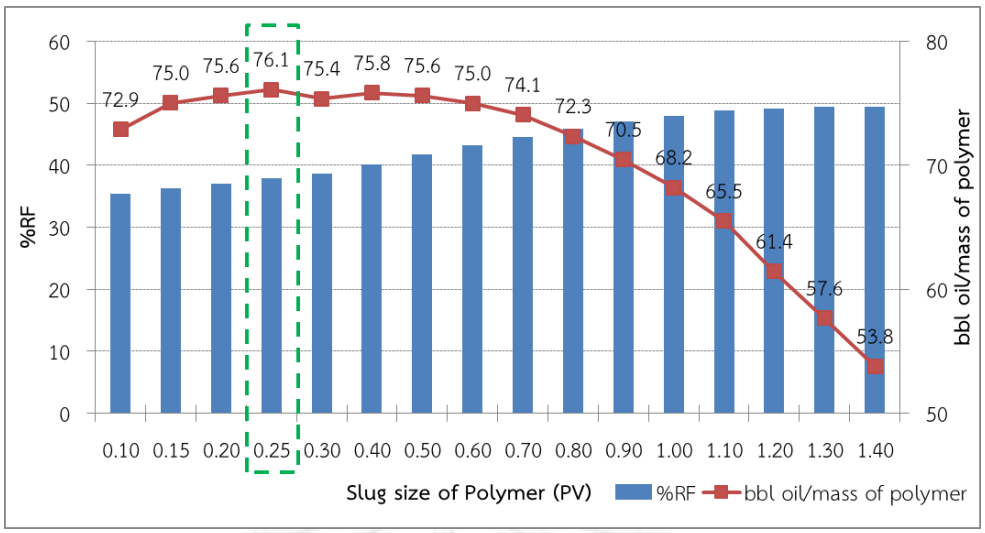

Figure 5.14 Recovery factors and additional oil produced per mass of polymer used of various polymer slug sizes of polymer concentration 500 ppm resistance factor 5

Table 5.2 Summary of optimal pre-flushed water slug with optimal polymer slug size at resistance factor 5

Cases	Optimal pre-flushed water slug (PV)	Optimal polymer slug (PV)
300 ppm R5	0.20	0.55
500 ppm R5	0.15	0.25

Table 5.3 Comparison of additional oil produced per mass of polymer used with the presence of chasing water

Cases	bbl oil/mass polymer (Section 5.2.1)	bbl oil/mass polymer (Section 5.2.2)
300 ppm R5	67.8	97.2
500 ppm R5	47.3	76.1

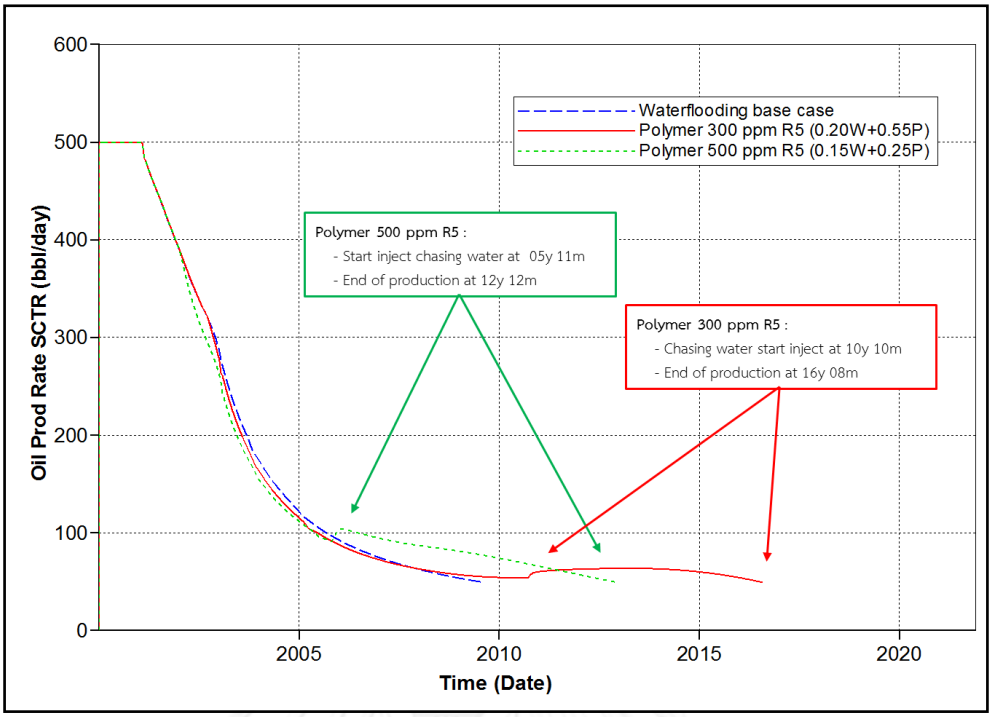

Figure 5.15 Oil production rates of optimal polymer slug size for 300 and 500 ppm concentration resistance factor 5 comparing with waterflooding base case

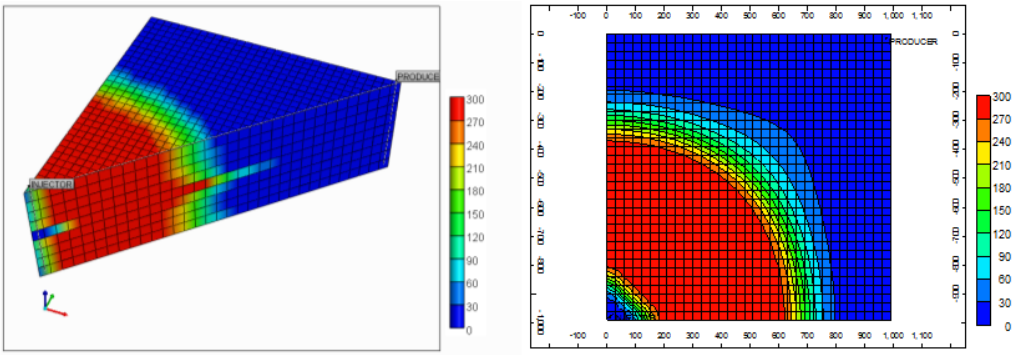

(a1) 3-D profile (a2) Areal plane in high permeability layer

(a) Start injecting chasing water at 10th year, 10th month

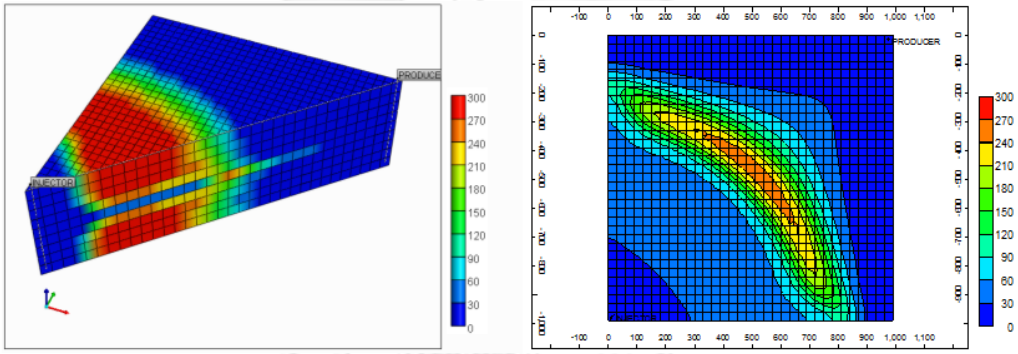

(b1) 3-D profile (b2) Areal plane in high permeability layer

(b) During injecting chasing water at 13th year, 1st month

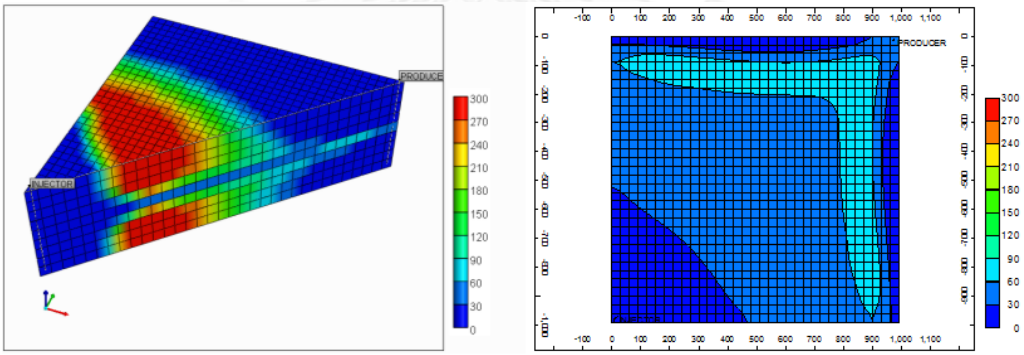

(c1) 3-D profile (c2) Areal plane in high permeability layer

(c) End of production at 16th year, 8th month

Figure 5.16 Polymer concentrations profiles at different production period of 300 ppm polymer concentration resistance factor 5

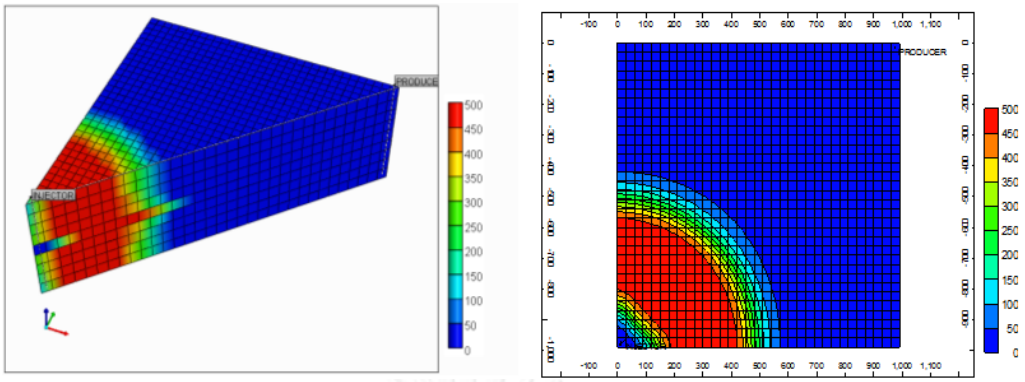

(a1) 3-D profile (a2) Areal plane in high permeability layer

(a) Start injecting chasing water at 5th year, 11th month

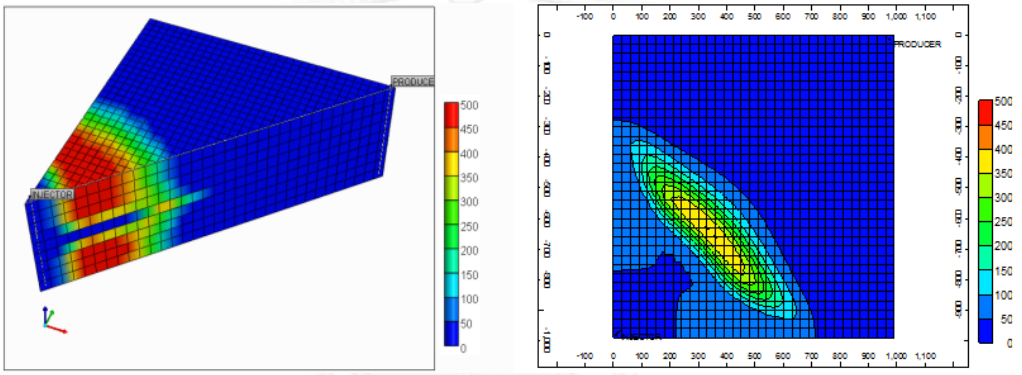

(b1) 3-D profile (b2) Areal plane in high permeability layer

(b) During injecting chasing water at 7th year, 1st month

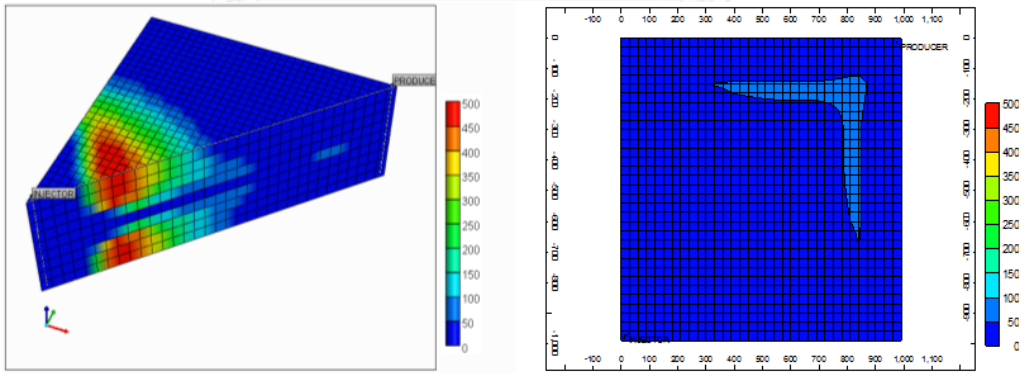

(c1) 3-D profile (c2) Areal plane in high permeability layer

(c) End of production at 12th year, 12th month

Figure 5.17 Polymer concentrations profiles at different production periods of 500 ppm polymer concentration resistance factor 5

5.2.3 Resistance Factor

After optimal slug size of pre-flushed water and polymer are determined in previous sections, resistance factor of polymer concentrations of 300 and 500 ppm is concerned in this section. Slug size of sequence fluids are kept as similar as previous section for both concentrations. Resistance factor is varied from 5.0 to 1.0, 2.5, 7.5, 10.0, 12.5 and 15. Again, recovery factor and amount of additional oil produced per mass of polymer used are used to select the best conditions as same as the previous sections.

Recovery factor and amount of additional oil produced per mass of polymer used of all cases are summarized from Figures 5.18 and 5.19. From the results, optimal resistance factor for polymer concentrations of 300 ppm and 500 ppm are 12.5 and 5.0, respectively. All details of optimized case of polymer in each concentration are summarized in Table 5.4. Consequently, the case of polymer concentration 300 ppm and resistance factor 12.5 is selected as the optimized single-slug polymer from the highest amount of additional oil produced per mass of polymer used. However, result from this section gives only the relative answer. Thus, confirmation test of resistance factor of 1.0 and 12.5 is performed in the next section.

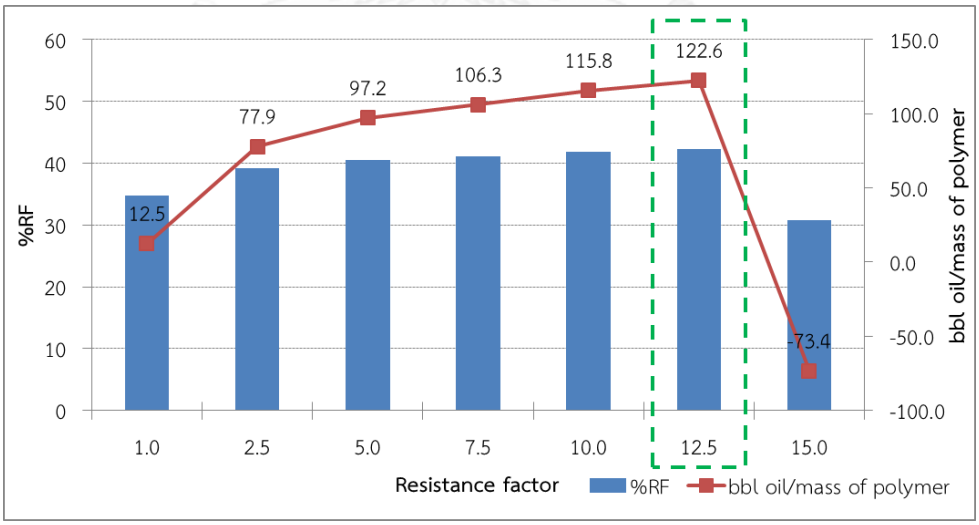

Figure 5.18 Recovery factors and additional oil produced per mass of polymer used of various resistance factors of polymer concentration 300 ppm

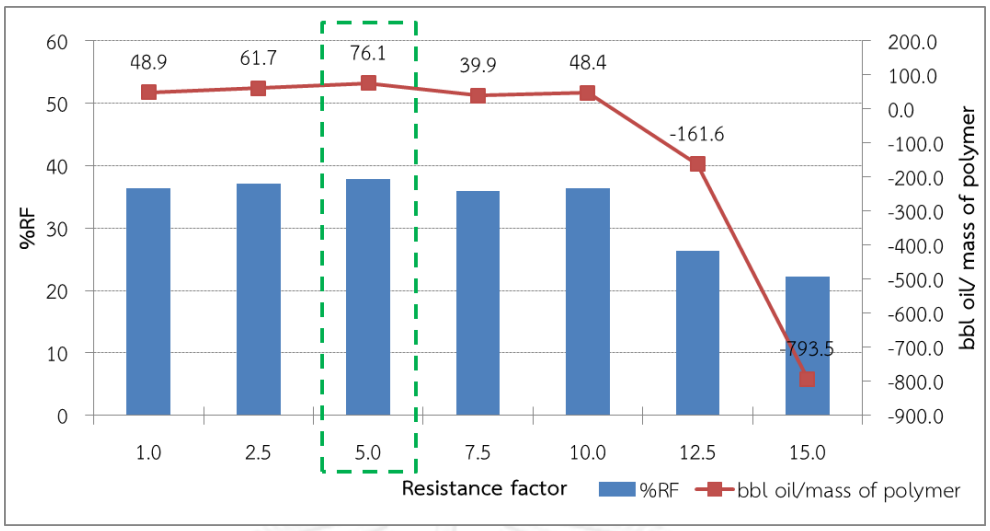

Figure 5.19 Recovery factors and additional oil produced per mass of polymer used of various resistance factors of polymer concentration 500 ppm

Table 5.4 Comparison and summary details of optimized cases of polymer concentrations of 300 and 500 ppm

Polymer concentration	Resistance factor	Pre-flushed water (PV)	Slug size of polymer (PV)	Recovery factor (%)	bbl oil /mass of polymer
300 ppm	12.50	0.20	0.55	42.26	122.60
500 ppm	5.00	0.15	0.25	37.84	76.10

Effect of resistance factor is demonstrated by using data obtained from the case 300 ppm polymer concentration and illustrated in Figure 5.20. In case of resistance factor of 1.0 and 15.0, productions are terminated before injecting of chasing water because oil production rate is lower than economic limit. In contrast, resistance factor 2.5, 5.0, 7.5, 10.0 and 12.5 can extend production period longer than 15 years. As mentioned in Chapter 3, main oil recovery mechanism of resistance factor is permeability reduction from polymer adsorption onto rock surface, causing pressure drop in reservoir. Average reservoir pressure of various resistance factors is illustrated in Figure 5.21. The higher the resistance factor, the higher the pressure drops in reservoir. High pressure drop from polymer injection decreases effective

permeability to water. Polymer shock front is stabilized and sweep efficiency is improved. Nevertheless, high resistance factor does not always yield good sweep efficiency. Resistance factor of 15.0 is a good example that causes high pressure drop. This is because at resistance factor of 15.0 polymer propagates very slowly in reservoir due to very high reduction of effective permeability to water as shown in Figure 5.22.

Resistance factor of 5.0 of 500ppm and resistance factor 12.5 of 300 ppm polymer concentrations are selected in order to describe areal sweep efficiency of various resistance factors during chasing water period. Oil saturation profile sequence starting from the point where chasing water is injected to the end of production is illustrated in Figures 5.23(a), (b) and (c). Oil saturation profile is not significantly different between two cases at the start of chasing water injection period as shown in Figure 5.23(a). Nevertheless, difference can be seen in Figure 5.23(b) showing that areal sweep efficiency of resistance factor of 12.5 of 300 ppm is better than that of resistance factor 5.0 of 500 ppm. However, oil saturation profile at the end of production truly expresses that the better areal sweep efficiency is on the other hand resistance factor of 5.0 as shown in Figure 5.23(c).

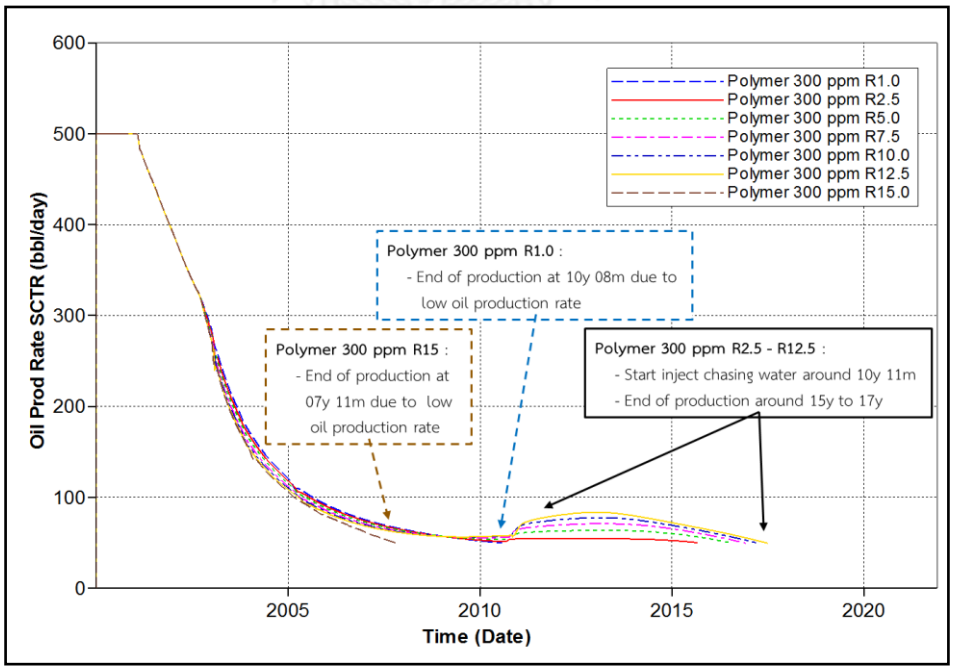

Figure 5.20 Oil production rates of various resistance factors of polymer concentration 300 ppm as a function of time

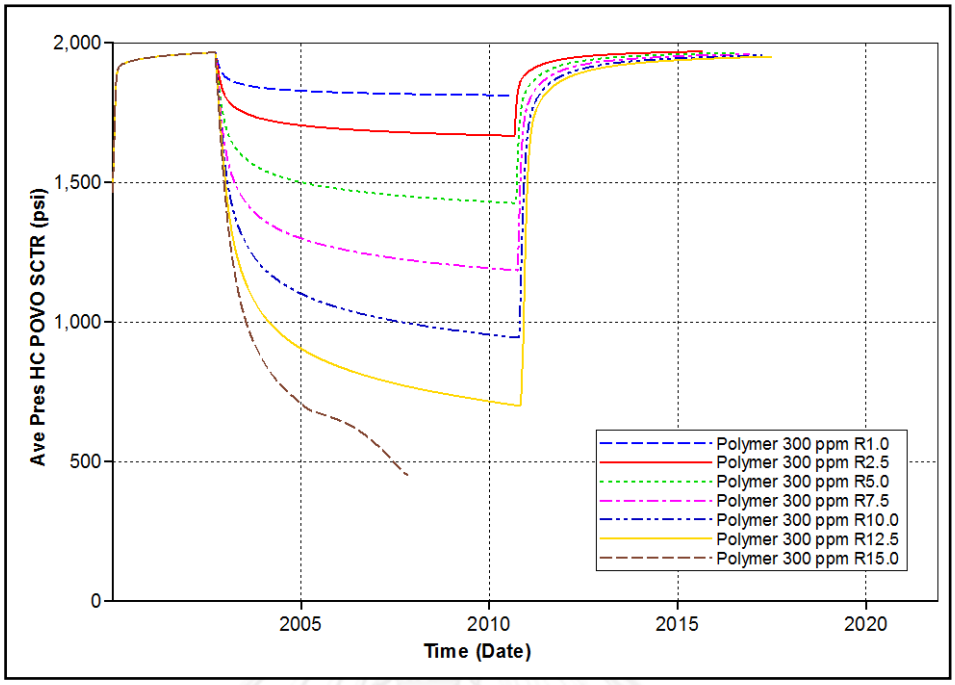

Figure 5.21 Average reservoir pressures of various resistance factor of polymer concentration 300 ppm as a function of time

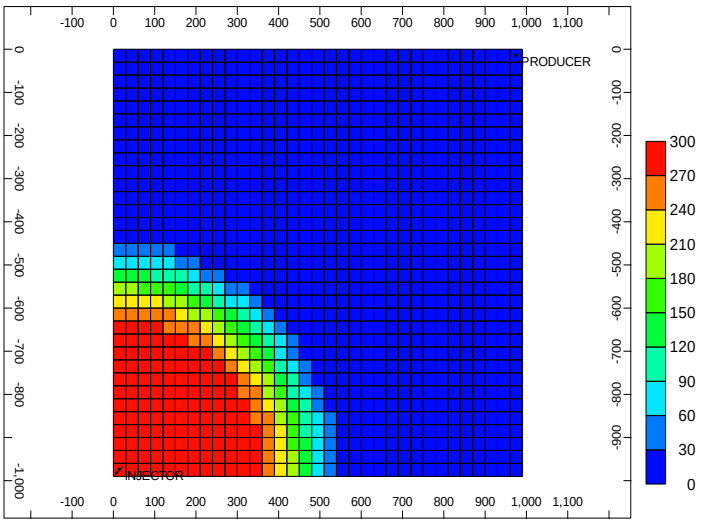

Figure 5.22 Polymer concentration profile from polymer concentration 300 ppm resistance factor 15 at the end of production

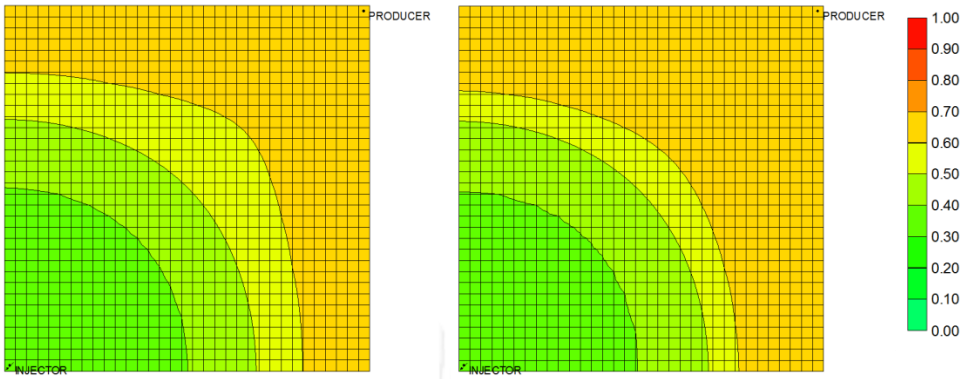

(a1) 500 ppm R5.0 (a2) 300 ppm R 12.5

(a) Start injecting chasing water at 10th year, 11th month

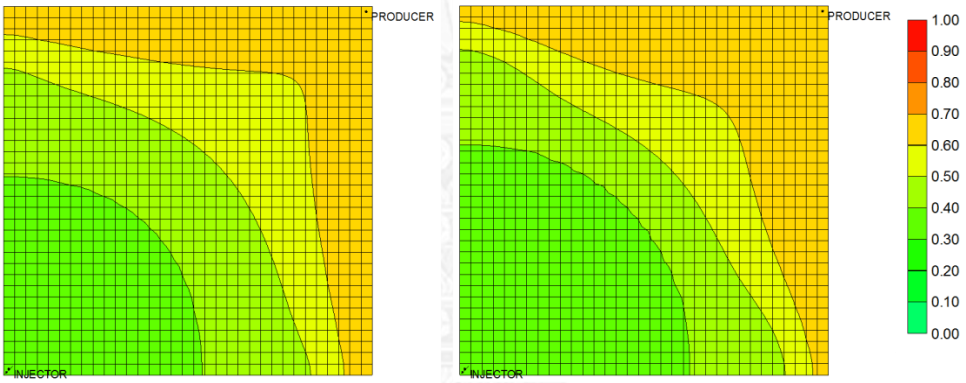

(b1) 500 ppm R5.0 (b2) 300 ppm R 12.5

(b) During injecting chasing water at 13th year, 1st month

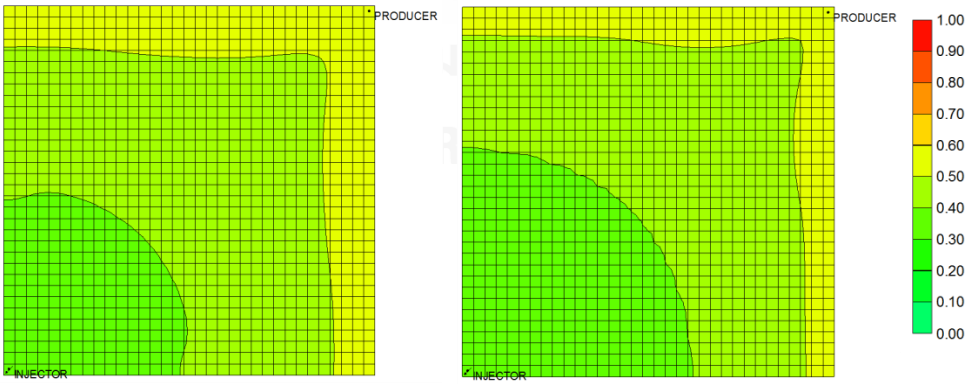

(c1) 500 ppm R5.0 (c2) 300 ppm R 12.5

(c) End of production of each case

Figure 5.23 Oil saturation profiles of polymer concentration 500 ppm R5.0 and 300 ppm R 12.5

5.2.4 Confirmation Test of *R*1.0 and *R*12.5 Polymer Flooding

In this section, resistance factors of 1.0 and 12.5 are performed in order to ensure the simulation results of single-slug polymer. Simulation tests are conducted in the same manner of resistance factor of 5.0 by using by optimal pre-flushed water slugs as shown in Table 5.5. Then, slug size of each case is varied to determine the recovery factor and amount of additional oil produced per mass of polymer used.

Table 5.5 Optimized pre-flushed water slug of various polymer concentrations and resistant factors

Polymer concentration	Resistance factor	Obtained pre-flushed water (PV)
300 ppm	1.0	0.10
500 ppm	1.0	0.20
700 ppm	1.0	0.25
300 ppm	5.0	0.20
500 ppm	5.0	0.15
300 ppm	12.5	0.20

Effect of pre-flushed water is illustrated in Figure 5.24. From the figure, recovery factors of each polymer concentration and resistance factor are plotted with slug size of pre-flushed water. The red horizontal line shows recovery factor obtained from waterflooding base case that is used to compare with all cases. For most cases, recovery factors drops to lower than waterflooding base case when pre-flushed water slug is higher than 0.20 PV. And only 700 ppm, resistance factor of 1.0 can yield the recovery factor higher than waterflooding base case when pre-flushed water is 0.25 PV. So that, the pre-flushed water should not be higher than 0.20 PV in order to yield high recovery factor. However, this value can be increased when production constraint is changed.

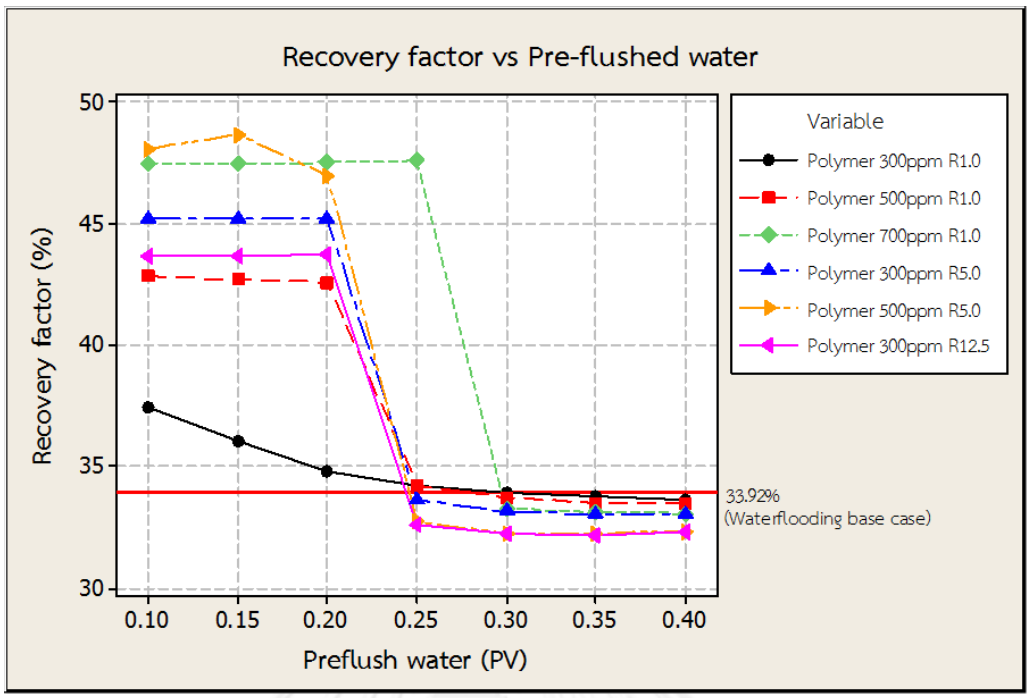

Figure 5.24 Recovery factors of cases with different polymer concentration and resistance factors as a function of pre-flushed water slug size

Effect of resistance factor is considered by varying polymer slug size of 300 ppm polymer concentration. The plot between recovery factor and slug size of 300 ppm polymer is shown in Figure 5.25. From the figure, recovery factor of 12.5 is the highest, resistance factor of 5.0 is in the middle and resistance factor of 1.0 is at the bottom of the curve. Recovery factor of each slug size of polymer is indeed increasing from resistance factor of 1.0 to 12.5. This can be expected that higher resistance factor can induce higher recovery factor in proper range. Moreover, higher resistance factor can reduce the amount of polymer required to yield the same recovery factor in proper range of resistance factor.

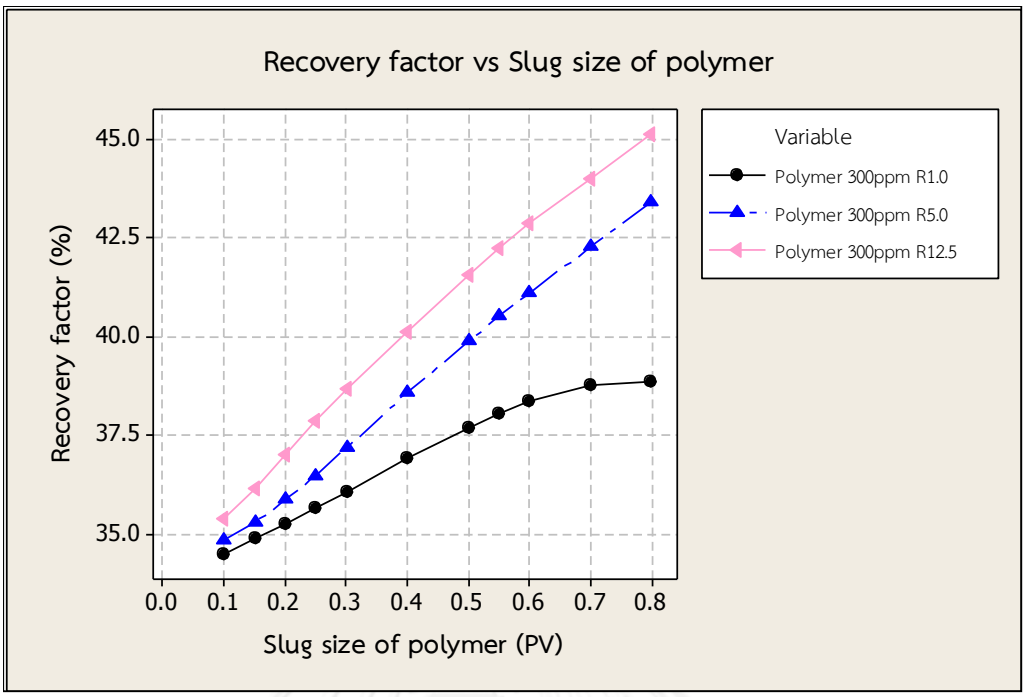

Figure 5.25 Recovery factors from polymer concentration of 300 ppm at different resistance factors as a function of polymer slug size

Optimized single-slug polymer flooding is assured by summary amount of additional oil produced per mass of polymer used and recovery factors of various polymer concentrations and resistance factors in Figures 5.26 and 5.27. Figure 5.26 shows that additional oil produced per mass of polymer used of polymer concentration 300 ppm resistance factor 12.5 is significantly higher than other cases. Therefore, polymer concentration of 300 ppm with resistance factor 12.5 is considered as an appropriate polymer concentration and resistance factor to yield maximum produced oil with proper amount of injected polymer. Figure 5.27 shows that recovery factor increases as slug size of polymer is raised. The highest curve of recovery factor is polymer concentration 300 ppm with resistance factor 12.5 (pink color) and polymer concentration 500 ppm with resistance factor 5.0 (yellow color) which yields the maximum produced oil comparing with the other cases. Moreover, polymer concentration of 300 ppm and resistance factor 12.5 curve is deviated from the latter case at 0.55 PV slug size of injected polymer. Therefore, 0.55 PV 300 ppm and resistance factor of 12.5 are optimized value of injected polymer to yield high recovery factor along with high additional oil produced per mass of polymer used.

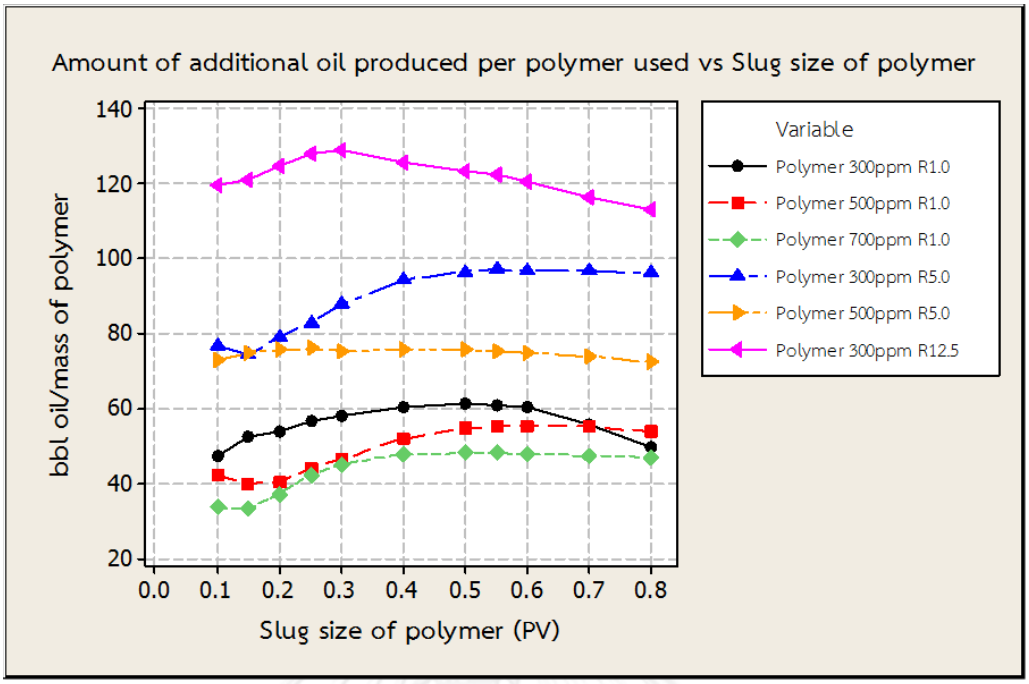

Figure 5.26 Additional oil produced per mass of polymer used of various polymer concentrations and resistance factors as a function of polymer slug size

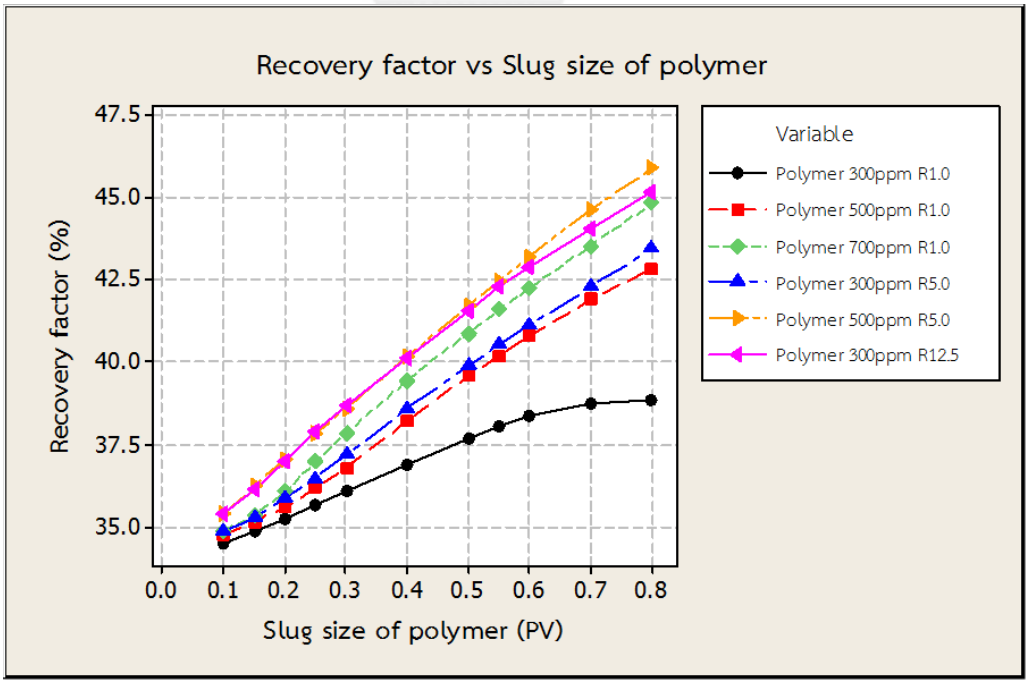

Figure 5.27 Recovery factors of various polymer concentrations and resistance factors as a function of polymer slug size

5.3 Double-slug Polymer Flooding in Heterogeneous Model 01A

Since polymer injection has shown an ability to maintain flood front and prevent water channeling, polymer injection at initial period (pre-flushed polymer) is foreseen to increase recovery by decreasing relative permeability to water. Therefore, double-slug polymer flooding is also implemented. Associated parameters include pre-flushed polymer, alkaline-surfactant (AS) and post-flushed polymer. Sequence of double-slug polymer flooding is starting with pre-flushed polymer followed by alkali-surfactant slug and chased by polymer slug (P+AS+P) as illustrated in Figure 5.28. By the way, optimized single-slug polymer flooding is already selected at concentration of 300 ppm 0.55 PV and resistance factor of 12.5 from the previous section. Then, post-flushed polymer is determined as same slug size as the optimized single-slug polymer flooding. Remaining parameters are pre-flushed polymer slug and AS slug.

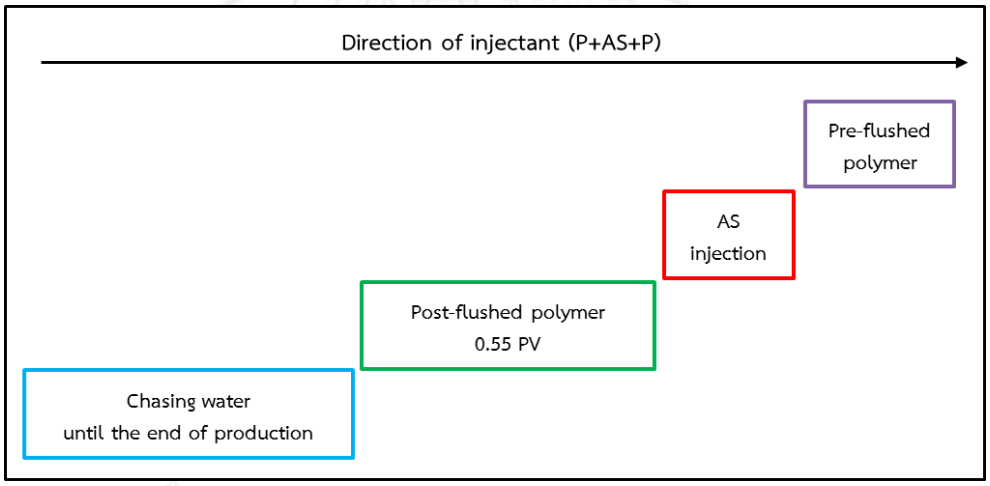

Figure 5.28 Sequence of double-slug polymer flooding (P+AS+P)

In this section, the pre-flushed polymer slug and AS slug are determined to find the optimized case. Therefore, the 1st optimized parameter is pre-flushed polymer by fixing the AS slug as base value (0.15 PV). After that AS slug is varied after the optimized pre-flushed polymer is determined. The alkaline and surfactant concentration in this study are specified as 1.3% and 0.28% as mentioned in the previous chapter, respectively. This double-slug polymer study contains:

5.3.1 slug-size of pre-flushed polymer

5.3.2 slug-size of alkaline-surfactant

5.3.1 Slug-size of Pre-flushed Polymer

The study of slug-size of pre-flushed polymer has objective to find the optimal slug of pre-flushed polymer before AS injection. The slug size of pre-flushed polymer is varied from 0.05 PV to 1.00 PV of pre-flushed polymer. After that 0.15 PV of alkaline-surfactant (AS), 300 ppm 0.55 PV R12.5 of post-flushed polymer are injected. Finally, the chasing water is injected until the end of production. The sequential injection is illustrated in Figure 5.29.

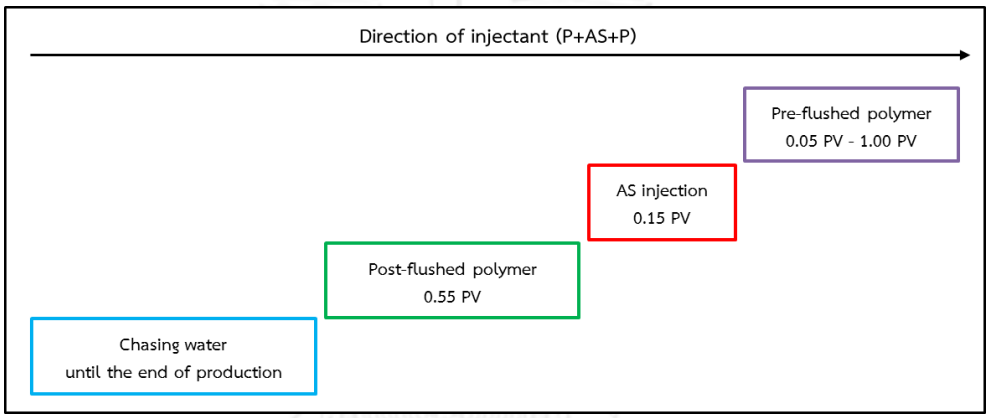

Figure 5.29 Sequential injection of study slug size of pre-flushed polymer

Recovery factor and amount of additional oil produced per mass of pre-flushed polymer used are used as criteria to select the best condition. Recovery factor is extracted from result in CMG, whereas amount of additional oil produced per mass of pre-flushed polymer used is calculated from the amount of incremental oil from 0.05 PV of pre-flushed polymer divided by mass of polymer used in pre-flushed slug. Due to the fact that pre-flushed polymer can prevent an early water early breakthrough and AS slug can remove the residual oil remained, therefore, oil recovery is remarkably improved compared to waterflooding base case. Significant of oil recovery from different case of various pre-flushed polymer slugs is decreased compared to improvement obtained from waterflooding base case. This is a reason why additional oil produced per mass of pre-flushed polymer used is used as criterion to select the optimized case with proper amount of injected pre-flushed polymer.

Recovery factor and amount of additional oil produced per mass of pre-flushed polymer used of all cases are summarized in Figure 5.30. From this figure, optimized slug for pre-flushed polymer is 0.25 PV, yielding the highest amount of additional oil produced per mass of pre-flushed polymer used.

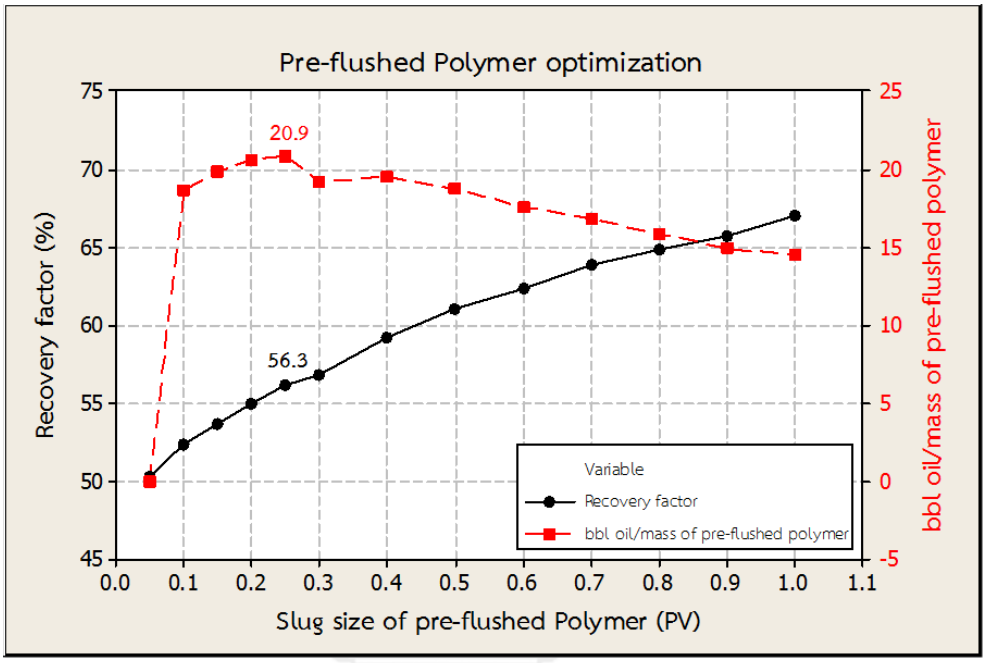

Figure 5.30 Recovery factors and additional oil produced per mass of pre-flushed polymer used as a function of pre-flushed polymer slug size

Recovery factor and oil production rate of 0.25 PV pre-flushed polymer slug in comparison with waterflooding base case are illustrated in Figures 5.31 and 5.32. Recovery factor of 0.25 PV pre-flushed polymer is about 56.3, increasing 66% from waterflooding base case (33.9%). Effect of sequential injection is demonstrated in Figure 5.32. From the figure, 0.25 PV of pre-flushed polymer injection is started from the first day of injection until 3rd year, 7th month. Effect of pre-flushed polymer is considered at 3rd year, 7th month in Figure 5.33. The 0.15 PV of AS injection is started after 0.25 PV of pre-flushed polymer slug until 5th year, 7th month. The effect of AS injection is considered at 5 years and 7 months in Figure 5.34. The 0.55 PV of post-flushed polymer and chasing water are injected after previous slug until the end of production. Effect of post-flushed polymer and chasing water injection are considered at 13th year, 8th month and 20th year, 8th month in Figures 5.35 and Figure 5.36, respectively.

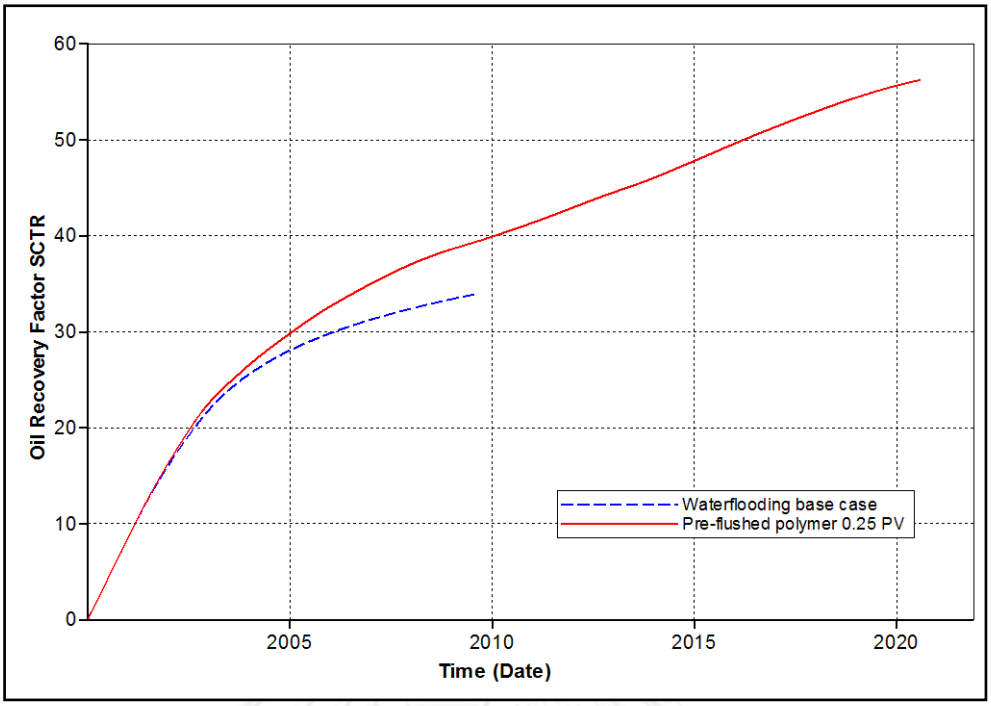

Figure 5.31 Recovery factors obtained from 0.25 PV of pre-flushed polymer slug compared to waterflooding base case as a function of time

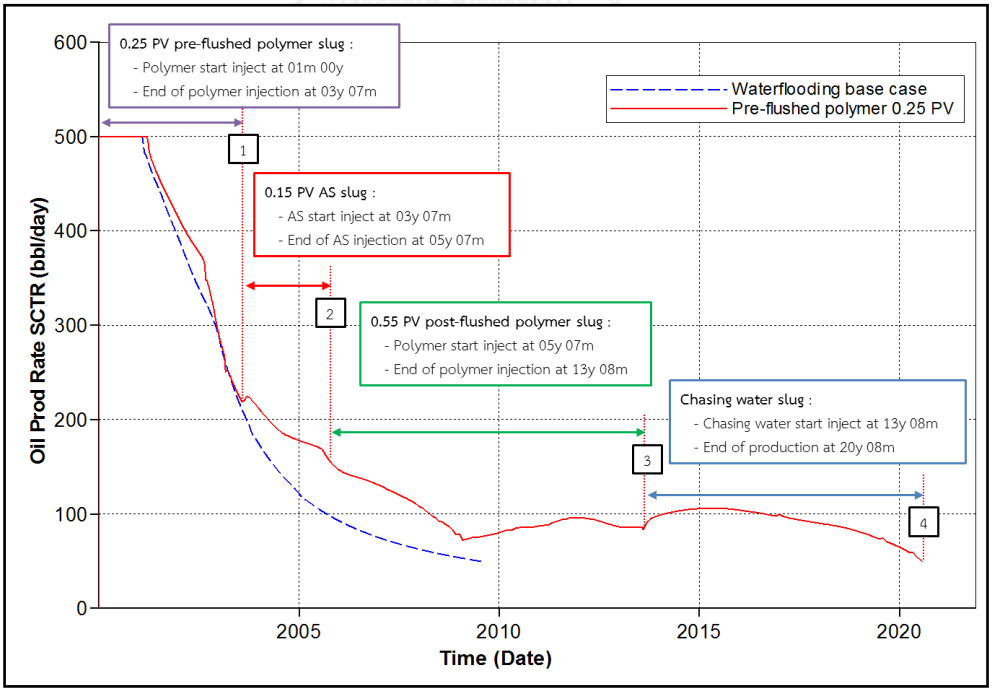

Figure 5.32 Oil production rates obtained from 0.25 PV pre-flushed polymer slug compared to waterflooding base case as a function of time

Effect of pre-flushed polymer is determined in Figure 5.33 at the end of 0.25 PV pre-flushed polymer injection (3rd year, 7th month). Polymer concentration, oil saturation and water saturation are tracked and compared to waterflooding base case. Polymer concentration profile in Figure 5.33(a) shows propagation of pre-flushed polymer in reservoir. Oil saturation shows that polymer front is stabilized both of 3-D perspective and areal plane in high permeability channel in Figure 5.33(b). Figure 5.33(c) shows the sharp interface of water front with presence of pre-flushed polymer. Therefore, results can imply that pre-flushed polymer can improve mobility ratio and hence early water breakthrough is prevented.

Effect of AS injection is determined in Figure 5.34 at the end of 0.15 PV AS injection (5th year, 7th month). The log capillary number, oil saturation and water saturation are tracked and compared to waterflooding base case. The log capillary number shows the area that relative permeability is changed due to lowering IFT value by means of alkali and surfactant in Figure 5.34(a). Yellow area is the zone that capillary number is in low IFT condition, whereas the orange area is the zone that represents ultra-low IFT condition. Occurrence result of alkali and surfactant to reduce residual oil saturation appears nearby the injector well. Accordingly, residual oil is totally removed only nearby injection well as shown in Figure 5.34(b). The presence of pre-flushed polymer forms itself like a buffer zone to prevent alkali-surfactant breakthrough as shown in Figure 5.34(c).

Effect of post-flushed polymer and chasing water are determined at the end of 0.55 PV post-flushed polymer injection (13th year, 8th month) in Figure 5.35 and at the end of production period (20th year, 8th month) in Figure 5.36. Polymer concentration, log capillary number, oil saturation and water saturation are tracked individually because waterflooding base case is stopped. Mechanism of post-slug polymer and chasing water are also same as the previous section, whereas the log capillary number in Figures 5.35(b) and 5.36(b) show that capillary number increases with an absence alkali and surfactant. Therefore, lowering IFT by means of alkali and surfactant occurred only in certain period.

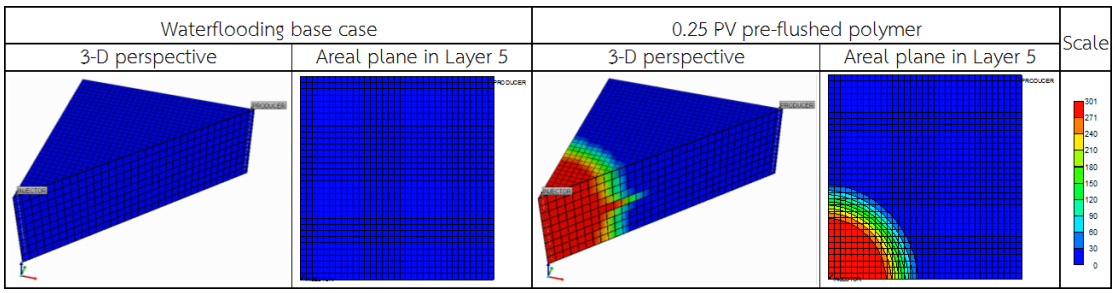

(a)

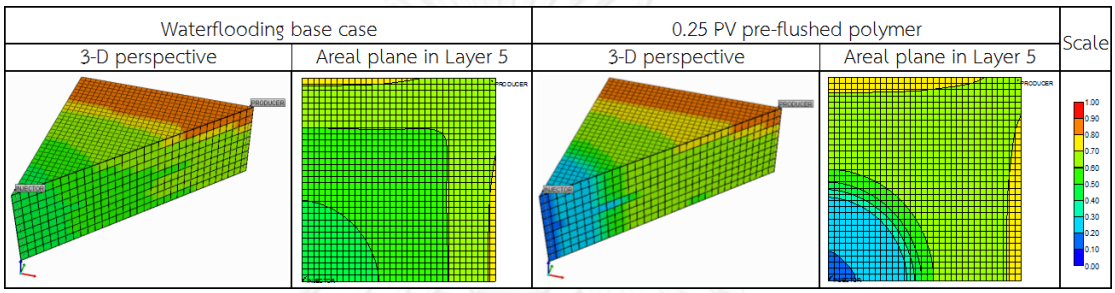

(b)

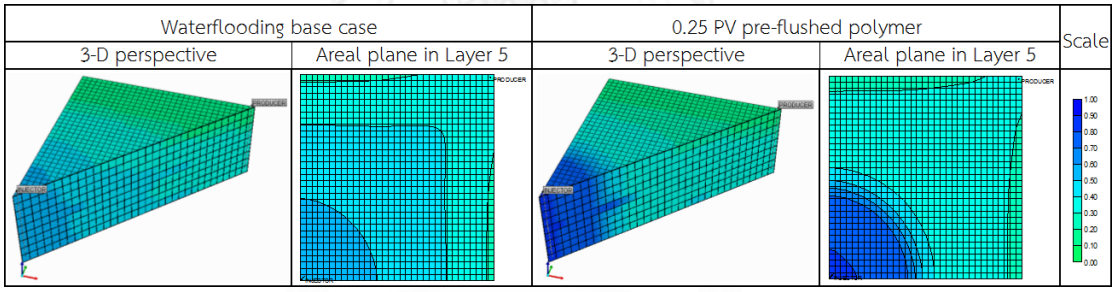

(c)

Figure 5.33 Effect of pre-flushed polymer on various tracked parameters at 3rd year, 7th month (a) Polymer concentration profiles (b) Oil saturation profiles (c) Water saturation profiles

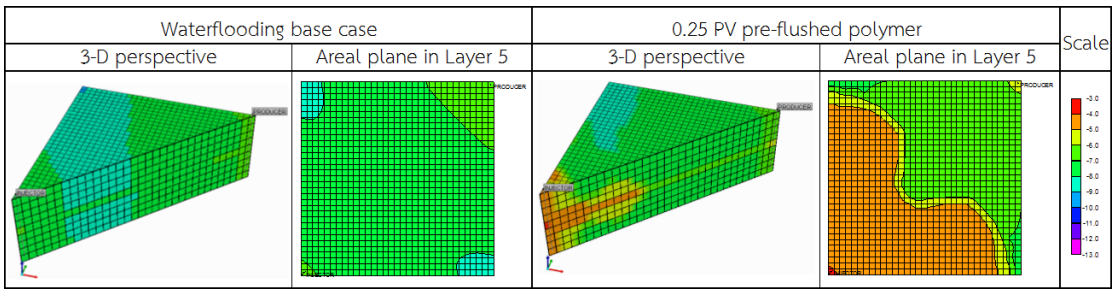

(a)

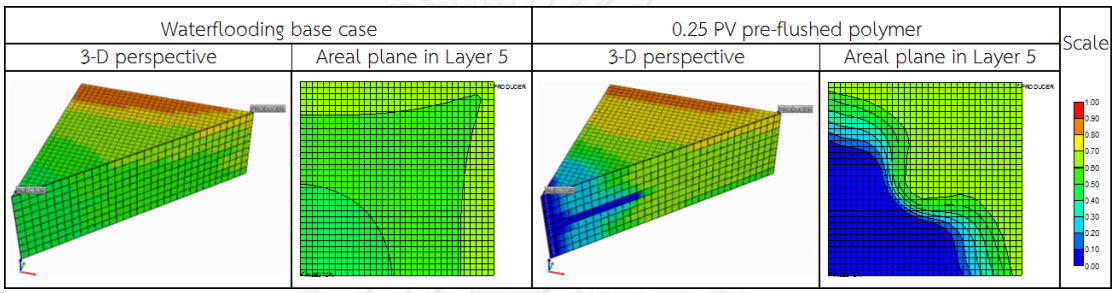

(b)

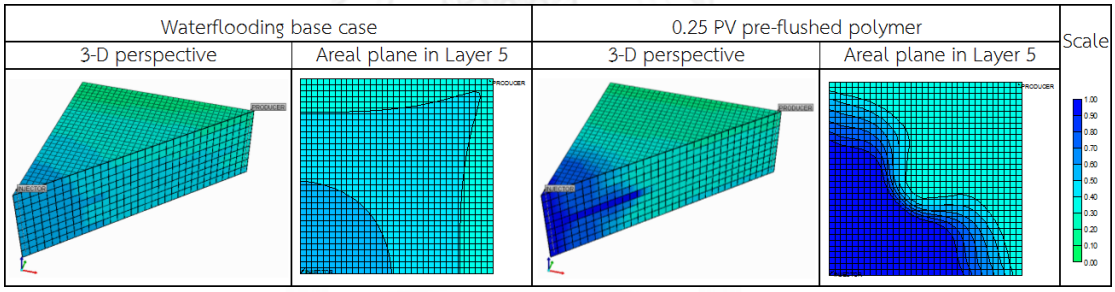

(c)

Figure 5.34 Effect of alkali-surfactant on various tracked parameters at 5^{th} year, 7^{th} month (a) Polymer concentration profiles (b) Oil saturation profiles (c) Water saturation profiles

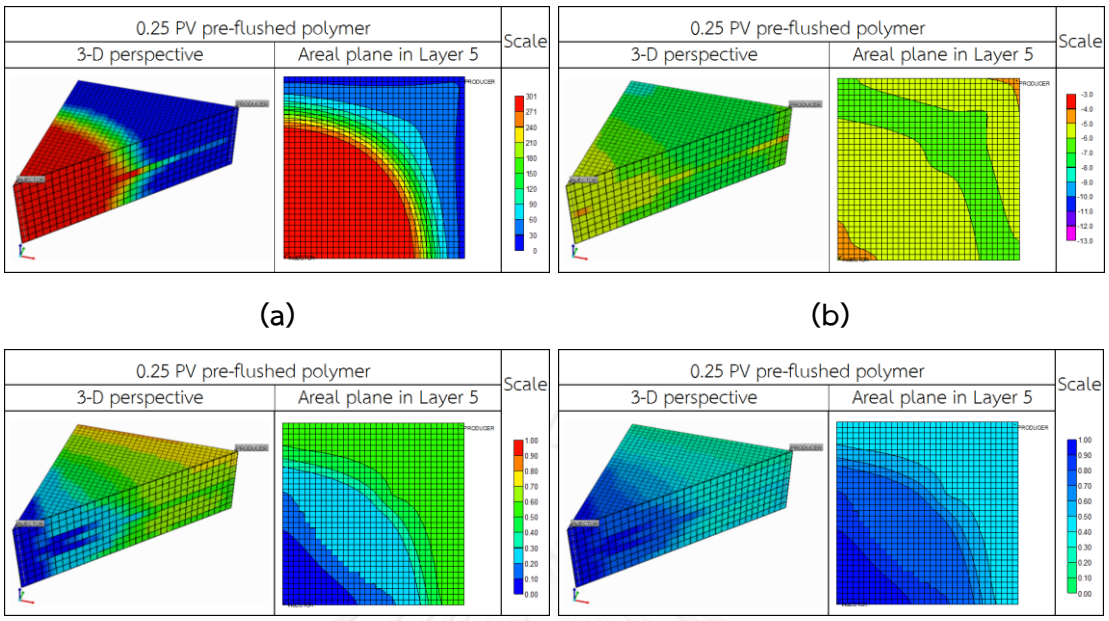

Figure 5.35Effect of post-flushed polymer on various tracked parameters at 13th year, 8th month (a) polymer concentration profiles (b) log capillary number profiles (c) oil saturation profiles (d) water saturation profiles

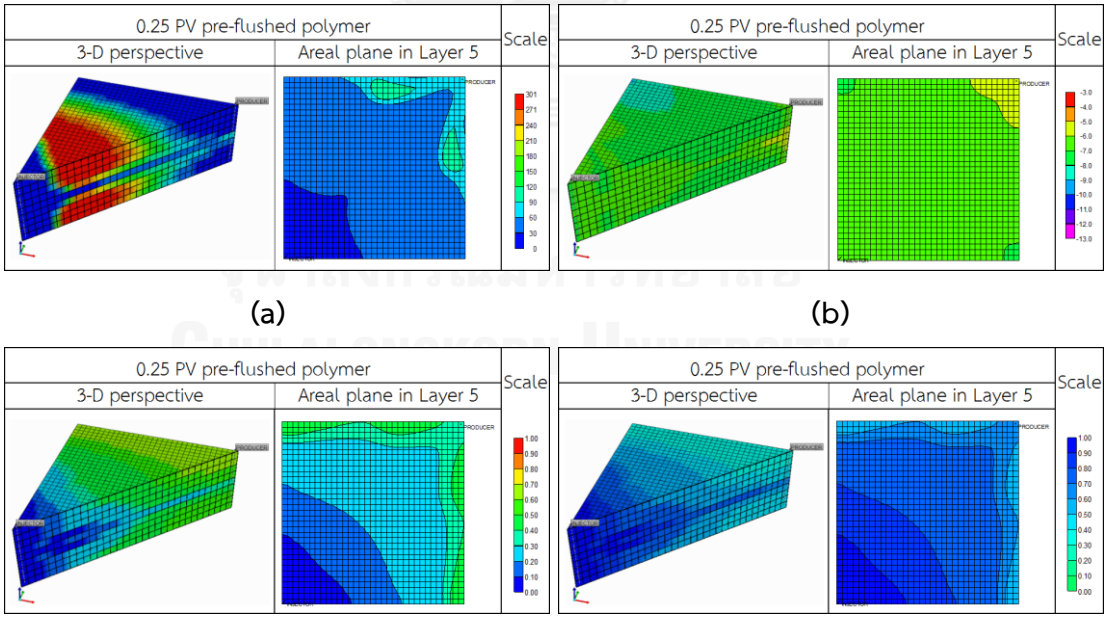

Figure 5.36 Effect of chasing water on various tracked parameters at 20th year, 8th month (a) polymer concentration profiles (b) log capillary number profiles (c) oil saturation profiles (d) water saturation profiles

5.3.2 Slug-size of Alkali-Surfactant

Before the slug size of alkali-surfactant (AS) in between double-slug polymer (P+AS+P) is identified, water is used to performed in between double-slug polymer (P+W+P) instead of AS slug by varying the slug size of water from 0.10 PV to 0.25 PV. Pre-flushed and post-flushed slugs are already determined as 0.25 PV and 0.55 PV in previous section, respectively. After that the chasing water is injected until the end of production. Sequential injection of water in between double-slug polymer (P+W+P) is illustrated in Figure 5.37. Recovery factors of various water slugs in between double-slug polymer are summarized in Figure 5.38. Results show that recovery factor is dropped when amount of water is increased. Effect of water slug can be considered from summary of oil and water production rates in Figures 5.39 and 5.40. In case of 0.20 PV and 0.25 PV of water slug, oil production rates are decreased to lower than economic limit during the post-flushed polymer injection period shown in Figure 5.39. Decreasing of oil production rate is caused by very high water production rate shown in Figure 5.40. Therefore, double-slug polymer can handle water slug in between not over than 0.15 PV.

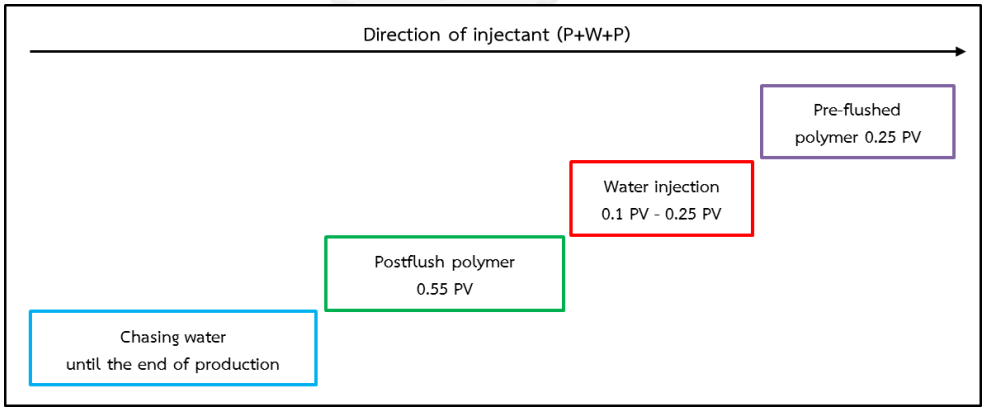

Figure 5.37 Sequential injection of study slug size of water in between double-slug polymer (P+W+P)

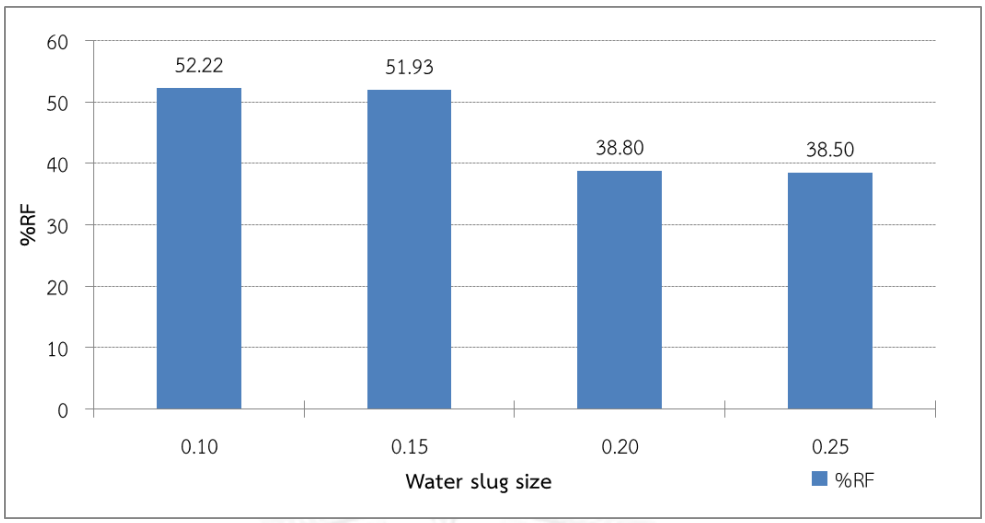

Figure 5.38 Recovery factors of various water slug sizes in between double-slug polymer

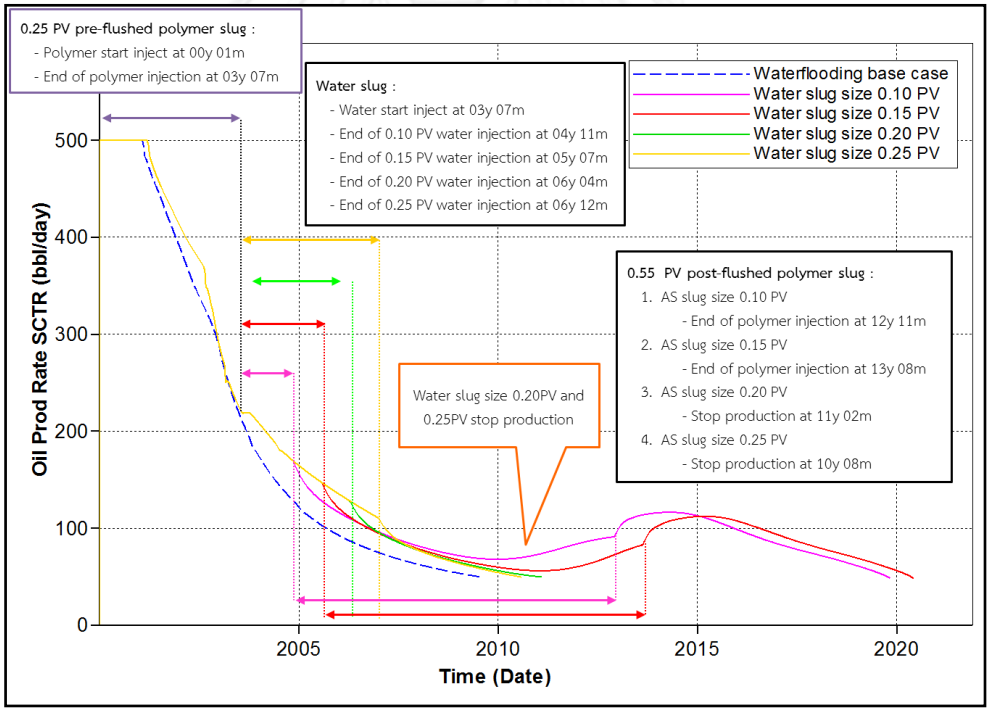

Figure 5.39 Oil production rates of various water slugs in between double-slug polymer compared to waterflooding base case as a function of time

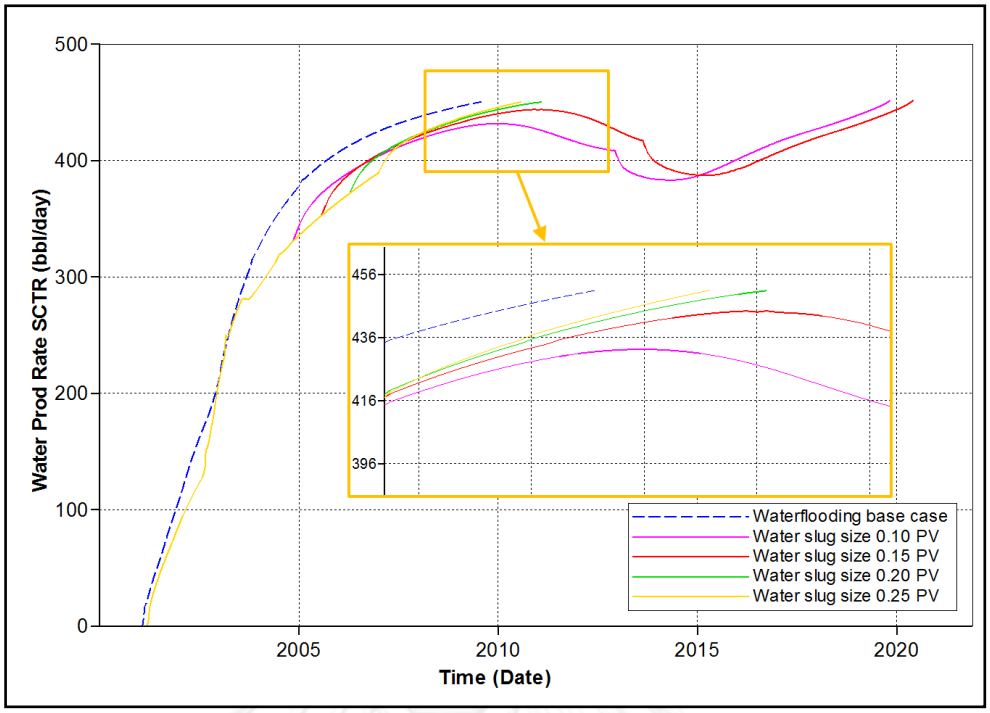

Figure 5.40 Water production rates of various water slugs in between double-slug polymer compared to waterflooding base case as a function of time

The study of AS slug size has an objective to identify the optimized slug of AS with proper amount of injected chemical. The slug size of AS is varied from 0.10 PV to 0.25 PV, placing in between pre-flushed and post-flushed polymer slugs which are fixed as 0.25 PV and 0.55 PV, respectively. After that, chasing water is injected until the end of production. Sequential injection of alkali and surfactant in between double-slug polymer (P+AS+P) is illustrated in Figure 5.41. Recovery factor and amount of additional oil produced per mass of surfactant used are used to select the best conditions. Recovery factor is also extracted from result in CMG, whereas the amount of additional oil produced per mass of surfactant used (bbl oil/mass of surfactant) is calculated from the amount of additional oil produced compared to water in between double-slug of polymer cases (P+W+P) divided by mass of surfactant used.

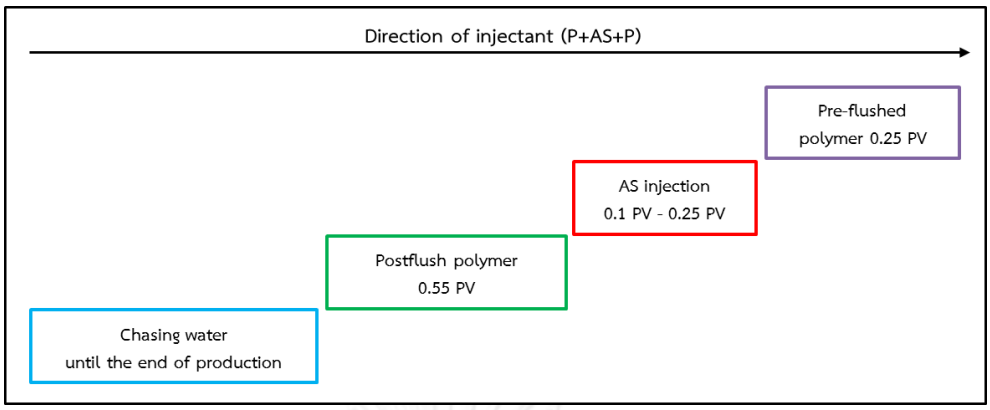

Figure 5.41 Sequential injection of study slug size of alkali and surfactant in between double-slug polymer (P+AS+P)

Recovery factor and amount of additional oil produced per mass of surfactant used of all various slug sizes of AS in between double-slug polymer cases are summarized in Figure 5.42, whereas recovery factors as a function of time are illustrated in Figure 5.43. From the results, optimal condition of AS slug is obtained at 0.10 PV. The 0.10 PV of AS slug yields the highest amount of additional oil produced per mass of surfactant used and recovery factor is not much different when increasing AS slug size.

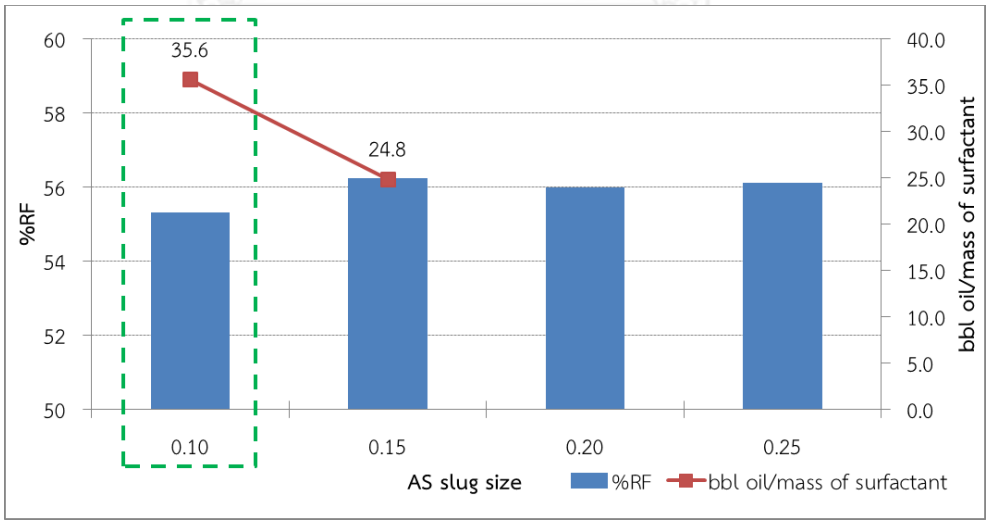

Figure 5.42 Recovery factors and additional oil produced per mass of surfactant used from various AS slug sizes

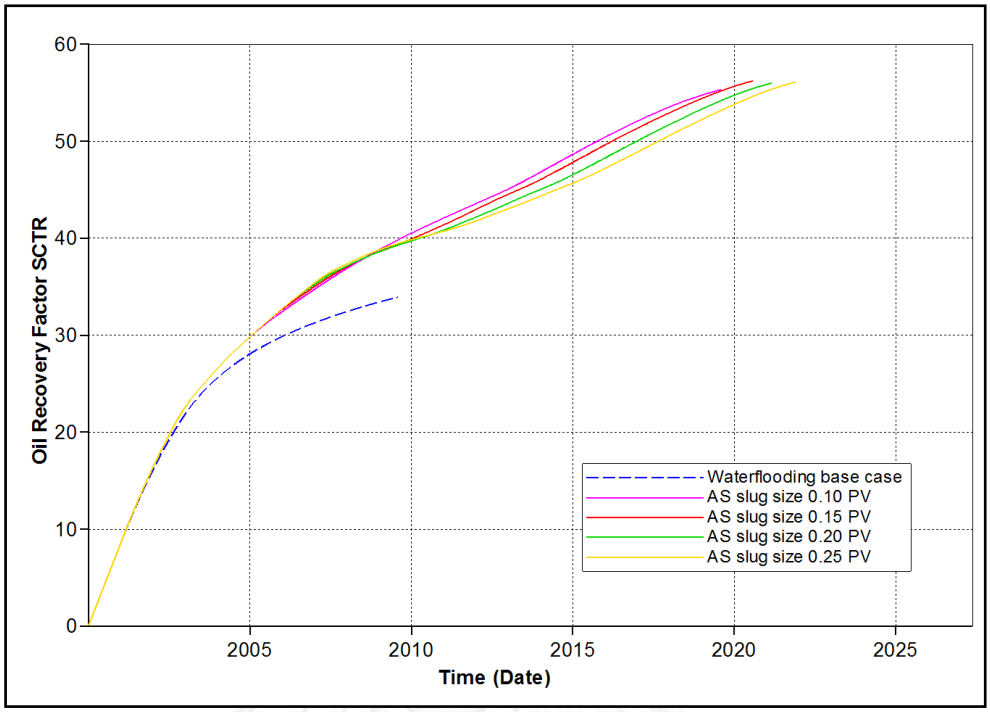

Figure 5.43 Recovery factors from various AS slug sizes in between double-slug polymer compared to waterflooding base case as a function of time

Effects of sequential injection of alkali-surfactant in between the P+AS+P flooding are demonstrated by oil and water production rate in Figures 5.44 and 5.45. AS slug is injected at the same time at 3rd year, 7th month but the end of injection depends on slug size as shown in Figures 5.44 and 5.45. Effects of various slug sizes of AS are considered at a month before seven years which is the end of 0.25 PV AS injection and 10th year, 7th month which is post-flushed polymer injection period. Parameters tracking at 6th year, 12th month and 10th year, 7th month are illustrated in Figures 5.46 and 5.47, respectively. In spite of the fact that incremental AS slug size from 0.1 PV to 0.25 PV increases oil production rate during 5th to 7th year as shown in Figure 5.44, water production rate is significantly increased during post-flushed polymer period. Therefore, AS gives both advantage and disadvantage at the same time. AS slug can reduce residual oil and increase relative permeability to water together resulting in increase of water saturation in reservoir as illustrated in Figure 5.46. Effect of AS slug cannot reach majority of reservoir volume except in high permeability channel as shown by log capillary number profile in Figure 5.46(a). Therefore, residual oil decreases very much only in high permeability channel as shown oil saturation profile in Figure 5.46(b), but water saturation is highly increased

as well in this location as shown by water saturation profile in Figure 5.46(c). Thus, this is the main reason that water production rate of incremental AS slug size is significantly increased during post-flushed polymer injection period. Oil saturation profile during post-flushed polymer injection in Figure 5.47(a) is not much different in each case, but water saturation profile shows more water channeling to producer when increasing AS slug size in Figure 5.47(b).

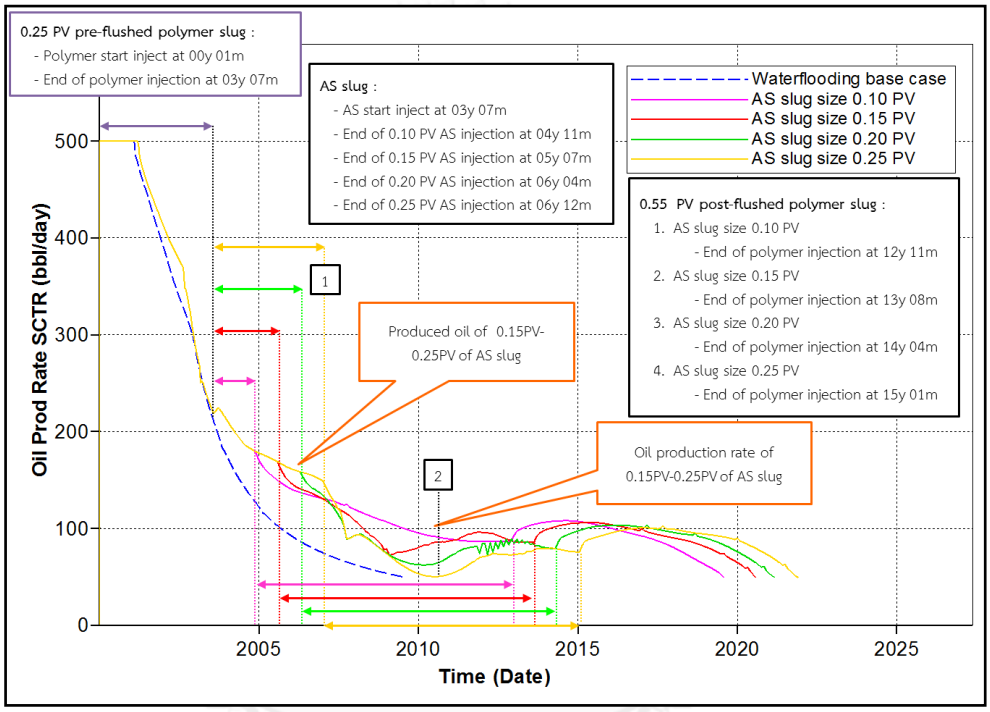

Figure 5.44 Oil production rates of various AS slugs in between double-slug polymer compared to waterflooding base case as a function of time

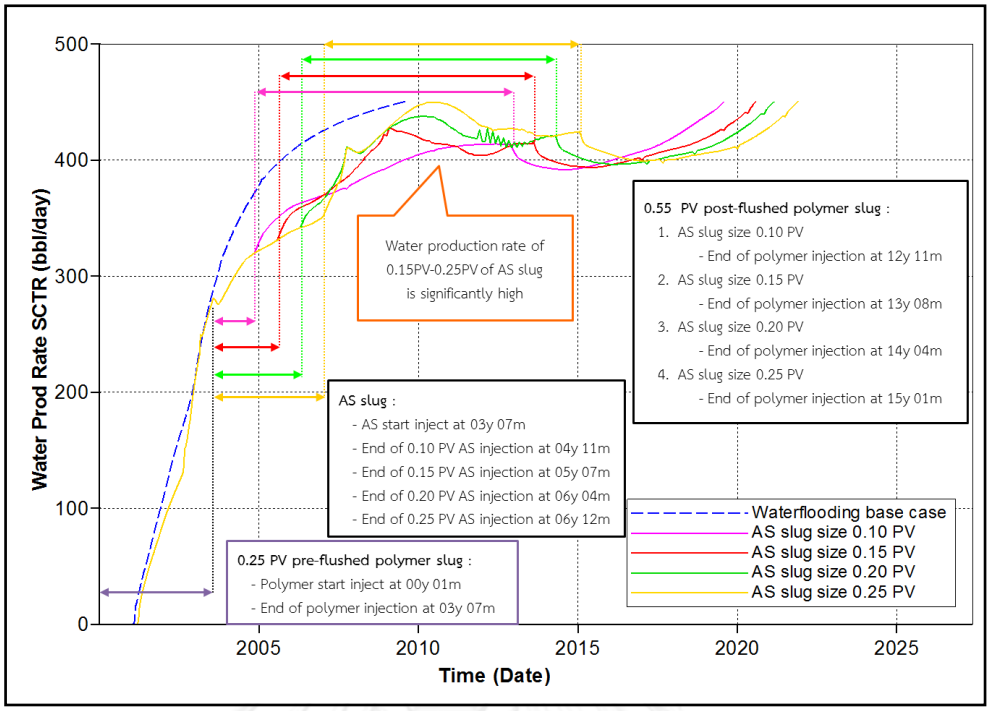

Figure 5.45 Water production rates of various AS slug in between double-slug polymer compared to waterflooding base case as a function of time

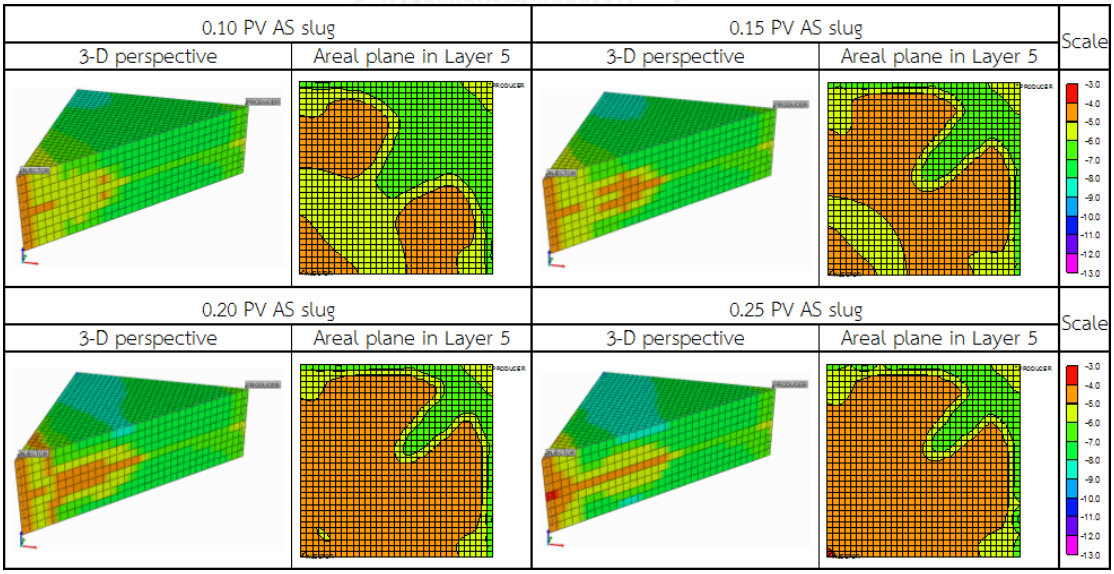

(a)

Figure 5.46 Effects of AS slug in various parameters at a 6th year, 12th month
(a) Log capillary number profile (b) Oil saturation profile
(c) Water saturation profile

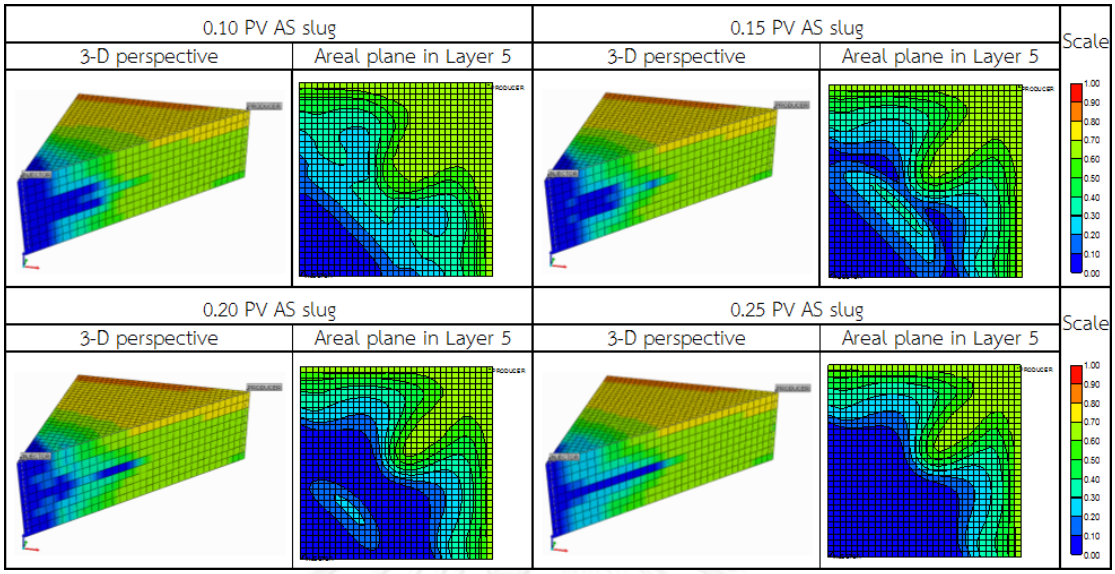

(b)

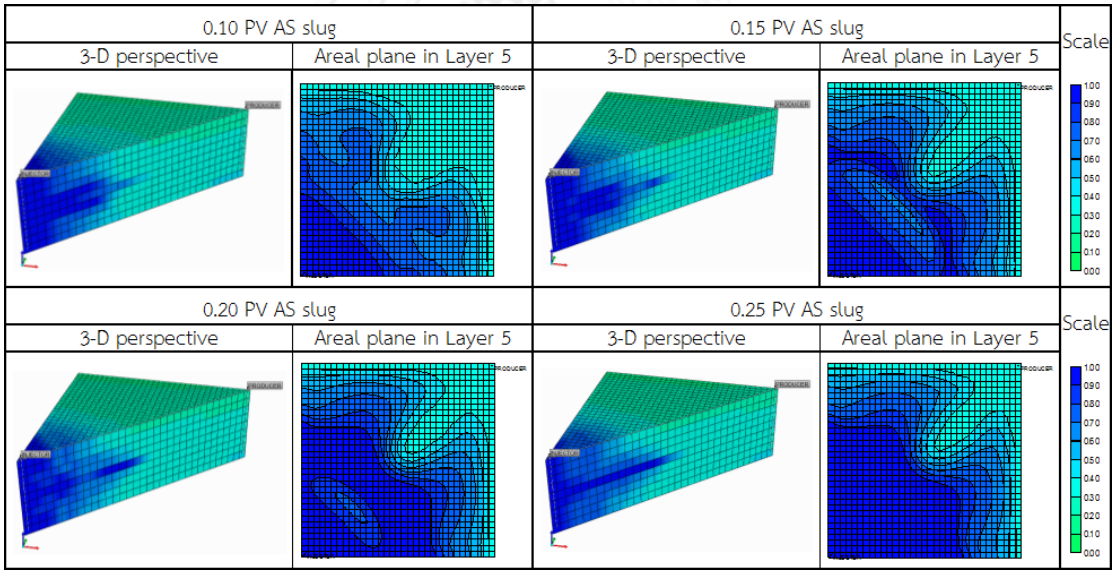

(c)

Figure 5.46 Effects of AS slug in various parameters at a 6th year, 12th month
(a) Log capillary number profile (b) Oil saturation profile
(c) Water saturation profile (continued)

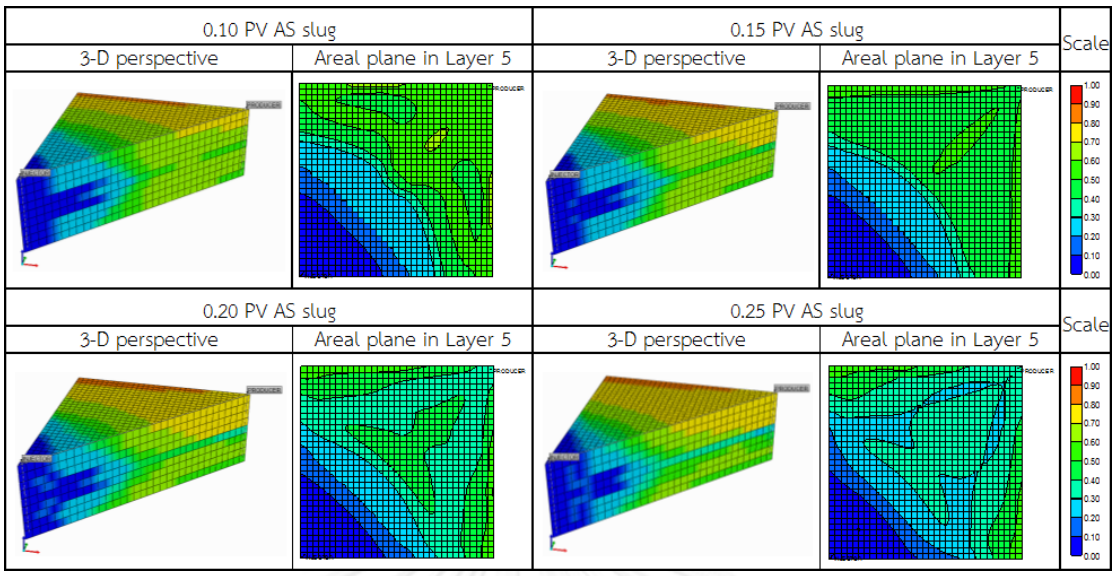

(a)

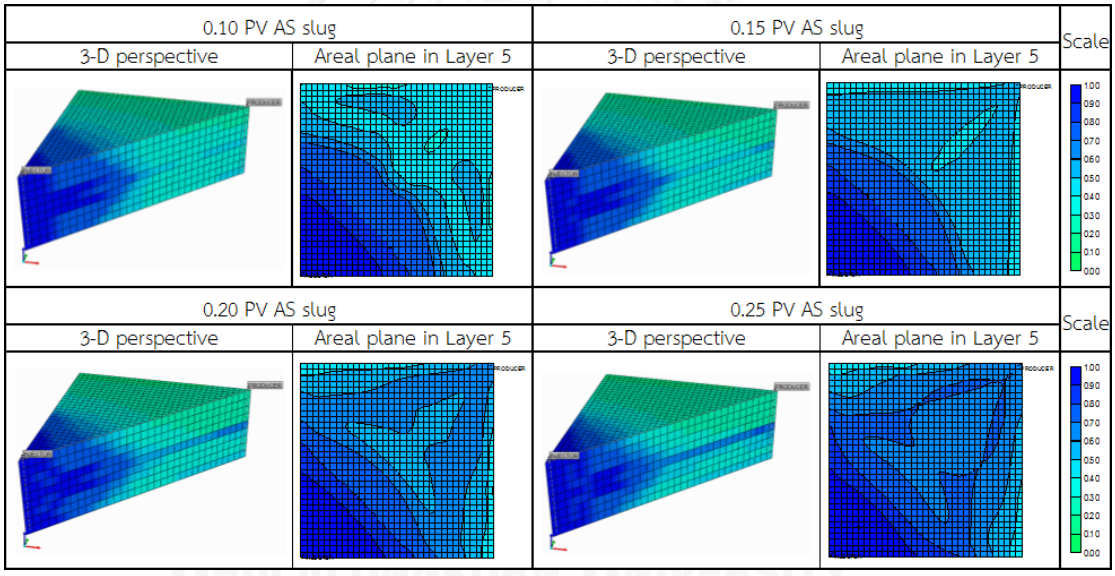

(b)

Figure 5.47 Effect of AS slug in various parameters at 10th year, 7th month
(a) Oil saturation profile (b) Water saturation profile

In summary, sequence of optimized case of pre-flushed polymer followed by alkali-surfactant slug and chased by polymer slug (P+AS+P) composes of 0.25 PV of pre-flushed polymer, 0.10 PV of AS slug, 0.55 PV of post-flushed polymer and chasing water until the end of production. Since total volume of injected chemical of P+AS+P case is specified, the case of alkali-surfactant slug chased by polymer slug (AS+P) is also kept at the same volume of injected chemical as same as P+AS+P flooding case to make both processes comparable. Hence, alkali-surfactant slug chased by polymer slug (AS+P) comprises 0.10 PV of AS slug, 0.80 PV of post-flushed polymer and chasing water until the end of production. Sequential injection of P+AS+P flooding and AS+P flooding are concluded in Figure 5.48.

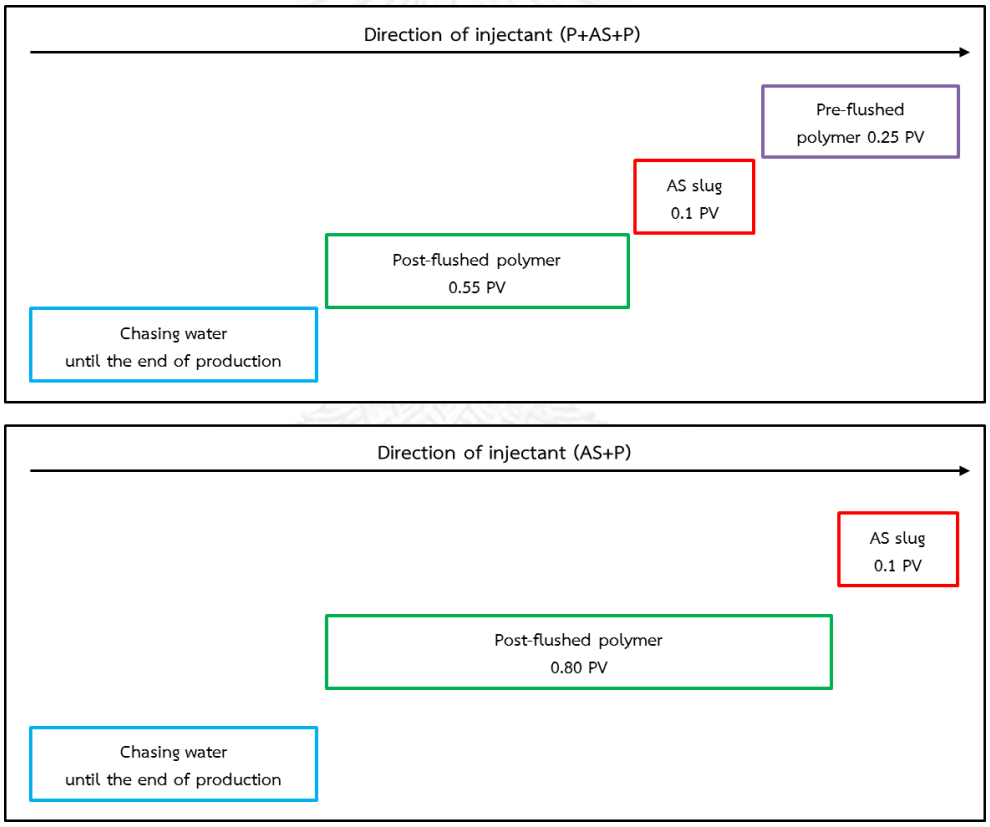

Figure 5.48 Sequential injection of P+AS+P flooding and AS+P flooding

5.4 Heterogeneous Models

In previous section, sequential injection of pre-flushed polymer followed by alkali-surfactant slug and chased by polymer slug (P+AS+P) and alkali-surfactant slug and chased by polymer slug (AS+P) are determined on the heterogeneous model 01A in which the middle layer is high permeability channel in x and y direction. In this section, high permeability channel is varied in both areal and vertical direction. However, volume of matrix containing high permeability is kept constant for all cases. Appearance of various high permeability channels are illustrated in Figure 4.23, and different models are summarized in Table 5.6. Waterflooding is performed in all models as reference before performing P+AS+P and AS+P flooding. Total production period, recovery factor and water/oil production ratio are the simulation outcome used to consider performance of each method. Water/oil production ratio is calculated from total water production divided by total oil production. Water/oil production ratio can be used to determine the amount of water produced at the same amount of oil produced. Result of each models are classified into groups in areal plane direction. After that, summary for all cases is discussed in last subsection.

Table 5.6 Summary of heterogeneous models

		Vertical Plane			
		All layer	In the middle	At the top	At the bottom
Arial Plane	Single layer	-	01A	02A	03A
	Parallel y-axis	01B	02B	03B	04B
	Parallel x-axis	01C	02C	03C	04C
	Across flow direction	01D	02D	03D	04D
	Single channel along flow direction	01E	02E	03E	04E
	Double channels along flow direction	01F	02F	03F	04F

5.4.1 Single-layered High Permeability Channel (Cases A)

Cases A comprise high permeability channel as single layer in one of nine layers of reservoir model. Cases A are divided into three patterns as shown in Figure 5.49. High permeability channel layer is located at the middle, top and bottom in Case 01A, 02A and 03A, respectively. Waterflooding, AS+P flooding and P+AS+P flooding performances are concluded in Table 5.7. Moreover, incremental of recovery factors of AS+P flooding and P+AS+P flooding compared to waterflooding are summarized in Figure 5.50. From these result, P+AS+P flooding can increase recovery factor approximately 20% from waterflooding in all cases, whereas differences of incremental recovery factor between AS+P flooding and P+AS+P flooding are around 3%. However, water/oil ratio shows that P+AS+P flooding produces less water than AS+P flooding in at the same amount of produced oil.

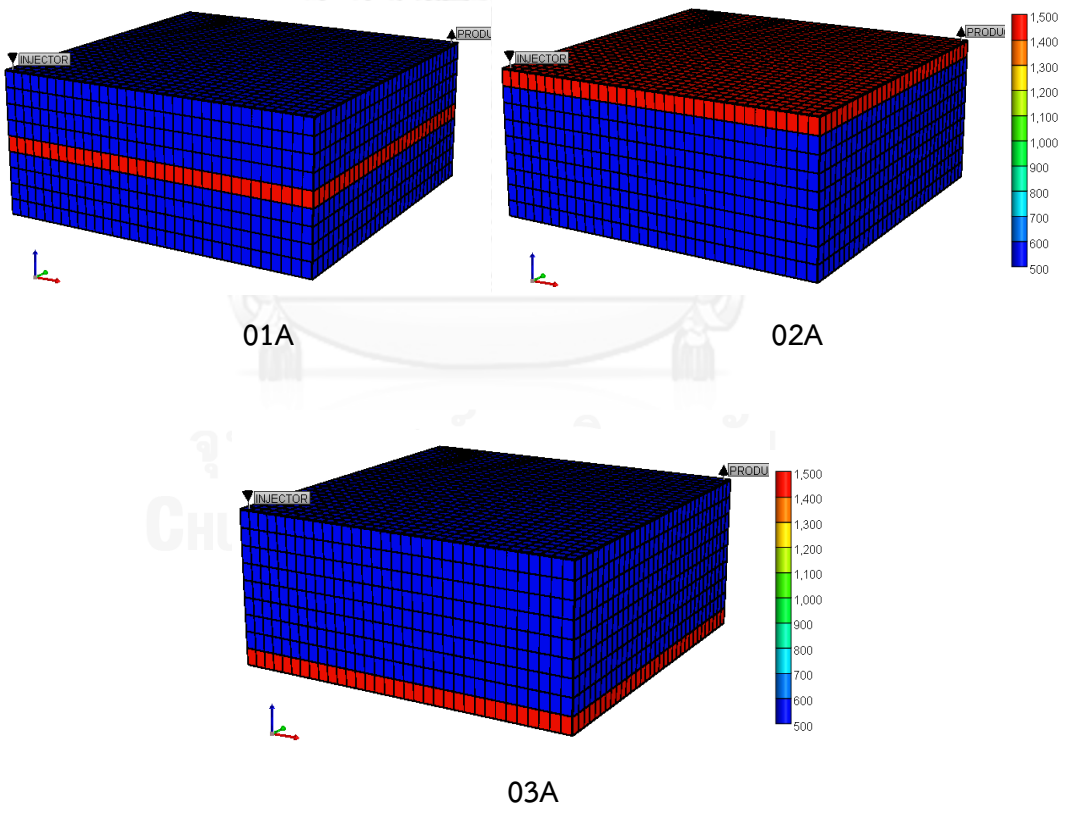

Figure 5.49 Location of high permeability channel in case A models, representing by red color

Table 5.7 Summary of simulation outcomes from waterflooding, AS+P flooding, P+AS+P flooding in reservoir models case A

Parameter	Strategy	01A	02A	03A
Production period	Waterflooding	09y 08m	09y 11m	10y 03m
	AS+P	18y 12m	19y 04m	19y 09m
	P+AS+P	19y 08m	20y 08m	20y 04m
Recovery factor (%)	Waterflooding	33.99	34.99	32.69
	AS+P	52.60	52.58	52.55
	P+AS+P	55.28	56.28	55.61
Water/Oil production ratio	Waterflooding	1.411	1.404	1.659
	AS+P	2.076	2.131	2.200
	P+AS+P	2.030	2.128	2.115

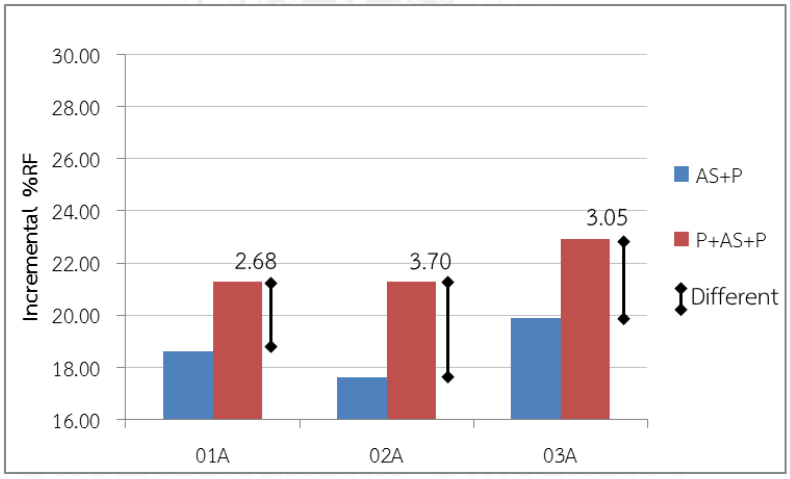

Figure 5.50 Comparison of incremental recovery factors of AS+P and P+AS+P flooding based on waterflooding in cases A

Recovery factor, oil and water production rates of waterflooding in cases 01A, 02A and 03A are illustrated in Figures 5.51 to 5.53. Results from waterflooding show that effects of gravity and water channeling in pronounced in case 03A in which high permeability channel is located at the bottom of reservoir. Comparing all cases, water production rate obtained from case 03A is the highest in first four years.

Afterward, water production rate of case 03A turns to the lowest due to replacement of residual oil by water after water breakthrough.

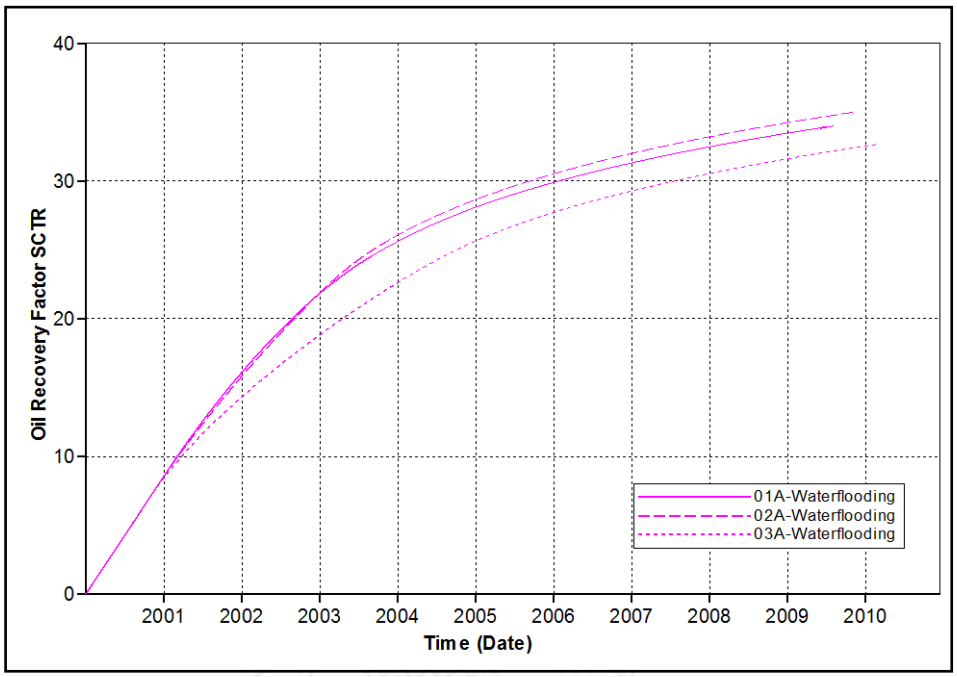

Figure 5.51 Recovery factors of waterflooding in cases A as a function of time

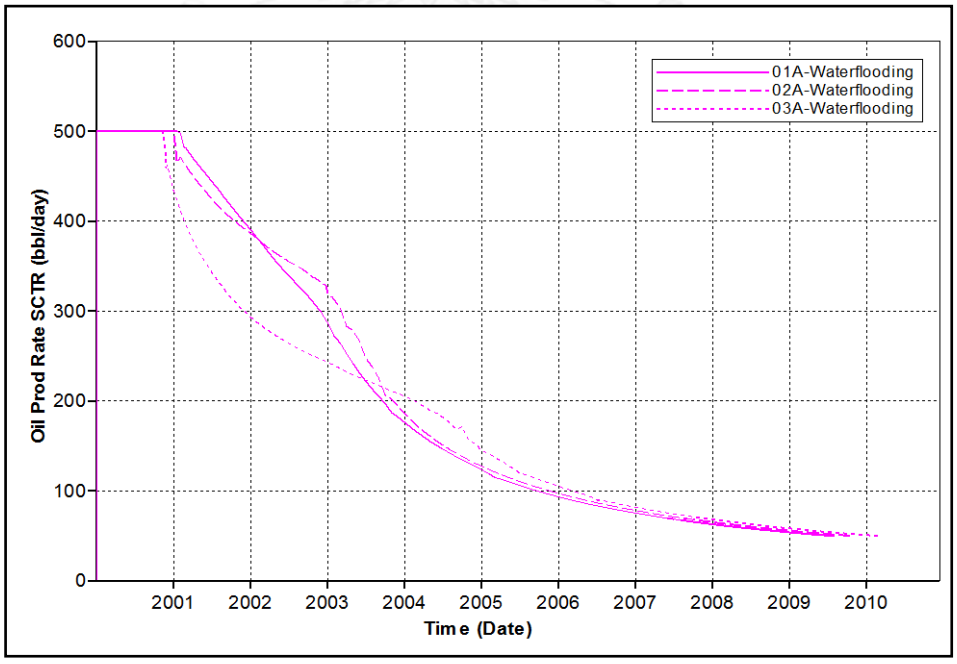

Figure 5.52 Oil production rates of waterflooding in cases A as a function of time

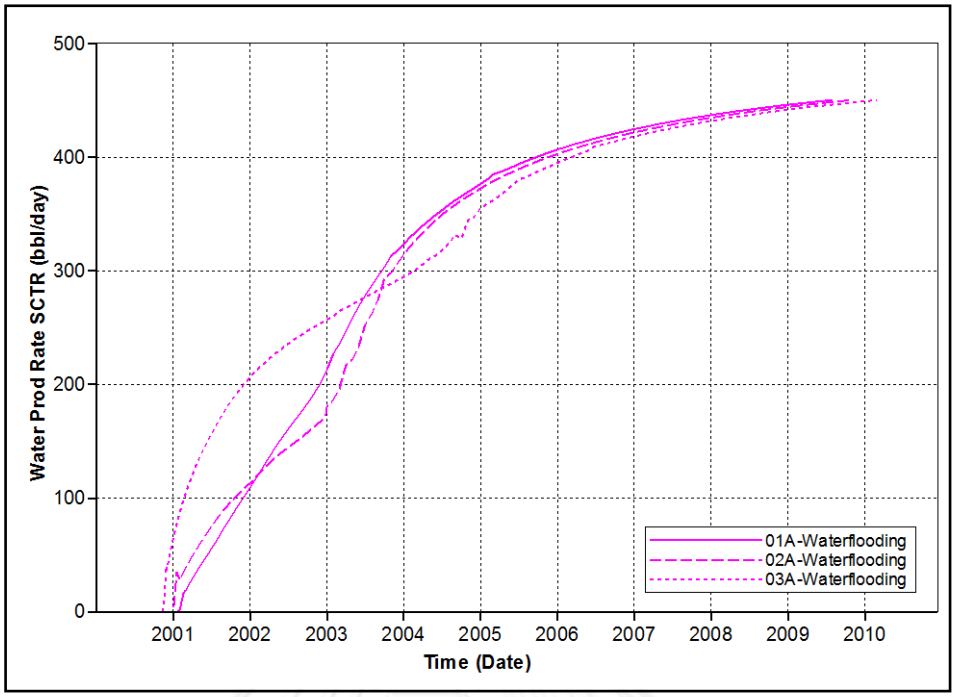

Figure 5.53 Water production rates of waterflooding in cases A as a function of time

Recovery factor, oil and water production rate of AS+P flooding and P+AS+P flooding from cases 01A, 02A and 03A are illustrated in Figures 5.54 to 5.56. From oil production rate shown in Figure 5.55, effects of gravity and water channeling can be noticed in both of AS+P and P+AS+P flooding. However, P+AS+P flooding can alleviate effect of gravity and water channeling better than AS+P flooding. Therefore, water production rate from AS+P flooding is higher than P+AS+P flooding for first four years. After that, post-flushed polymer can maintain stable front and improve sweep efficiency. Hence, oil production rate in the case AS+P flooding, which previously leaves highly un-swept oil in formation, is higher than P+AS+P flooding during post-flushed polymer period. Overall recovery factor of P+AS+P flooding is higher than that of AS+P flooding when combining the result of two periods.

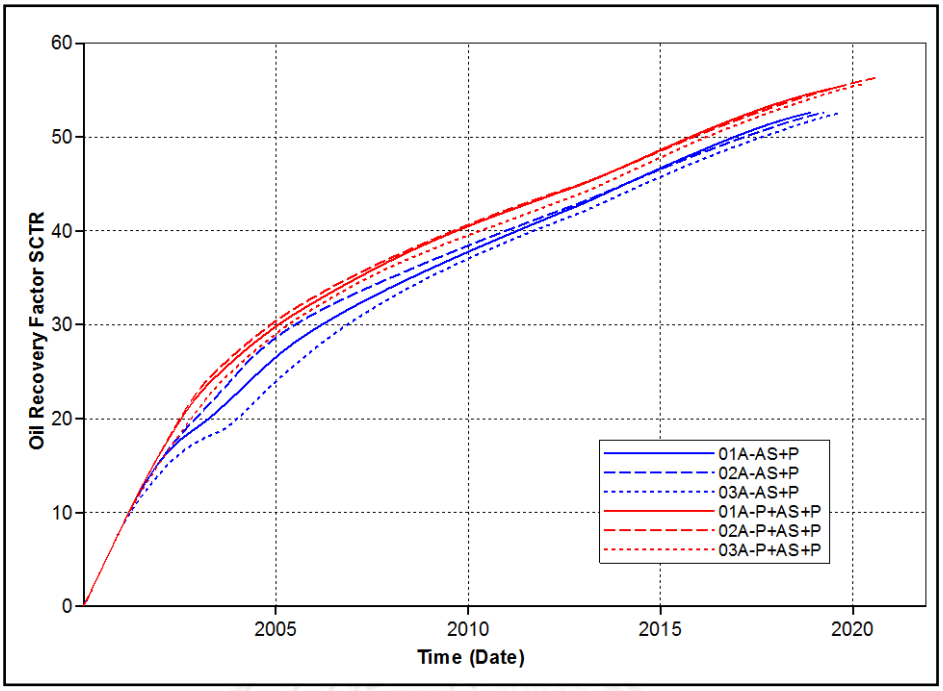

Figure 5.54 Recovery factors of AS+P and P+AS+P flooding in cases A as a function of time

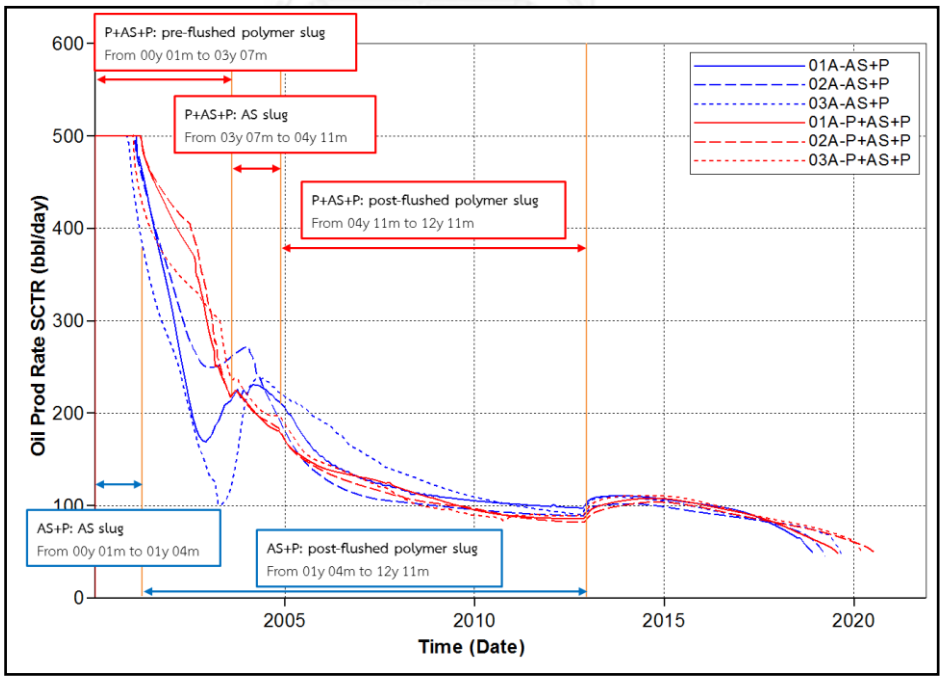

Figure 5.55 Oil production rates of AS+P and P+AS+P flooding in cases A as a function of time

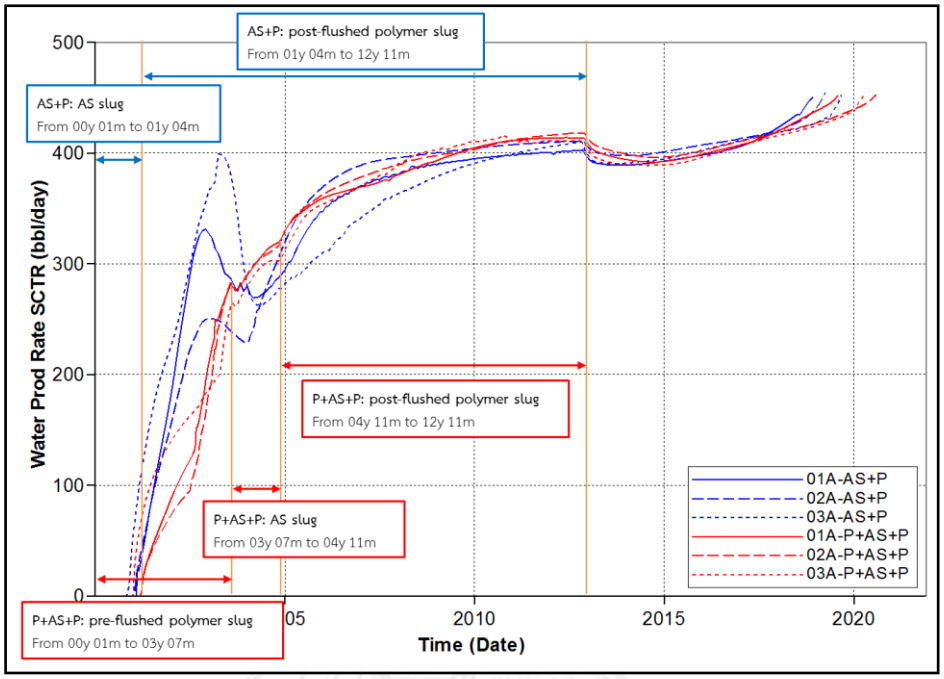

Figure 5.56 Water production rates of AS+P and P+AS+P flooding in cases A as a function of time

5.4.2 Parallel y-axis of High Permeability Channel (Cases B)

High permeability channel in cases B is located parallel to y-axis direction and in the middle between injector and producer as shown in Figure 5.57. High permeability channel is varied in all layers, at the middle, top and bottom and consecutively labeled as cases 01B, 02B, 03B and 04B, respectively. Results of waterflooding, AS+P and P+AS+P flooding performed in these models are summarized in Table 5.8. Moreover, incremental of recovery factor of AS+P and P+AS+P flooding based on waterflooding are summarized in Figure 5.58. Results show that incremental recovery factor of P+AS+P flooding compared to waterflooding can be distinguished from AS+P flooding in case 01B where high permeability channel is narrow, whereas difference of two methods in other cases are just visible. Water/oil ratio shows that P+AS+P flooding produces less water than AS+P flooding at the same amount of produced oil in every case.

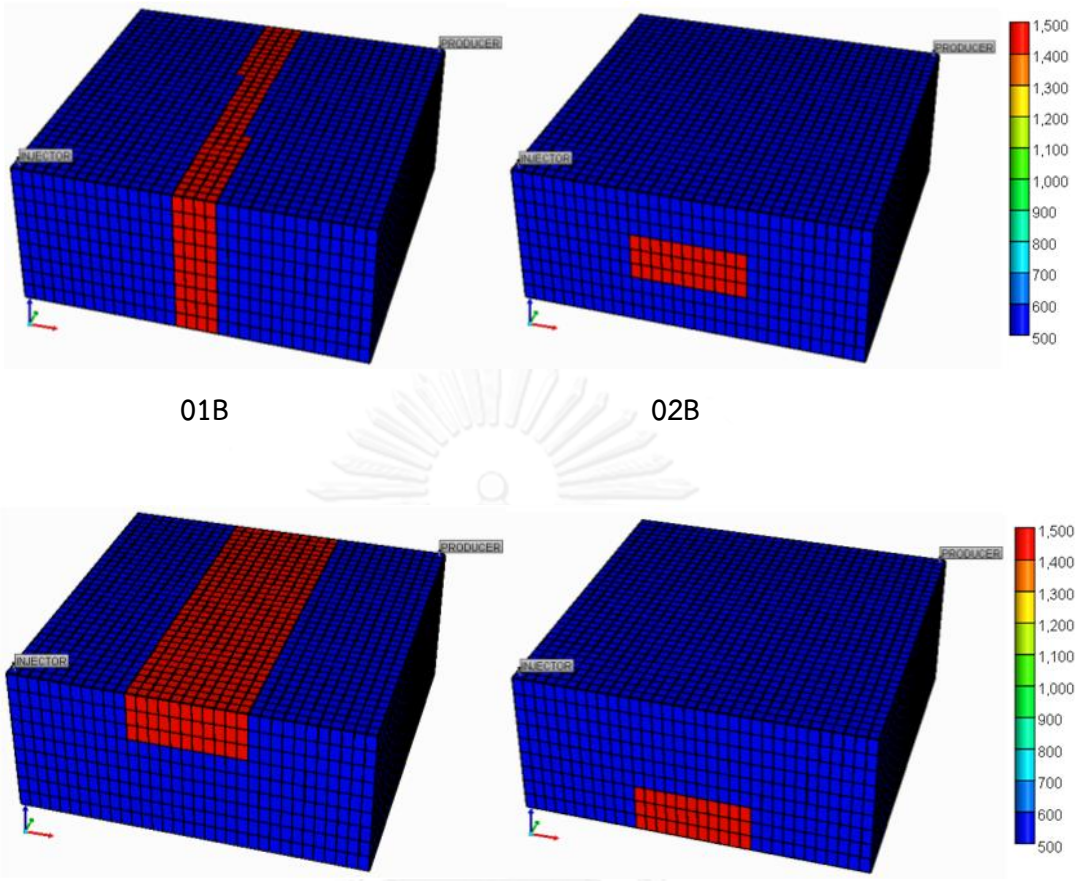

01B 02B

03B 04B

Figure 5.57 Location of high permeability channel in case B models, representing by red color

Table 5.8 Summary of simulation outcomes from waterflooding, AS+P flooding, P+AS+P flooding in reservoir models case B

Parameter	Strategy	01B	02B	03B	04B
Production period	Waterflooding	09y 05m	09y 06m	09y 05m	09y 07m
	AS+P	23y 02m	22y 04m	23y 03m	22y 11m
	P+AS+P	25y 09m	22y 07m	23y 05m	23y 08m
Recovery factor (%)	Waterflooding	34.03	34.03	34.19	33.95
	AS+P	56.21	55.33	56.02	55.85
	P+AS+P	63.73	60.19	61.06	61.29
Water/Oil production ratio	Waterflooding	1.345	1.367	1.334	1.393
	AS+P	2.513	2.439	2.536	2.496
	P+AS+P	2.445	2.196	2.268	2.290

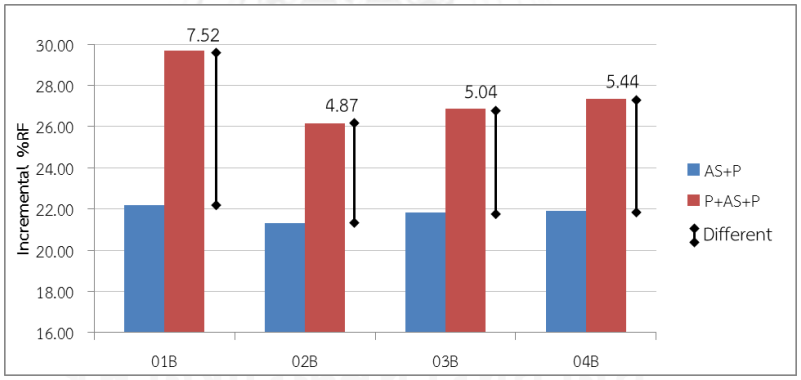

Figure 5.58 Comparison of incremental recovery factors of AS+P and P+AS+P flooding based on waterflooding in cases B

Recovery factor, oil and water production rates of waterflooding from cases 01B, 02B, 03B and 04B are illustrated in Figures 5.59 to 5.61. Recovery factors of all cases are not differentiated by means of waterflooding. By the way, effect from gravity segregation causes an early breakthrough in case 04B, resulting high water production rate around 2nd year of production life. Recovery factor, oil and water production rates of AS+P and P+AS+P flooding from cases 01B, 02B, 03B and 04B are

illustrated in Figures 5.62 to 5.64. Main mechanisms of each chemical can be described as same as in the previous section.

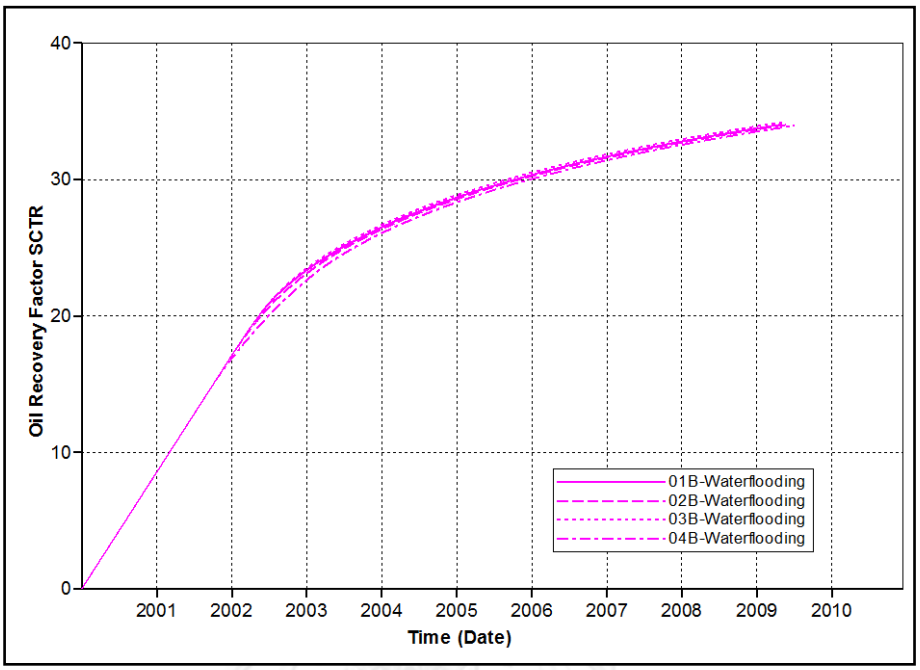

Figure 5.59 Recovery factors of waterflooding from cases B as a function of time

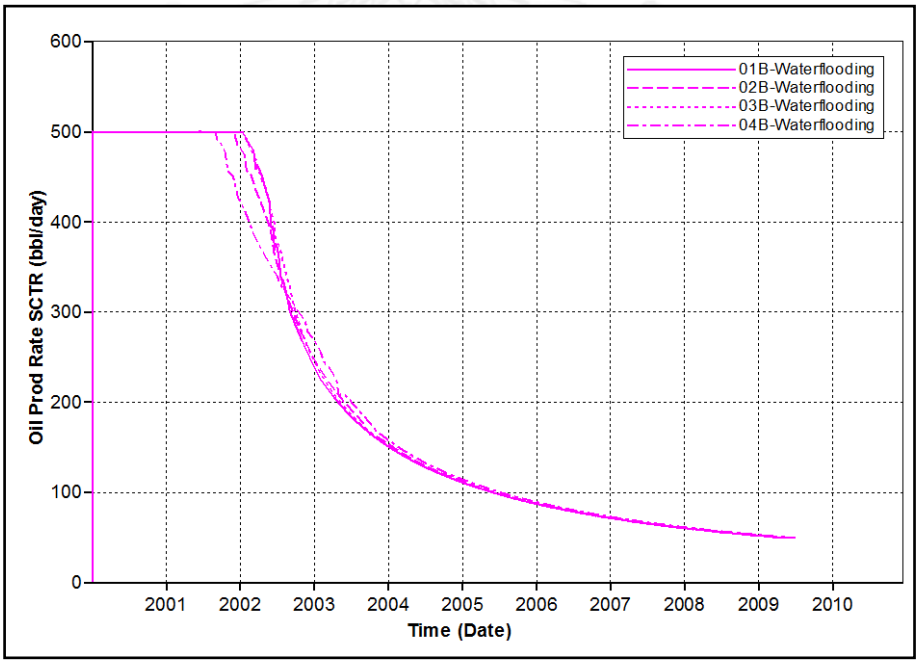

Figure 5.60 Oil production rates of waterflooding from cases B as a function of time

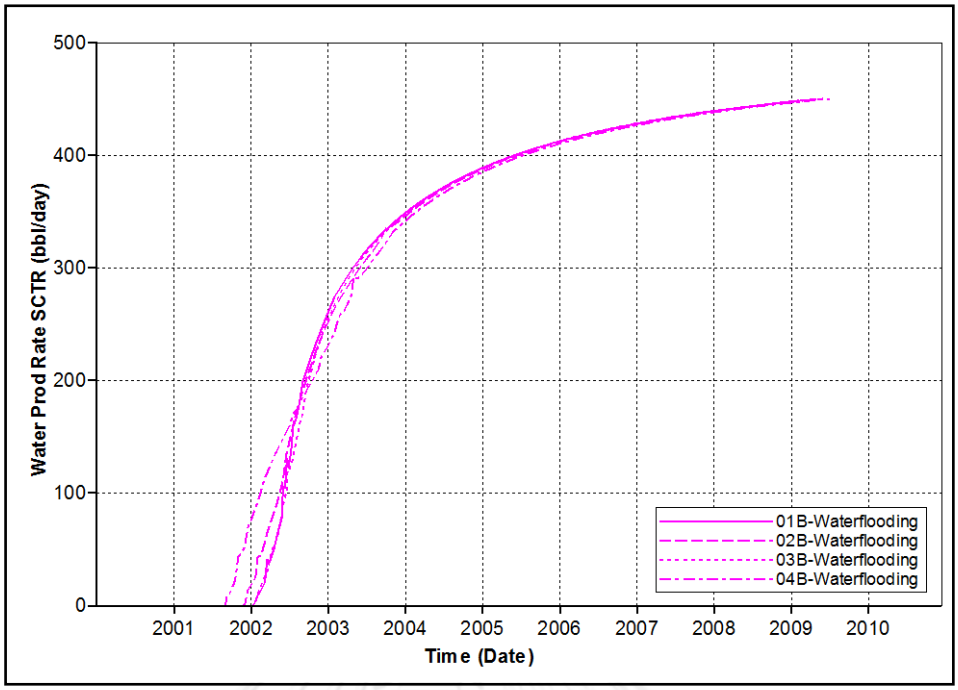

Figure 5.61 Water production rates of waterflooding from cases B as a function of time

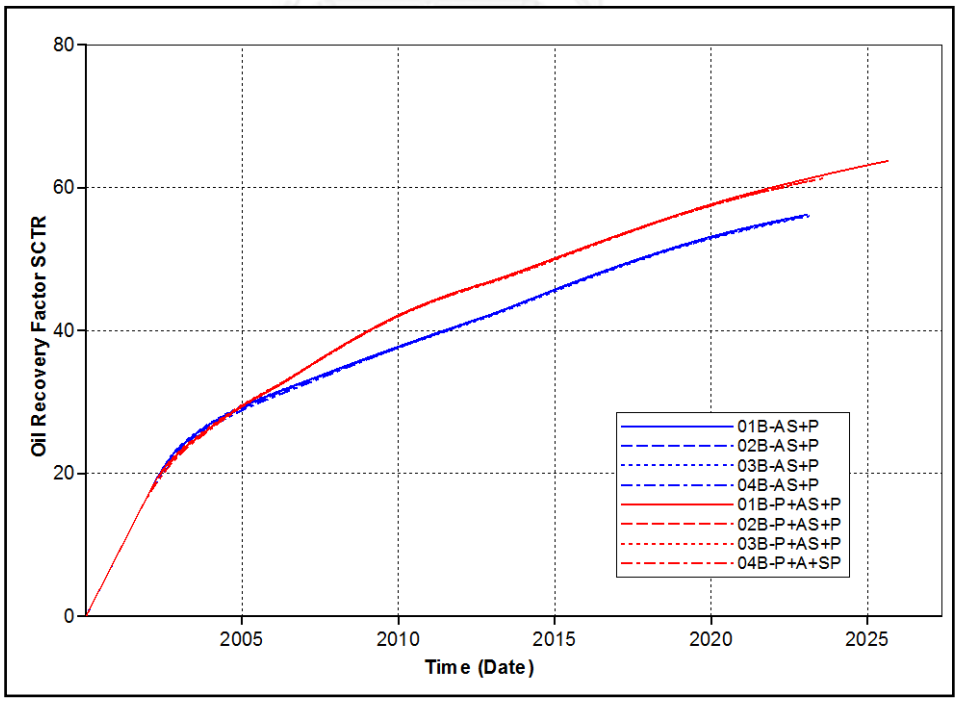

Figure 5.62 Recovery factors of AS+P and P+AS+P flooding from cases B as a function of time

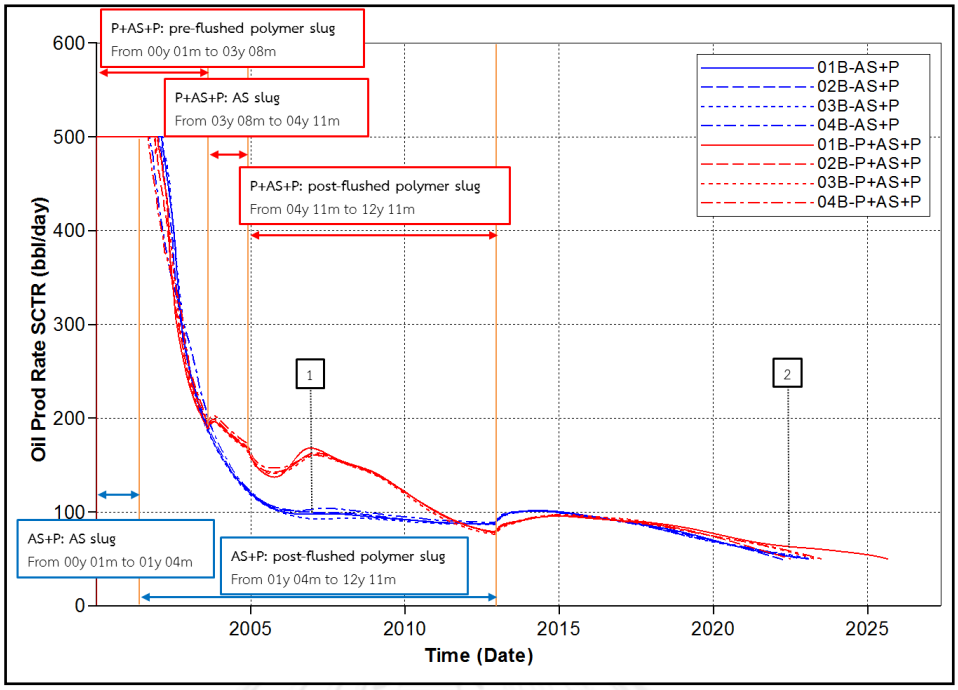

Figure 5.63 Oil production rates of AS+P and P+AS+P flooding in cases B as a function of time

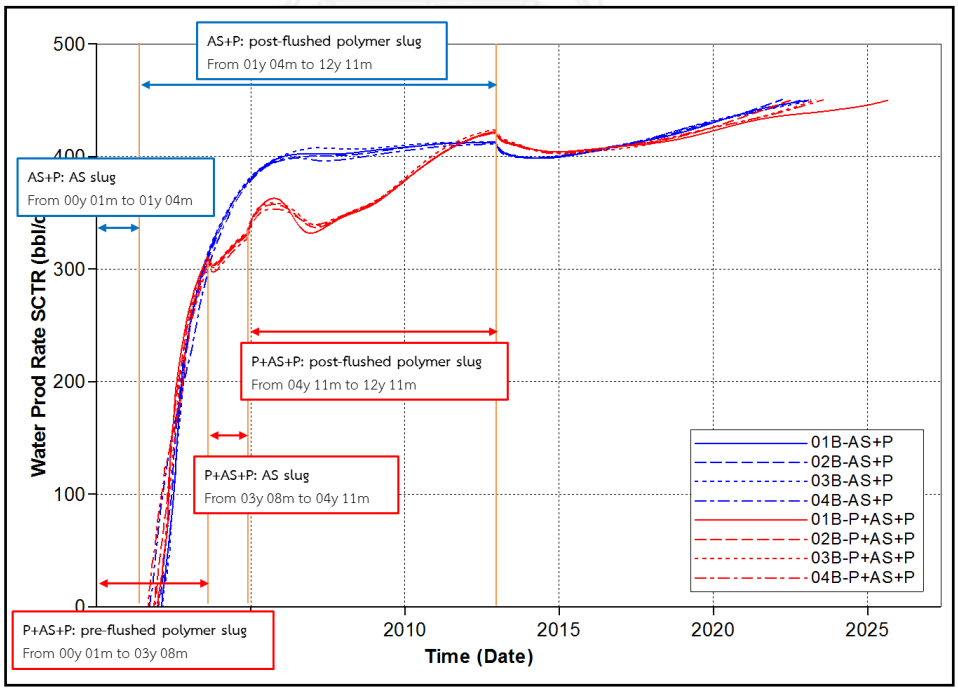

Figure 5.64 Water production rates of AS+P and P+AS+P flooding in cases B as a function of time

Difference between AS+P and P+AS+P flooding can be observed during 3rd to 12th year of production period. Even though AS slug and post-flushed polymer slug are injected during 3rd to 12th year of production period, pre-flushed polymer slug is the main part which creates difference between AS+P and P+AS+P flooding. Effect of pre-flushed polymer slug in case 01B model at 7th year, 1st month is shown in Figure 5.65. Figure 5.65(a) illustrates pre-flushed polymer concentration profile, where oil and water saturation profiles are shown in Figures 5.65(b) and 5.65(c). In case of P+AS+P flooding, blue color in oil saturation profile, which represents the area containing no residual oil from the result of AS slug, is larger than that of AS+P flooding case. It is a result of the presence of pre-flushed polymer that acts as buffer for AS slug to remove residual oil efficiently. Therefore, P+AS+P flooding can remove residual oil better than AS+P flooding in this period.

Comparison of P+AS+P flooding from case 01B and case 02B shows obviously different recovery factor. Post-flushed polymer is a reason which prolongs production period for case 01B. Effect of post-flushed polymer is considered in Figure 5.66 at 22nd year, 6th month which is near the end of production of case 02B. Post-flushed polymer slug of case 02B in Figure 5.6 (a) is broken and water saturation profile in Figure 5.66 (b) shows that chasing water tends propagate and by-pass polymer slug into producer. Therefore, production of case 02B is terminated. Although post-flushed of case 01B can maintain stability of flood front when high permeability channel is narrower than case 02B, production of case 01B can only be extended until post-flushed polymer slug is unstable by chasing water at around 25th year.

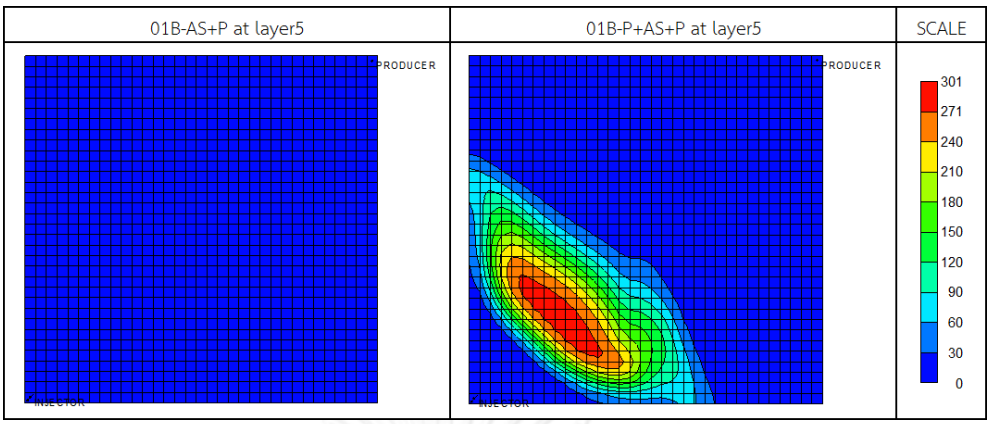

(a)

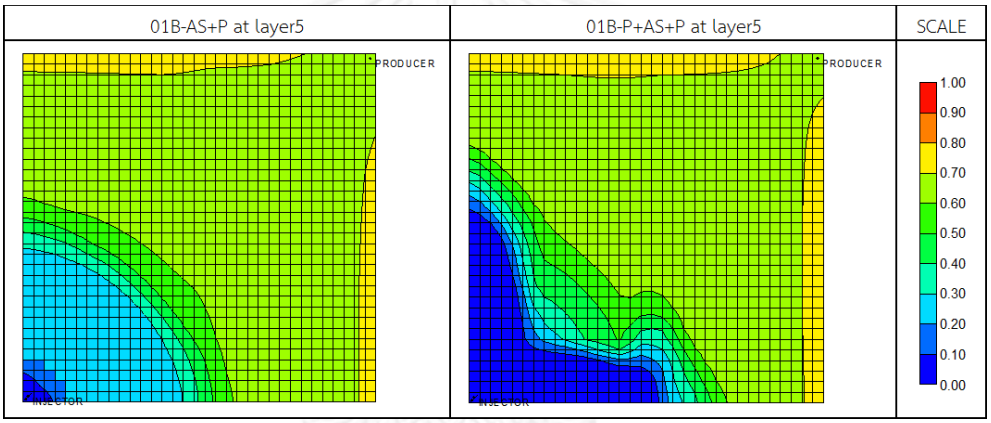

(b)

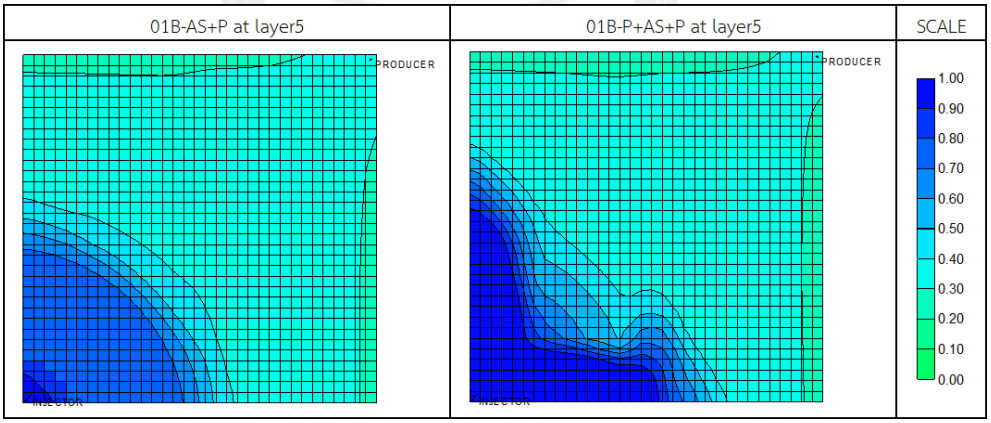

(c)

Figure 5.65 Effect of pre-flushed polymer in case 01B at 7th year, 1st month

(a) Polymer concentration profiles (b) Oil saturation profiles

(c) Water saturation profiles

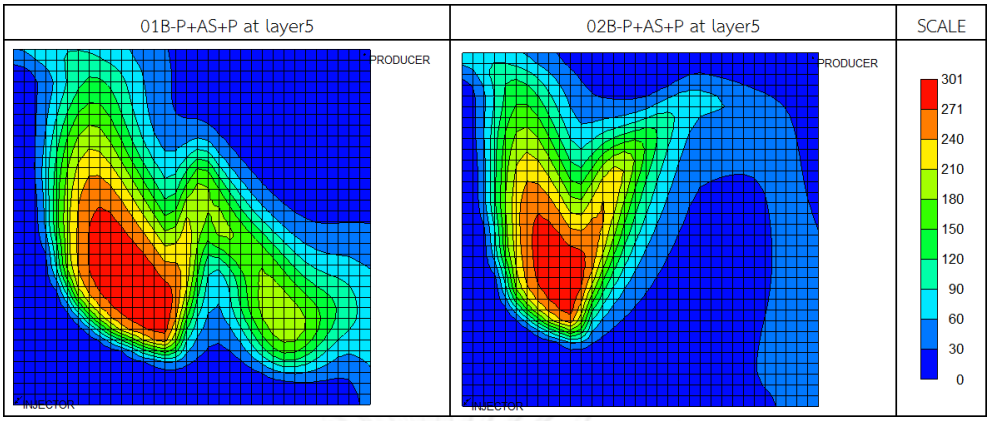

(a)

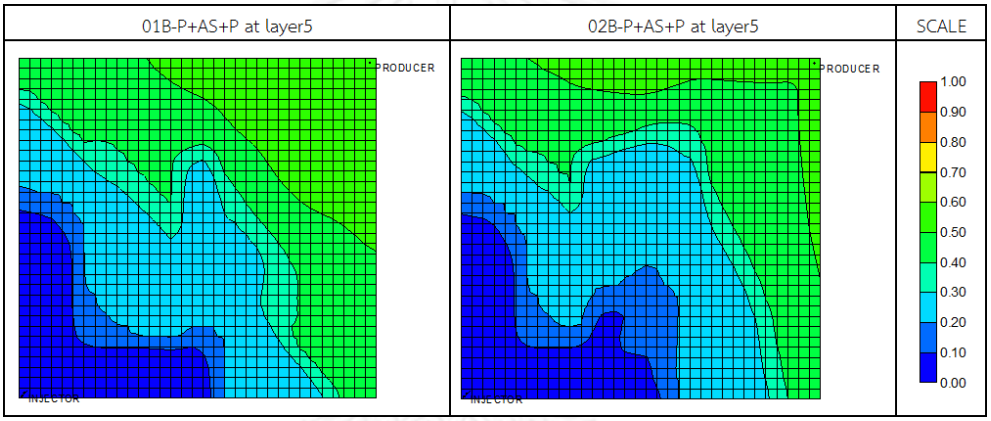

(b)

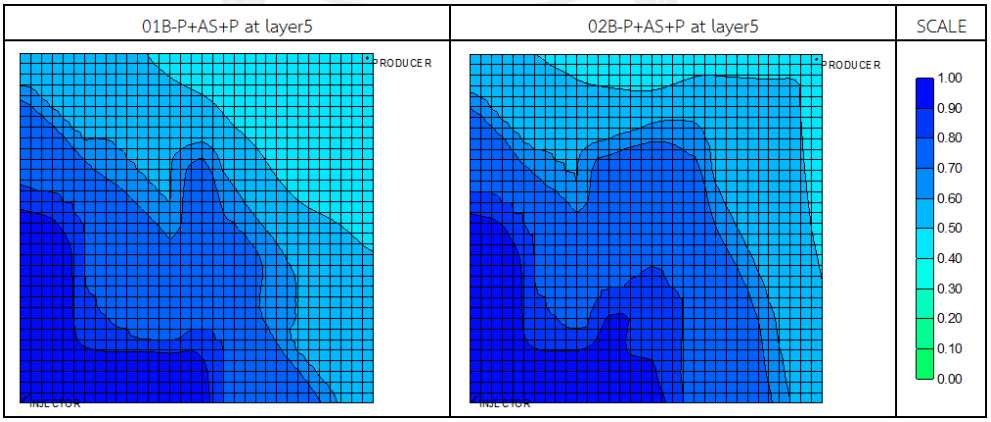

(c)

Figure 5.66 Effect of post-flushed polymer in cases 01B and 02B at 22nd year, 7th month (a) Polymer concentration profile (b) Oil saturation profile (c) Water saturation profile

5.4.3 Parallel x-axis of High Permeability Channel (Cases C)

High permeability channel in cases C is located parallel to x-axis direction and in the middle between injector and producer as shown in Figure 5.67. High permeability channel is located in all layers, at the middle, top and bottom in cases 01C, 02C, 03C and 04C, respectively. Result of waterflooding, AS+P and P+AS+P flooding performances are summarized in Table 5.9. Moreover, incremental of recovery factor of AS+P and P+AS+P flooding compared to waterflooding are shown in Figure 5.68. Incremental recovery factor of AS+P and P+AS+P flooding from waterflooding in cases C is as similar as cases B. Incremental recovery factor of P+AS+P flooding from waterflooding can be distinguished from cases of AS+P flooding in cases C as well as in cases B. Therefore, symmetric of high permeability structure yields the same result in cases B and cases C.

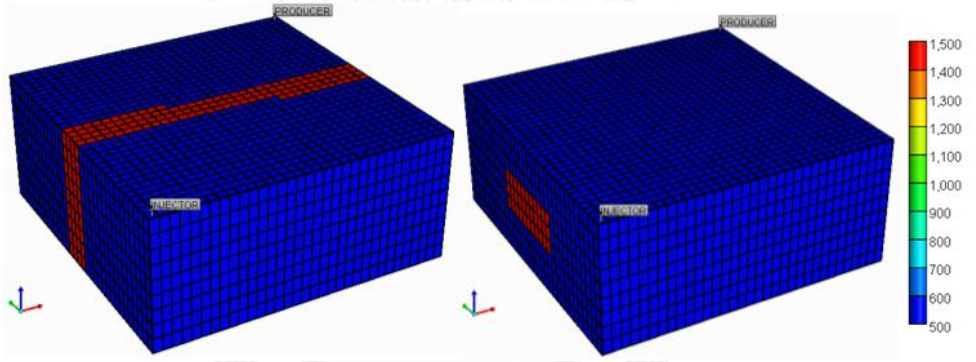

01C 02C

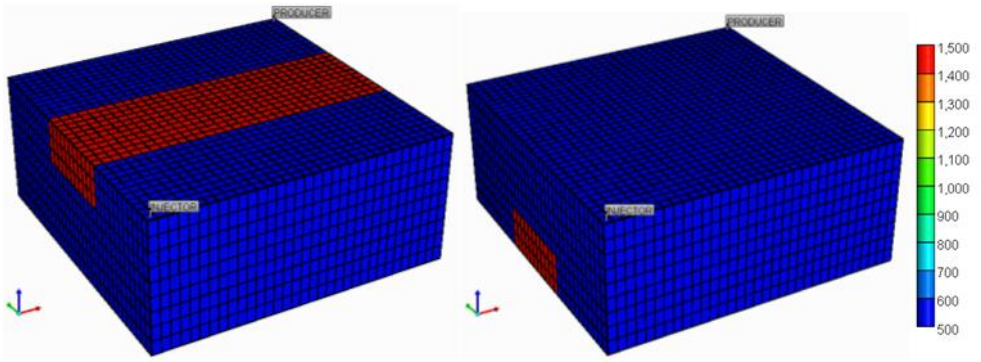

03C 04C

Figure 5.67 Location of high permeability channel in cases C models, representing by red color

Table 5.9 Summary of simulation outcomes from waterflooding, AS+P flooding, P+AS+P flooding in reservoir models case C

Parameter	Strategy	01C	02C	03C	04C
Production period	Waterflooding	09y 05m	09y 06m	09y 05m	09y 07m
	AS+P	23y 02m	22y 03m	23y 03m	22y 07m
	P+AS+P	25y 10m	22y 08m	23y 05m	23y 07m
Recovery factor (%)	Waterflooding	33.93	34.03	34.15	34.02
	AS+P	56.13	55.23	56.16	55.45
	P+AS+P	63.84	60.24	61.05	61.24
Water/Oil production ratio	Waterflooding	1.352	1.367	1.337	1.388
	AS+P	2.517	2.432	2.527	2.470
	P+AS+P	2.450	2.206	2.268	2.281

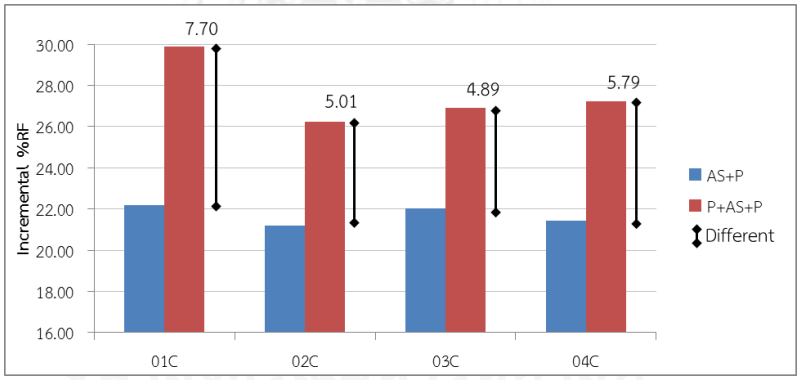

Figure 5.68 Comparison of incremental recovery factors of AS+P and P+AS+P flooding based on waterflooding in cases C

5.4.4 High Permeability Channel across Flow Direction (Cases D)

High permeability channel in Case D is located across direction and in the middle between injector and producer as shown in Figure 5.69. High permeability channel is varied in all layers, placed at the middle, top and bottom. These cases are labeled as cases 01C, 02C, 03C and 04C, respectively. Results of waterflooding, AS+P and P+AS+P flooding performance are summarized in Table 5.10. Moreover,

incremental of recovery factor of AS+P flooding and P+AS+P flooding compared to waterflooding are shown in Figure 5.70. From the figure, incremental recovery factors of AS+P and P+AS+P flooding from waterflooding of cases 01D, 02D, 03D and 04D are completely different in cases applied with AS+P flooding. Distinguish results of case D are similar to case 01B or 01C. Water/oil ratio shows that P+AS+P flooding produces less water than AS+P flooding at the same amount of produced oil in every case.

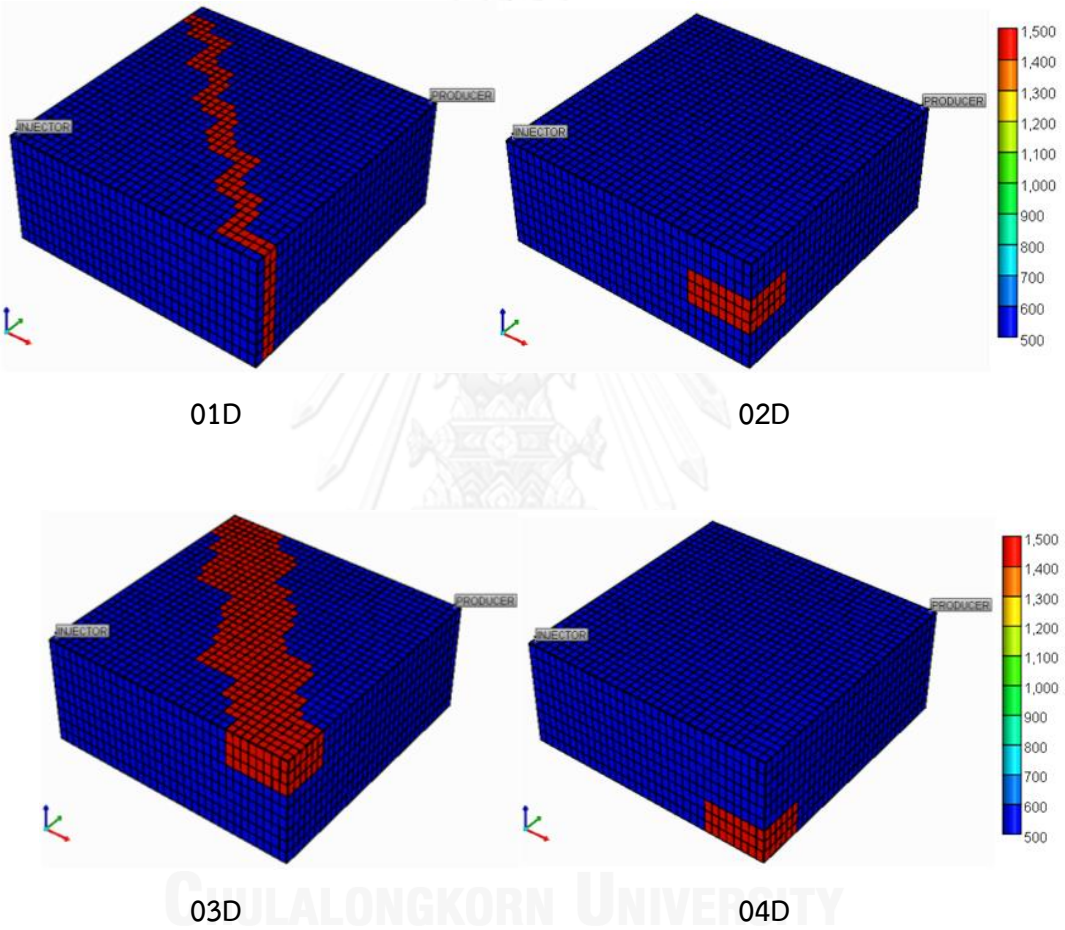

Figure 5.69 Location of high permeability channel in cases D models, representing by red color

Table 5.10 Summary of simulation outcomes from waterflooding, AS+P flooding, P+AS+P flooding in reservoir models case D

Parameter	Strategy	01D	02D	03D	04D
Production period	Waterflooding	09y 03m	09y 04m	09y 04m	09y 04m
	AS+P	22y 10m	23y 02m	23y 02m	22y 11m
	P+AS+P	24y 07m	23y 12m	23y 11m	24y 02m
Recovery factor (%)	Waterflooding	34.23	34.06	34.40	33.78
	AS+P	55.88	56.28	56.12	55.88
	P+AS+P	62.75	62.10	62.04	62.24
Water/Oil production ratio	Waterflooding	1.290	1.323	1.300	1.342
	AS+P	2.482	2.508	2.518	2.495
	P+AS+P	2.339	2.294	2.286	2.310

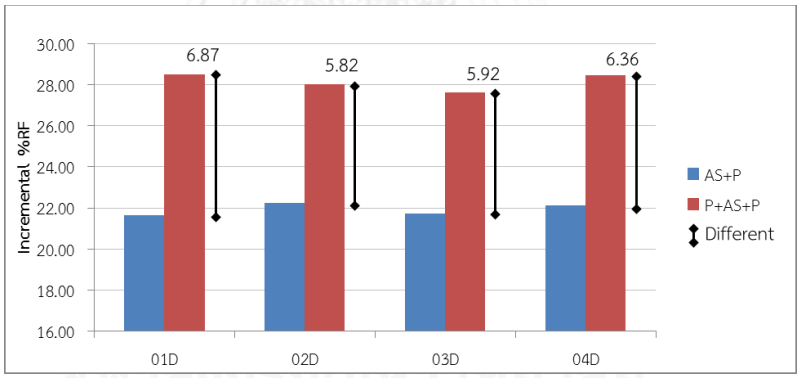

Figure 5.70 Comparison of incremental recovery factors of AS+P and P+AS+P flooding based on waterflooding in cases D

Recovery factor, oil and water production rates of waterflooding in cases 01D, 02D, 03D and 04D are illustrated in Figures 5.71 to 5.73. Recovery factors are not much different among each model by waterflooding technique. By the way, effect from gravity segregation causes an early breakthrough in case 04D, increasing abruptly water production rate around 2nd year. Recovery factor, oil and water production rates of AS+P and P+AS+P flooding in cases 01D, 02D, 03D and 04D are illustrated in Figures 5.74 to 5.76. Main mechanisms provided by pre-flushed polymer, AS slug and post-flushed polymer can be explained in the same way as explained in cases 01B

and 01C. However, size and location of high permeability channel in case D does not have any effect on two recovery techniques. Therefore, it can be implied that size and location of high permeability channel does not have much influence when direction of high permeability channel is perpendicular to flow direction in AS+P and P+AS+P flooding.

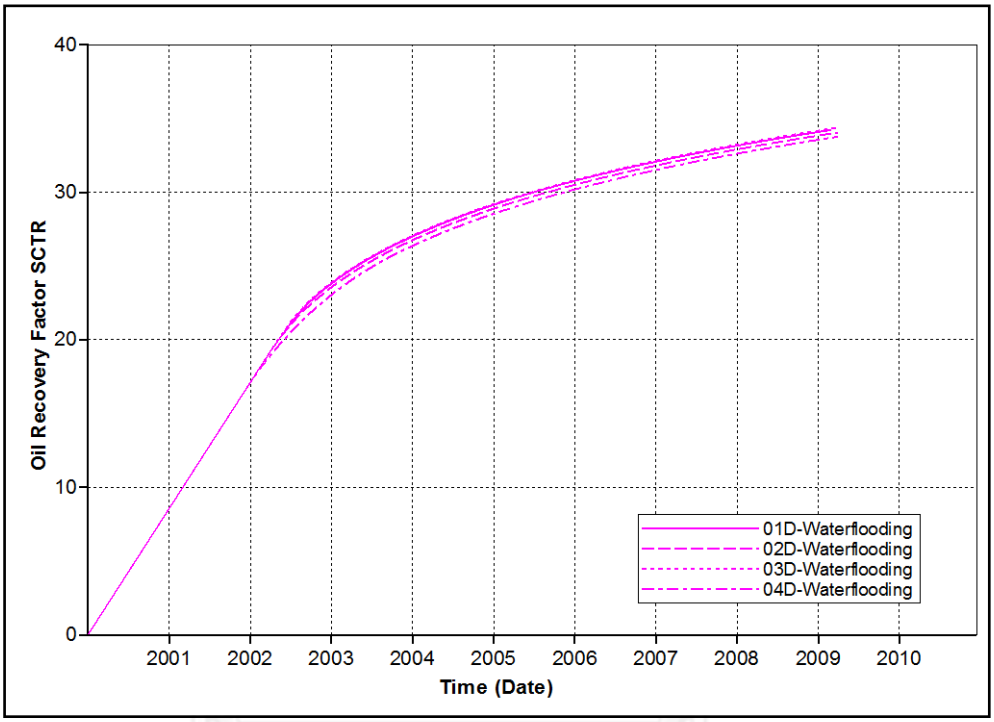

Figure 5.71 Recovery factors of waterflooding in cases D as a function of time

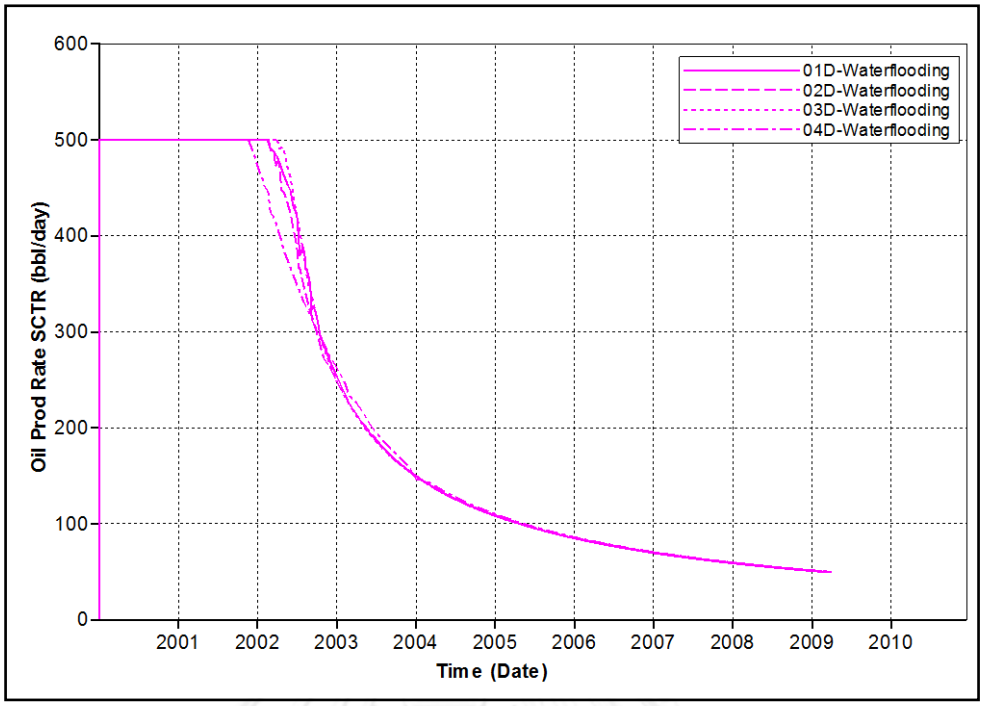

Figure 5.72 Oil production rates of waterflooding in cases D as a function of time

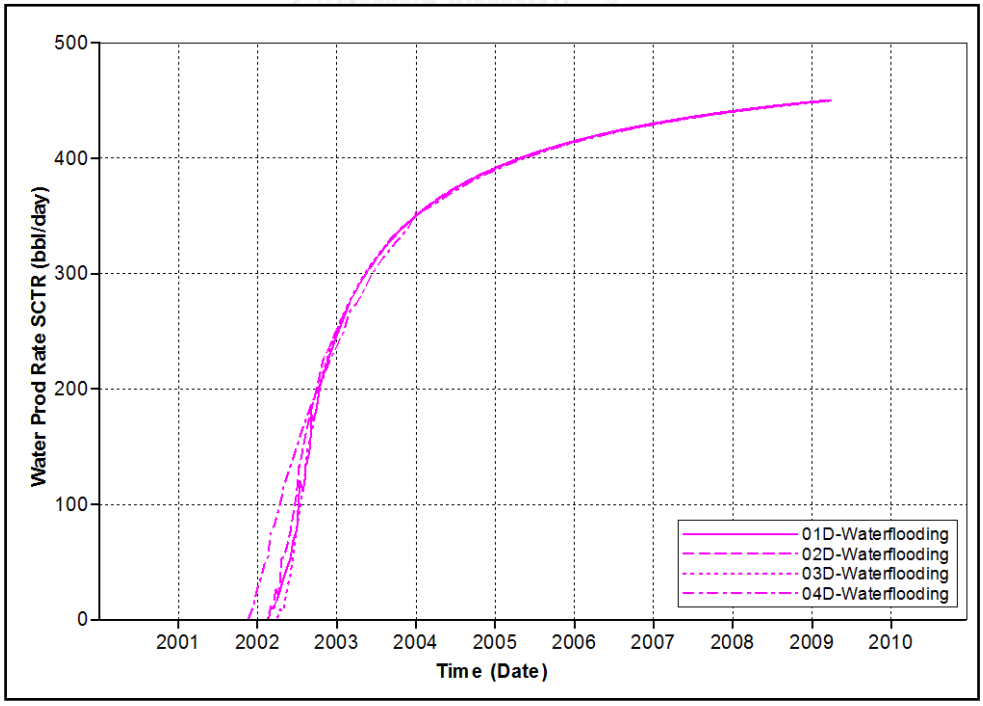

Figure 5.73 Water production rates of waterflooding in cases D as a function of time

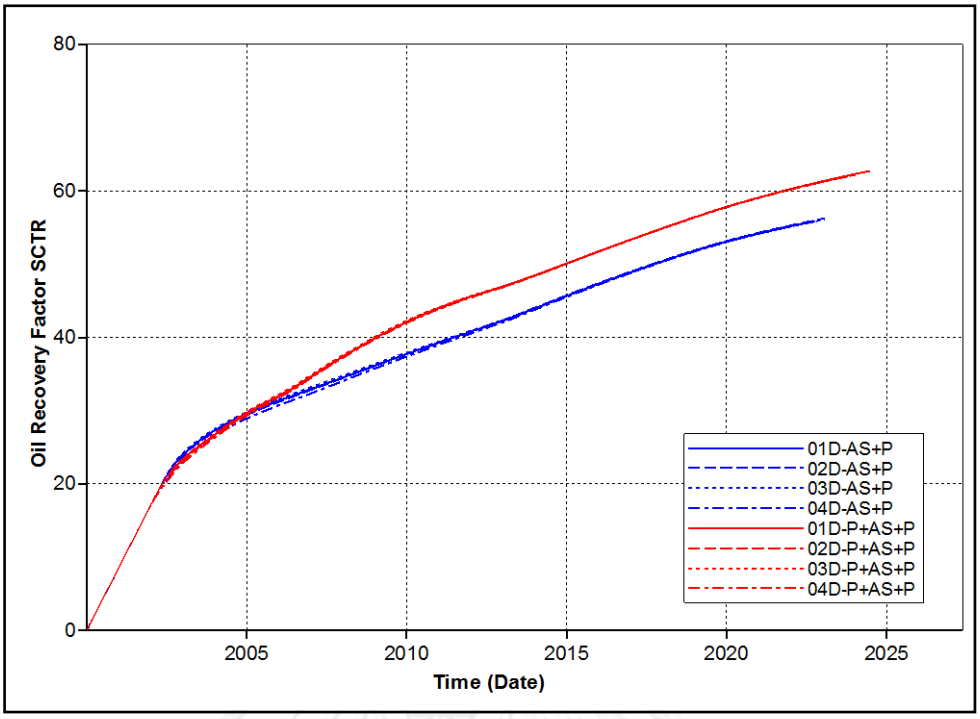

Figure 5.74 Recovery factors of AS+P and P+AS+P flooding in cases D as a function of time

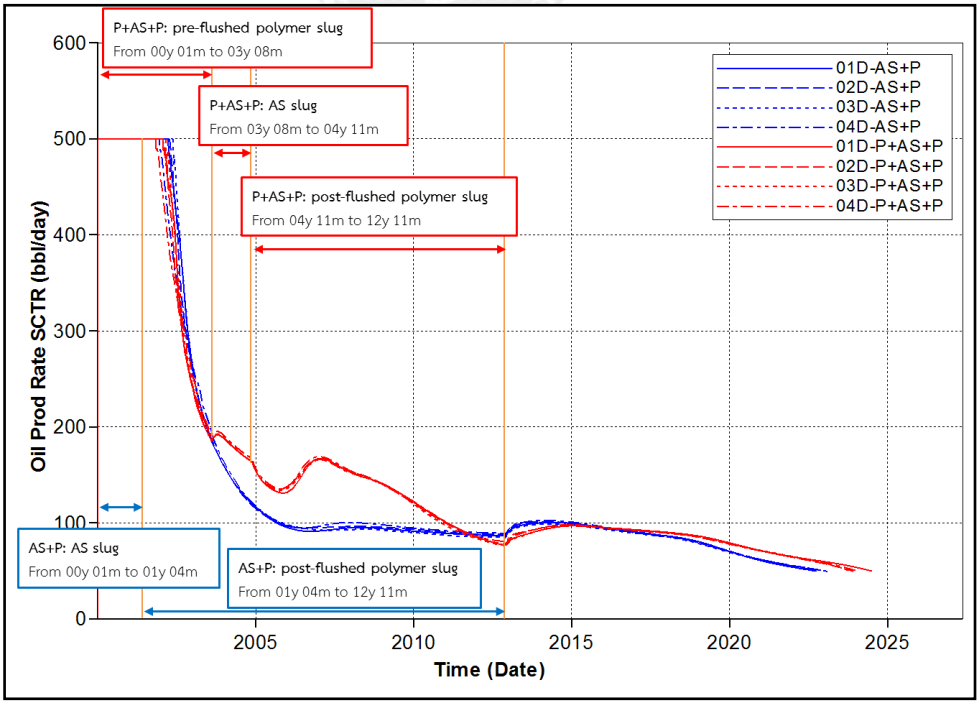

Figure 5.75 Oil production rates of AS+P and P+AS+P flooding in cases D as a function of time

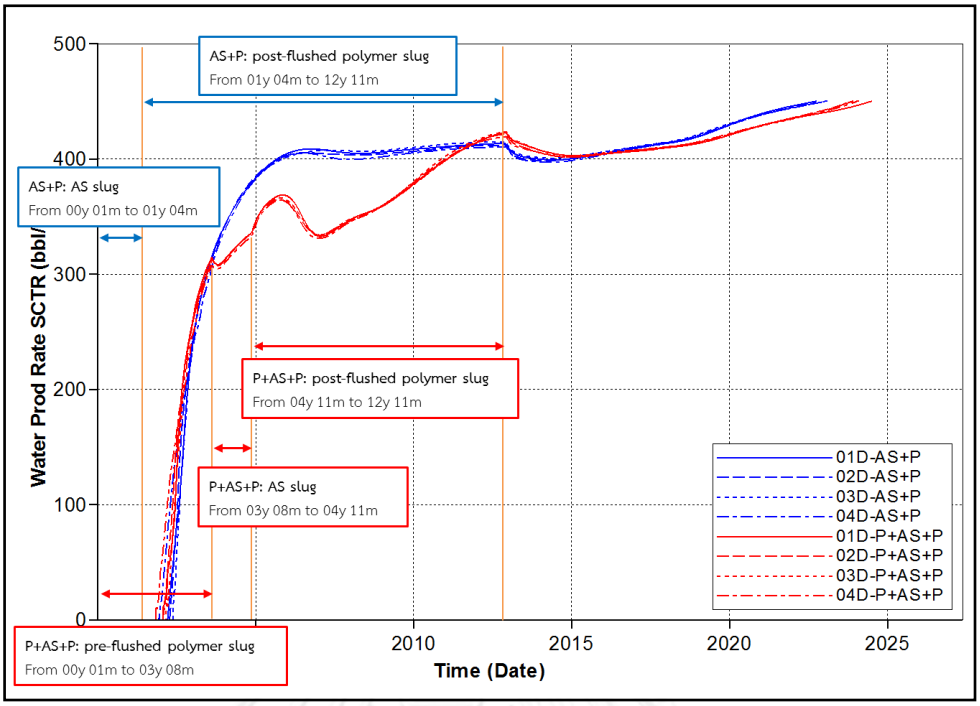

Figure 5.76 Water production rates of AS+P and P+AS+P flooding in cases D as a function of time

5.4.5 High Permeability Channel along Flow Direction (Cases E)

High permeability channel in cases E is located along with direction of traveling front from injector to producer as shown in Figure 5.77. High permeability channel is varied in all layers, located at the middle, top and bottom. These models are labeled as cases 01E, 02E, 03E and 04E, respectively. Result of waterflooding, AS+P and P+AS+P flooding are summarized in Table 5.11. Incremental of recovery factor of AS+P and P+AS+P flooding compared to waterflooding are depicted in Figure 5.78. Incremental recovery factor of AS+P and P+AS+P flooding based on waterflooding of cases 01E, 02E, 03E and 04E can be subdivided into two groups which are high different (case 01E) and slight different (cases 02E, 03E and 04E). Water/oil ratio shows that P+AS+P flooding produces less water than AS+P flooding at the same amount of produced oil for all cases.

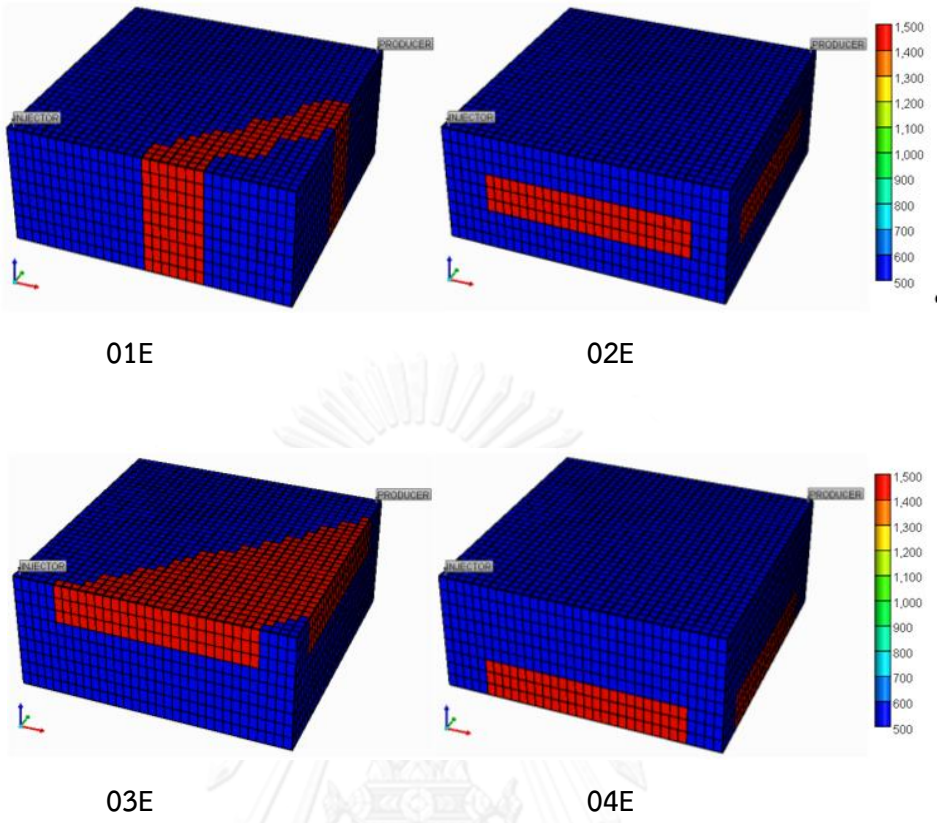

01E 02E

03E 04E

Figure 5.77 Location of high permeability channel in cases E models, representing by red color

Table 5.11 Summary of simulation outcomes from waterflooding, AS+P flooding, P+AS+P flooding in reservoir models case E

Parameter	Strategy	01E	02E	03E	04E
Production period	Waterflooding	09y 01m	09y 04m	09y 06m	09y 07m
	AS+P	22y 06m	20y 10m	20y 12m	20y 12m
	P+AS+P	23y 07m	19y 12m	20y 11m	21y 04m
Recovery factor (%)	Waterflooding	34.48	34.06	34.61	33.62
	AS+P	55.62	53.76	53.71	53.76
	P+AS+P	61.90	56.15	56.85	57.32
Water/Oil production	Waterflooding	1.233	1.322	1.327	1.417
	AS+P	2.447	2.301	2.331	2.328

ratio	P+AS+P	2.246	2.033	2.135	2.171

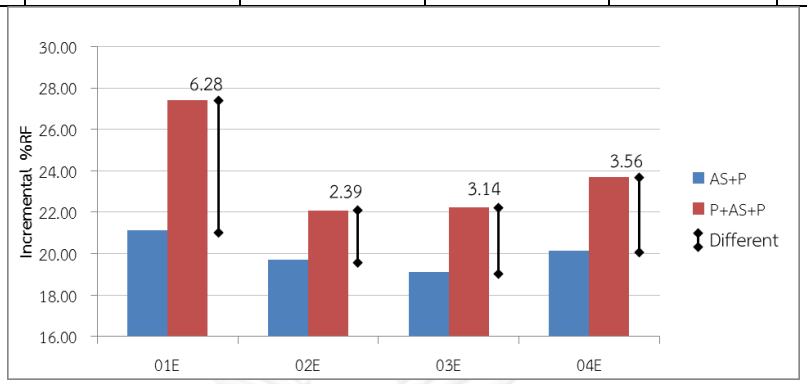

Figure 5.78 Comparison of incremental recovery factors of AS+P and P+AS+P flooding based on waterflooding in cases E

Recovery factor, oil and water production rate of waterflooding from cases 01E, 02E, 03E and 04E are illustrated in Figures 5.79 to 5.81. Water production rate shows an early breakthrough in order of the highest to the lowest impacts as 04E, 02E, 03E and 01E, respectively. Therefore, an impact of early water breakthrough when high permeability channel is located along flow direction is more pronounced when the location is at the bottom. Moreover, an impact is higher when width of high permeability channel is large compared to smaller width.

Recovery factor, oil and water production rate of AS+P and P+AS+P flooding in cases 01E, 02E, 03E and 04E are illustrated in Figures 5.82 to 5.84. Oil recovery mechanisms of all cases can be separated into two groups by using oil production rate. Plateau production of case 01E is significantly different from others. Therefore, difference of incremental recovery factors between AS+P and P+AS+P flooding is high. Case 01E can be explained as same as cases 01B, 01C and 01D by effect of pre-flushed polymer and post-flushed polymer.

In cases of 02E, 03E and 04E, water production rate before the 2nd year shows that both of AS+P and P+AS+P flooding cannot mitigate large area of high permeability channel along direction flow direction. Case 02E is chosen to represent an explanation for the less different incremental recovery factor between AS+P and P+AS+P flooding based on waterflooding. Polymer concentration, oil saturation and water saturation profiles are illustrated in Figure 5.85 at 7th year 1st month. The left side of polymer concentration profile shown in Figure 5.85(a) indicates pre-flushed polymer concentration tracking, whereas the right side indicates post-flushed

polymer concentration tracking. In case of P+AS+P flooding, pre-flushed polymer cannot stabilize flood front, spreading out in high permeability channel. Pre-flushed polymer hence cannot form itself like a buffer slug to prevent high water saturation as shown in Figure5.85(c). Therefore, oil production rate between AS+P and P+AS+P flooding of case 02E is not much different. That makes result of incremental recovery factor of AS+P and P+AS+P flooding compared to waterflooding to be less different.

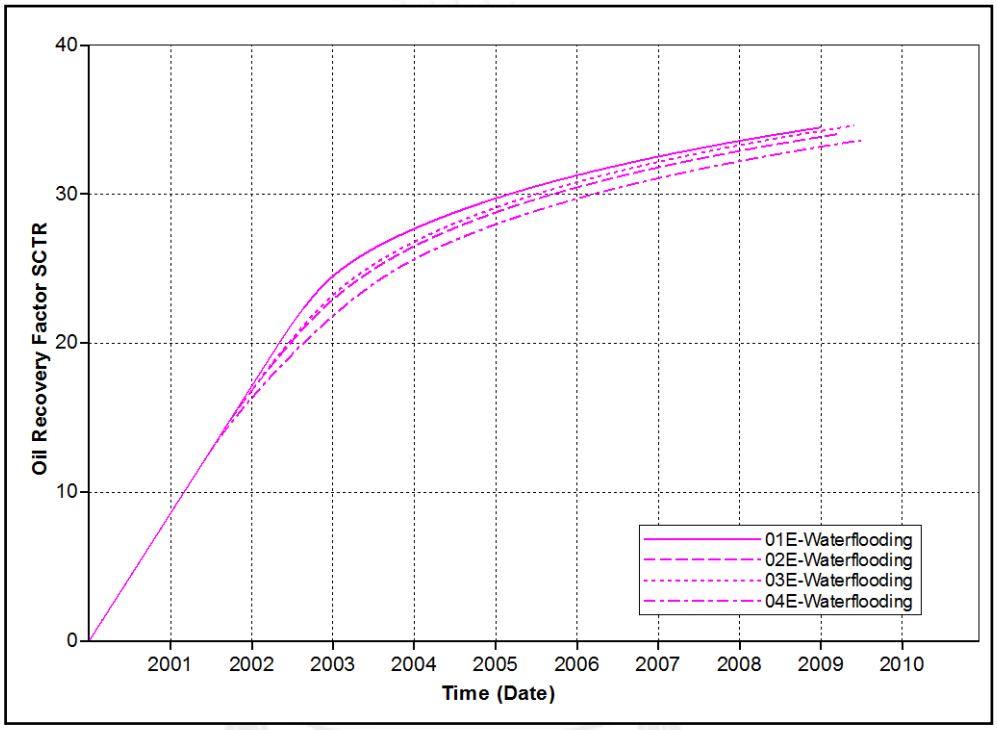

Figure 5.79 Recovery factors of waterflooding in cases E as a function of time

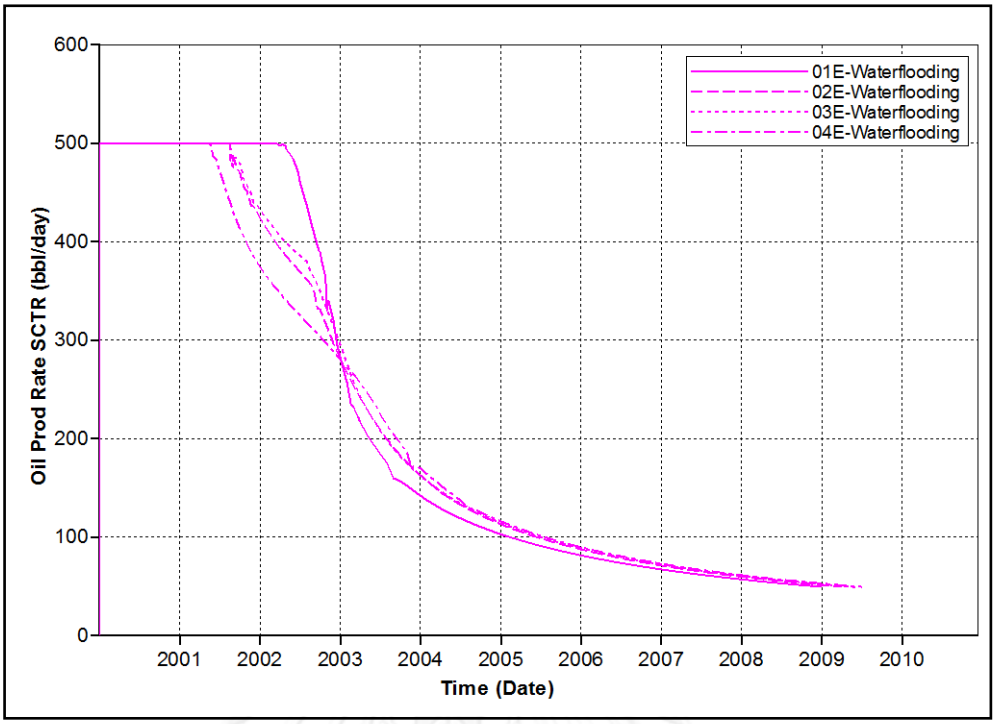

Figure 5.80 Oil production rates of waterflooding in cases E as a function of time

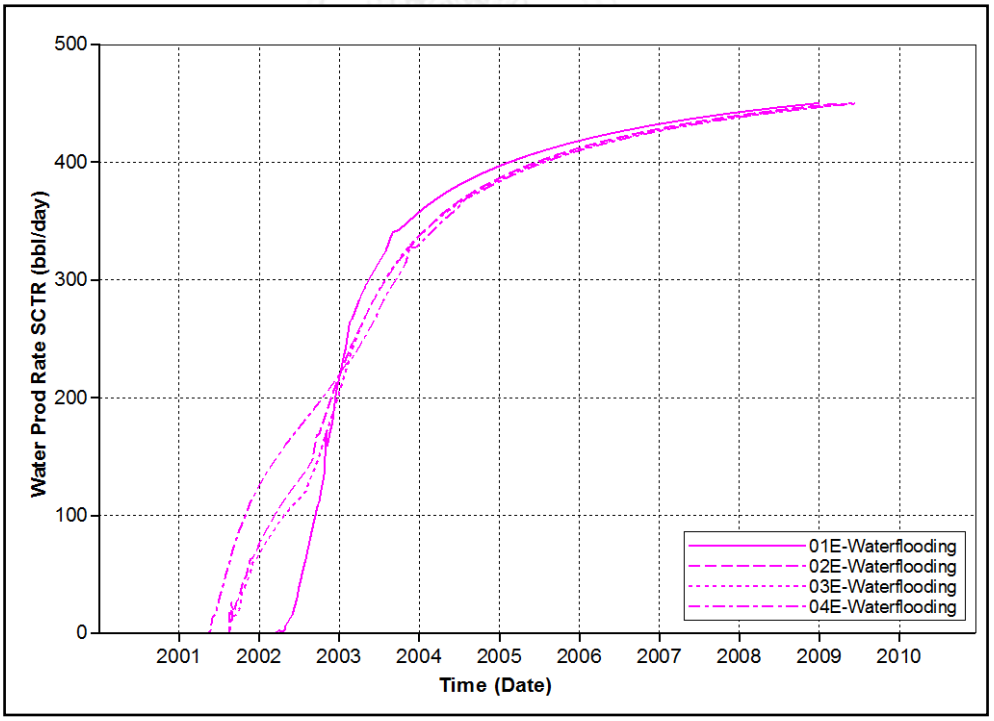

Figure 5.81 Water production rates of waterflooding in cases E as a function of time

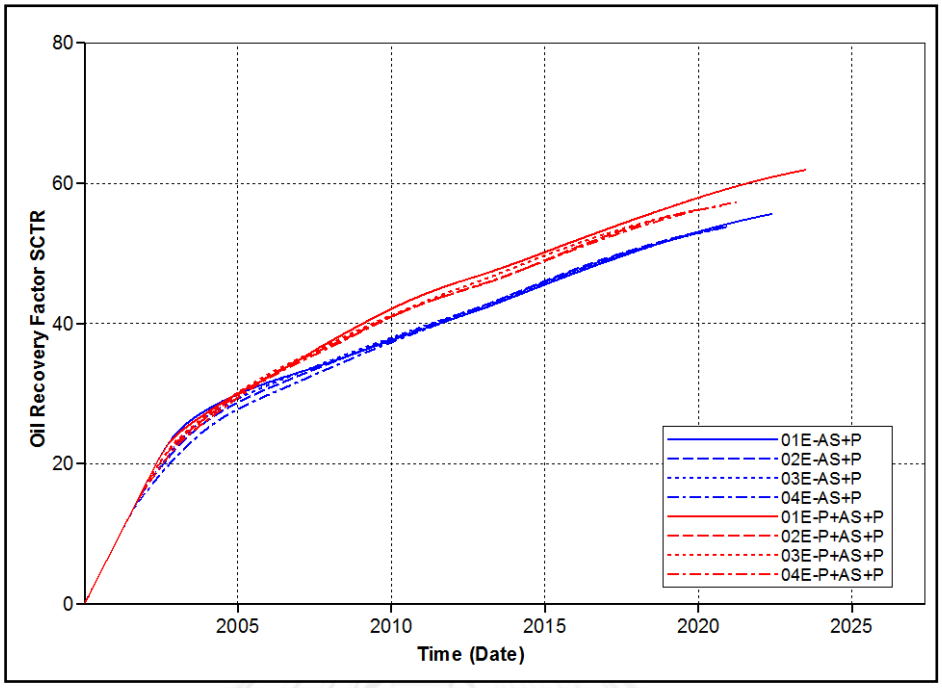

Figure 5.82 Recovery factors of AS+P and P+AS+P flooding in cases E as a function of time

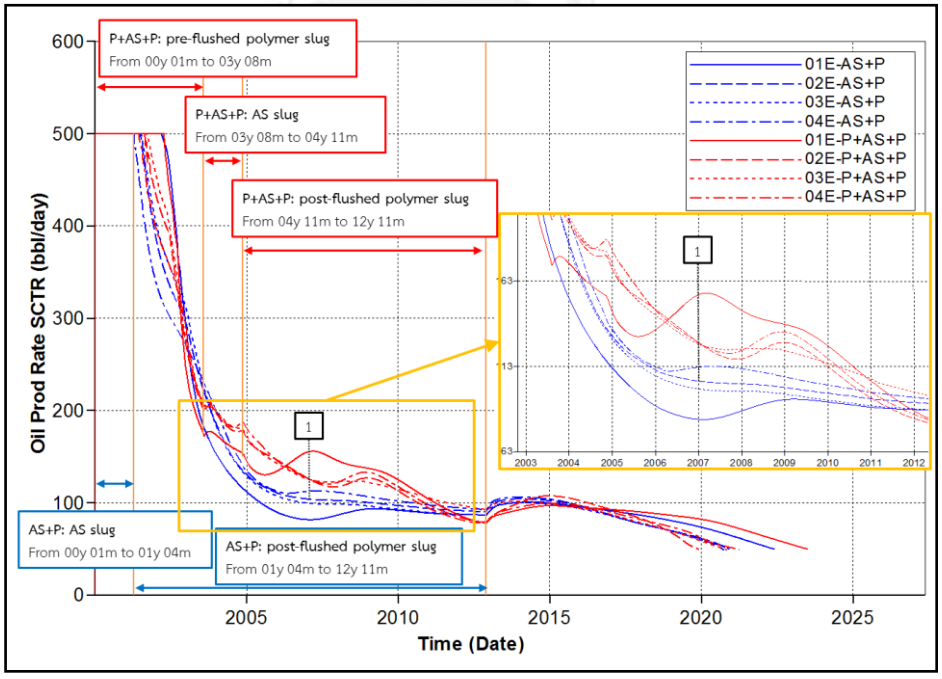

Figure 5.83 Oil production rates of AS+P and P+AS+P flooding in cases E as a function of time

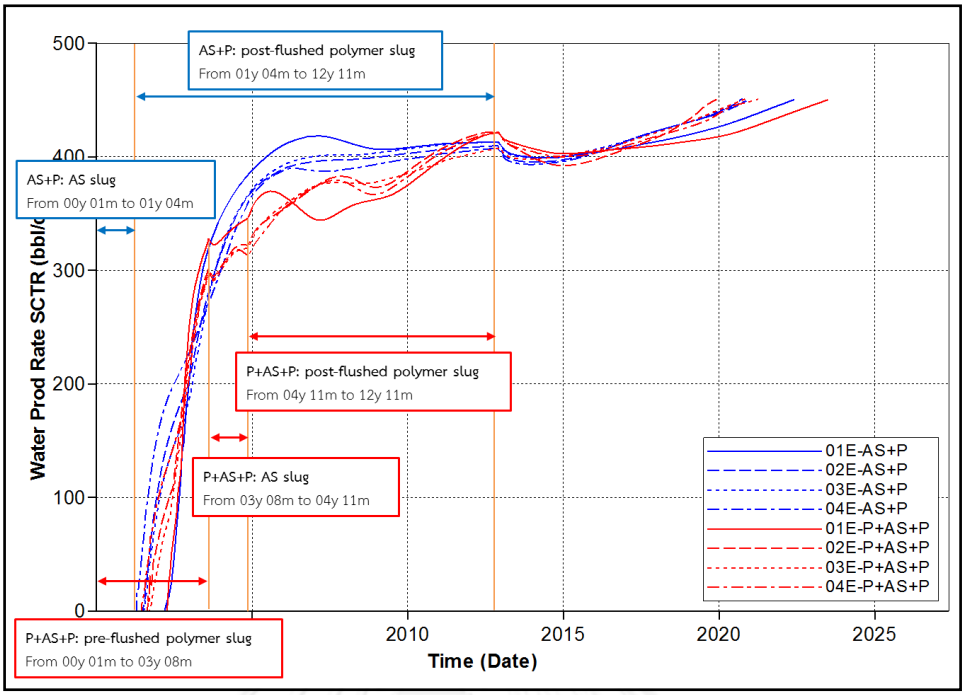

Figure 5.84 Water production rates of AS+P and P+AS+P flooding in cases E as a function of time

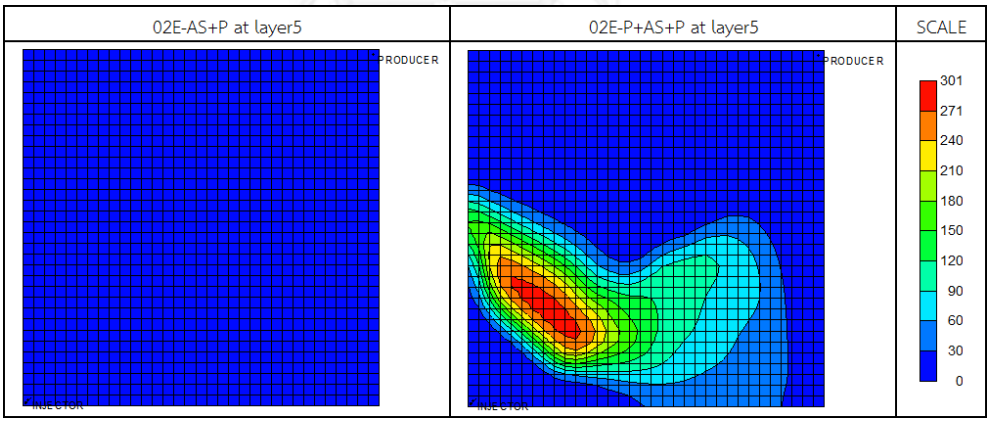

(a)

Figure 5.85 Effect of pre-flushed polymer slug in case 02E at 7th year, 1st month (a) Pre-flushed polymer concentration profile (b) Post-flushed polymer concentration profile (c) Oil saturation profile (d) Water saturation profile

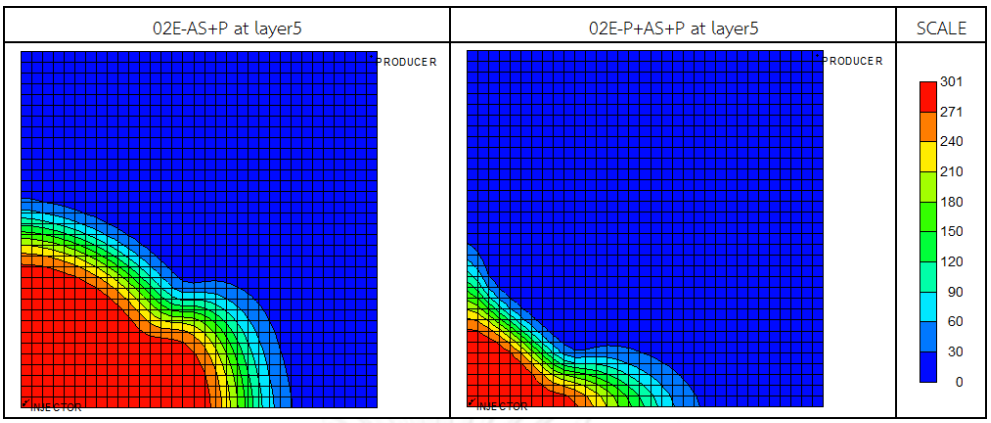

(b)

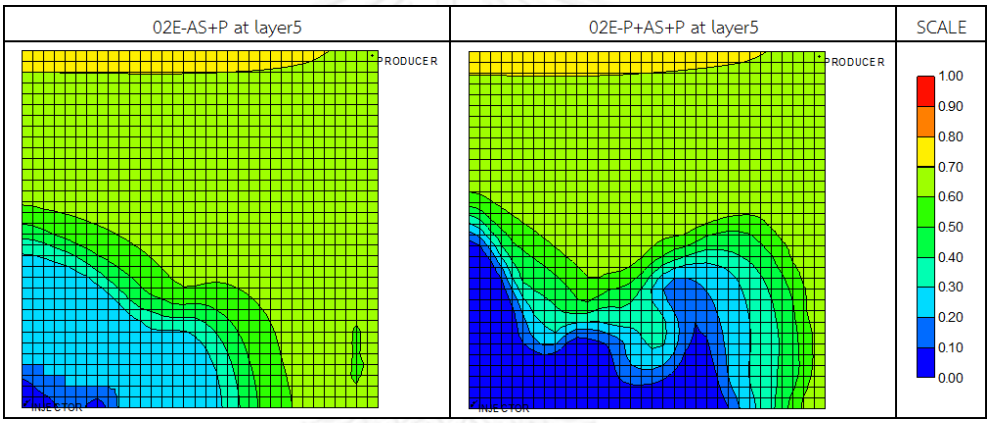

(c)

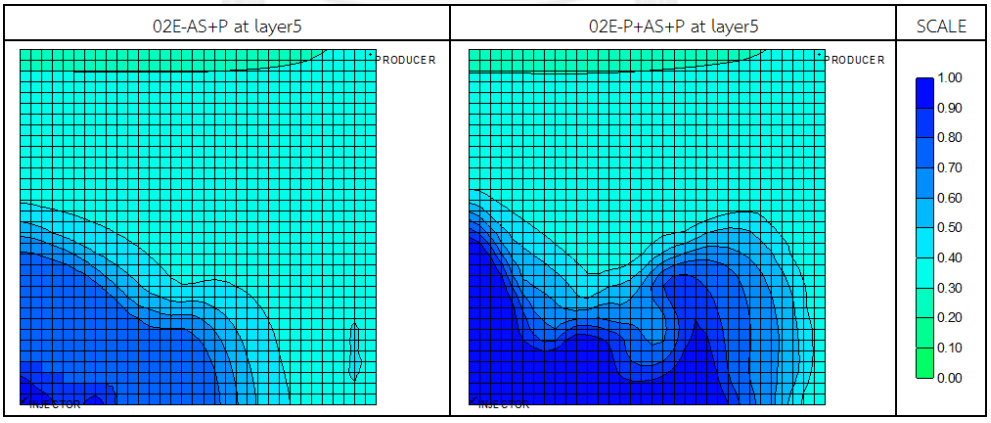

(d)

Figure 5.85 Effect of pre-flushed polymer slug in case 02E at 7th year, 1st month (b) Post-flushed polymer concentration profile (c) Oil saturation profile (d) Water saturation profile (continued)

5.4.6 Double High Permeability Channels along Flow Direction (Cases F)

Two high permeability channels in Case F are located along direction of traveling front from injector to producer as shown in Figure 5.86. Cases comprise high permeability channel varied in all layers, located at the middle, top and bottom. These cases are labeled as 01E, 02F, 03F and 04F, respectively. Direction of high permeability channels in cases F is as same as that of cases E. But cases F are composed of two high permeability channels one on at the left and another one on right of reservoir. Due to matrix volume of high permeability channel is kept to constant for all cases, width of high permeability channels in cases F is narrower than single channel of cases E. Result of waterflooding, AS+P and P+AS+P flooding are summarized in Table 5.12. Incremental of recovery factors of AS+P and P+AS+P flooding compared to waterflooding are summarized in Figure 5.87. Incremental recovery factor of P+AS+P flooding from waterflooding of 01F, 02F, 03F and 04F are outstandingly different from AS+P flooding. Comparing with cases E, it can be concluded that width of high permeability channel has a significant affect more than direction. However, water/oil ratio shows that P+AS+P flooding produces less water than AS+P flooding at the same amount of produced oil in all cases.

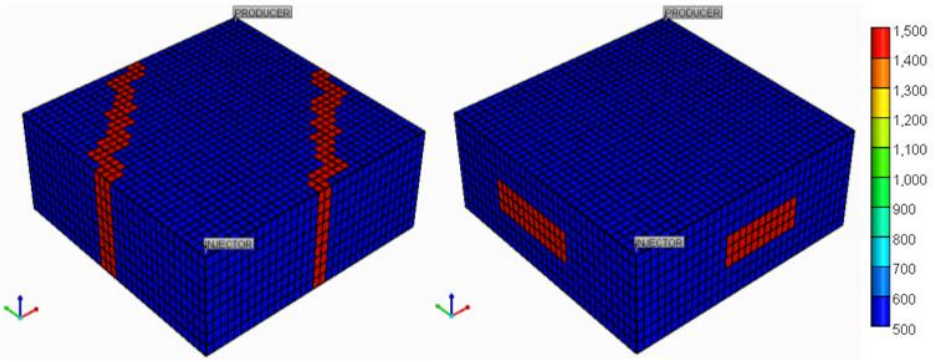

01F **02F**

Figure 5.86 Location of high permeability channels in cases F models, representing by red color

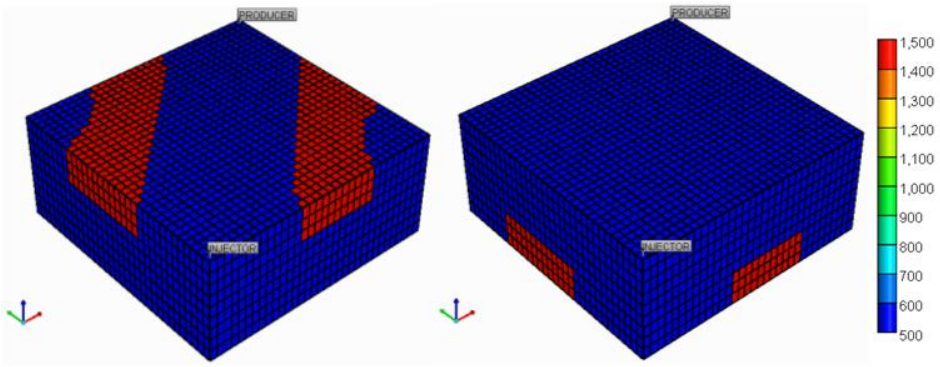

03F 04F

Figure 5.86 Location of high permeability channels in cases F models, representing by red color (continued)

Table 5.12 Summary of simulation outcomes from waterflooding, AS+P flooding, P+AS+P flooding in reservoir models case F

Parameter	Strategy	01F	02F	03F	04F
Production period	Waterflooding	08y 11m	09y 01m	08y 12m	09y 03m
	ASP	22y 10m	21y 06m	22y 10m	22y 02m
	PASP	23y 04m	21y 12m	23y 03m	22y 08m
Recovery factor (%)	Waterflooding	34.34	34.32	34.84	33.84
	ASP	56.12	54.36	55.67	55.18
	PASP	61.73	59.56	61.22	60.14
Water/Oil production ratio	Waterflooding	1.201	1.244	1.190	1.316
	ASP	2.467	2.370	2.495	2.423
	PASP	2.221	2.148	2.236	2.212

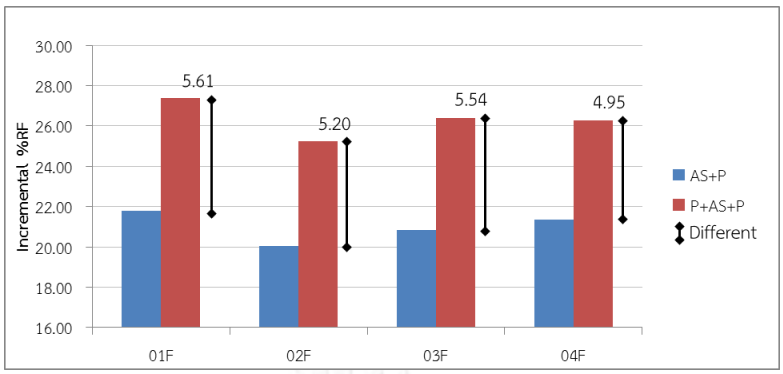

Figure 5.87 Comparison of incremental recovery factors of AS+P and P+AS+P flooding based on waterflooding in cases F

Recovery factor, oil and water production rate of waterflooding performed in cases 01F, 02F, 03F and 04F are illustrated in Figures 5.88 to 5.90. These results show that gravity segregation causes underrunning of water in especially the case 04F where high permeability channel is located at the bottom of reservoir. Water production rate of case 04F is the highest around 2nd year. Recovery factor, oil and water production rates of AS+P and P+AS+P flooding in cases 01D, 02D, 03D and 04D are illustrated in Figures 5.91 to 5.93. Mechanisms of pre-flushed polymer slug, AS slug and post-flushed polymer slug can be explained as same as case 01B and 01C.

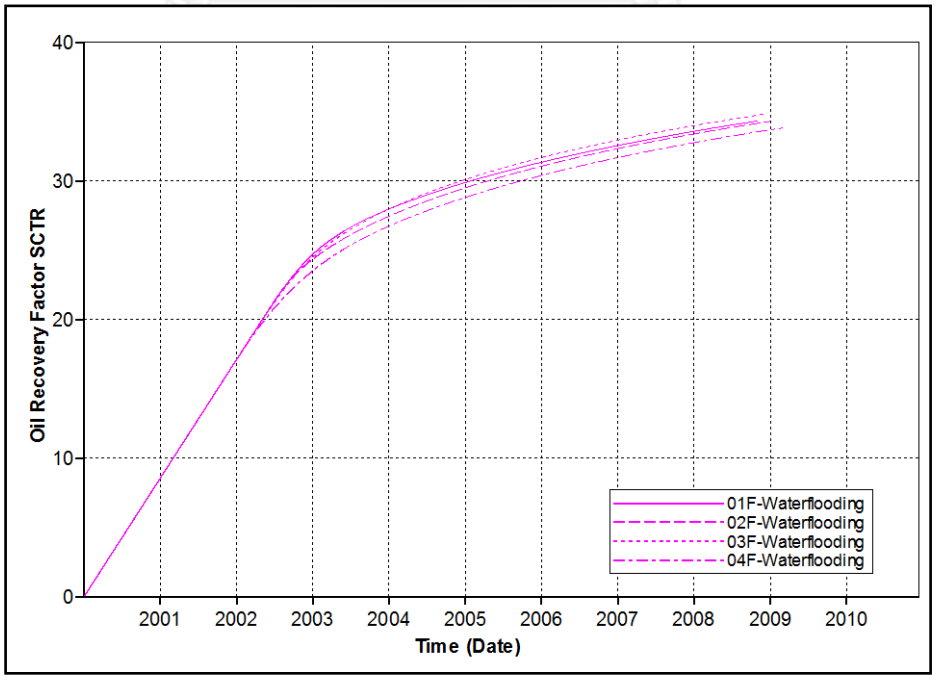

Figure 5.88 Recovery factors of waterflooding in cases F as a function of time

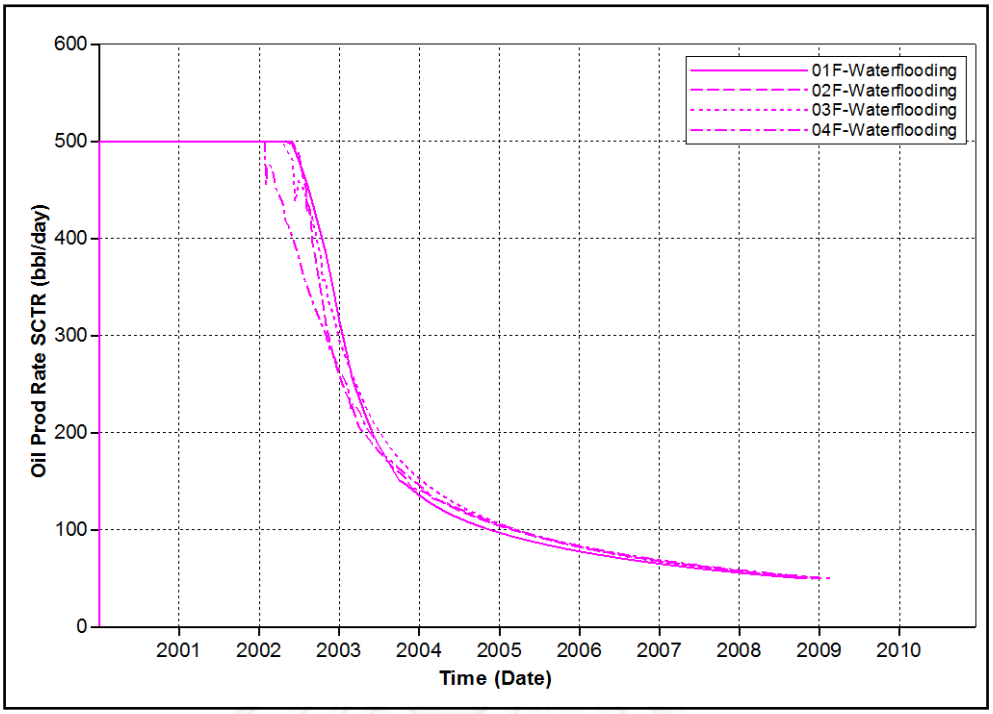

Figure 5.89 Oil production rates of waterflooding in cases F as a function of time

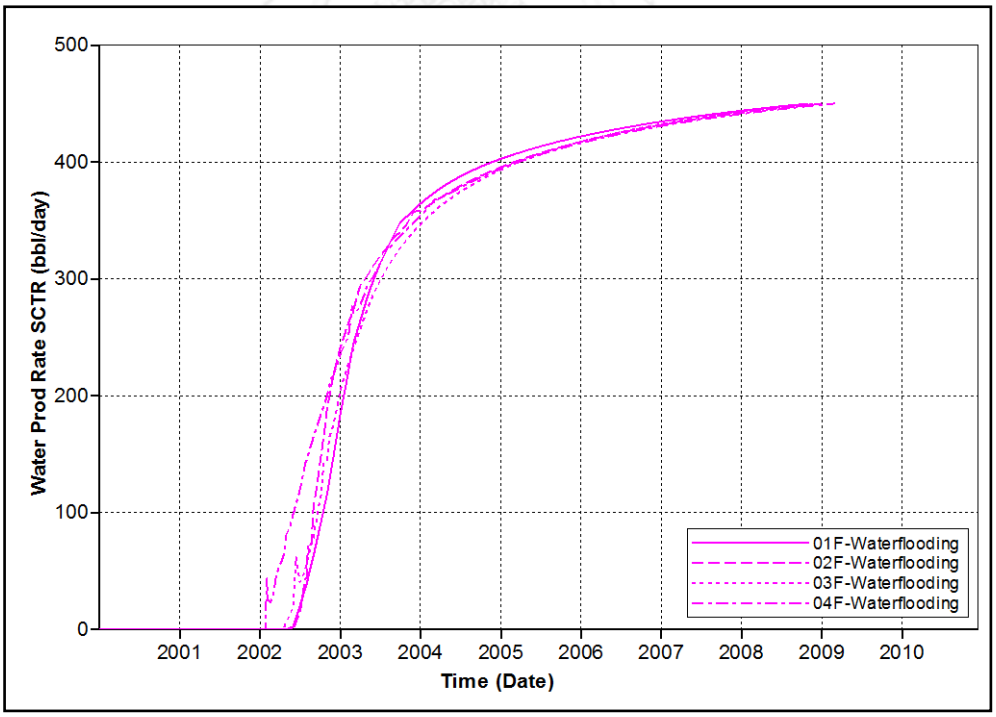

Figure 5.90 Water production rates of waterflooding in cases F as a function of time

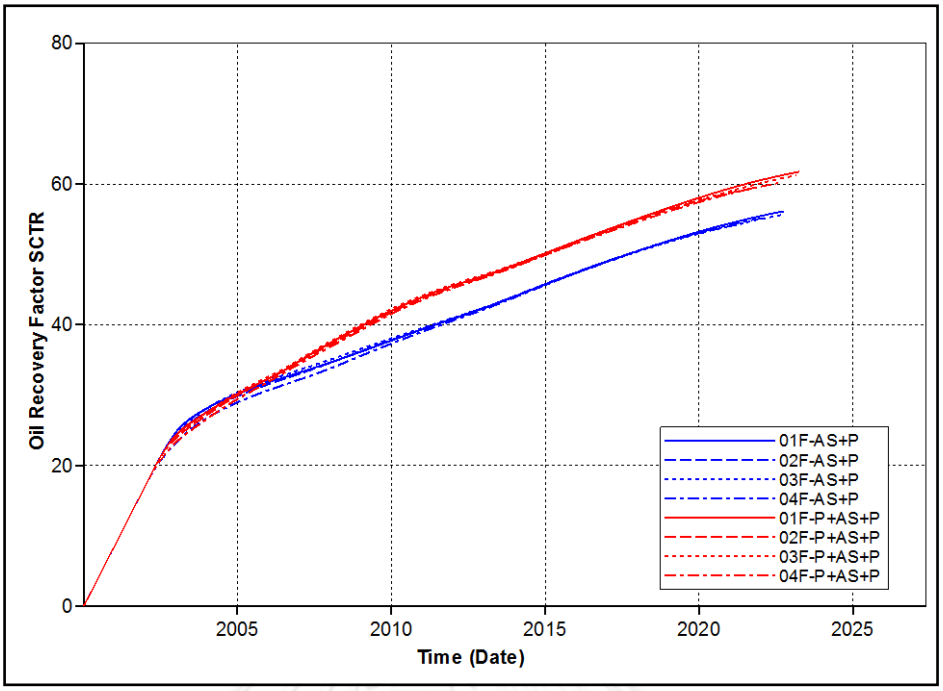

Figure 5.91 Recovery factors of AS+P and P+AS+P flooding in cases F as a function of time

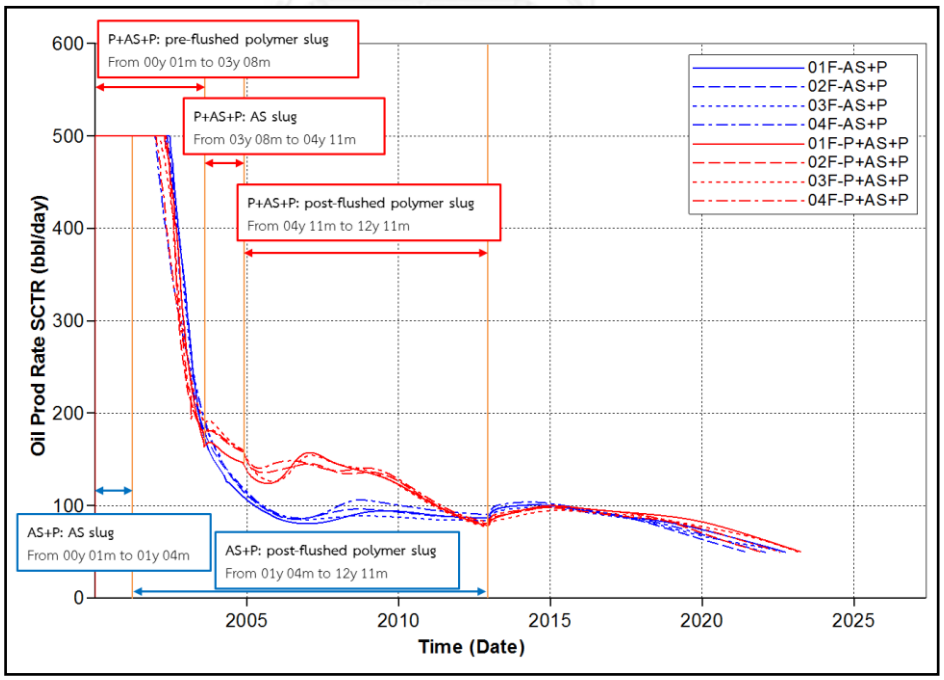

Figure 5.92 Oil production rates of AS+P and P+AS+P flooding in cases F as a function of time

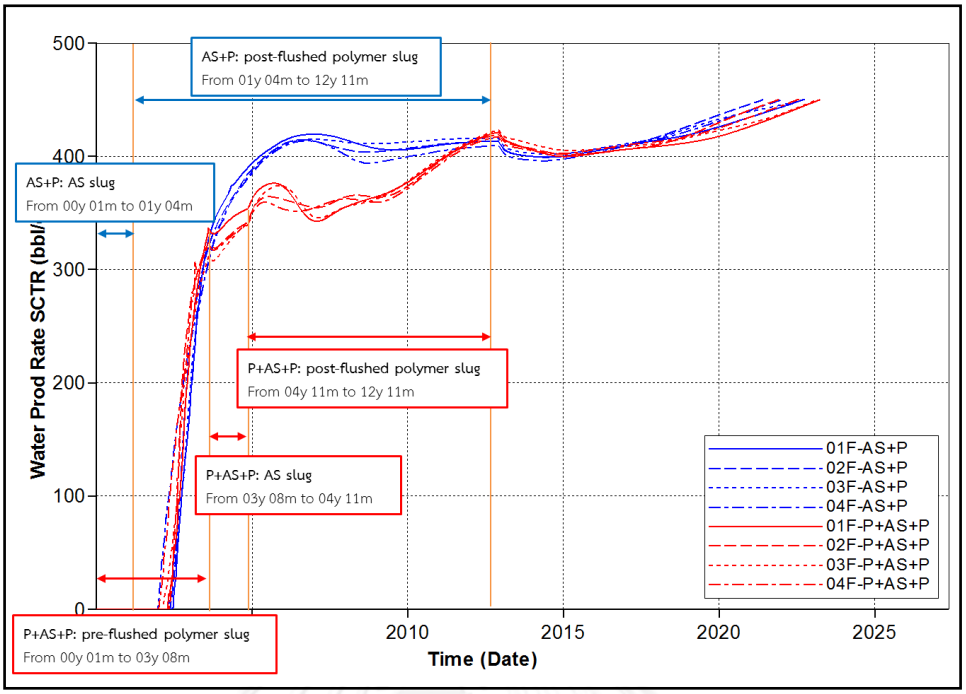

Figure 5.93 Water production rates of AS+P and P+AS+P flooding in cases F as a function of time

5.4.7 Summary of Heterogeneous Models

In this section, incremental of recovery factor of AS+P and P+AS+P flooding from waterflooding of all cases are concluded and plotted together in the same graph. According to variation of high permeability channel, width/height ratio (w/h ratio) of high permeability channel is defined to use for sorting criteria. Width/height ratio of high permeability channel is calculated from width of the narrowest location of one high permeability channel in x-direction divided by height of high permeability channel in z-direction. Sorting result is shown in Table 5.13. Summary of incremental recovery factors of AS+P and P+AS+P flooding are illustrated in Figure 5.94, where summary of difference of incremental recovery factors between AS+P flooding and P+AS+P flooding are illustrated in Figure 5.95. From results, data can be separated into two groups. The 1st group contains cases 01A, 02A, 03A, 02E, 03E and 04E with high w/h ratio. Width of high permeability channel in this group is much larger than height. It can be seen that, incremental recovery factors of both AS+P and P+AS+P flooding are very less improved compared to solely waterflooding among this group. Moreover, difference between AS+P and P+AS+P flooding is inconsiderable. On the

other hand, incremental recovery factors of both AS+P and P+AS+P flooding from waterflooding as well as difference between AS+P flooding and P+AS+P flooding are obvious in 2nd group.

It could be concluded that w/h ratio of high permeability channel can be used to predict incremental recovery factor of AS+P and P+AS+P compared to waterflooding and also difference between AS+P and P+AS+P flooding. When w/h ratio is high, both methods yield less incremental recovery factor and less different between two methods. For low value of w/h ratio, more difference incremental recovery factor between two methods is obtained. However, increment result also depends on direction of high permeability channel. For instance, in case 01F where w/h ratio is very low, incremental recovery factor is still dropped. Therefore, direction of high permeability channel to fluid flow direction has to be taken in account together with w/h ratio.

Table 5.13 Width/height ratio of all heterogeneity models

Case	w/h ratio	Case	w/h ratio
01A	82.50	02C	9.17
02A	82.50	03C	9.17
03A	82.50	04C	9.17
02E	18.33	02D	7.50
03E	18.33	03D	7.50
04E	18.33	04D	7.50
02F	9.17	01E	1.39
03F	9.17	01B	0.83
04F	9.17	01C	0.83
02B	9.17	01F	0.56
03B	9.17	01D	0.56
04B	9.17		

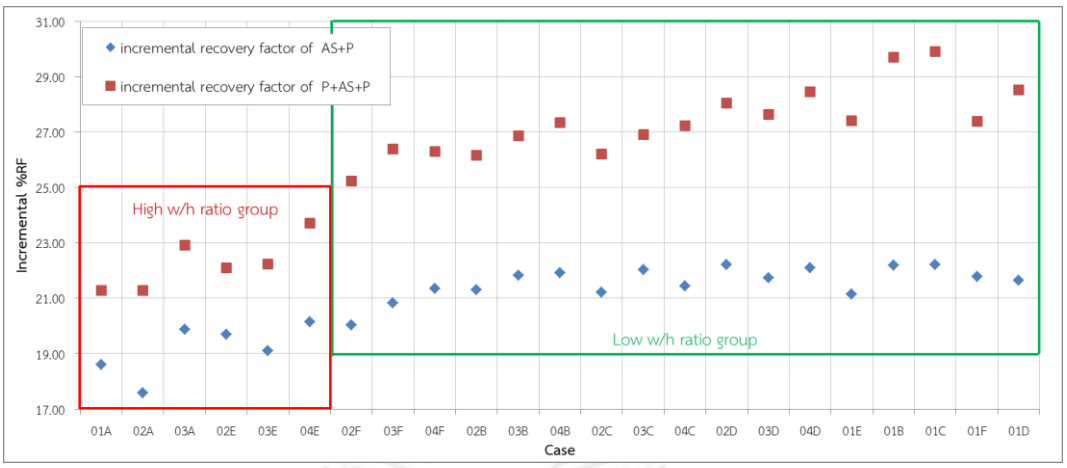

Figure 5.94 Summary of incremental recovery factors of AS+P and P+AS+P flooding compared to waterflooding as a function of sorted models by w/h ratio

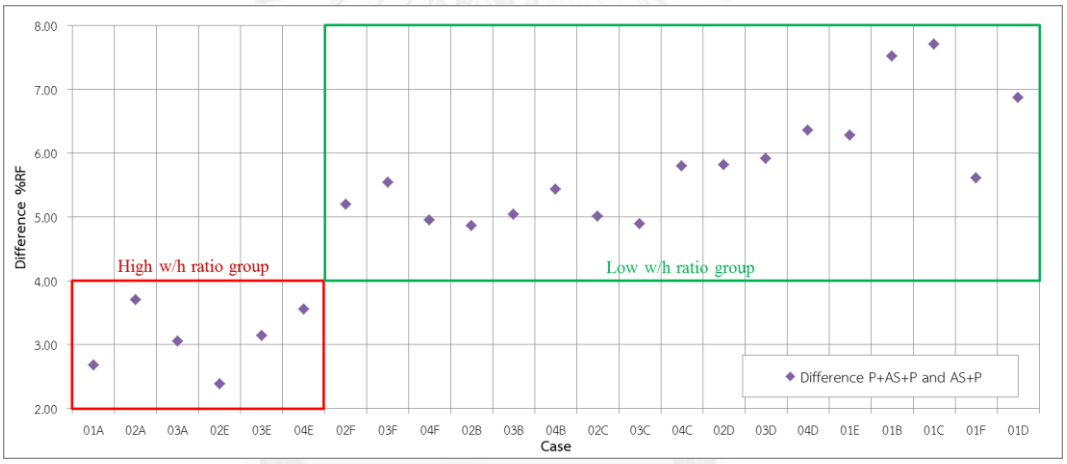

Figure 5.95 Summary of difference of incremental recovery factors between AS+P and P+AS+P flooding as a function of sorted models by w/h ratio

5.5 Sensitivity Analysis

In this section, the highest incremental recovery factor from waterflooding is used for choosing the representative AS+P and P+AS+P methods for the sensitivity analysis. Result from this section can indicate significance and uncertainty of each parameter on the interest outcome which is recovery factor. Models of chosen AS+P flooding and P+AS+P flooding are summarized in Table 5.14. Sensitivity analysis parameters compose of Corey's exponent of relative permeability, rock wettability, permeability contrast, ratio of vertical to horizontal permeabilities and porosity in high permeability channel. Recovery factors from both AS+P and P+AS+P are compared to waterflooding and relative data are used for comparison among each interest parameter.

Table 5.14 Descriptive summary of chosen models for sensitivity analysis

Strategy	Model	Description
AS+P flooding	01C	High permeability channel locates across direction in all layers.
P+AS+P flooding	02D	High permeability channel locates across direction in the middle layers.

5.5.1 Corey's Exponent of Relative Permeability

Since relative permeability curves are constructed from correlation by using end-points of oil and water saturations to calculate relative permeability values and exact relative permeability curves can only be determined from special core analysis in laboratory, this parameter is therefore necessary for sensitivity analysis on simulation outcomes. Curvature of relative permeability curves of oil and water are determined by the Corey's exponent of oil (C_o) and water (C_w) as mentioned in equation (3.4) and (3.5) in Chapter 3. In this study, main relative permeability curve sets are subdivided into relative permeability curves of rock at normal condition and at ultra-low IFT condition. Relative permeability curves of rock at normal condition is

general relative permeability curves based on theory when capillary number is less than 10^{-7} or only water is presented as an aqueous phase. Relative permeability curves of ultra-low IFT condition occurs when alkali and surfactant are presented in aqueous phase, increasing capillary number above 10^{-4}. Therefore, sensitivity analysis of Corey's exponent is sub-divided into the study of relative permeability curves of rock at normal condition (cases N) and at ultra-low IFT condition (cases U). In this study, Corey's exponent of oil (C_o) is set to be equal to that of water (C_w) for every specific case.

5.5.1.1 Corey's exponent of Rock at Normal Condition (Cases N)

Normal condition of relative permeability curve is so called the interpolation set1 in STAR. Corey's exponent of rock at condition is previously set as 2.0 for base case. In this section, Corey's exponents of rock at normal condition are varied to 1.0, 1.5, and 2.5. Various relative permeability curves generated from different Corey's exponent values at normal condition are illustrated in Figure 5.96.

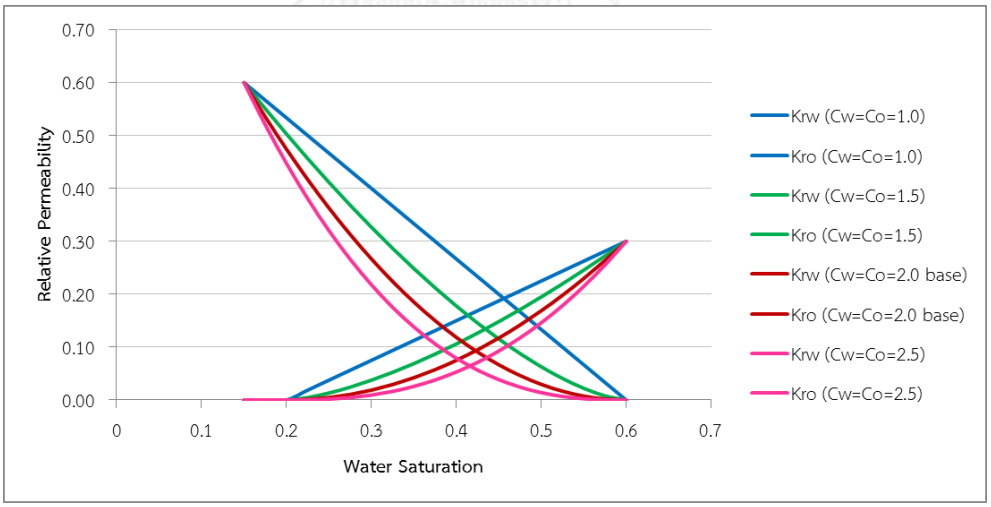

Figure 5.96 Summary of relative permeability curves generated from different Corey's exponent values for rock at normal condition

Summary of interest simulation outcomes which are recovery factors and incremental recovery factor compared to waterflooding for both AS+P and P+AS+P flooding are illustrated in Figures 5.97 and 5.98, respectively. Results show that incremental recovery factors of AS+P flooding compared to waterflooding does not fluctuate with Corey's exponents of rock at normal condition, whereas incremental recovery factor of P+AS+P flooding based on waterflooding is more dominant at elevated values of Corey's exponent. Stable incremental recovery factors by means of AS+P flooding is caused by decreasing of both recovery factors obtained from waterflooding and AS+P flooding at the same magnitude. On the other hand, increasing of the incremental recovery factor of P+AS+P flooding is caused by decreasing recovery factor of waterflooding while recovery factor of P+AS+P flooding is maintained constant.

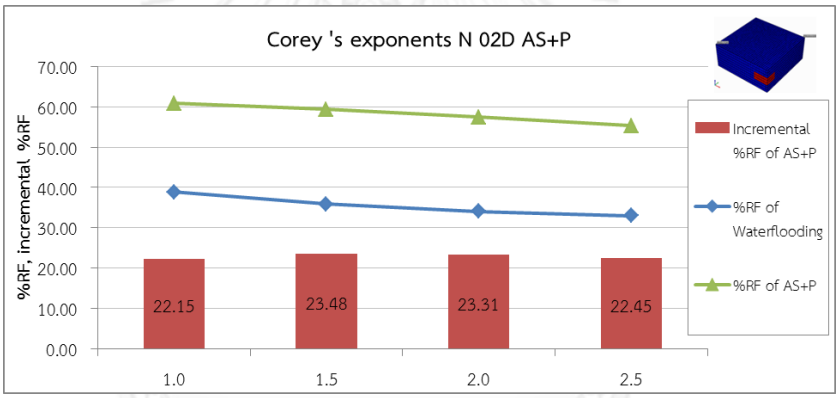

Figure 5.97 Recovery factors and incremental recovery factors compared to waterfloofing of various Corey's exponents of rock at normal condition by AS+P flooding

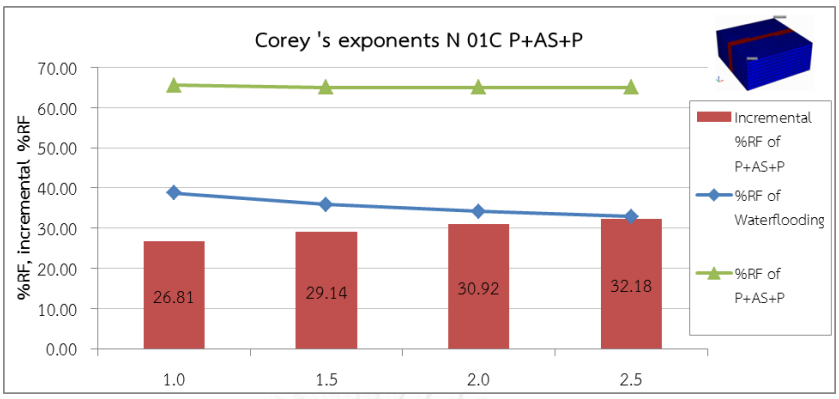

Figure 5.98 Recovery factors and incremental recovery factors compared to waterflooding of various Corey's exponents of rock at normal condition by P+AS+P flooding

Oil recovery factors and production rates of waterflooding in the study of Corey's exponent on chosen models 02D and 01C are illustrated in Figures 5.99 to 5.101. Comparing results between these models, the trend of each waterflooding case is similar. Hence, effect of Corey's exponent on waterflooding is explained using 01C model. Result from the plot can be divided into two periods. The 1st period is started from the first day of production until 3rd year, 6th month. In this 1st period, water production rate shows the earliest breakthrough when Corey's exponent is 1.0 and the latest when Corey's exponent is 2.5 as shown in Figure 5.102. Therefore, oil rate is the highest at Corey's exponent of 2.5. This is effect of curvature of relative permeability curve when water saturation is low. However, oil and water production rates in 2nd period are switched from maximum to minimum after 3rd year, 6th month. Alternation is caused from displacement mechanism at saturation closer to residual oil saturation. Due to high oil saturation that is remained in reservoir, relative permeability to oil near residual oil saturation in the case of 1.0 Corey's exponent is then higher than the case of Corey's exponent of 2.5. This therefore, results in better flow of oil in case of lower value of Corey's exponent. Consecutively, residual oil of case 1.0 Corey's exponent can be reduced to residual oil saturation as shown as blue area in Figure 5.103. Figure 5.103 illustrates oil saturation profile at the end of production of each Corey's exponent value. When Corey's exponent increases from 1.0 to 2.5, volumetric sweep efficiency is increased but displacement efficiency is reduced. Even if volumetric sweep efficiency of case 1.0 Corey's exponent is not as high, displacement efficiency is the best that reaches residual oil saturation. Recovery factor is the highest when Corey's exponent is 1.0.

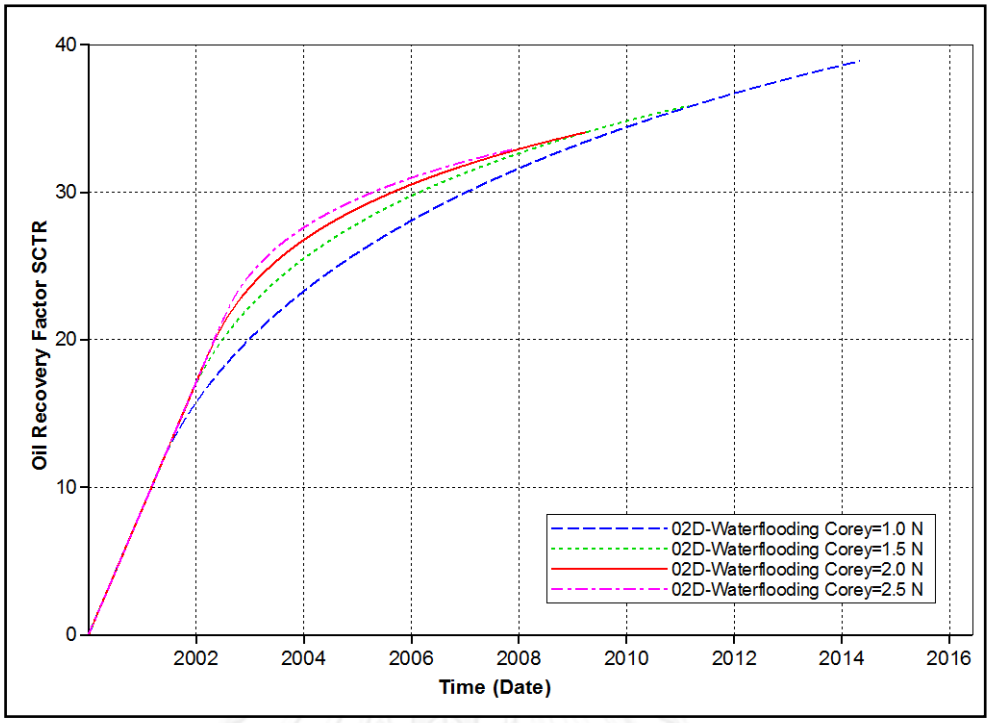

(a)

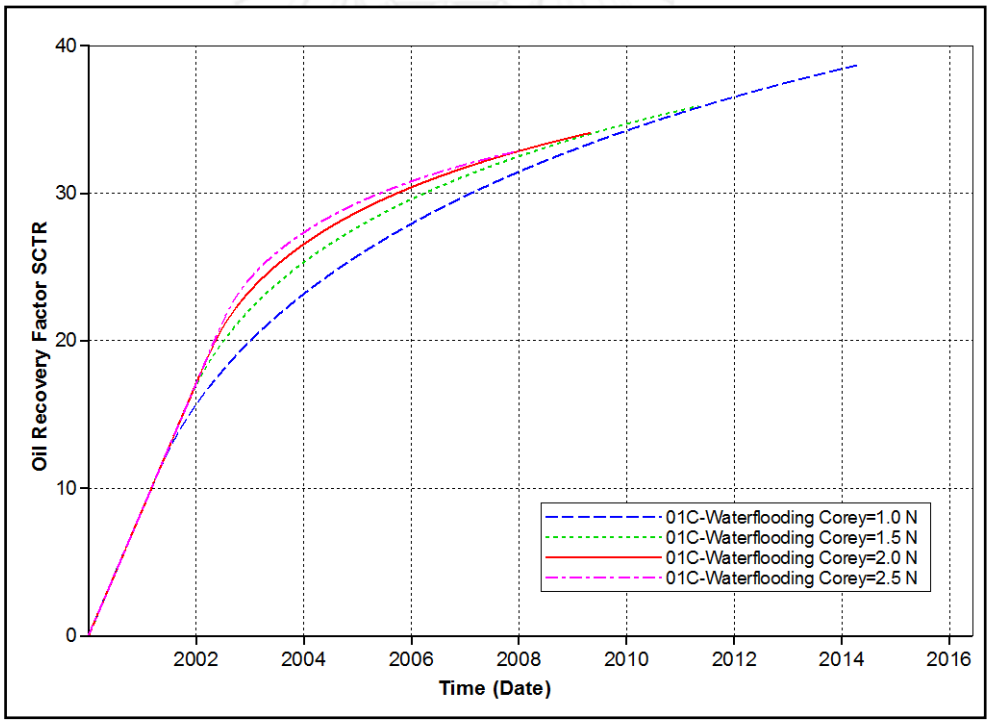

(b)

Figure 5.99 Recovery factors of various Corey's exponents of rock at normal condition by waterflooding (a) model 02D (b) model 01C

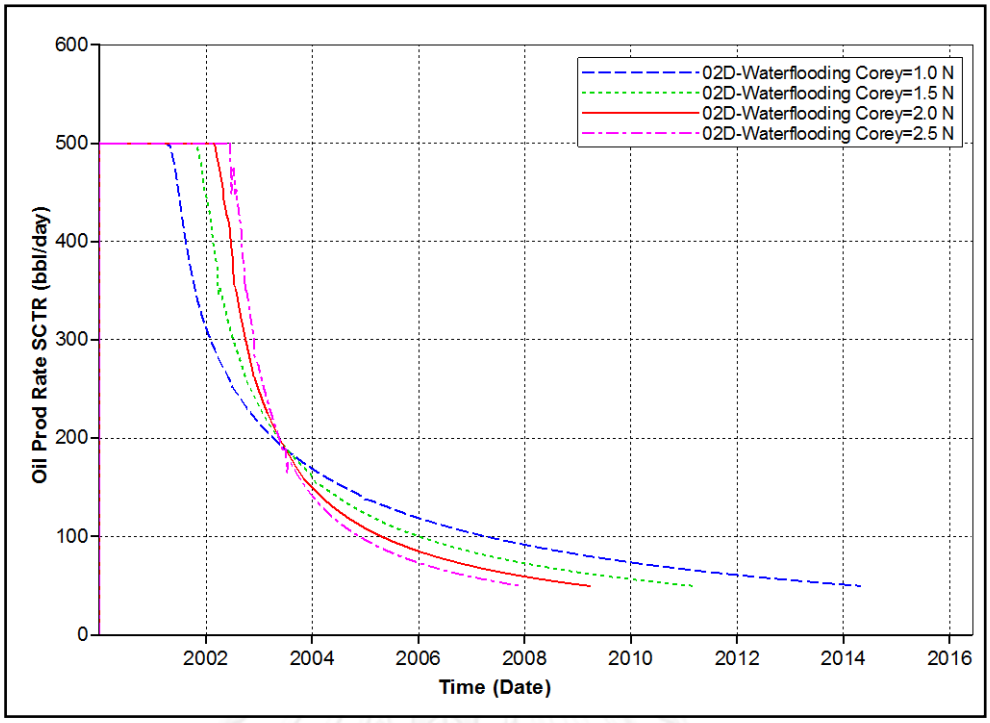

(a)

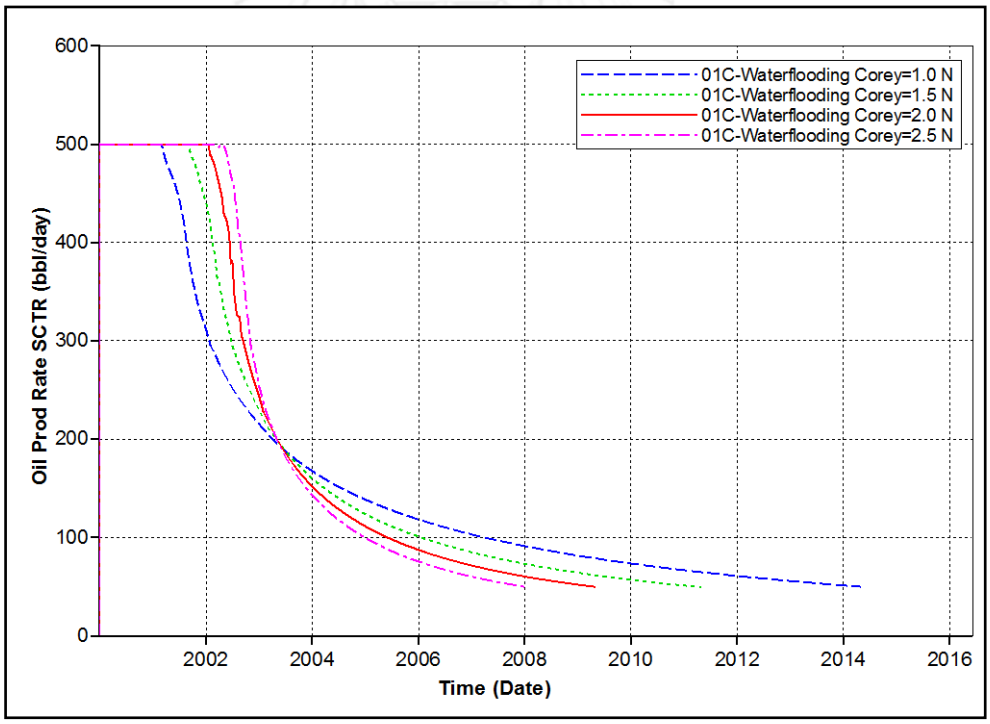

(b)

Figure 5.100 Oil production rates of various Corey's exponents of rock at normal condition by waterflooding (a) model 02D (b) model 01C

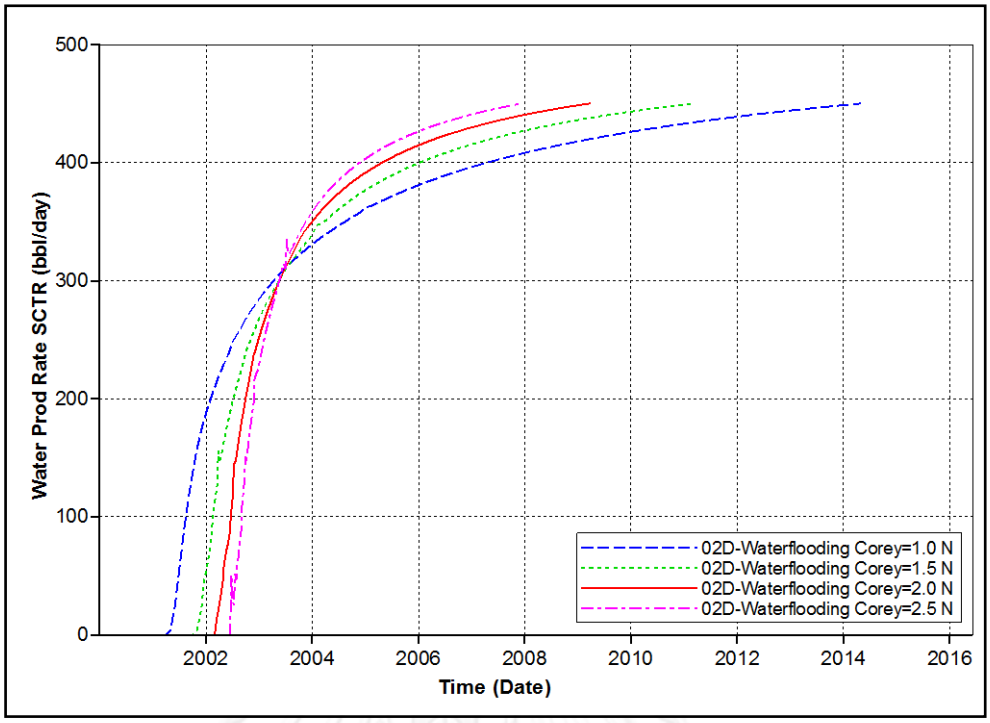

(a)

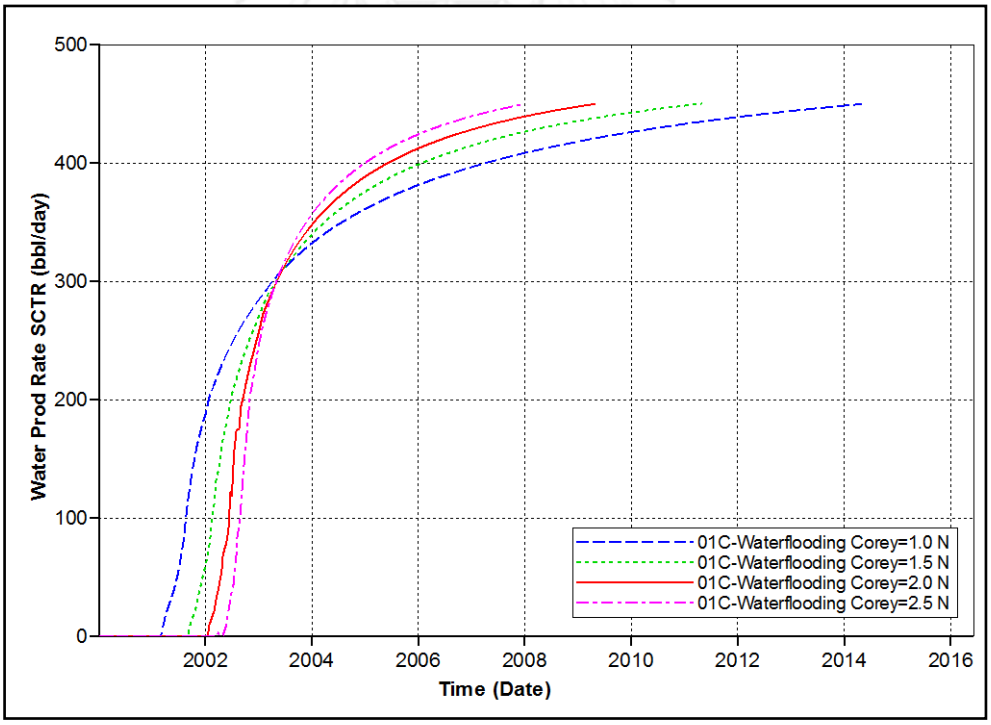

(b)

Figure 5.101 Water production rates of various Corey's exponents of rock at normal condition by waterflooding (a) model 02D (b) model 01C

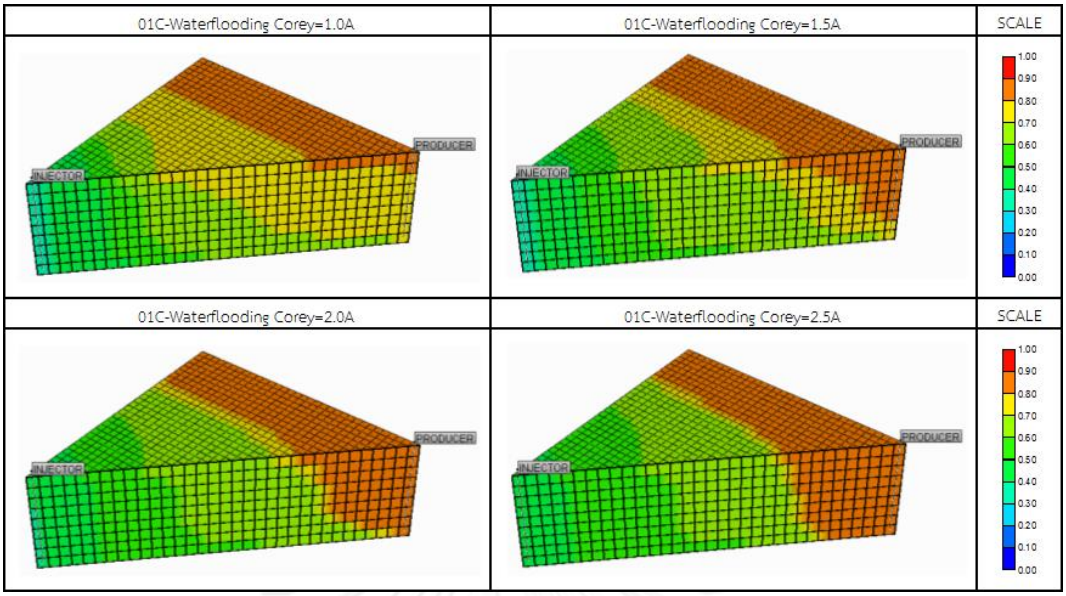

Figure 5.102 Oil saturation profiles of various Corey's exponents of rock at normal condition by waterflooding at 2nd year 1st month

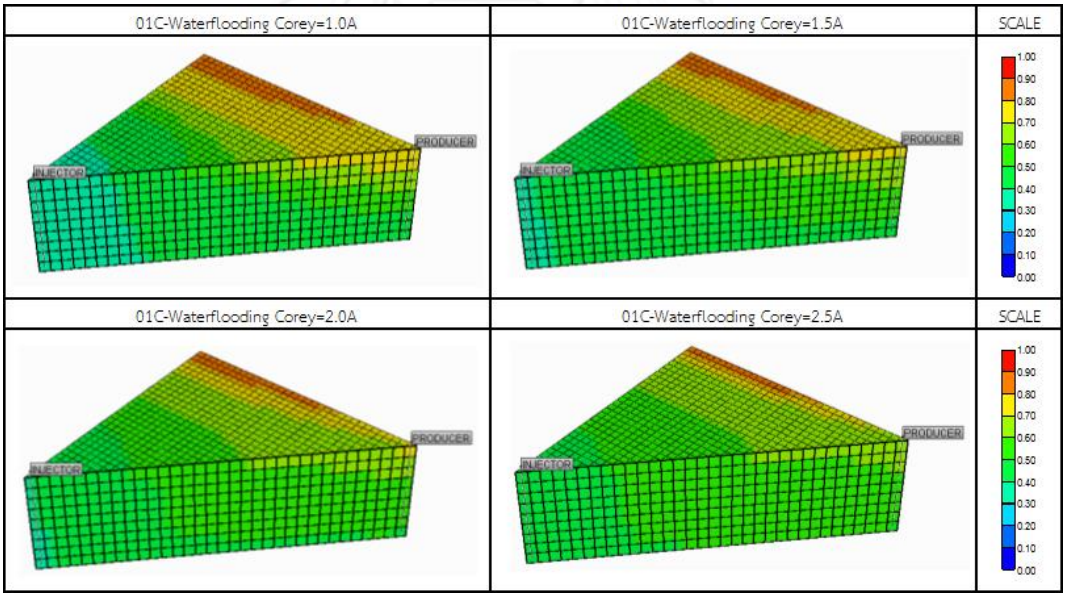

Figure 5.103 Oil saturation profiles of various Corey's exponents of rock at normal condition by waterflooding at the end of production

Oil recovery factors and production rates of AS+P flooding in model 02D are illustrated in Figures 5.104 to 5.106. From these figures, recovery mechanisms by means of AS+P flooding is more or less as same as waterflooding. Water production rate shows that the earliest water breakthrough occurs when Corey's exponent is 1.0 and the latest when Corey's exponent is 2.5. And so, oil production rate is the highest in case of Corey's exponent 2.5 prior to 4th year and 2nd month. After that, sweep efficiency is improved by post-flushed polymer slug. Chasing water is injected until flood front of post-flushed polymer slug can be stabilized. Therefore, recovery factor of AS+P flooding is decreasing when Corey's exponent is increased.

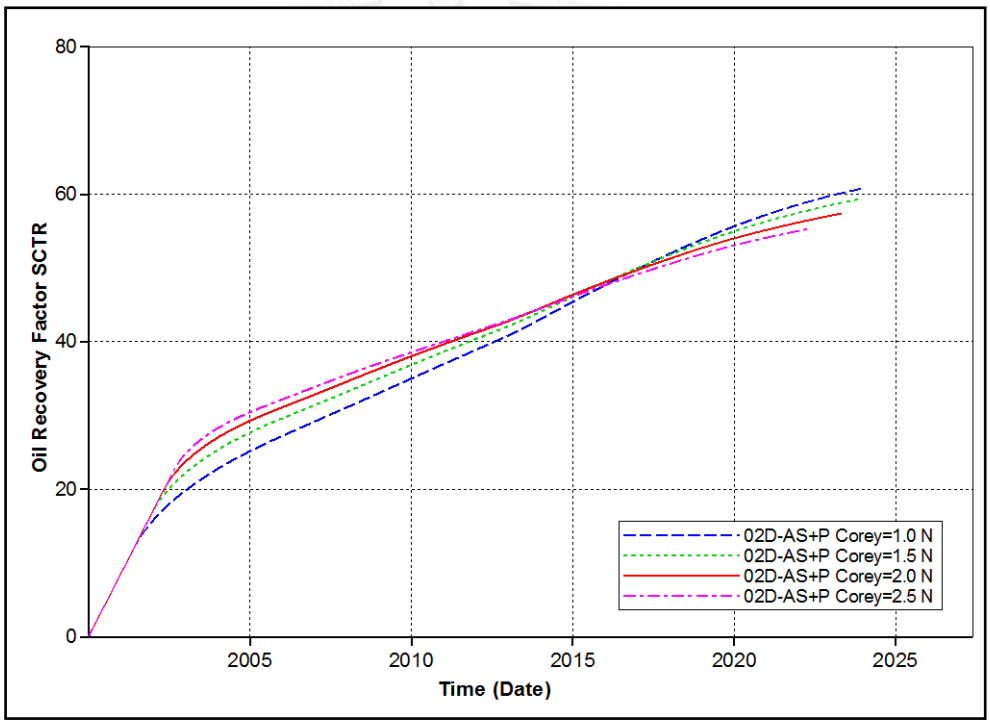

Figure 5.104 Recovery factors of various Corey's exponents of rock at normal condition by AS+P flooding in model 02D

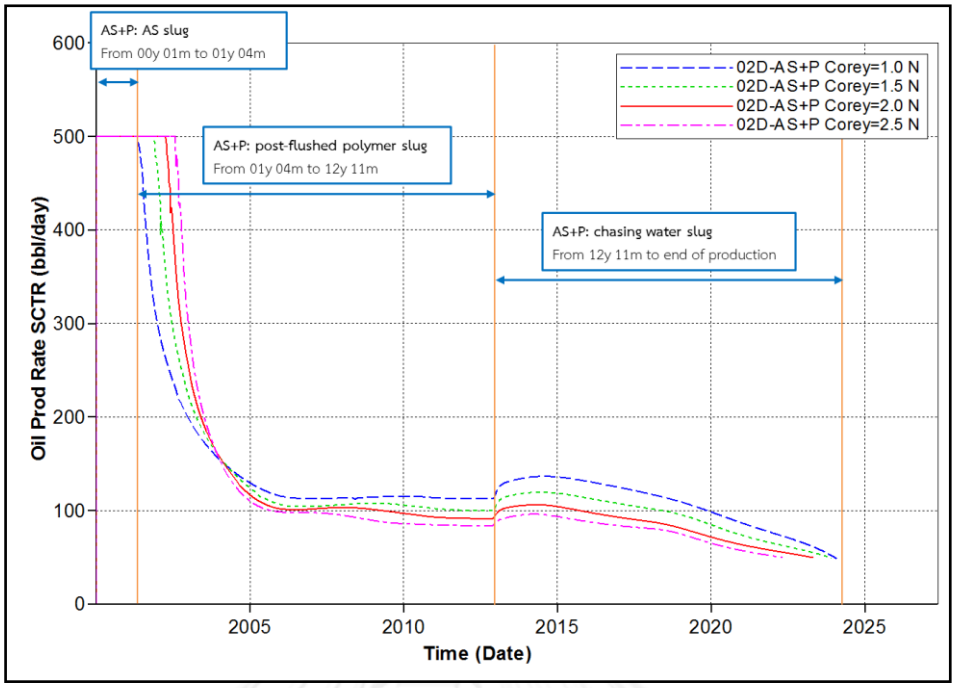

Figure 5.105 Oil production rates of various Corey's exponents of rock at normal condition by AS+P flooding in model 02D

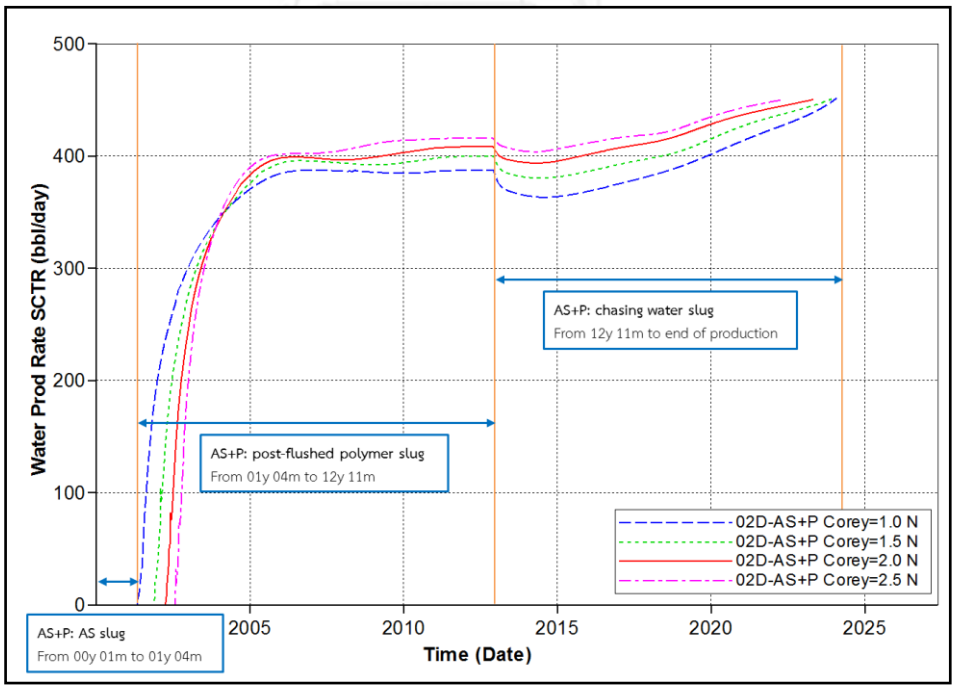

Figure 5.106 Water production rates of various Corey's exponents of rock at normal condition by AS+P flooding in model 02D

Oil recovery factor, production rates of P+AS+P flooding in model 01C are illustrated in Figures 5.107 to 5.109. From these figures, mechanisms during pre-flushed polymer slug, AS slug and post-flushed polymer slug are similar to those of waterflooding and AS+P flooding. Result of separating polymer slug can improve recovery factor not only in AS injection period, but also during chasing water period near the end of production. Pre-flushed polymer slug can compensate recovery factor in case 2.5 Corey's exponent by stabilizing flood front, extending production period. Therefore, recovery factors of P+AS+P flooding are quite constant throughout the chosen Corey's exponents.

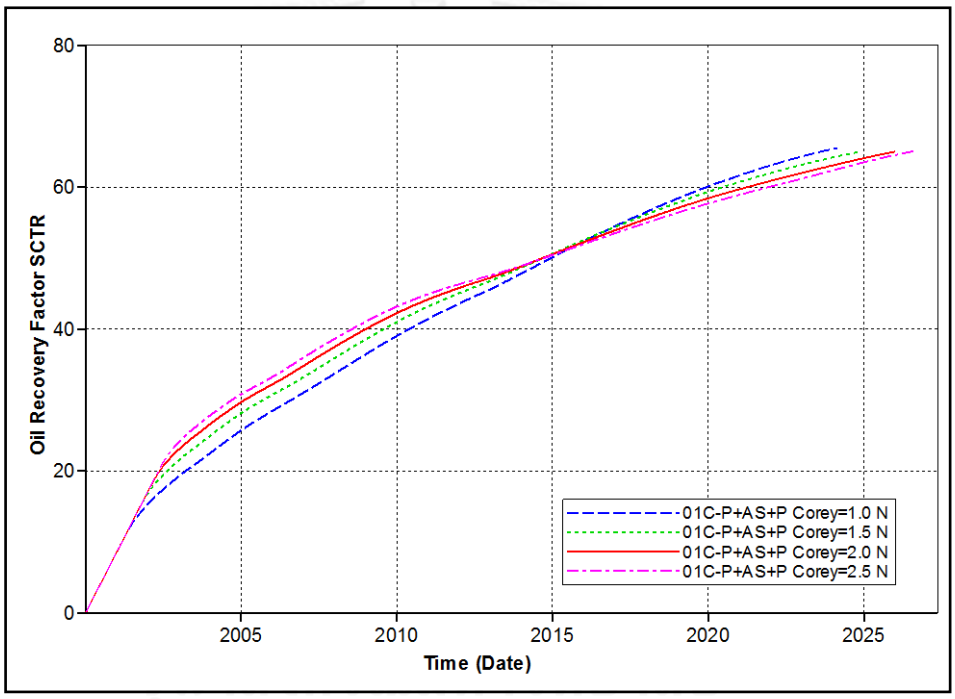

Figure 5.107 Recovery factors of various Corey's exponents of rock at normal condition by P+AS+P flooding in model 01C

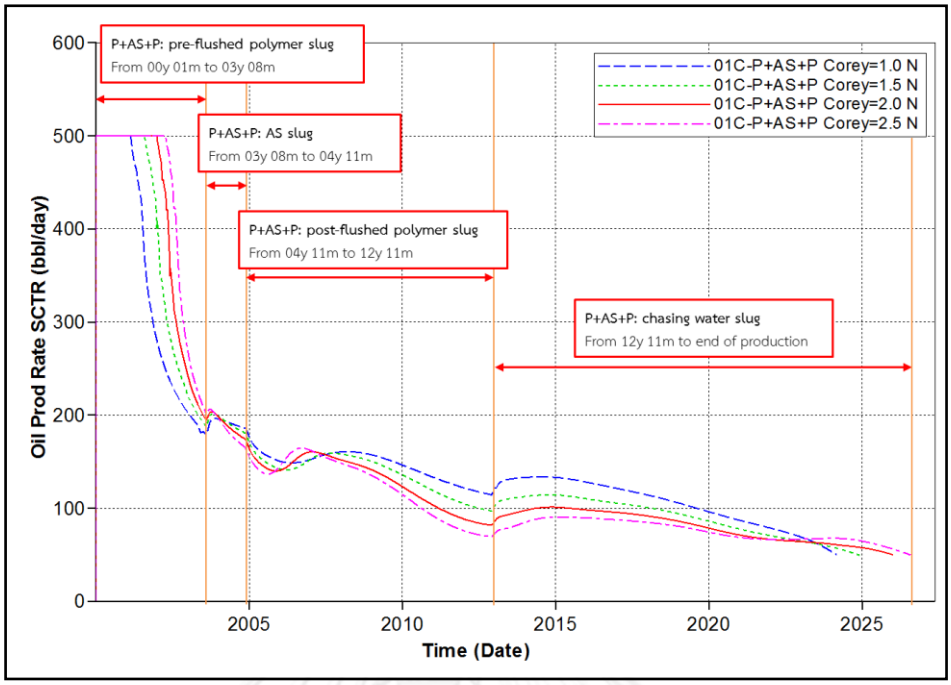

Figure 5.108 Oil production rates of various Corey's exponents of rock at normal condition by P+AS+P flooding in model 01C

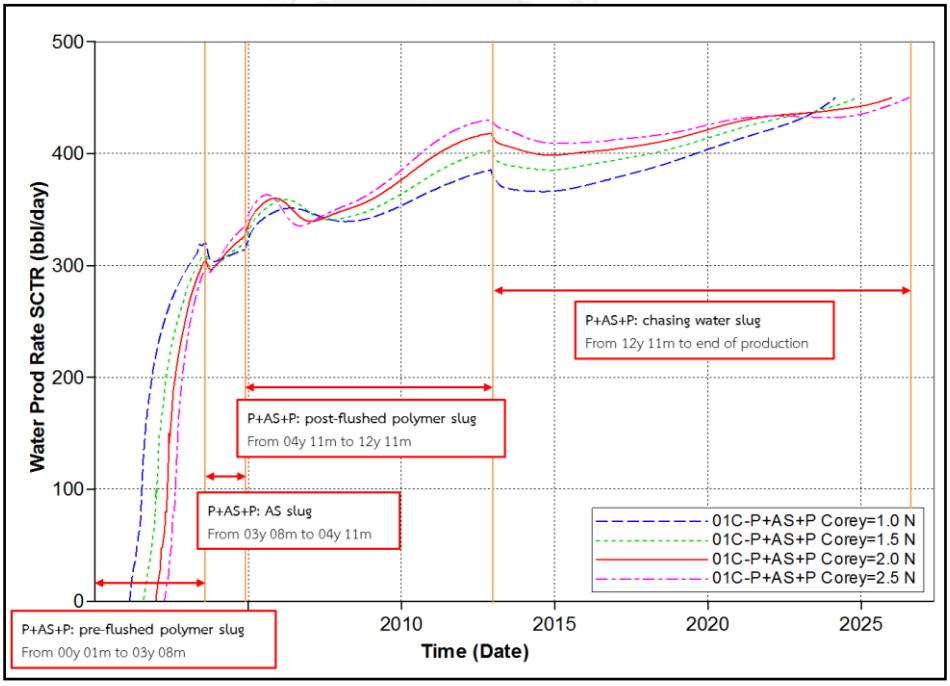

Figure 5.109 Water production rates of various Corey's exponents of rock at normal condition by P+AS+P flooding in model 01C

5.5.1.2 Corey's exponent of Rock at Ultra-low IFT Condition (Cases U)

Relative permeability curves at ultra-low IFT condition is represented by interpolation set3 in the STAR. Corey's exponent of rock at ultra-low IFT condition is 1.0 for base case. Corey's exponents of ultra-low IFT condition are varied to 1.5 and 2.0. Various Corey's exponents of rock ultra-low IFT condition are illustrated in Figure 5.110.

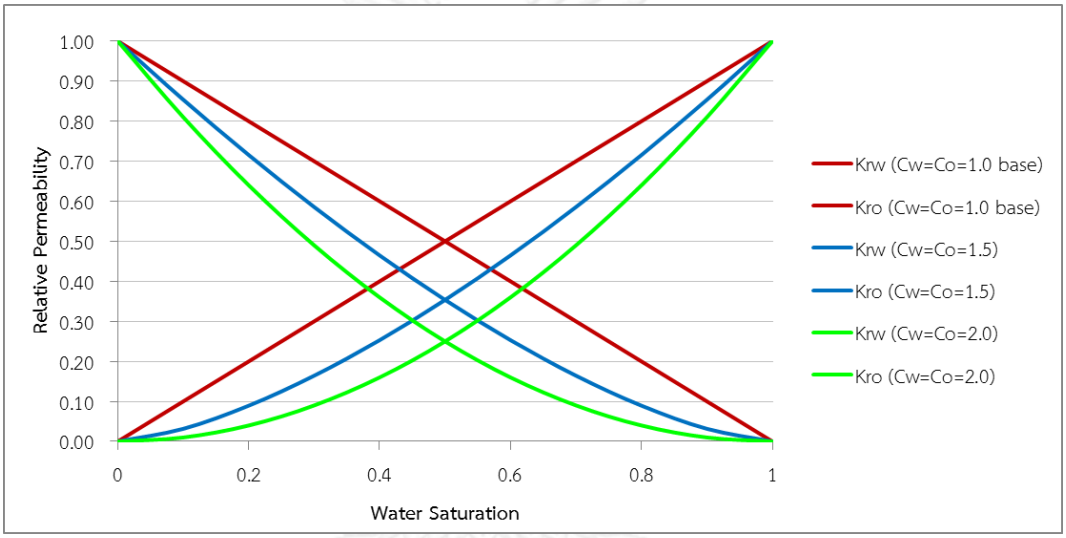

Figure 5.110 Summary of relative permeability curves generated from different Corey's exponent values for rock at ultra-low IFT condition

Summary of recovery factors and incremental recovery factors of waterflooding, AS+P flooding and P+AS+P flooding are illustrated in Figures 5.111 and 5.112, respectively. Incremental recovery factors of both AS+P and P+AS+P flooding compared to waterflooding is reduced when Corey's exponent of rock at ultra-low IFT condition is raised. Decreasing of incremental recovery factor is caused by constant recovery factor in all waterflooding cases and reducing recovery factor of both of AS+P and P+AS+P flooding. Since Corey's exponent of rock at ultra-low IFT condition is activated when capillary number decreases by means of alkali and surfactant, recovery factor of all waterflooding cases does not change because IFT is still high.

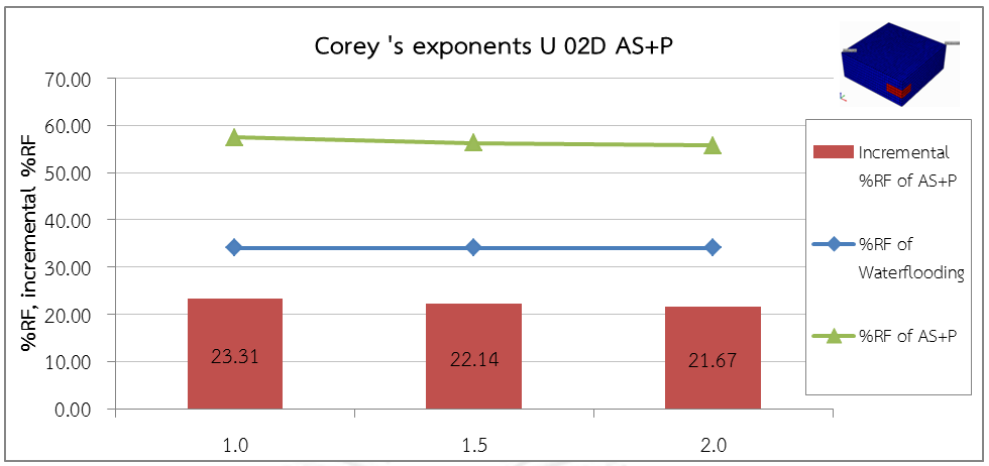

Figure 5.111 Recovery factors and incremental recovery factors compared to waterflooding of various Corey's exponents of rock at ultra-low IFT condition by AS+P flooding

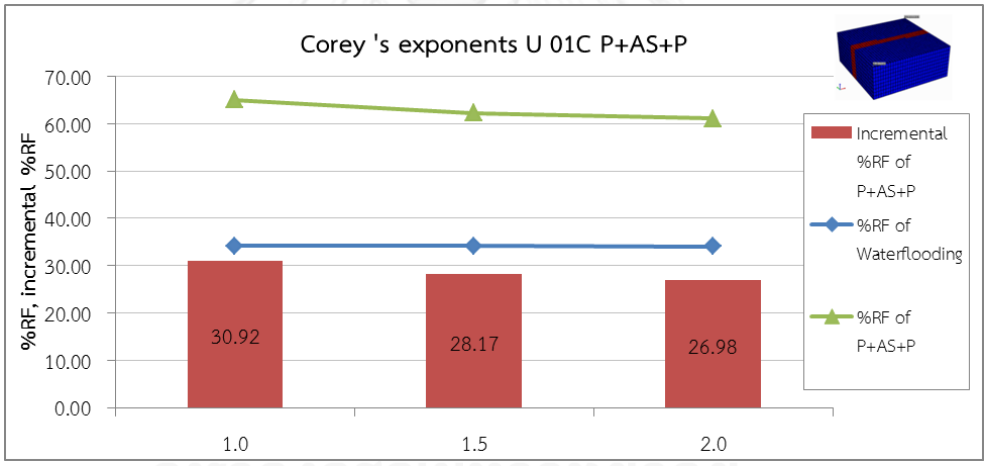

Figure 5.112 Recovery factors and incremental recovery factors compared to waterflooding of various Corey's exponents of rock at ultra-low IFT condition by P+AS+P flooding

Recovery factor, oil and water production rates of AS+P flooding in model 02D are illustrated in Figures 5.113 to 5.115, whereas recovery factor, oil and water production rates of P+AS+P flooding in model 01C are depicted in Figures 5.116 to 5.118. Main mechanism which is caused by variation of Corey's exponent of rock at ultra-low IFT condition occurs in AS injection period. Oil production rates of AS+P flooding in Figure 5.114 show very less difference during post-flushed polymer period after AS injection for all cases. But, oil production rates of P+AS+P flooding in Figure

5.117 are obviously difference during post-flushed polymer period after AS injection for all cases. Therefore, impact of Corey's exponent of rock at ultra-low IFT condition is explained by using P+AS+P flooding in model 01C at 7th year, 1st month in Figure 5.119. Oil saturation profile in each case shows similar ultra-low IFT area altered by AS injection. However, residual oil after AS injection is different from case to case. For Corey's exponent of rock at ultra-low condition IFT equal to 1.0, residual oil is reduced nearly to near zero, whereas residual oil increases when Corey's exponent of rock ultra-low IFT condition increases to 2.5. This is again the effect from curvature of relative permeability to oil close to end point of 100 percent water saturation. In case of Corey's exponent of rock at ultra-low IFT condition of 1.0 or 1.5, oil can flow nearly to 100 percent water saturation. Therefore, very less amount of residual oil is left in ultra-low IFT zone. On the other hand, residual oil cannot flow at water saturation around 1.0 when Corey's exponent of rock at ultra-low IFT condition is 2.5. Therefore, displacement efficiency of AS injection depends mainly on Corey's exponent of rock at ultra-low IFT condition.

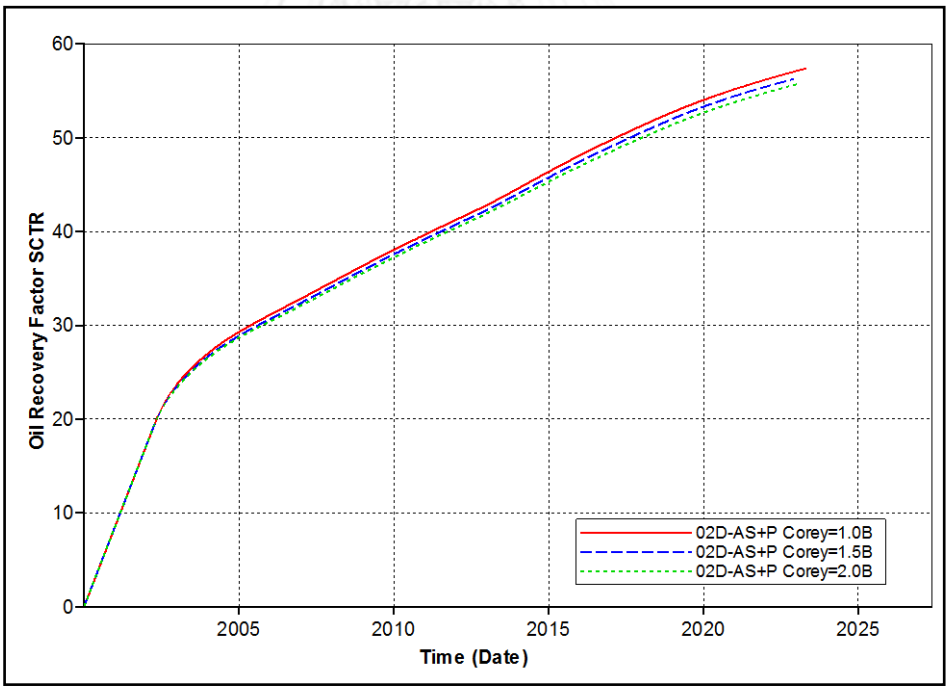

Figure 5.113 Recovery factors of various Corey's exponents of rock at ultra-low IFT condition by AS+P flooding in model 02D

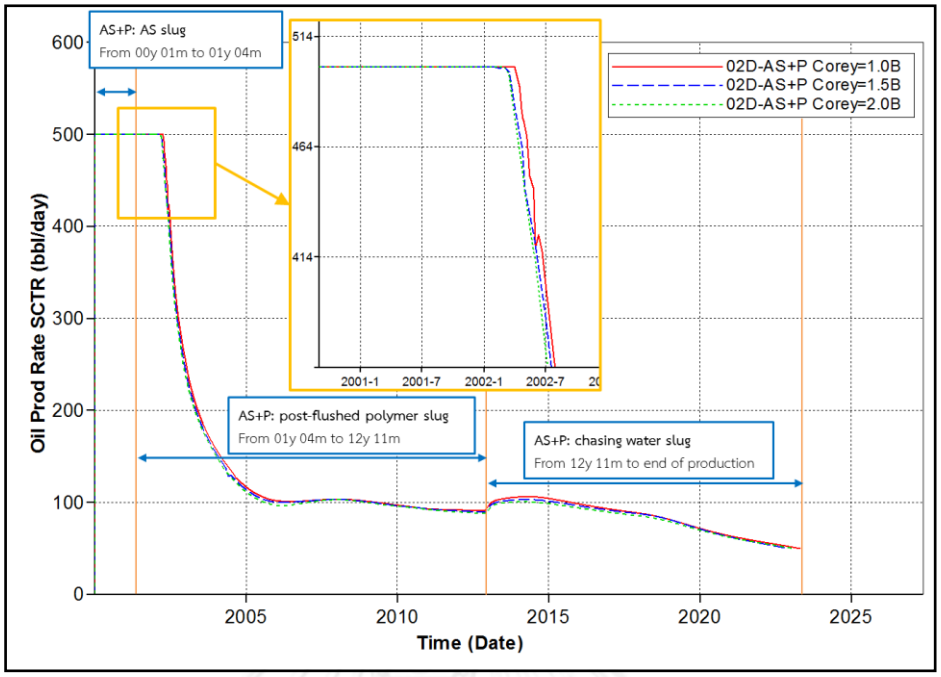

Figure 5.114 Oil production rates of various Corey's exponents of rock at ultra-low IFT condition by AS+P flooding in model 02D

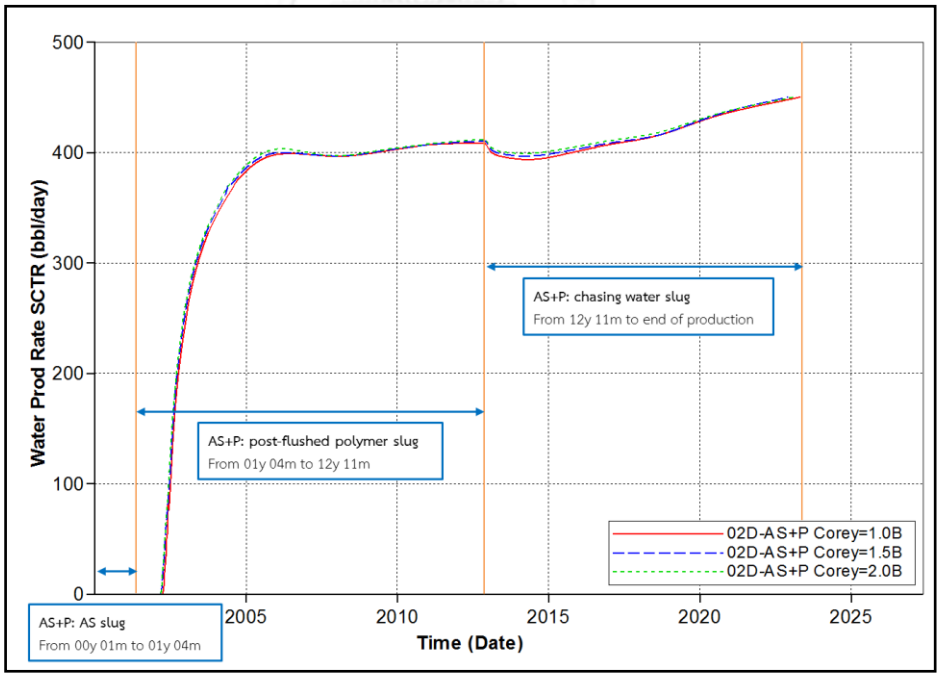

Figure 5.115 Water production rates of various Corey's exponents of rock at ultra-low IFT condition by AS+P flooding in model 02D

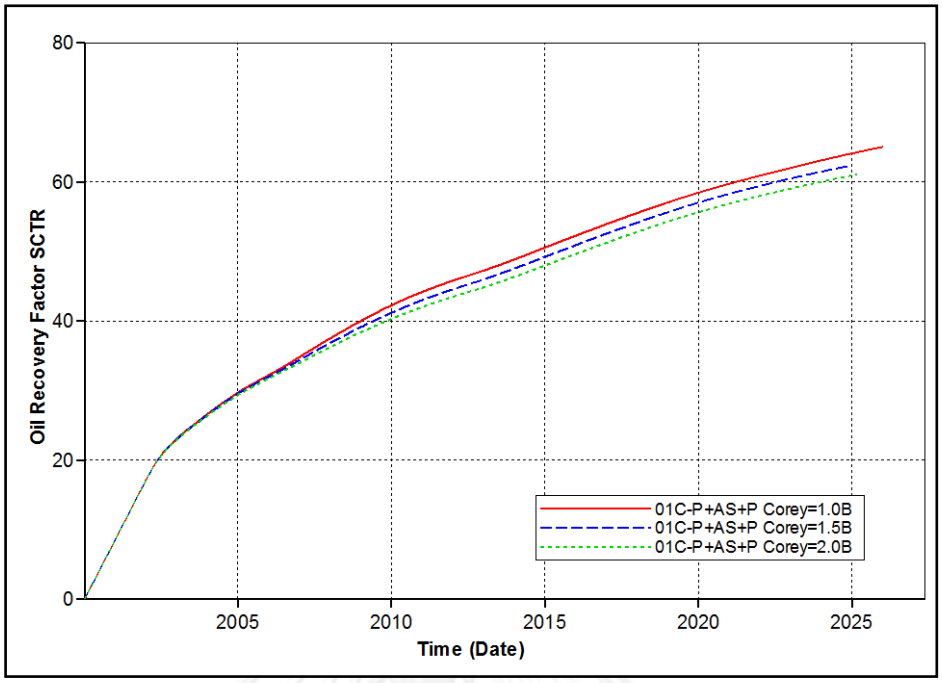

Figure 5.116 Recovery factors of various Corey's exponents of rock at ultra-low IFT condition by P+AS+P flooding in model 01C

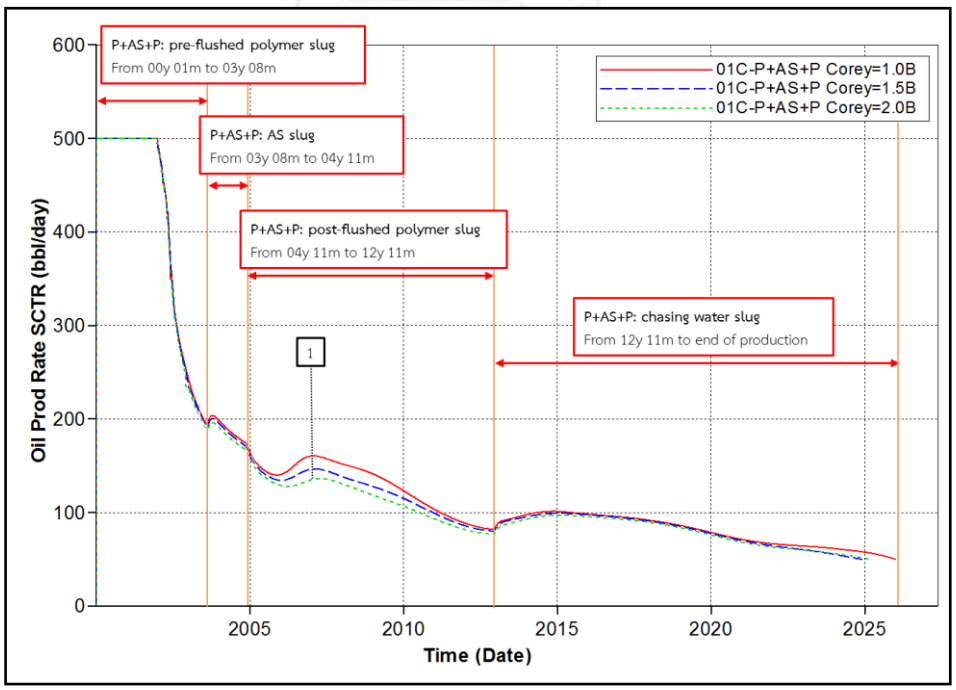

Figure 5.117 Oil production rates of various Corey's exponents of rock at ultra-low IFT condition by P+AS+P flooding in model 01C

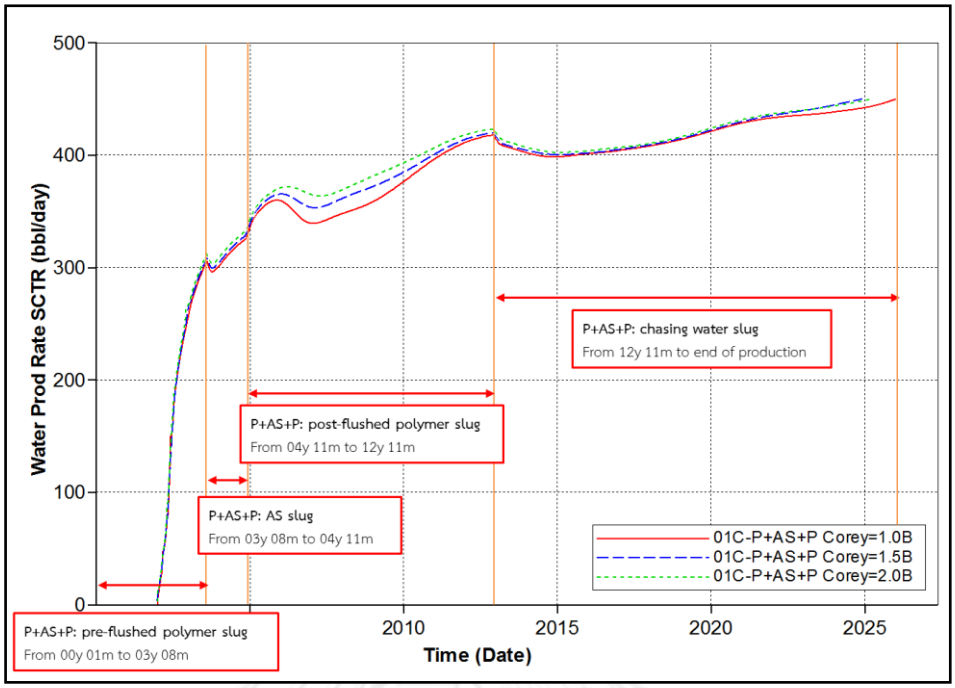

Figure 5.118 Water production rates of various Corey's exponents of rock at ultra-low IFT condition by P+AS+P flooding in model 01C

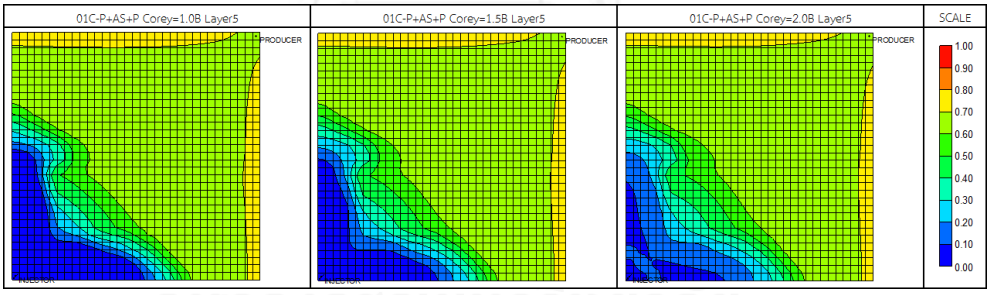

Figure 5.119 Oil saturation profiles of various Corey's exponents of rock at ultra-low IFT condition by P+AS+P flooding at 7th year, 1st month

5.5.2 Wettability

In this section, sensitivity of rock wettability on AS+P and P+AS+P flooding is considered. In general, wetting condition can be distinguished from relative permeability curves to oil and water as well as capillary pressure which are precisely measured from special core analysis in laboratory. Previously mentioned in Chapter 4 (section 4.1.3) wettability of base case reservoir model is moderately oil-wet. Various wetting conditions are considered including mildly oil-wet, strongly oil-wet and very strongly oil-wet. Summary of essential parameters to generate these wetting conditions are summarized in Table 5.15. Essential parameters are set to align with the rule of thumb by Craig Jr. [19]. Movable oil saturation is fixed in all cases by controlling constant difference between irreducible water saturation (S_{wi}) and residual oil saturation (S_{or}). Relative permeability curves and capillary pressure of each wetting condition are illustrated in Figures 5.120 and 5.121. Relative permeability curve shifts to the left with the same movable oil saturation gap when wettability moves to stronger oil-wet condition. Irreducible water saturation is decreasing, whereas residual oil saturation is increasing when wettability tends to be stronger oil-wet. Moreover, relative permeability to water at residual oil saturation ($k_{rw@}S_{orw}$) is increasing when wettability tends to be stronger oil-wet. End-point capillary pressure (P_c) is decreasing when wettability tends to be stronger oil-wet.

Table 5.15 Essential parameters required to represent all wetting conditions

Wetting condition	S_{wi}	S_{or}	Mobile oil saturation	$k_{rw@}S_{orw}$	P_c
Mildly oil-wet	0.2	0.35	0.45	0.225	-1
Moderately oil-wet	0.15	0.4	0.45	0.3	-2
Strongly oil-wet	0.13	0.42	0.45	0.375	-4
Very strongly oil-wet	0.11	0.44	0.45	0.45	-6

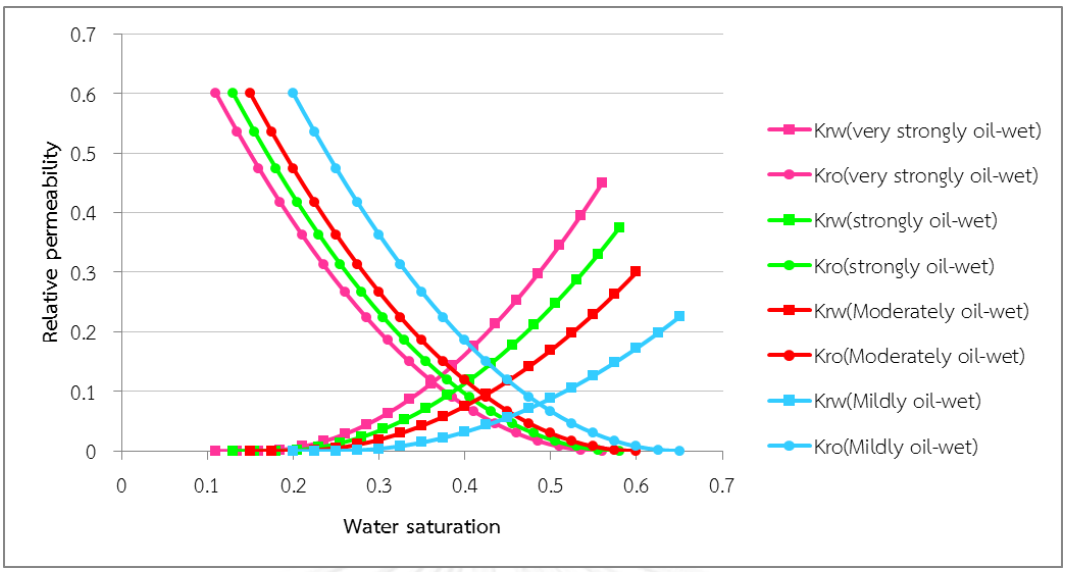

Figure 5.120 Summary of relative permeability curves of various wetting conditions

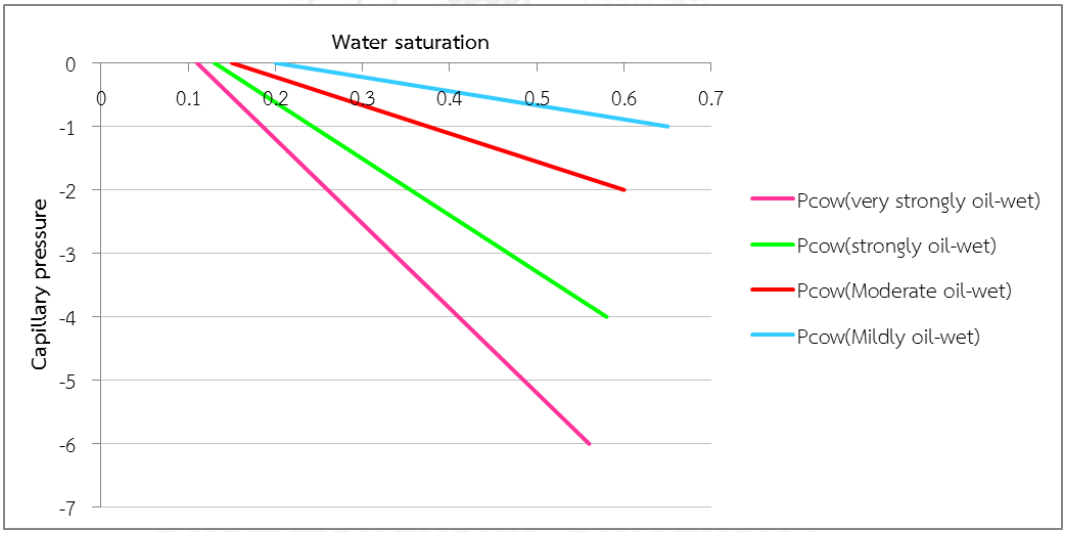

Figure 5.121 Summary of capillary pressures of various wetting conditions

Summary of recovery factor and incremental recovery factor of waterflooding, AS+P and P+AS+P flooding are illustrated in Figures 5.122 and 5.123, respectively. Both of incremental recovery factors by means of AS+P and P+AS+P flooding based on waterflooding are quite stable in all wetting conditions. These results can be implied that all of waterflooding, AS+P and P+AS+P flooding are equally affected from wettability conditions. Therefore, incremental recovery factors compared to waterflooding remain stable. However, these stable incremental recovery factors among wetting conditions means that both AS+P and P+AS+P flooding can guarantee improvement on recovery factor from conventional waterflooding in all chosen wetting conditions.

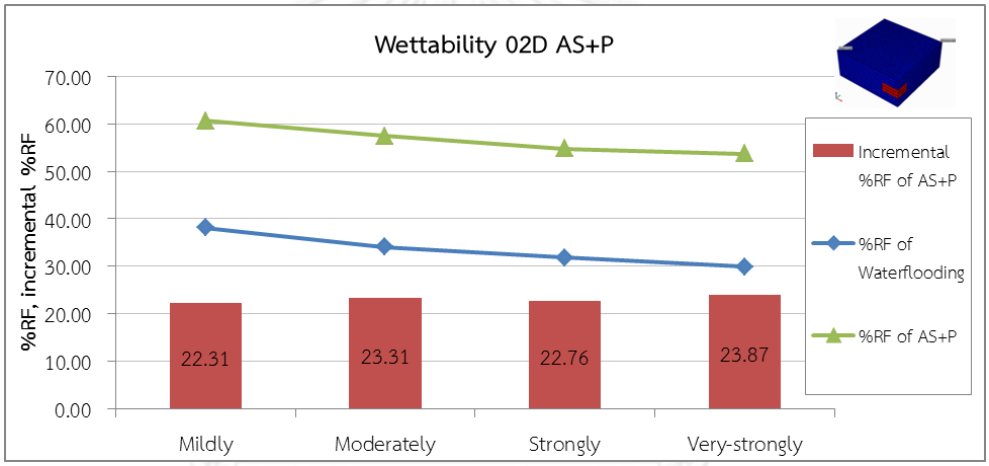

Figure 5.122 Recovery factors and incremental recovery factors of various wetting conditions by AS+P flooding

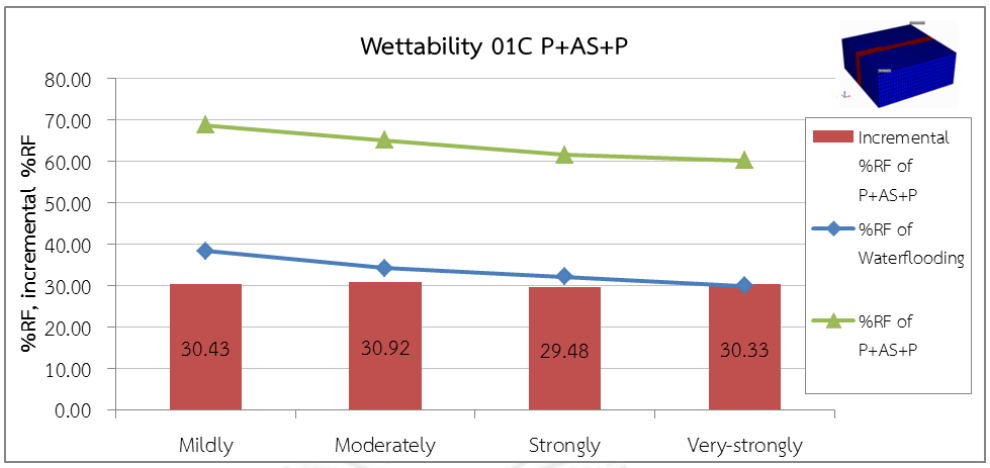

Figure 5.123 Recovery factors and incremental recovery factor of various wetting conditions by P+AS+P flooding

Recovery factor, oil and water production rate of waterflooding in model 02D and 01C are illustrated in Figures 5.124 to 5.126. Comparing these results between two models, trend of each waterflooding case is similar. Therefore, effect of wettability condition on waterflooding is explained through model 02D. Water production rate shows that water early breakthrough is remarkable when wetting condition is very strongly oil-wet. Therefore, sweep efficiency by waterflooding is less. Volumetric sweep efficiency and displacement efficiency are considered from oil saturation profile of various wetting conditions by waterflooding at the end of production shown in Figure 5.127. Oil saturation profile of mildly oil-wet case shows better of both displacement and volumetric sweep efficiency. Displacement efficiency can be distinguished from blue area nearby injector which is minimum residual oil saturation, whereas volumetric sweep efficiency can be observed from area covered by orange and yellow colors near producer which is residual oil remained in the reservoir.

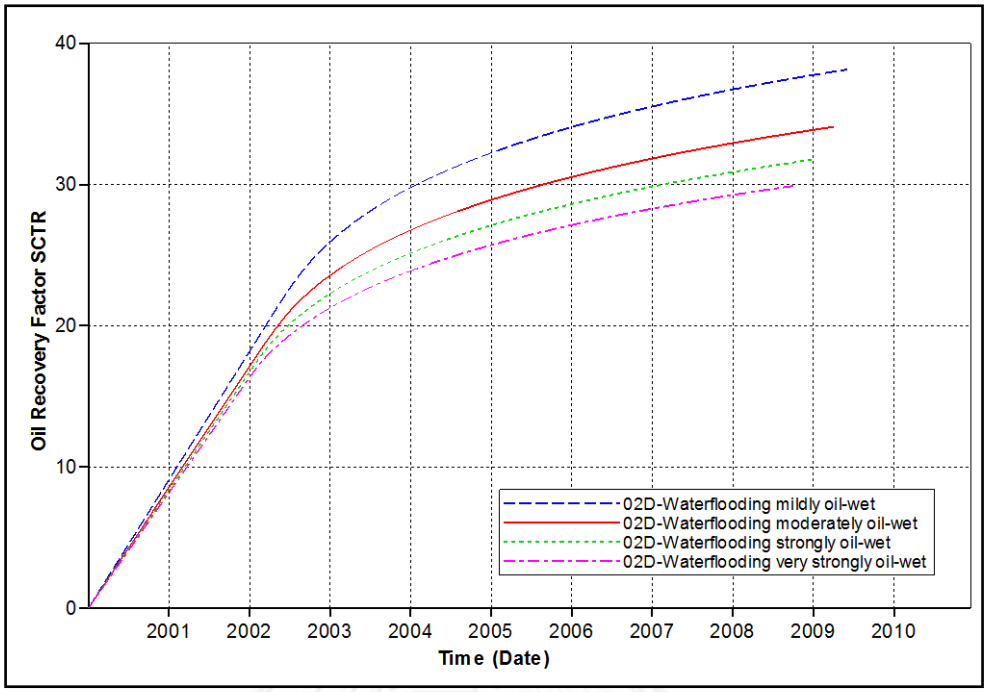

(a)

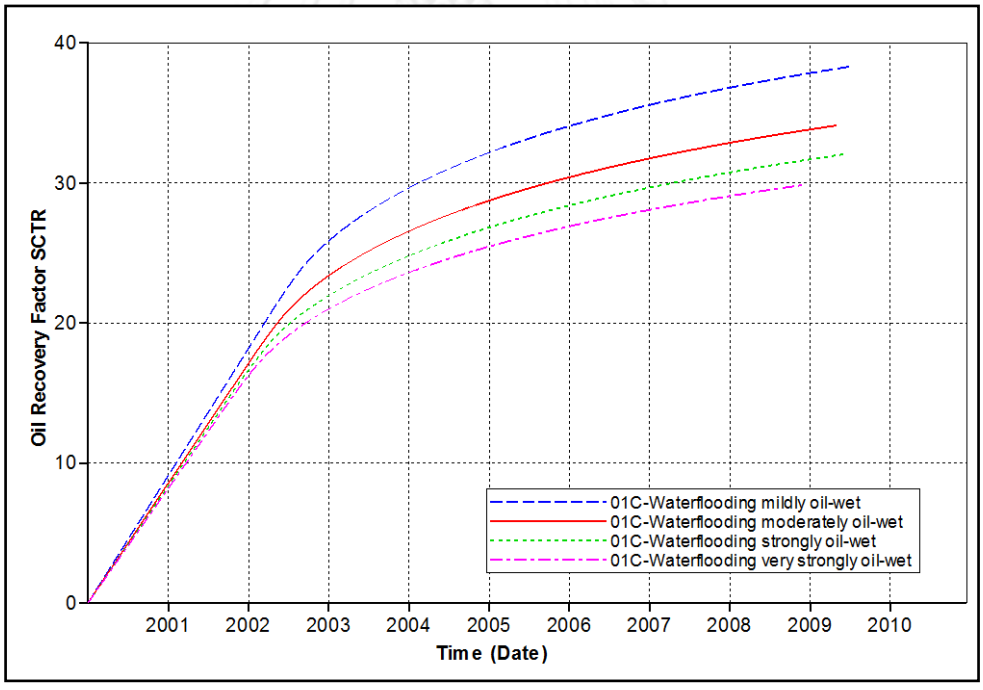

(b)

Figure 5.124 Recovery factors of various wetting conditions by waterflooding as a function of time (a) model 02D (b) model 01C

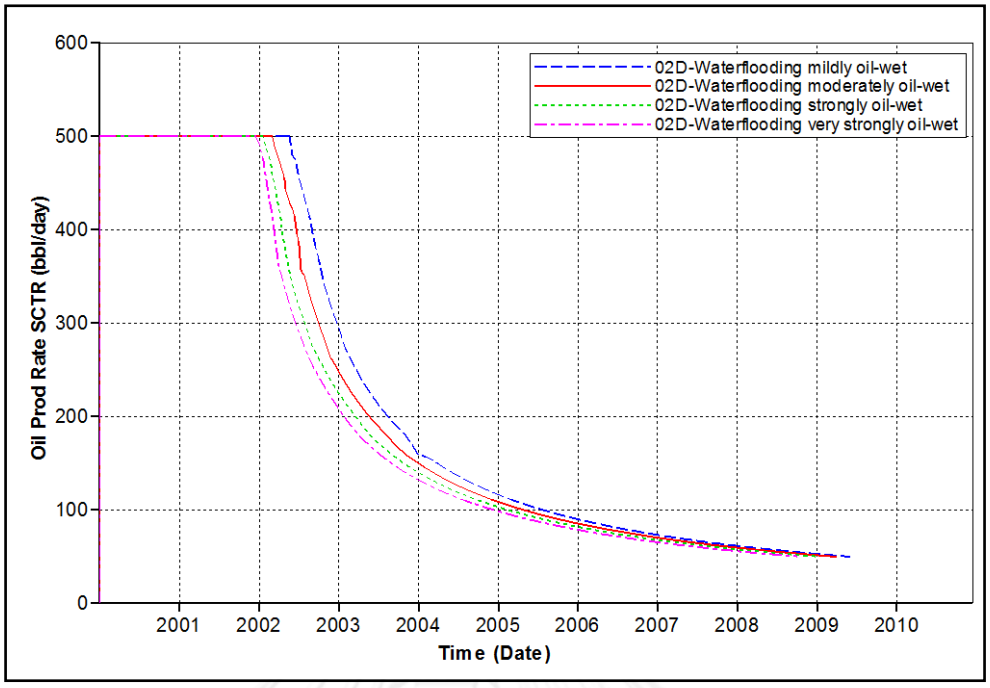

(a)

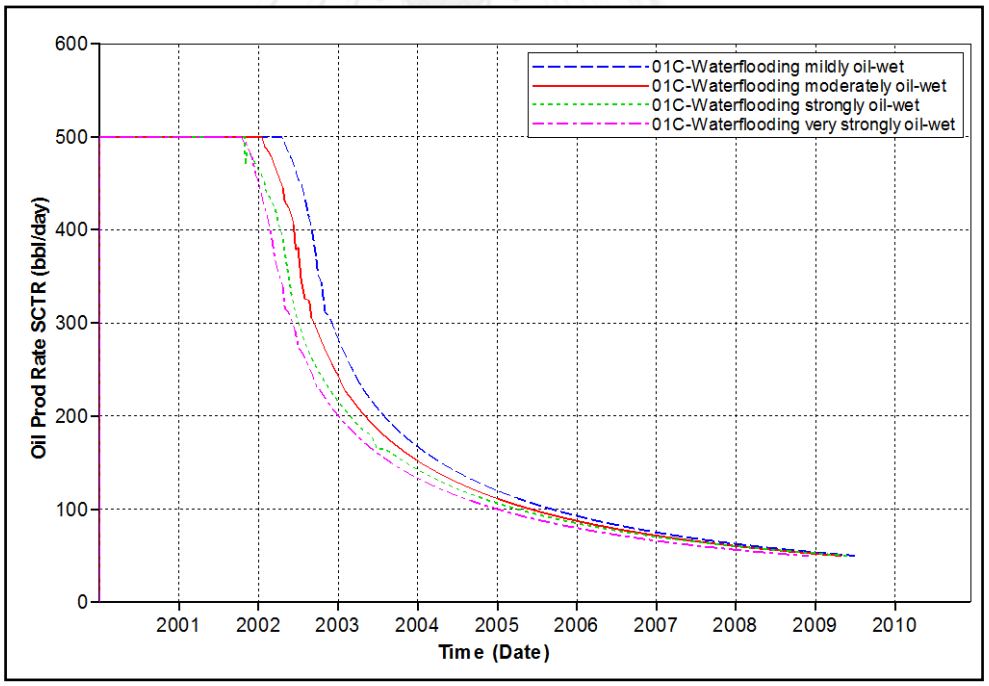

(b)

Figure 5.125 Oil production rates of various wetting conditions by waterflooding as a function of time (a) model 02D (b) model 01C

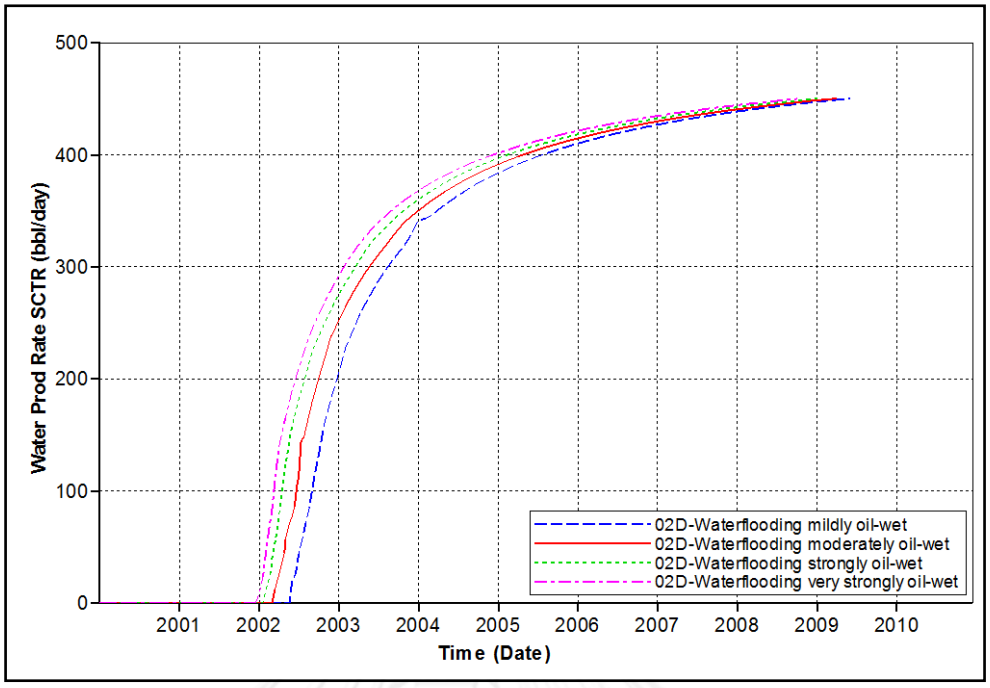

(a)

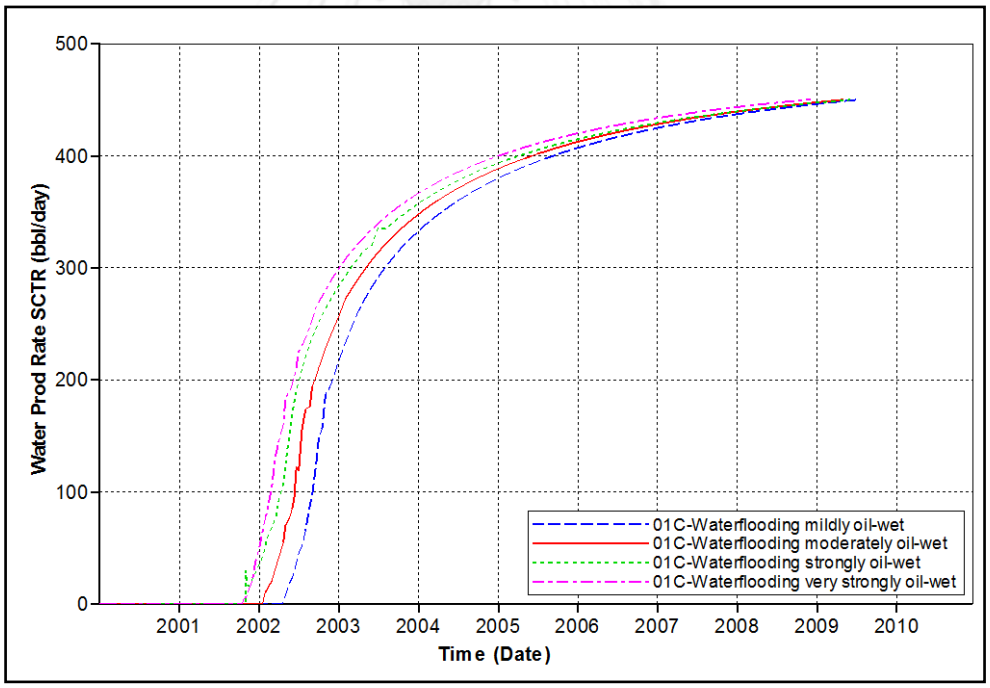

(b)

Figure 5.126 Water production rates of various wetting conditions by waterflooding as a function of time (a) model 02D (b) model 01C

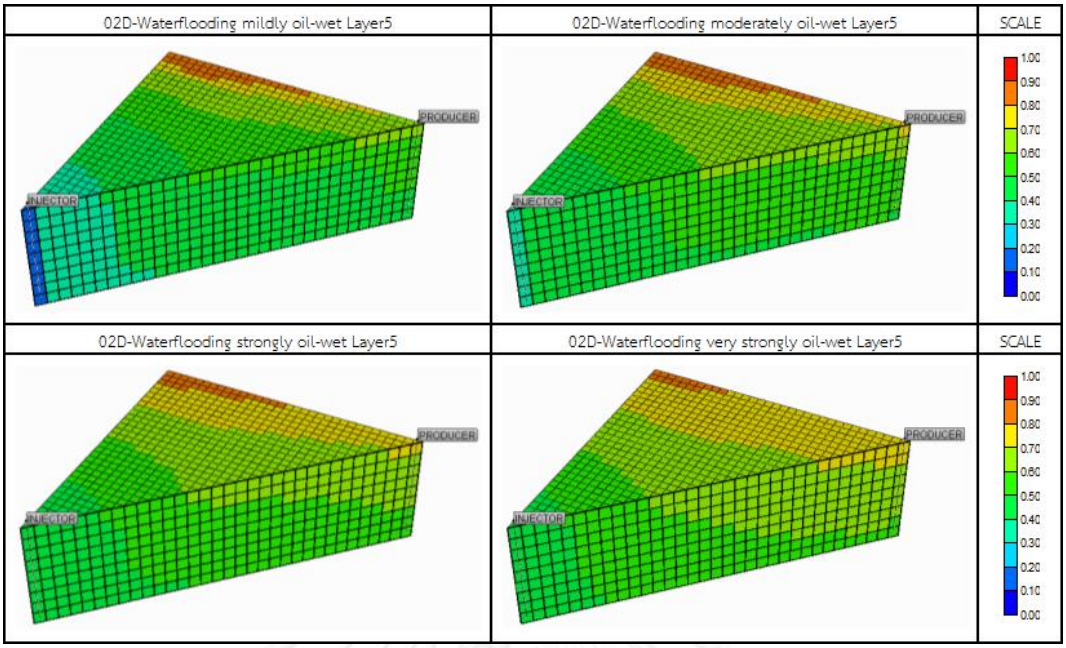

Figure 5.127 Oil saturation profiles of various wetting conditions by waterflooding at the end of production

Recovery factor, oil and water production rates of AS+P flooding in model 02D are illustrated in Figures 5.128 to 5.130, whereas recovery factor, oil and water production rates of P+AS+P flooding in model 01C are illustrated in Figures 5.131 to 5.133. From these results, mechanism which is affected from wetting condition occurs during post-flushed polymer slug and chasing water period. Oil recovery mechanism can be explained by using oil saturation profile of various wetting conditions of both AS+P and P+AS+P flooding at the end of production as shown in Figures 5.134 and 5.135, respectively. Area of deep blue color is a result from ultra-low IFT condition. This area, none of residual oil is left. Lighter blue color area shows the area that low-IFT condition is achieved. Area of ultra-low IFT condition is equal for all cases, but low-IFT zone is different. Low-IFT area is vast when wetting condition is mildly oil-wet. Low-IFT condition is the condition in between normal condition and ultra-low IFT condition. Therefore, amount of residual oil is different reduced based on low-IFT area in different wettability condition.

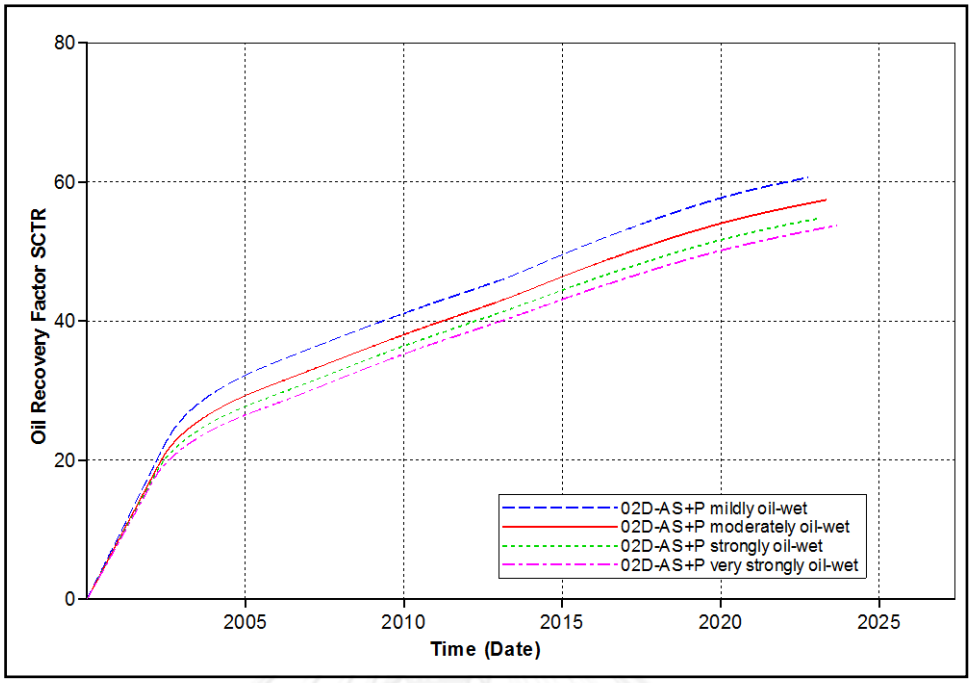

Figure 5.128 Recovery factors of various wetting conditions by AS+P flooding in model 02D as a function of time

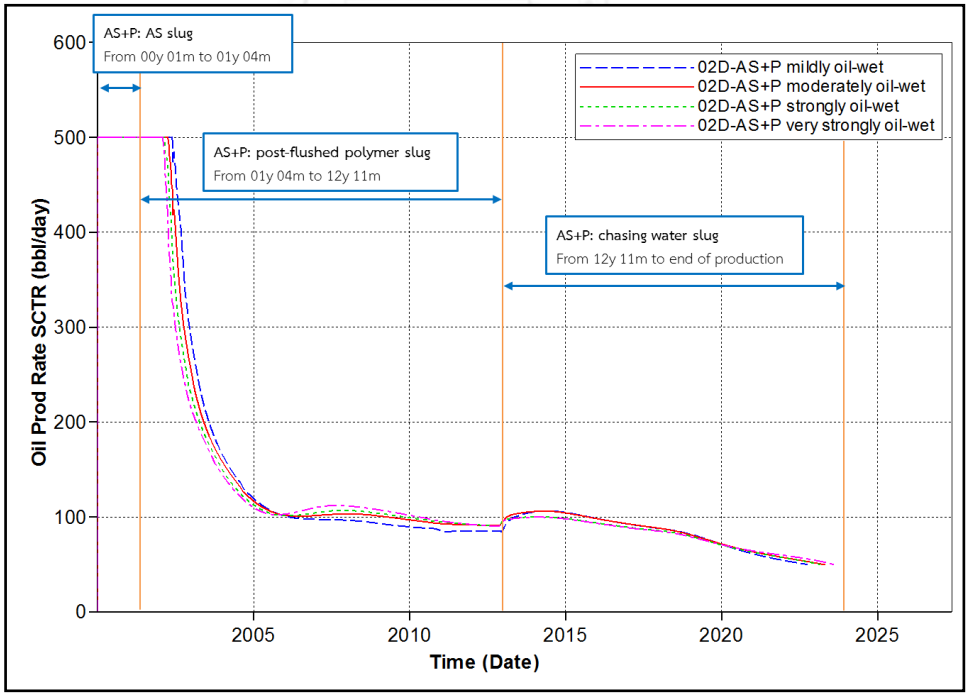

Figure 5.129 Oil production rates of various wetting conditions by AS+P flooding in model 02D as a function of time

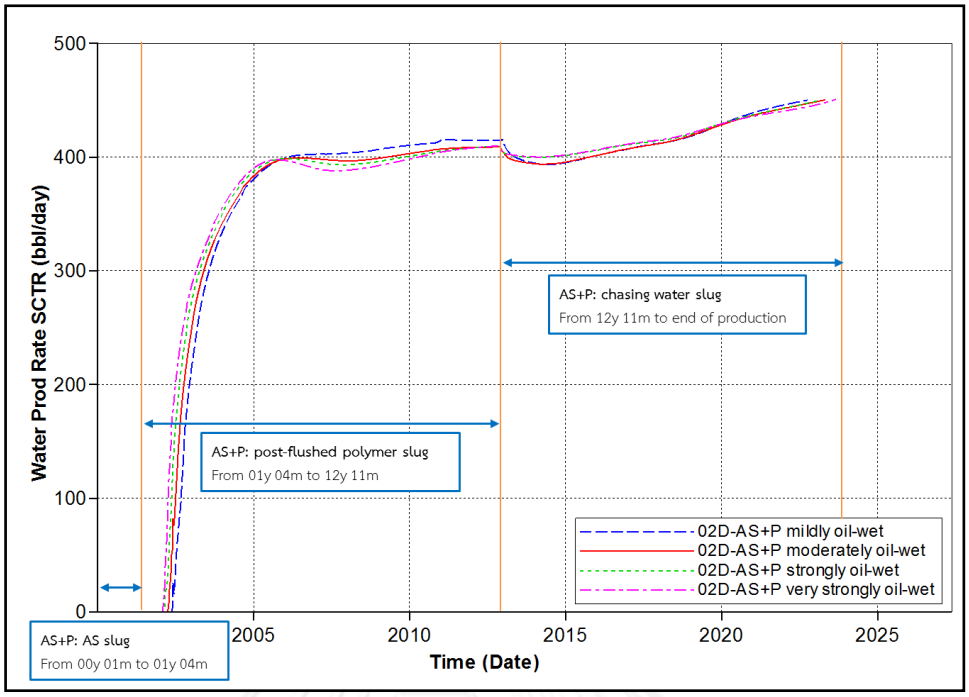

Figure 5.130 Water production rates of various wetting conditions by AS+P flooding in model 02D as a function of time

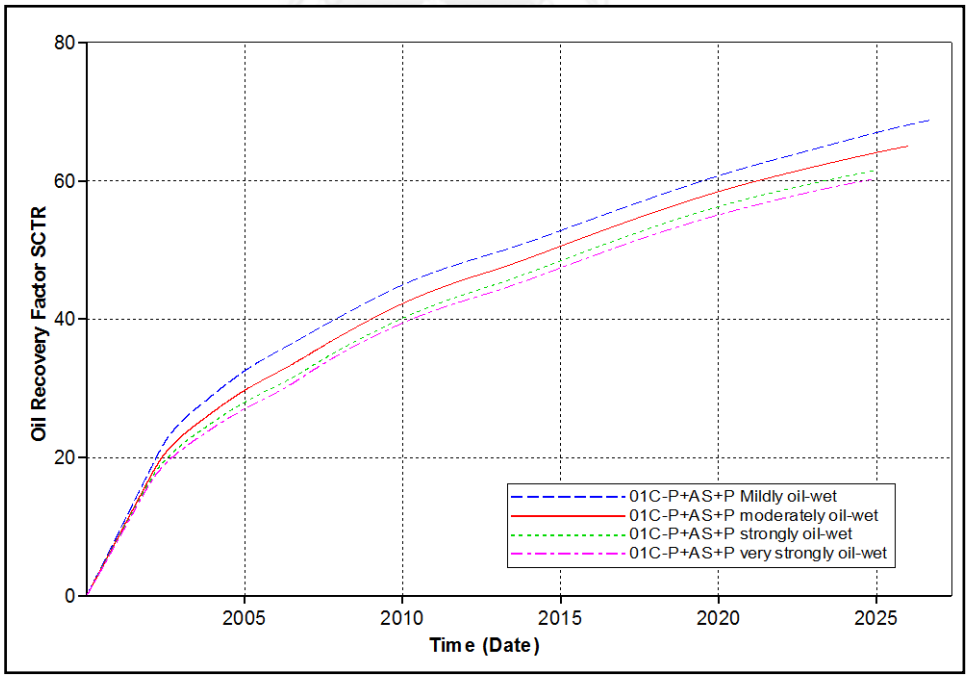

Figure 5.131 Recovery factors of various wetting conditions by P+AS+P flooding in model 01C as a function of time

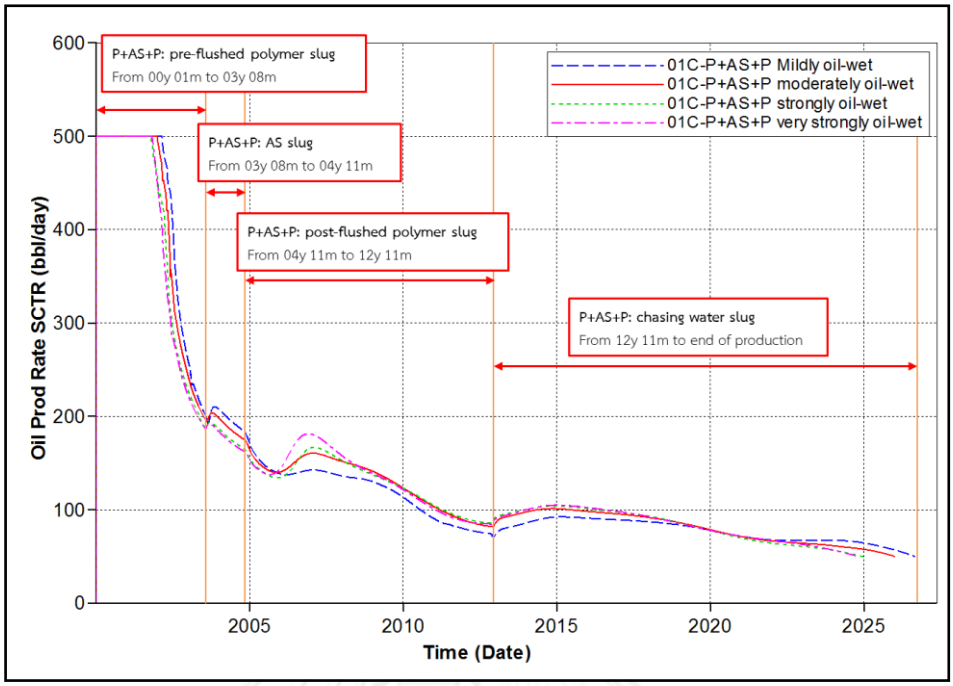

Figure 5.132 Oil production rates of various wetting conditions by P+AS+P flooding in model 01C as a function of time

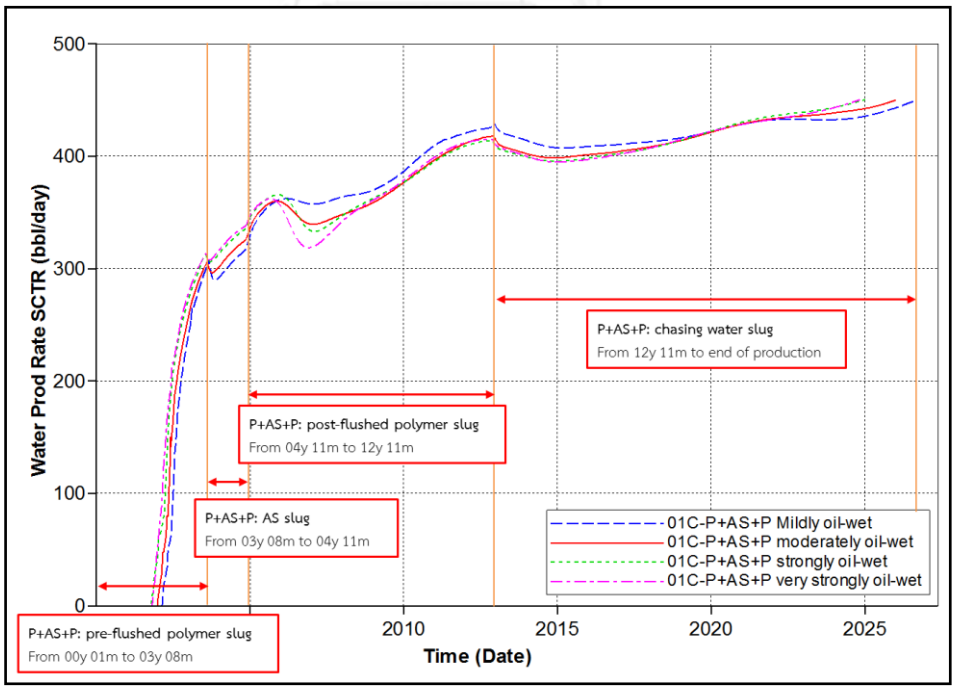

Figure 5.133 Water production rates of various wetting condition by P+AS+P flooding in model 01C as a function of time

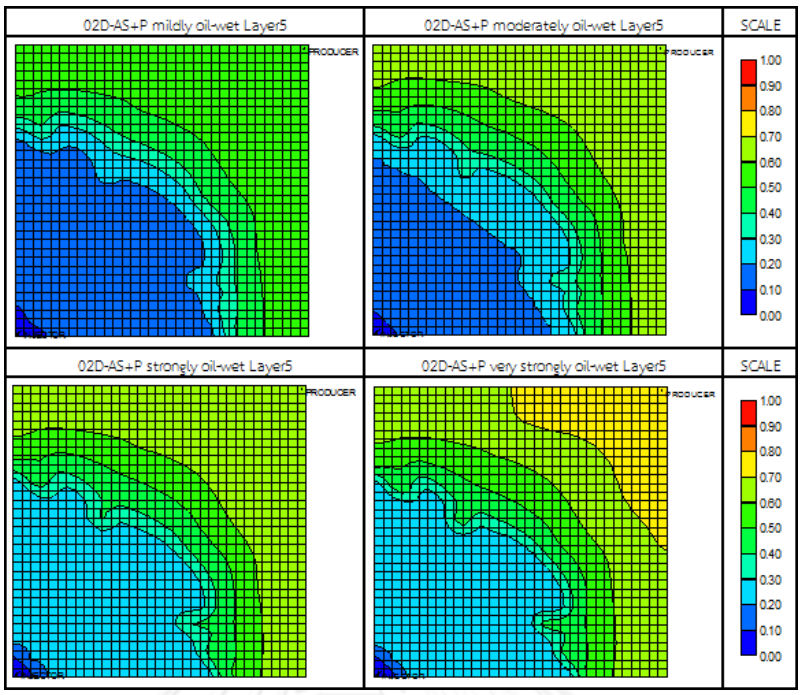

Figure 5.134 Oil saturation profiles of various wetting conditions by AS+P flooding at the end of production

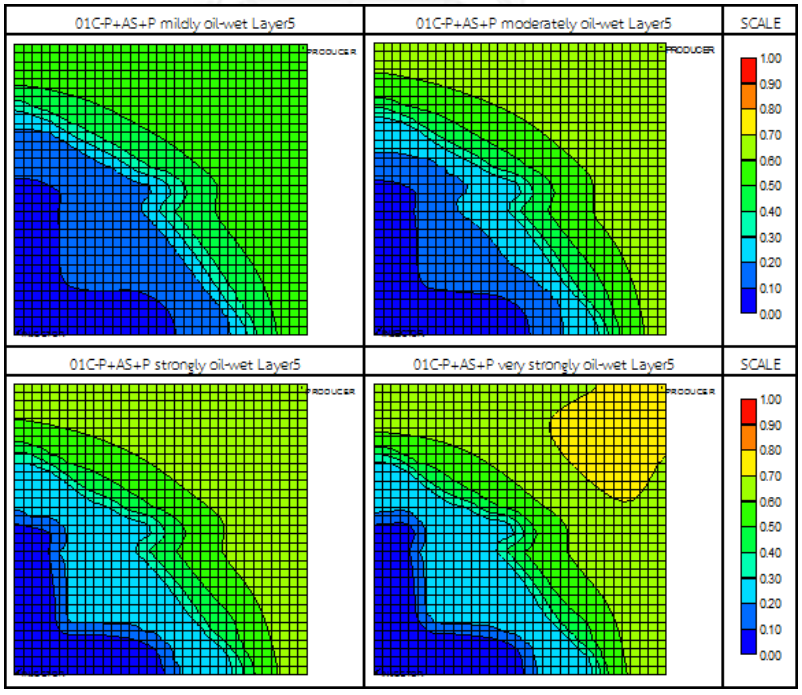

Figure 5.135 Oil saturation profiles of various wetting conditions by P+AS+P flooding at the end of production

5.5.3 Permeability Contrast between Channel and Matrix

Permeability contrast between channel and matrix is parameter that exhibits relationship between matrix permeability and channel permeability. Chosen values of matrix permeability and channel permeability are summarized in Table 5.16. Higher permeability contrast between channel and matrix infers to higher capability of fluid to flow through channel. Three times permeability contrast between channel and matrix is used in base case. Values of 5 and 10 times permeability contrast between channel and matrix are chosen to determine effect of this interest parameter.

Table 5.16 Summary of permeability contrast between channel and matrix

Permeability contrast	Matrix permeability	Channel permeability
3 times	500 mD	1,500 mD
5 times	500 mD	2,500 mD
10 times	500 mD	5,000 mD

Summary of recovery factor and incremental recovery factor of waterflooding, AS+P and P+AS+P flooding are illustrated in Figures 5.136 and 5.137, respectively. Entire recovery factors by means of waterflooding and AS+P flooding in model 02D remain the same for all permeability contrast values. Therefore, incremental recovery factor of AS+P flooding compared to waterflooding remains constant. For model 01C, recovery factors of waterflooding gradually decrease, whereas recovery factors obtained from P+AS+P flooding sharply decline. Therefore, incremental recovery factors of P+AS+P flooding based on waterflooding shows a declining trend. Oil saturation profile at the end of production of various permeability contrasts between channel and matrix by waterflooding in model 02D and 01C shown in Figures 5.138 and 5.139 are used to describe difference of these two models.

In model 02D, front of waterflooding at the end of production is not much different even channel permeability is changed. Therefore, water can sweep oil at the same level. However, volumetric sweep efficiency is worse when channel permeability is increased in model 01C. This is effect of the direction of high

permeability channel in reservoir. High permeability channel is located across direction of flow between injector and producer in model 02D, whereas high permeability channel is located parallel x-axis in model 01C. Hence, increasing channel permeability normal to direction of flow between injector and producer is sensitive compared to parallel direction of high permeability to the flow direction.

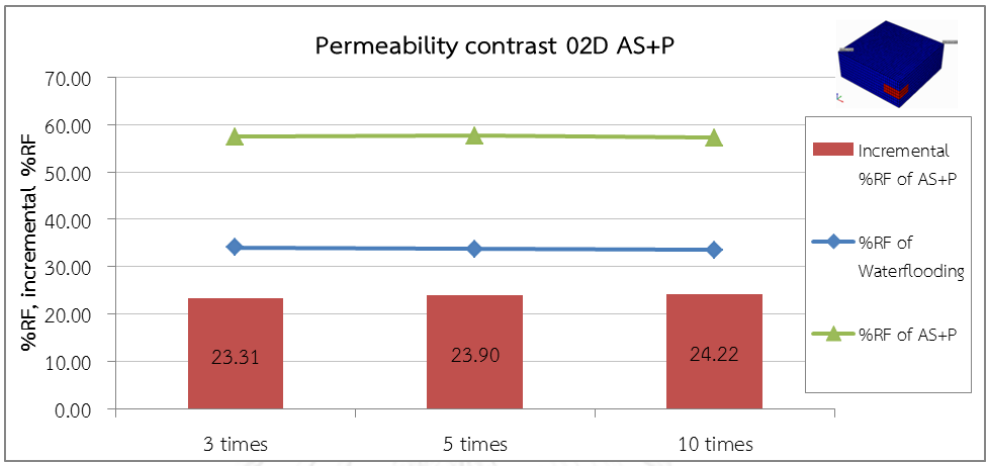

Figure 5.136 Recovery factors and incremental recovery factors of various permeability contrasts between channel and matrix by AS+P flooding

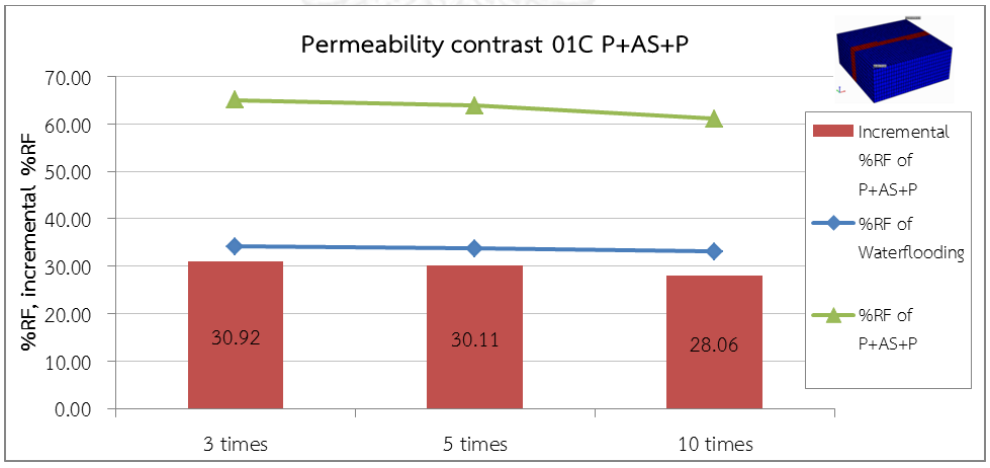

Figure 5.137 Recovery factors and incremental recovery factors of various permeability contrasts between channel and matrix by P+AS+P flooding

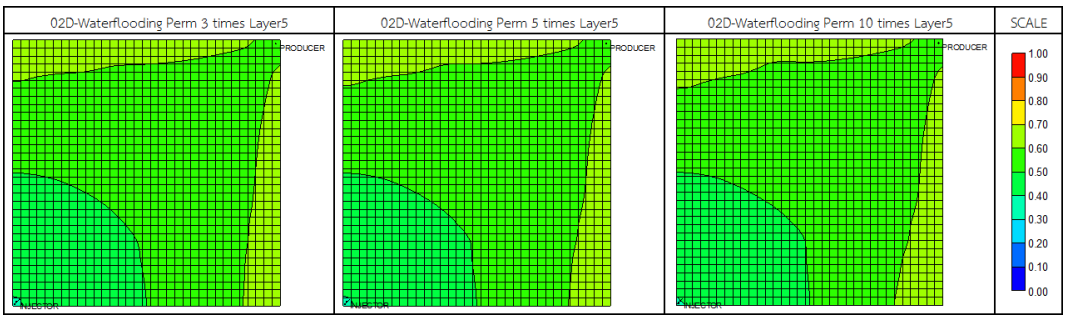

Figure 5.138 Oil saturation profiles at the end of production of various permeability contrasts between channel and matrix by waterflooding in model 02D

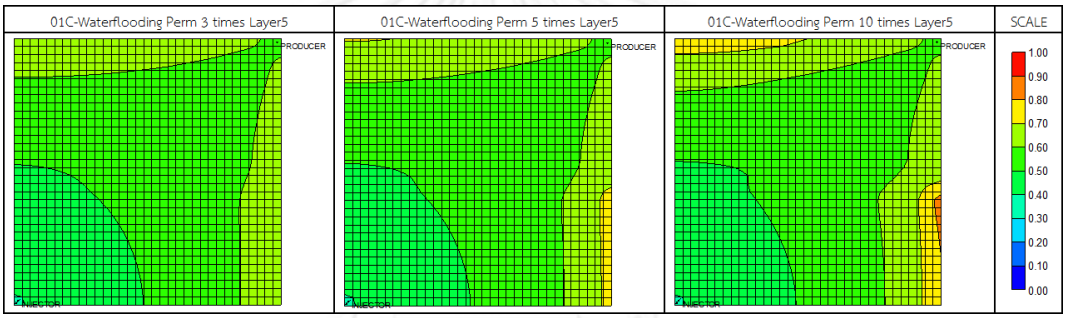

Figure 5.139 Oil saturation profiles at the end of production of various permeability contrasts between channel and matrix by waterflooding in model 01C

Recovery factor, oil and water production rates of AS+P flooding in model 02D are illustrated in Figures 5.140 to 5.142, whereas recovery factor, oil and water production rates of P+AS+P flooding in model 01C are illustrated in Figure 5.143 to 5.145. Different result of AS+P and P+AS+P flooding in each model can be observed from oil saturation profile of various permeability contrasts between channel and matrix at the end of production as shown in Figures 5.146 and 5.147. From these figures, AS+P and P+AS+P flooding are affected from increment of channel permeability in different direction as same as waterflooding process.

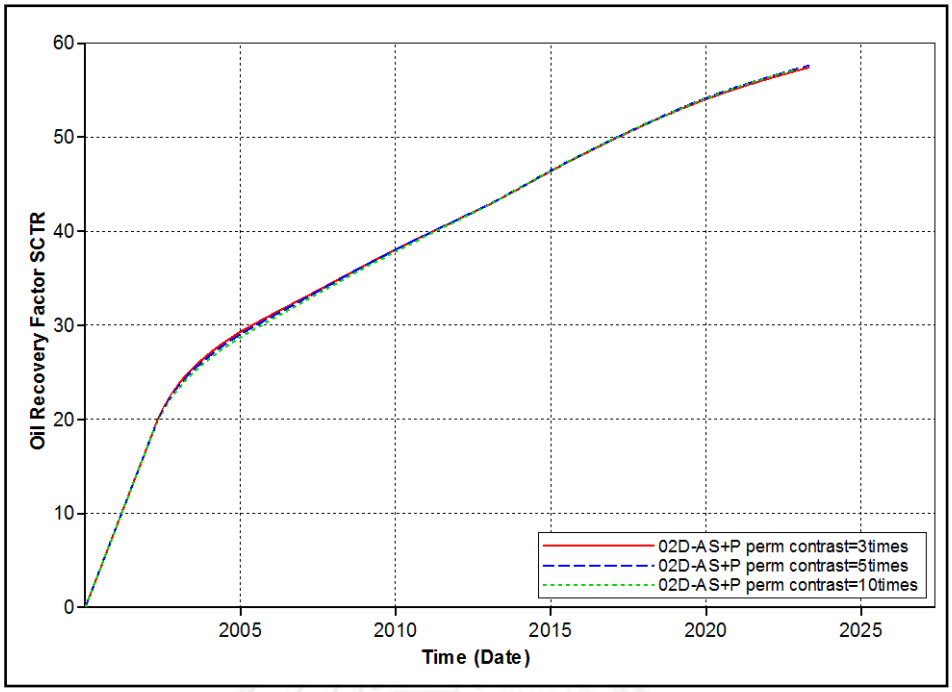

Figure 5.140 Recovery factors of various permeability contrasts between channel and matrix by AS+P flooding in model 02D as a function of time

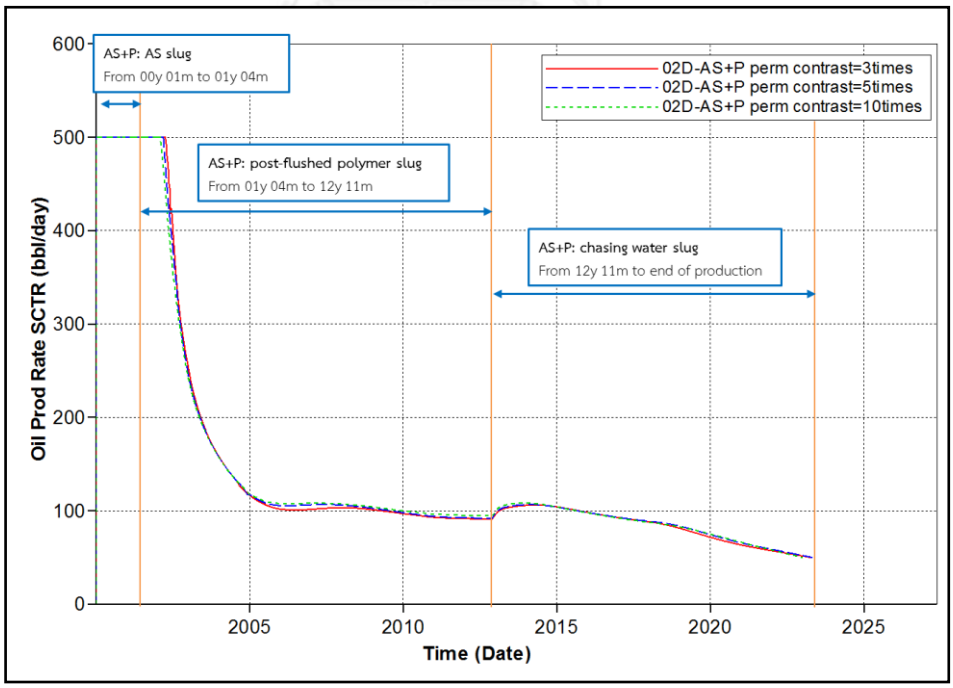

Figure 5.141 Oil production rates of various permeability contrast between channel and matrix by AS+P flooding in model 02D as a function of time

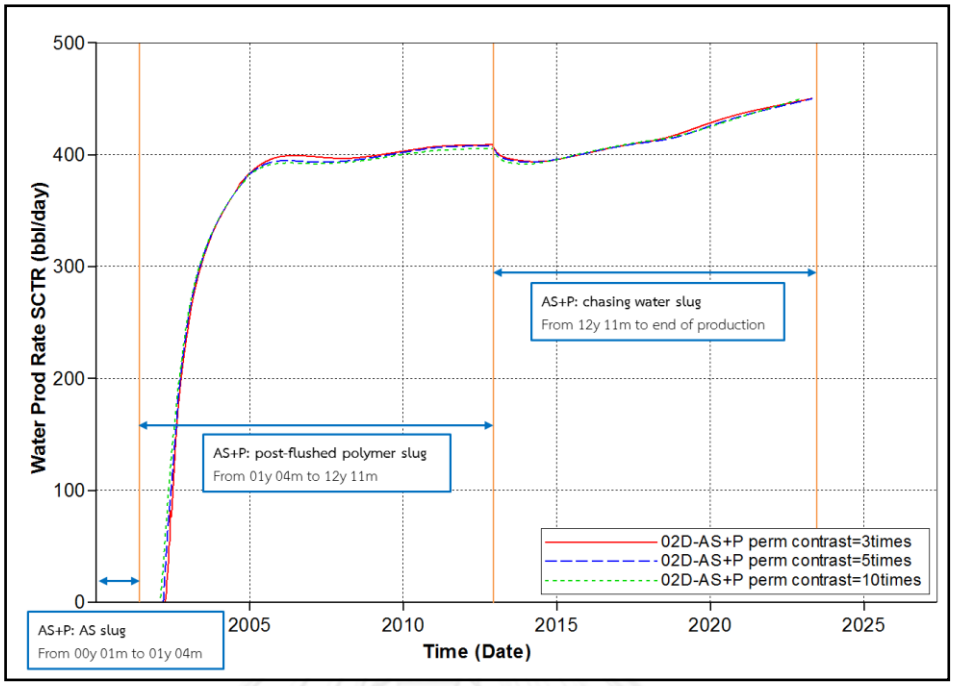

Figure 5.142 Water production rates of various permeability contrasts between channel and matrix by AS+P flooding in model 02D as a function of time

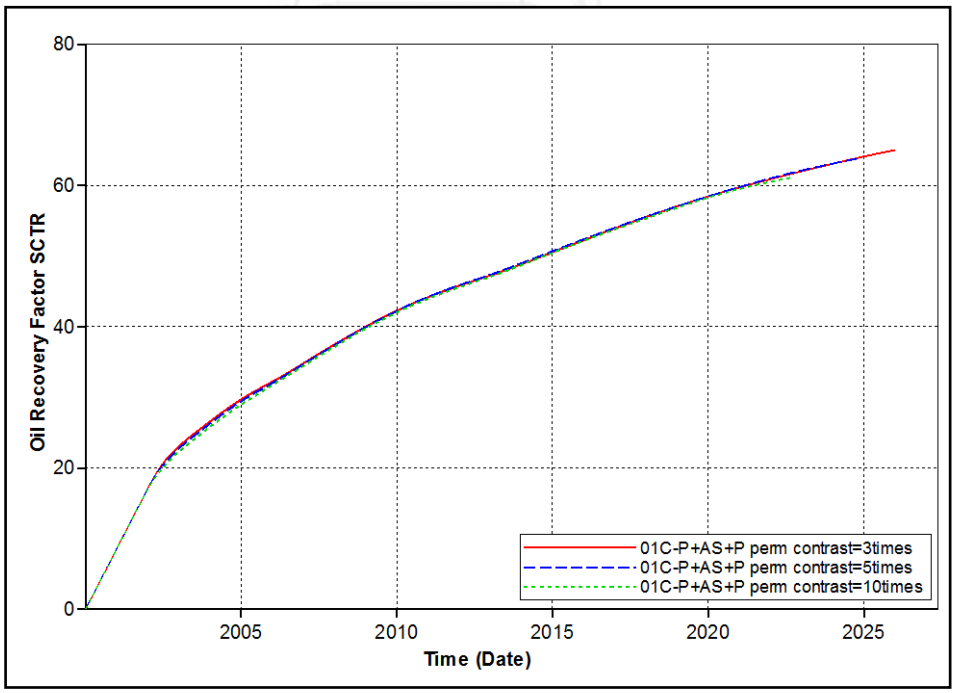

Figure 5.143 Recovery factors of various permeability contrasts between channel and matrix by P+AS+P flooding in model 01C as a function of time

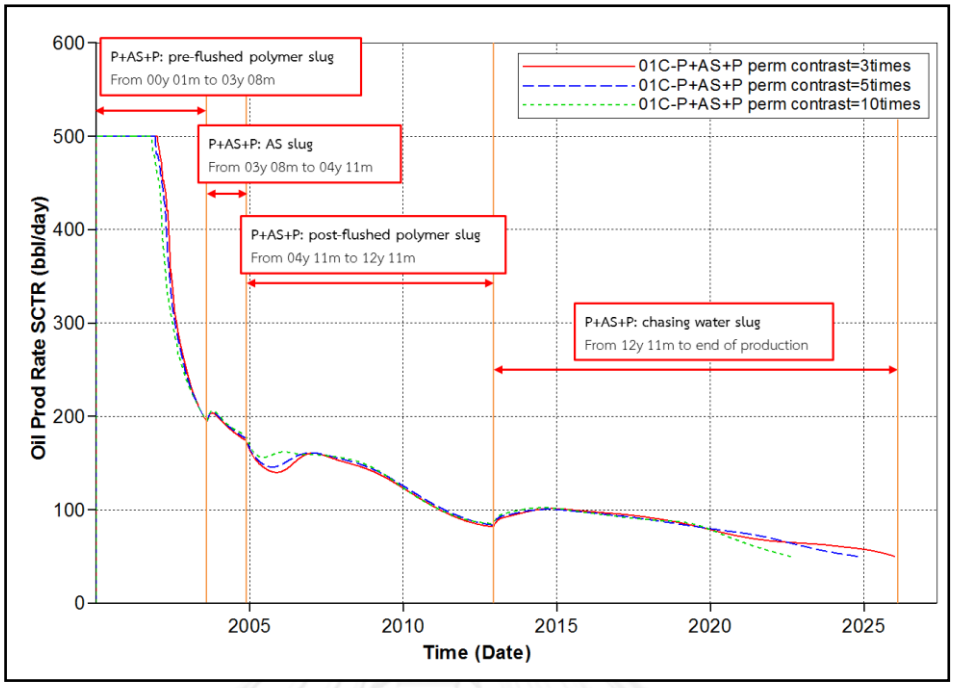

Figure 5.144 Oil production rates of various permeability contrasts between channel and matrix by P+AS+P flooding in model 01C as a function of time

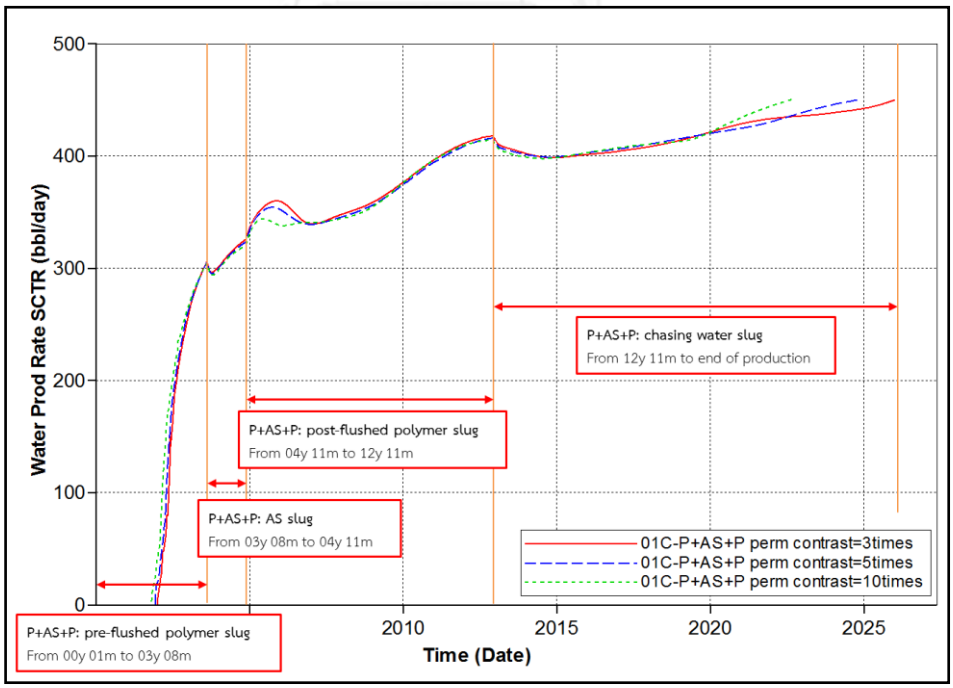

Figure 5.145 Water production rates of varied permeability contrasts between channel and matrix by P+AS+P flooding in model 01C as a function of time

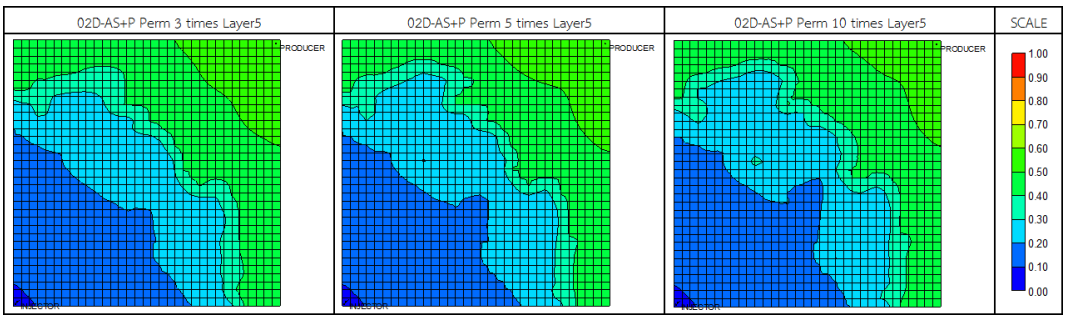

Figure 5.146 Oil saturation profiles of various permeability contrasts between channel and matrix by AS+P flooding at the end of production

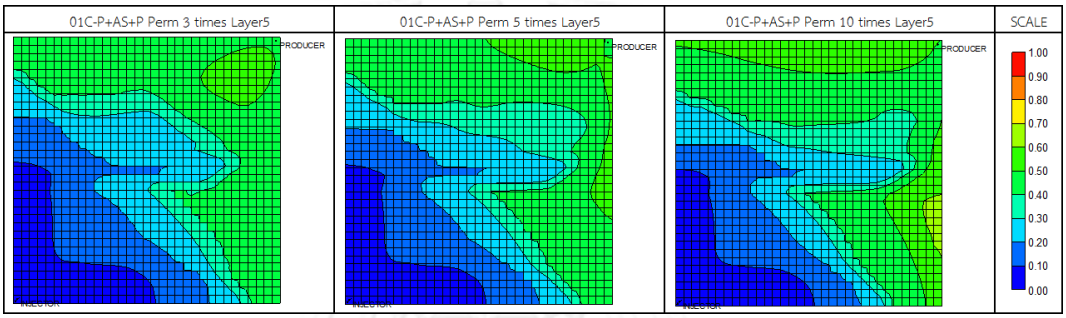

Figure 5.147 Oil saturation profiles of various permeability contrasts between channel and matrix by P+AS+P flooding at the end of production

5.5.4 Ratio of Vertical to Horizontal Permeability

In most reservoirs, vertical permeability is generally related to horizontal permeability due to grain shape, grain size, sedimentation process and lithification. This anisotropy property is represented by ratio of vertical to horizontal permeability (k_v/k_h). In this study, matrix permeability is fixed as 500 mD of all cases. This matrix permeability is horizontal permeability value. Ratio of vertical to horizontal permeability of base case is set at 0.10. Therefore, vertical permeability of base case is 50 mD. In this section, three different ratios of vertical to horizontal permeability are used to replace the previous values of 0.10. These three values include 0.05, 0.20, and 0.25 as summarized in Table 5.17.

Table 5.17 Summary of ratio of vertical to horizontal permeability

Ratio of vertical to horizontal permeability	Matrix horizontal permeability	Vertical permeability
0.05	500 mD	25 mD
0.10	500 mD	50 mD
0.20	500 mD	100 mD
0.25	500 mD	125 mD

Summary of recovery factors and incremental recovery factors of waterflooding, AS+P and P+AS+P flooding are illustrated in Figures 5.148 and 5.149, respectively. Entire recovery factors of waterflooding in two models remain stable. Recovery factors of AS+P flooding remain stable as same as waterflooding, whereas recovery factors obtained from P+AS+P flooding gradually decreases when ratio of vertical to horizontal permeability is higher than 0.10. Recovery factor, oil and water production rates of waterflooding in model 02D and 01C are illustrated in Figures 5.150 to 5.152. If ratio of vertical to horizontal permeability increases, underrunning of water is induced by due to gravity. Underrunning of water is a significantly effect in case of high vertical to horizontal permeability ratio. Effect of underrunning of water is observed by using oil saturation profile by waterflooding at the end of production as depicted in Figure 5.153. High residual oil left after waterflooding process at the top of reservoir can be seen from Figure 5.153(a) in 3-D perspective. Even for vertical to horizontal permeability ratio of 0.25, high residual oil remains un-swept. Oil saturation profile of areal plane of layer 9 in Figure 5.153(b) shows very good sweep efficiency by underrunning of water at the lower part of reservoir. Therefore, recovery factor of waterflooding after water breakthrough does not have any significant difference when combining results of top and bottom parts of reservoir.

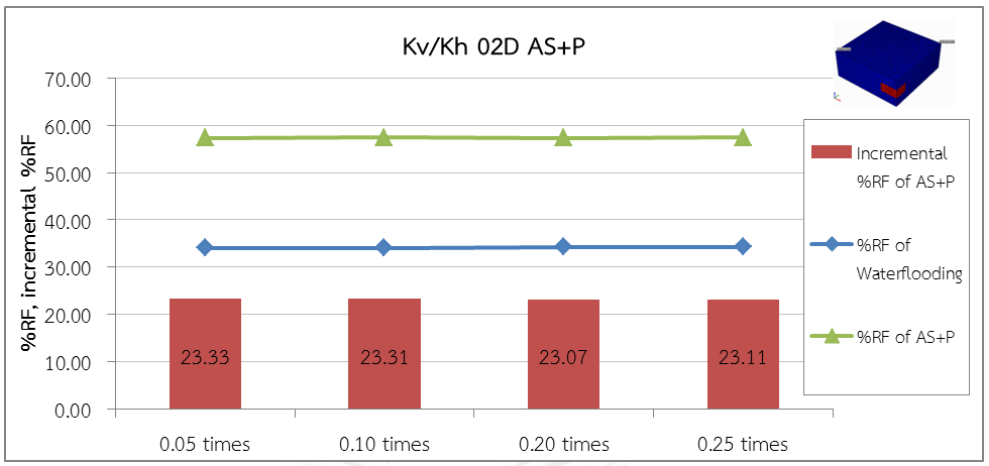

Figure 5.148 Recovery factors and incremental recovery factors of various ratios of vertical to horizontal permeability by AS+P flooding

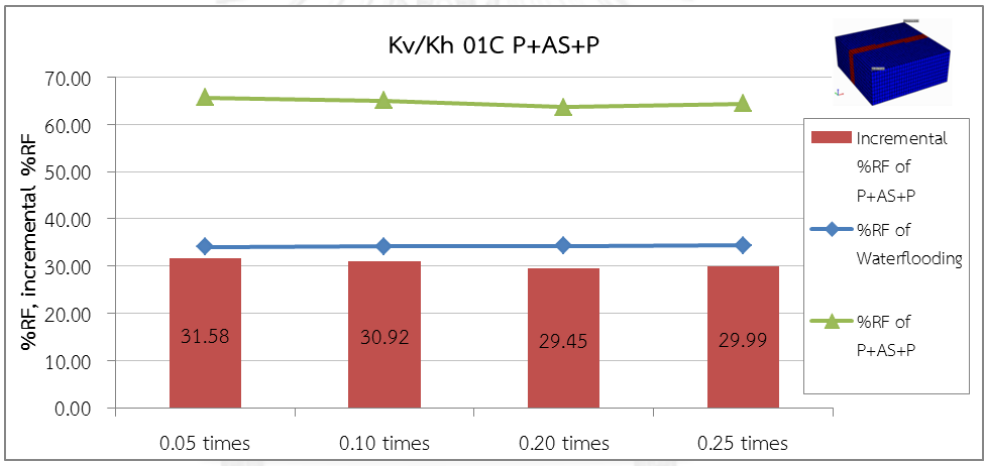

Figure 5.149 Recovery factors and incremental recovery factors of various ratios of vertical to horizontal permeability by P+AS+P flooding

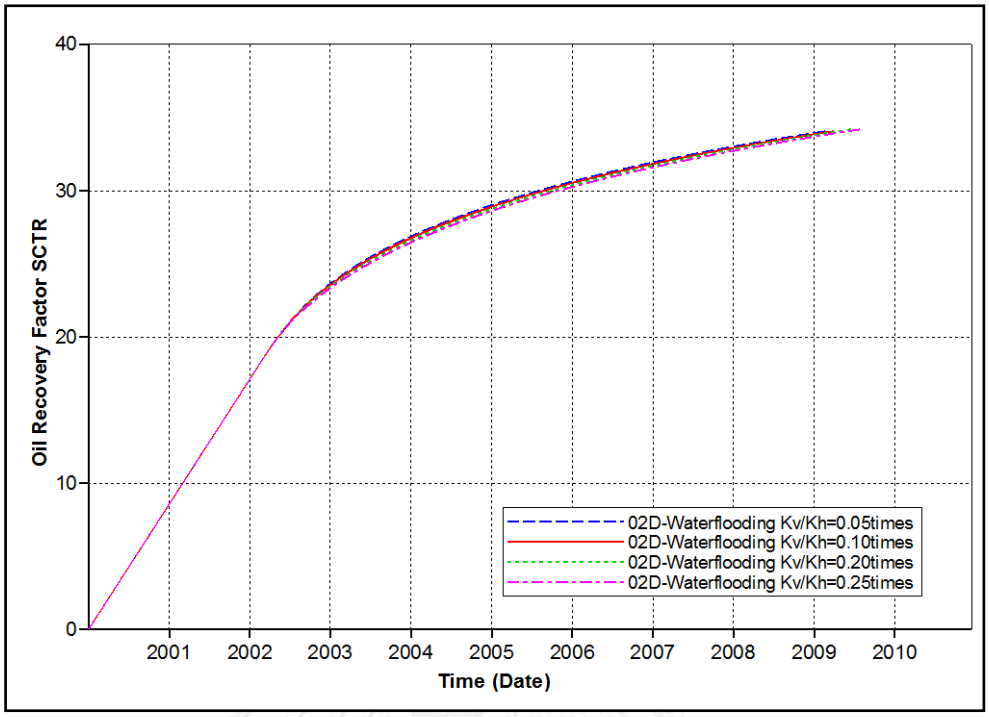

(a)

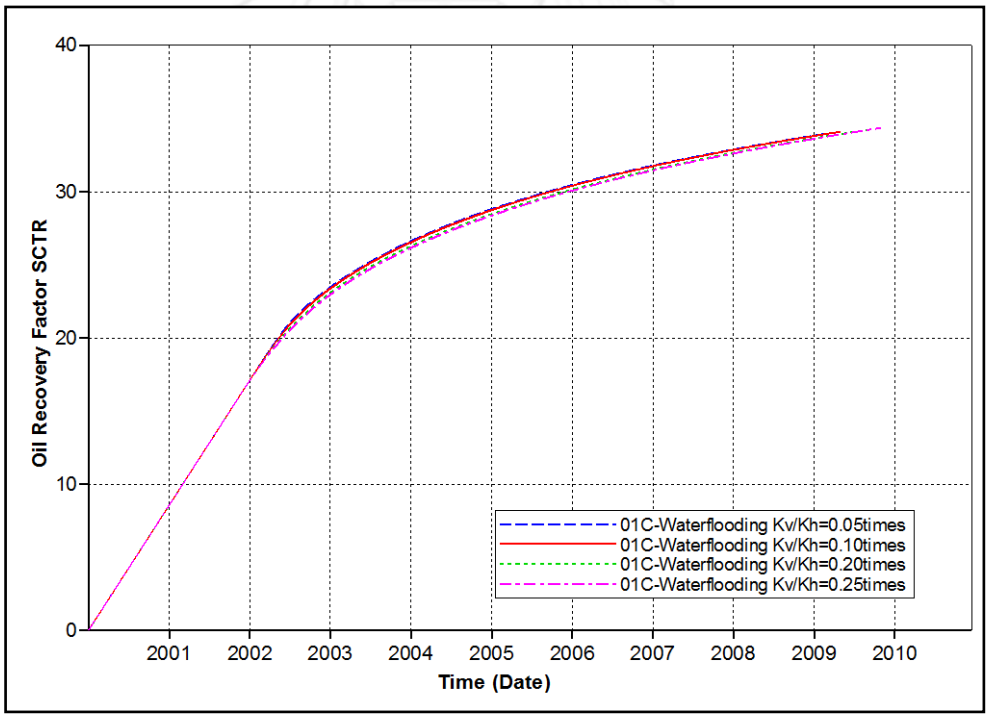

(b)

Figure 5.150 Recovery factors of various ratios of vertical to horizontal permeability by waterflooding as a function of time (a) model 02D (b) model 01C

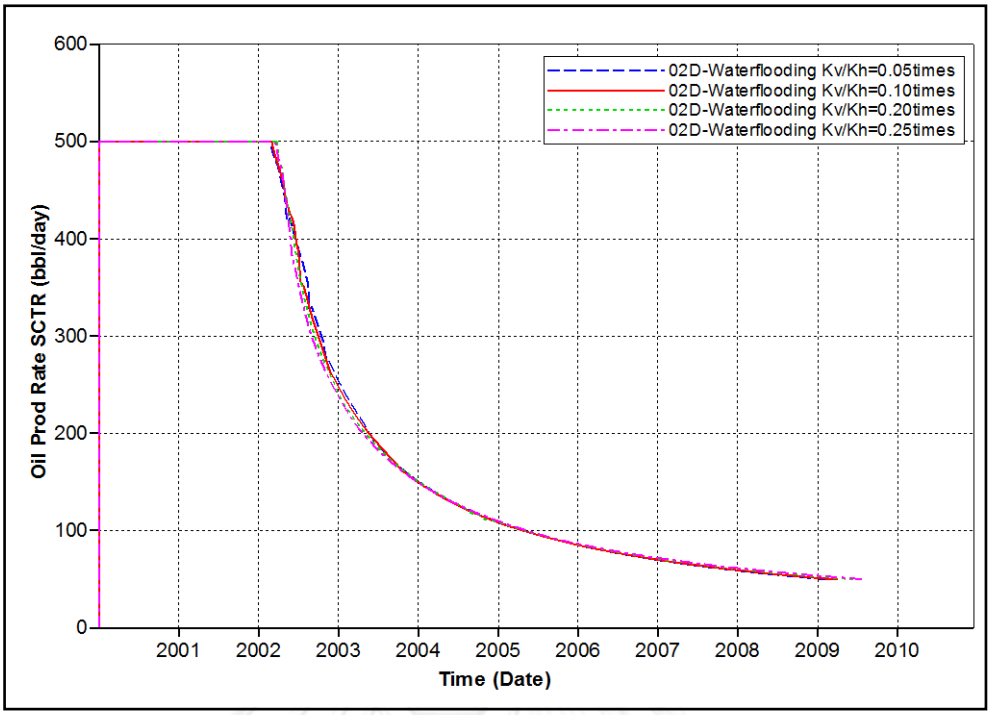

(a)

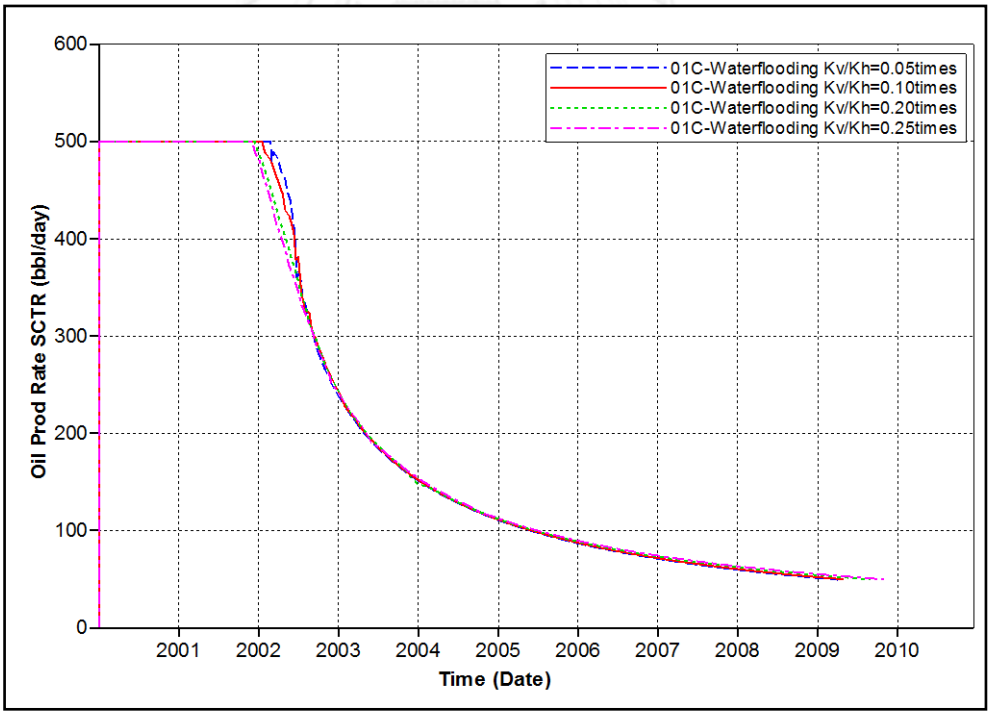

(b)

Figure 5.151 Oil production rates of various ratios of vertical to horizontal permeability by waterflooding as a function of time (a) model 02D (b) model 01C

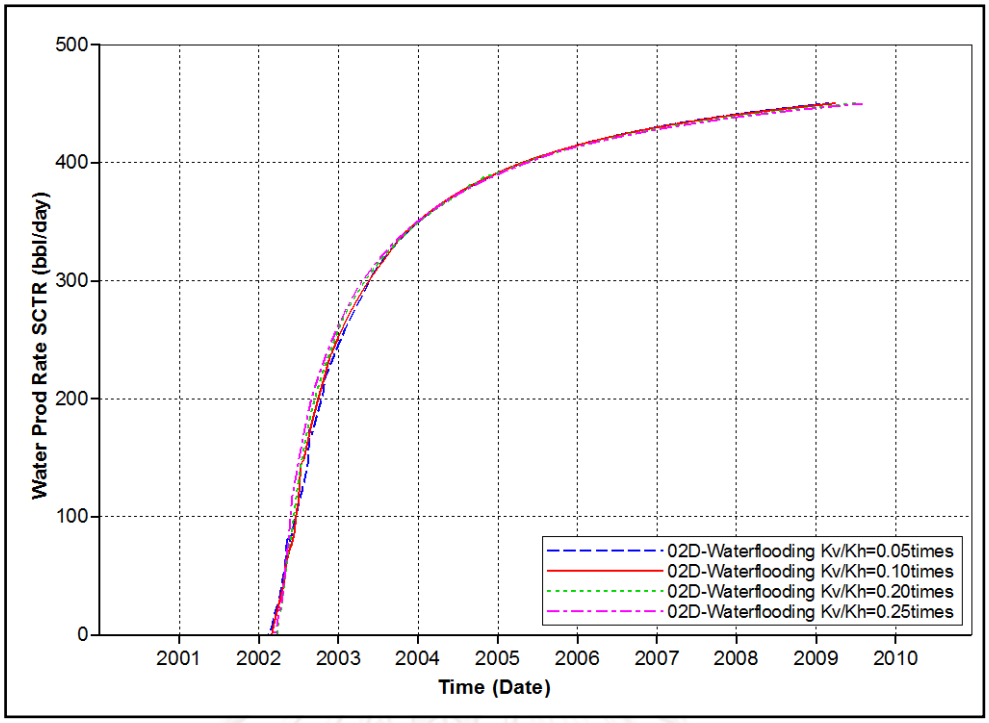

(a)

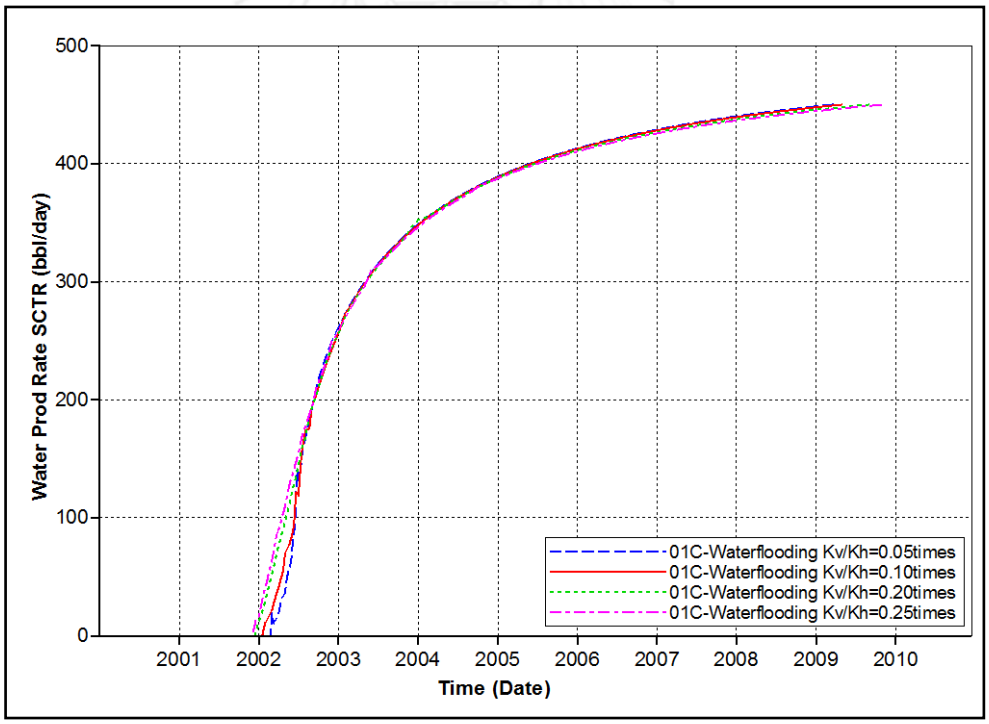

(b)

Figure 5.152 Water production rates of various ratios of vertical to horizontal permeability by waterflooding as a function of time (a) model 02D (b) model 01C

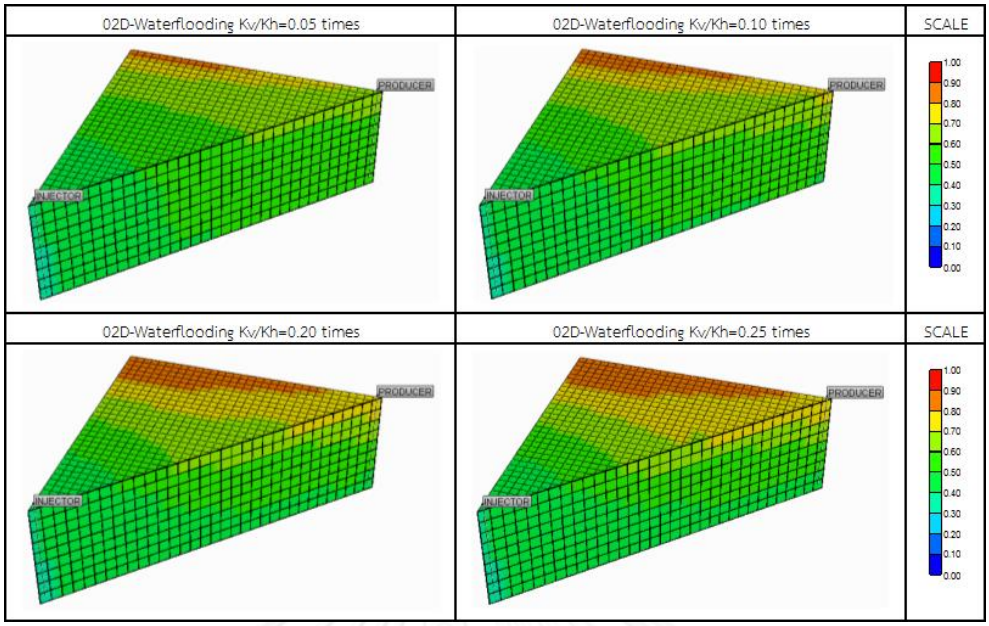

(a)

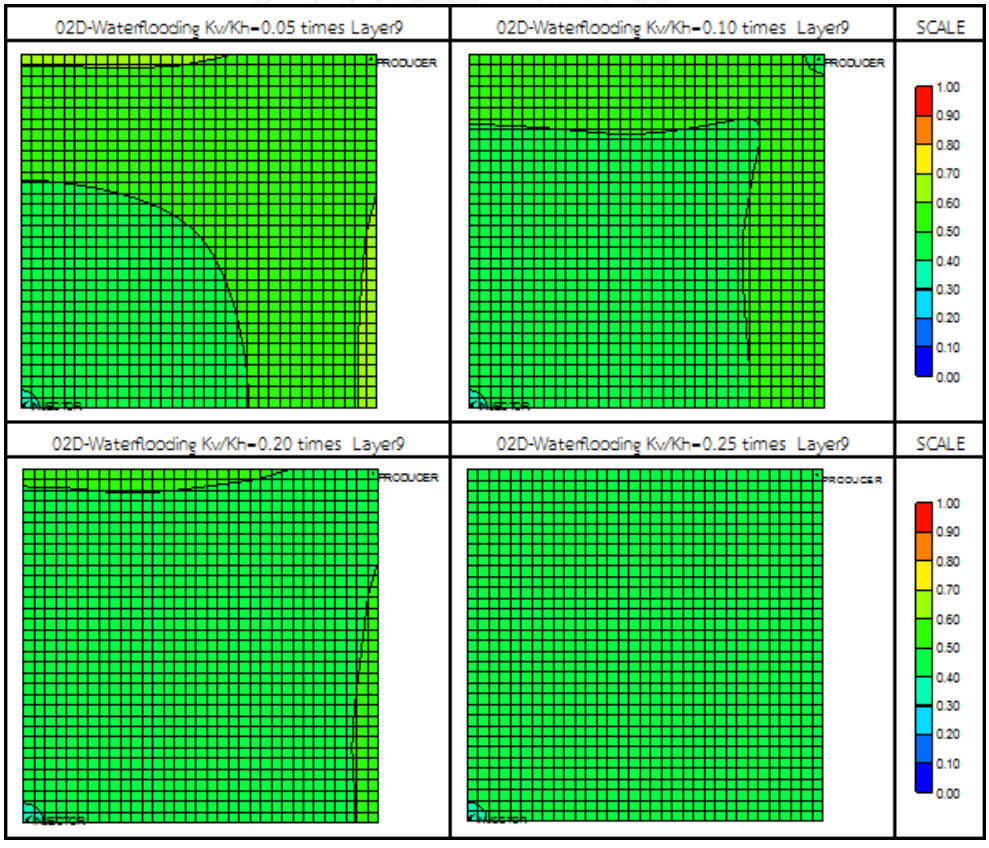

(b)

Figure 5.153 Oil saturation profiles of various ratios of vertical to horizontal permeability by waterflooding at the end of production

(a) 3-D perspective (b) areal plane layer 9

Recovery factor, oil and water production rates of AS+P flooding in model 02D are illustrated in Figures 5.154 to 5.156, whereas recovery factor, oil and water production rates of P+AS+P flooding in model 01C are illustrated in Figures 5.157 to 5.159. Results show that, AS+P flooding is not much affected from variation of vertical to horizontal permeability ratio. On the other hand, P+AS+P flooding is obviously affected from variation of the vertical to horizontal permeability ratio especially at the time close to end of production period. Difference of two techniques is presence and absence of pre-flushed polymer slug. Therefore, pre-flushed polymer of P+AS+P flooding is malfunctioned related to change of vertical to horizontal permeability ratio. Effect of vertical to horizontal permeability ratio to pre-flushed polymer slug in P+AS+P is explained in 3-D perspective and areal plane of layer 9 in Figure 5.160. From the figure, the top part of pre-flushed polymer remains stable from 3-D perspective, but the bottom part of pre-flushed slug is affected from underrunning of chasing water. Therefore, higher ratio of vertical to horizontal permeability results in lower stability of pre-flushed polymer slug and consequently production period is reduced due to early water breakthrough.

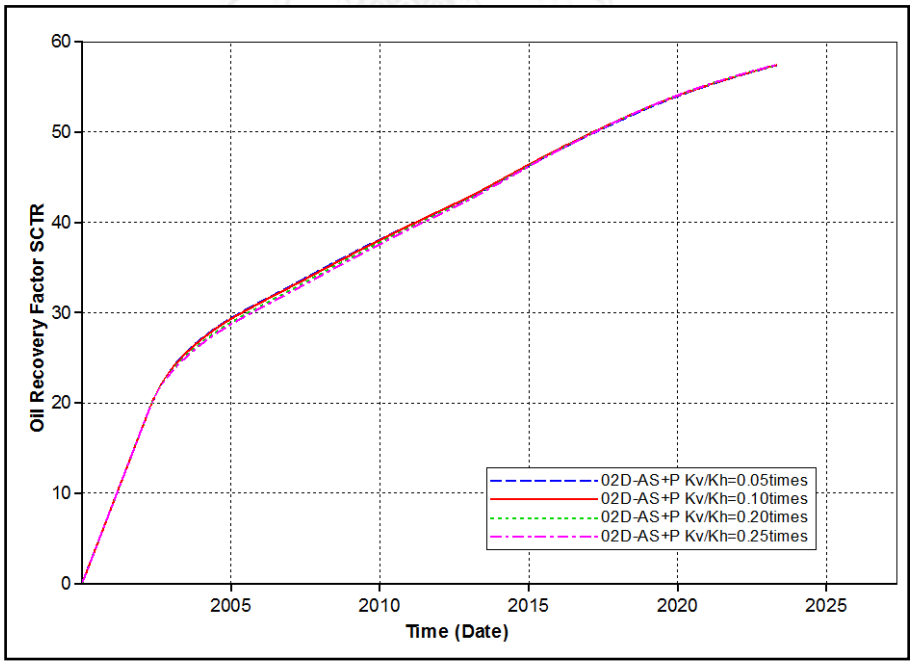

Figure 5.154 Recovery factors of various ratios of vertical to horizontal permeability by AS+P flooding in model 02D as a function of time

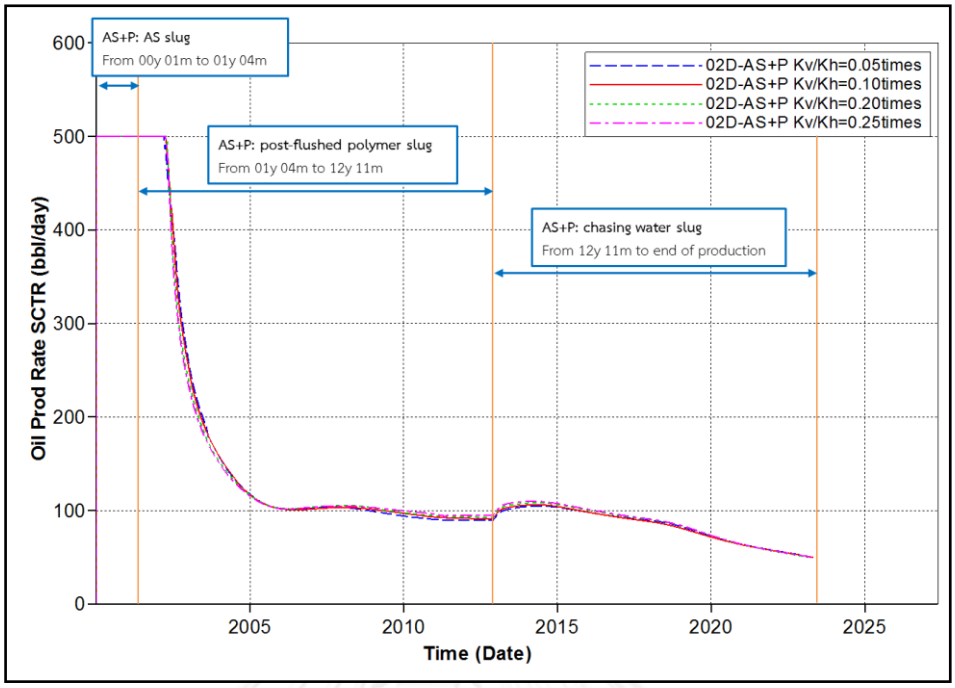

Figure 5.155 Oil production rates of various ratios of vertical to horizontal permeability by AS+P flooding in model 02D as a function of time

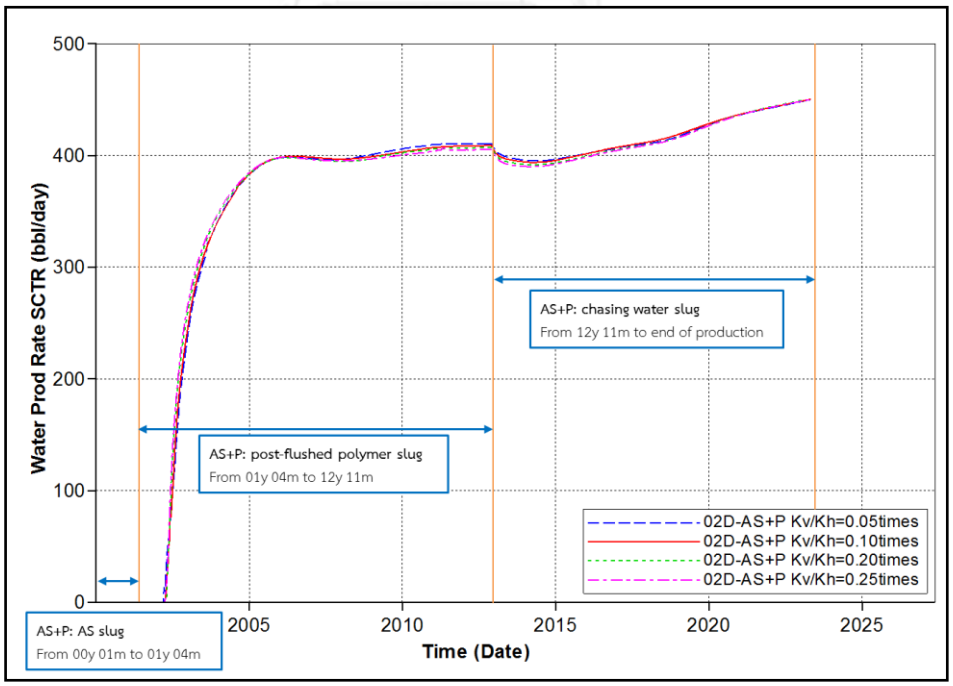

Figure 5.156 Water production rates of various ratios of vertical to horizontal permeability by AS+P flooding in model 02D as a function of time

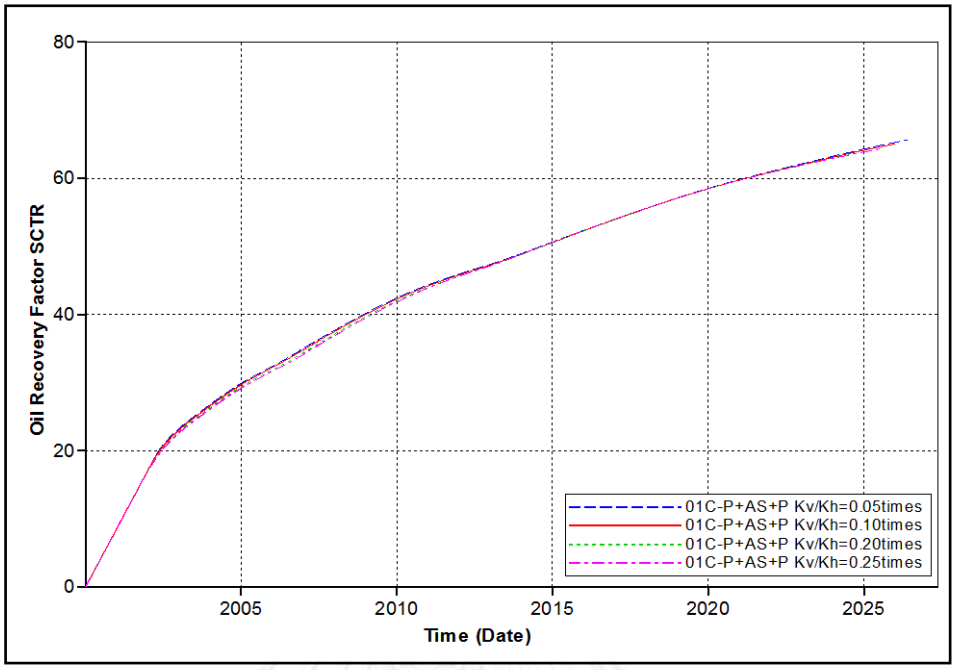

Figure 5.157 Recovery factors of various ratios of vertical to horizontal permeability by P+AS+P flooding in model 01C as a function of time

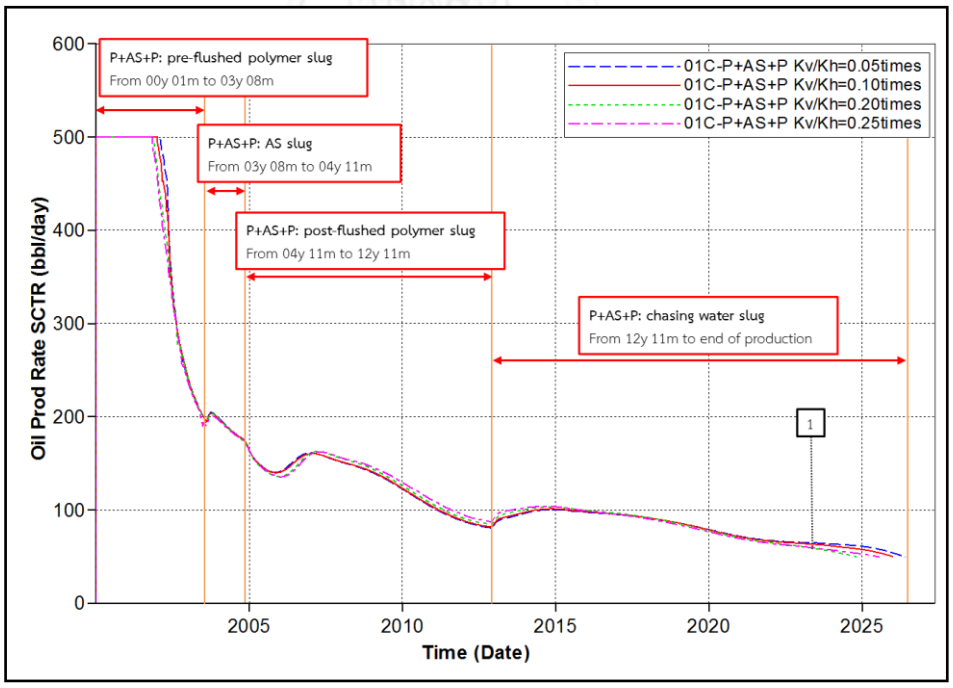

Figure 5.158 Oil production rates of various ratios of vertical to horizontal permeability by P+AS+P flooding in model 01C as a function of time

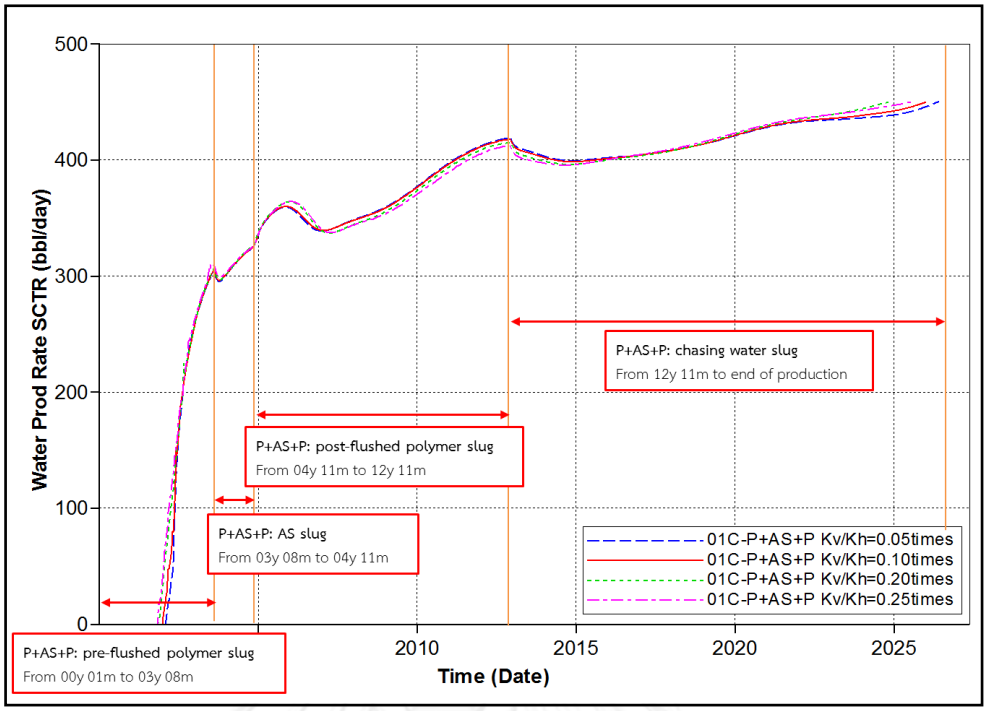

Figure 5.159 Water production rates of various ratios of vertical to horizontal permeability by P+AS+P flooding in model 01C as a function of time

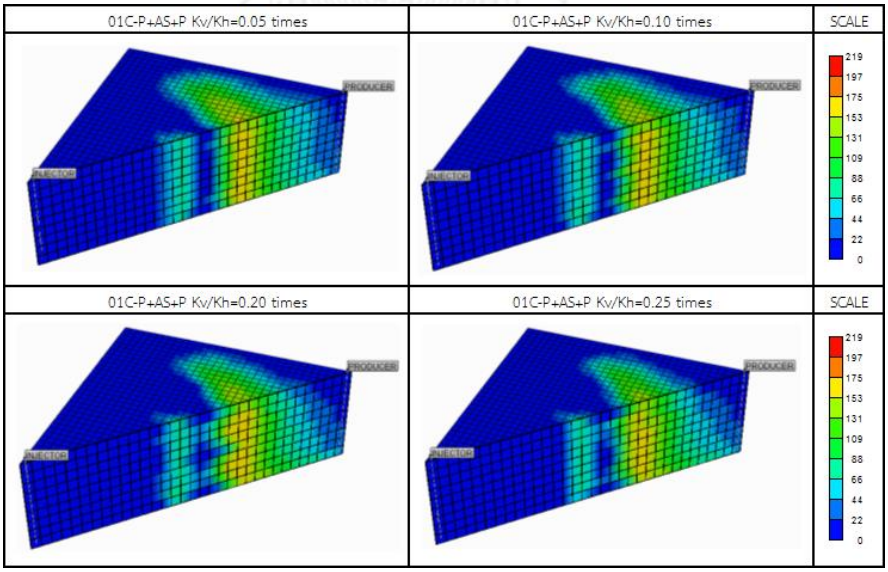

(a)

Figure 5.160 Pre-flushed polymer concentration profiles of varied ratio of vertical to horizontal permeability by P+AS+P flooding at 23rd year, 1st month (a) 3-D perspective (b) Areal plane layer 9

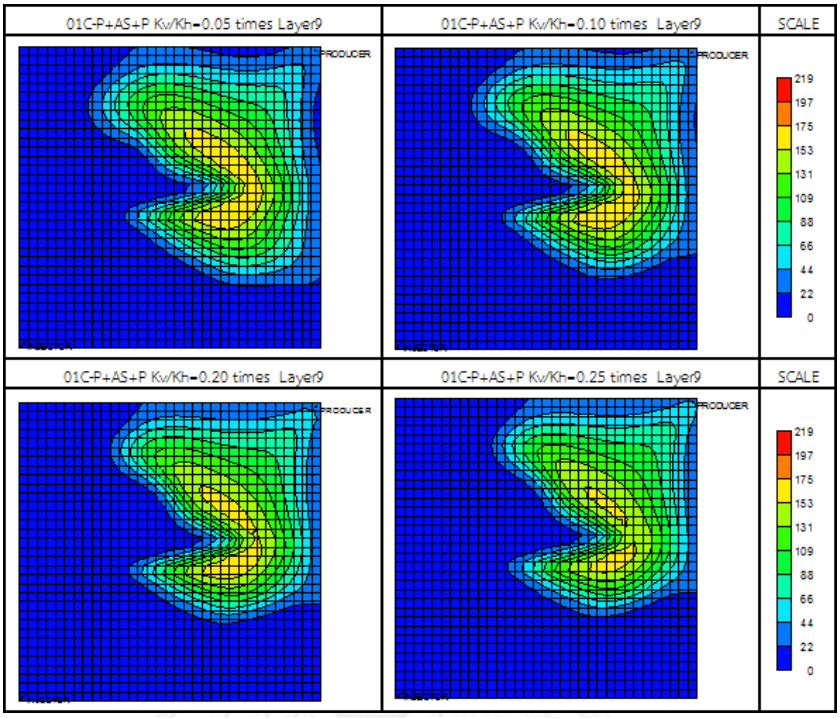

(b)

Figure 5.160 Pre-flushed polymer concentration profiles of varied ratio of vertical to horizontal permeability by P+AS+P flooding at 23rd year, 1st month (a) 3-D perspective (b) Areal plane layer 9 (continued)

5.5.5 Porosity in High Permeability Channel

Even though relationship between permeability and porosity of high permeability channel cannot be directly identified, relationship between permeability and porosity of matrix of carbonate reservoir can still be determined by using grain size coefficient and cementation-compaction coefficient from the equation (3.9). General values of grain size coefficient (A_{gr}) and cementation-compaction coefficient (A_{mcp}) are listed in Table 3.2. The reef limestone which is used to represent oil-wet reservoir in this study possesses porosity and permeability as shown in Table 4.1. Therefore, grain size coefficient and cementation-compaction coefficient of this matrix reef limestone can be considered as summarized in Table 5.18. Estimated porosity in high permeability channel can be accomplished using grain size coefficient and cementation-compaction coefficient parameters as shown in Table 5.18. Porosity value of high permeability channel of base case is 0.14. Then, values of 0.17, 0.20 and 0.23 porosity of high permeability channel are used to performed

sensitivity study of this interest parameter. Pore volume of each case is summarized in Table 5.19 since porosity in high permeability channel is altered from base case value.

Table 5.18 Summary of parameters used to calculate various porosities of high permeability channel

Location	A_{gr}	A_{mcp}	Permeability(mD)	Porosity
Matrix	8.25×10^8	7.29	500	0.14
High permeability channel	8.25×10^8	6.73	1,500	0.14
	8.25×10^8	7.29	1,500	0.17
	8.25×10^8	8.18	1,500	0.20
	8.25×10^8	9.00	1,500	0.23

Table 5.19 Total pore volume of various porosities in high permeability channel

Porosity in high permeability channel	Pore volume (MMbbl)
0.14	2.64
0.17	2.70
0.20	2.76
0.23	2.82

Summary of recovery factors and incremental recovery factor of waterflooding, AS+P and P+AS+P flooding are illustrated in Figures 5.161 and 5.162, respectively. Even though incremental recovery factor of P+AS+P flooding based on waterflooding is differ from incremental of recovery factor of P+AS+P flooding, most of recovery factors in all cases remain unchanged. Recovery factor, oil and water production rates of waterflooding in model 02D and 01C are illustrated in Figures 5.163 to 5.165. Recovery factor, oil and water production rates of AS+P flooding in model 02D and P+AS+P flooding in model 01C are illustrated in Figures 5.166 to 5.168 and Figures 5.169 to 5.171, respectively. These figures indicate that all

phenomena in reservoir are retarded by increasing of storage in high permeability channel. High storage means that amount of fluids are increased. Hence, injectant has to be increased in order to sweep whole fluids in reservoir. Summary of AS+P and P+AS+P flooding in various porosities in high permeability channel shows retarding of injectant interval period due to incremental of porosity in high permeability channel in Table 5.20 and 5.21. Therefore, it can be concluded that increasing in porosity in high permeability channel delays responds of reservoir to the injectant.

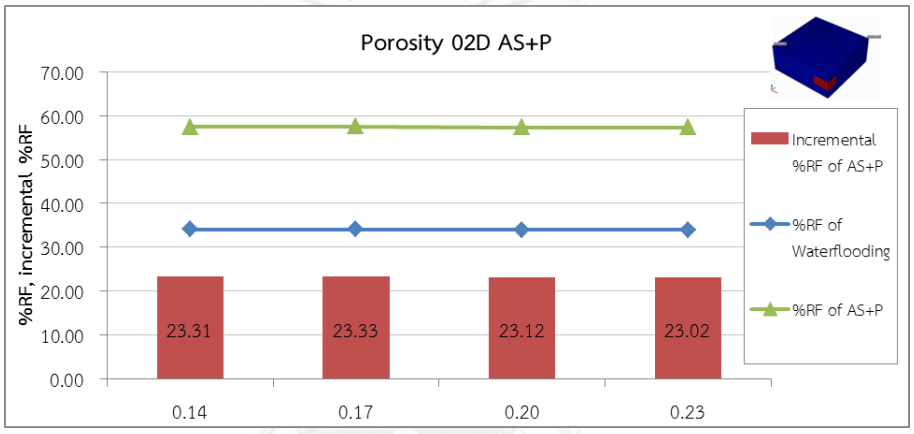

Figure 5.161 Recovery factors and incremental recovery factors of various porosities in high permeability channel by AS+P flooding

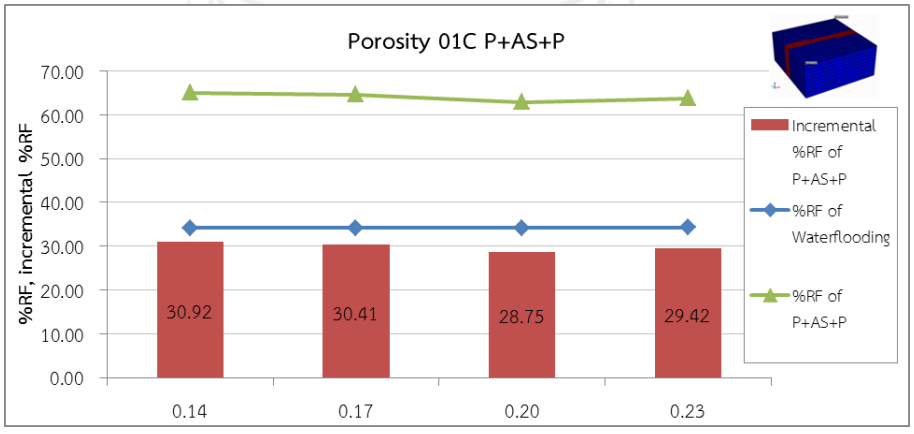

Figure 5.162 Recovery factors and incremental recovery factors of various porosities in high permeability channel by P+AS+P flooding

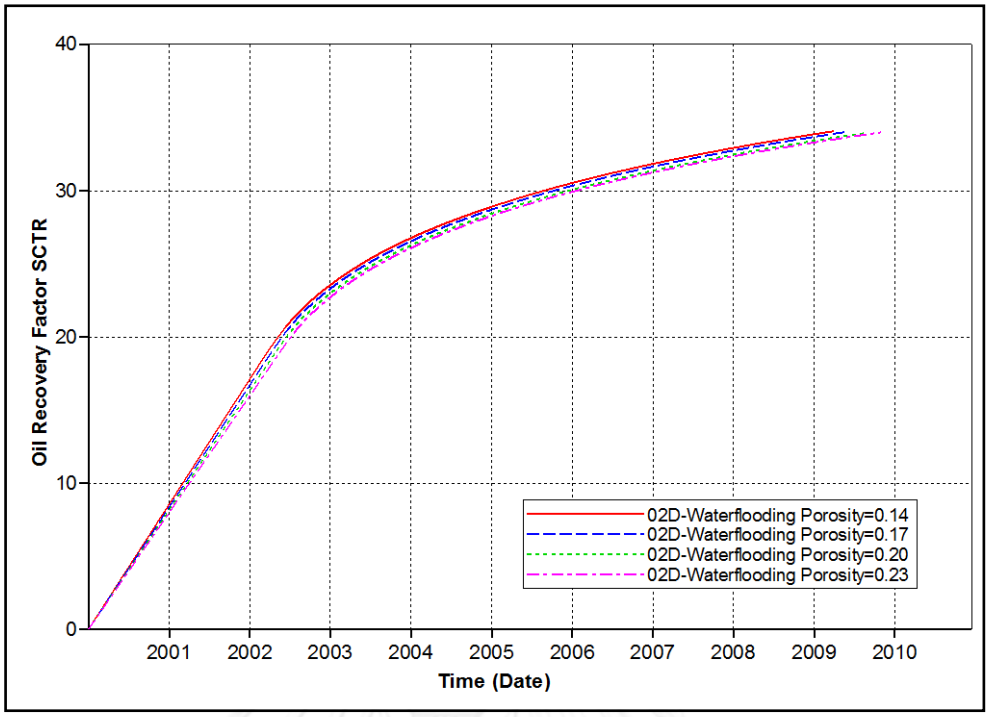

(a)

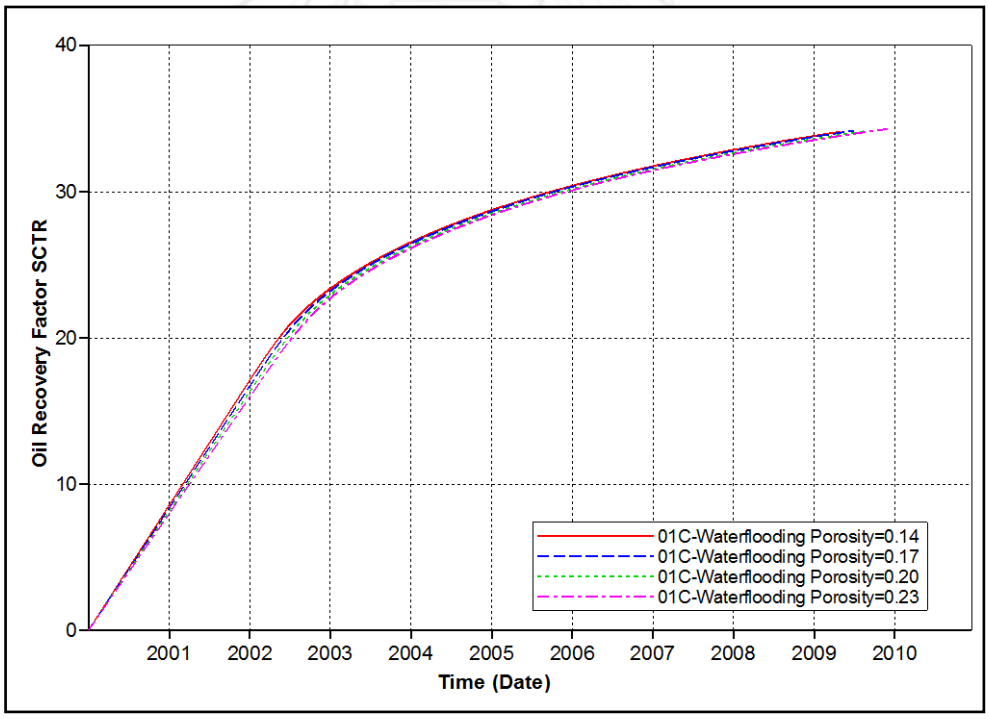

(b)

Figure 5.163 Recovery factors of various porosities in high permeability channel by waterflooding as a function of time (a) model 02D (b) model 01C

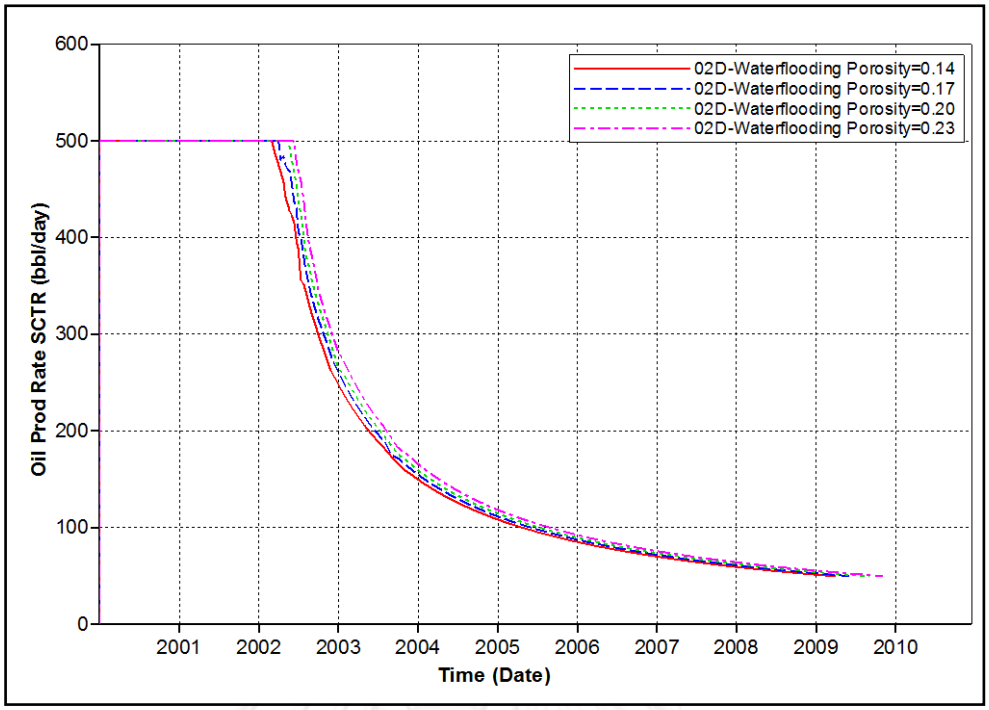

(a)

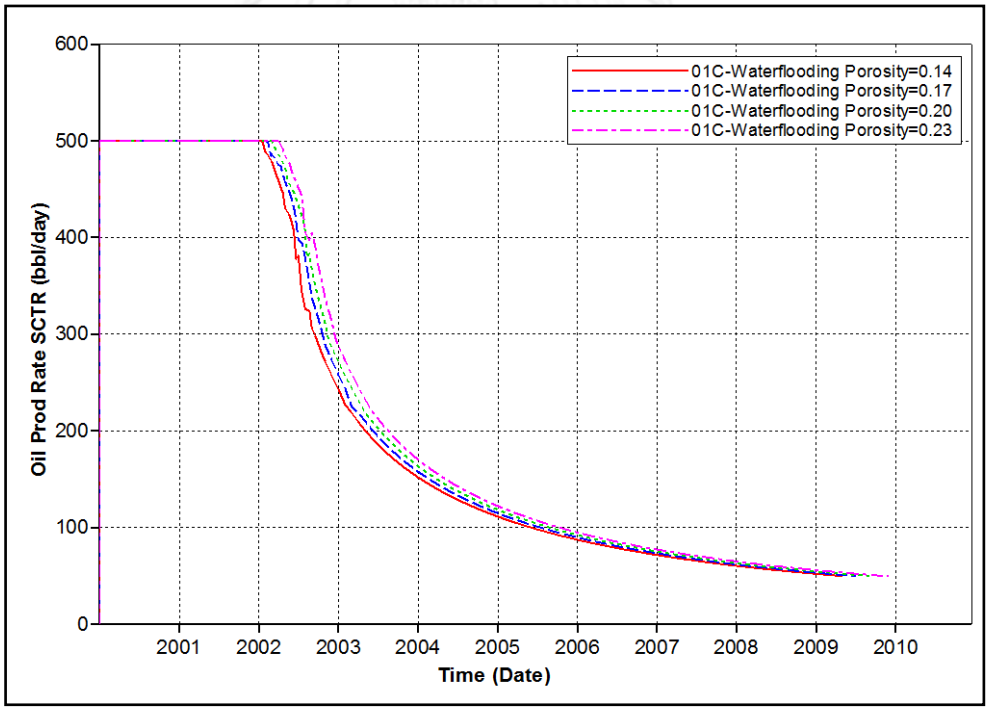

(b)

Figure 5.164 Oil production rates of various porosities in high permeability channel by waterflooding as a function of time (a) model 02D (b) model 01C

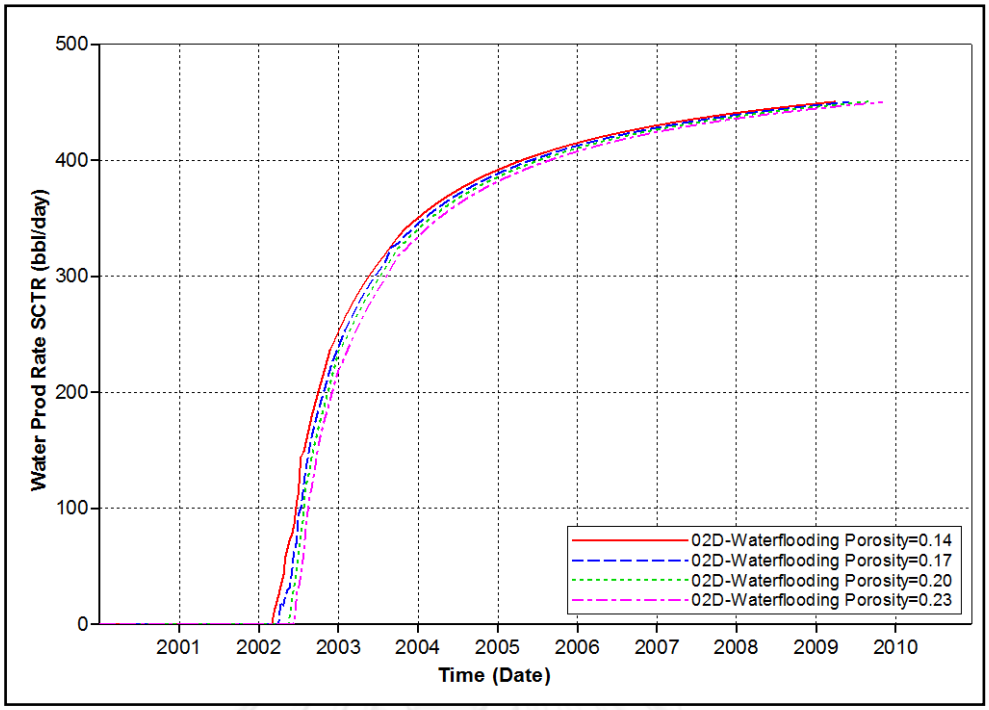

(a)

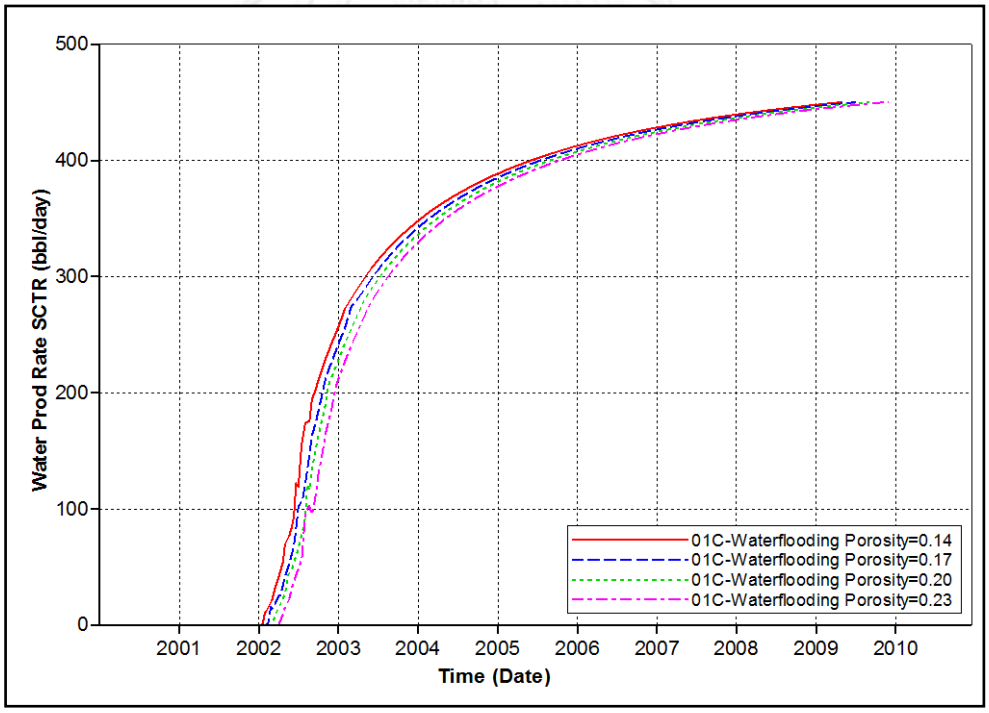

(b)

Figure 5.165 Water production rates of various porosities in high permeability channel by waterflooding as a function of time (a) model 02D (b) model 01C

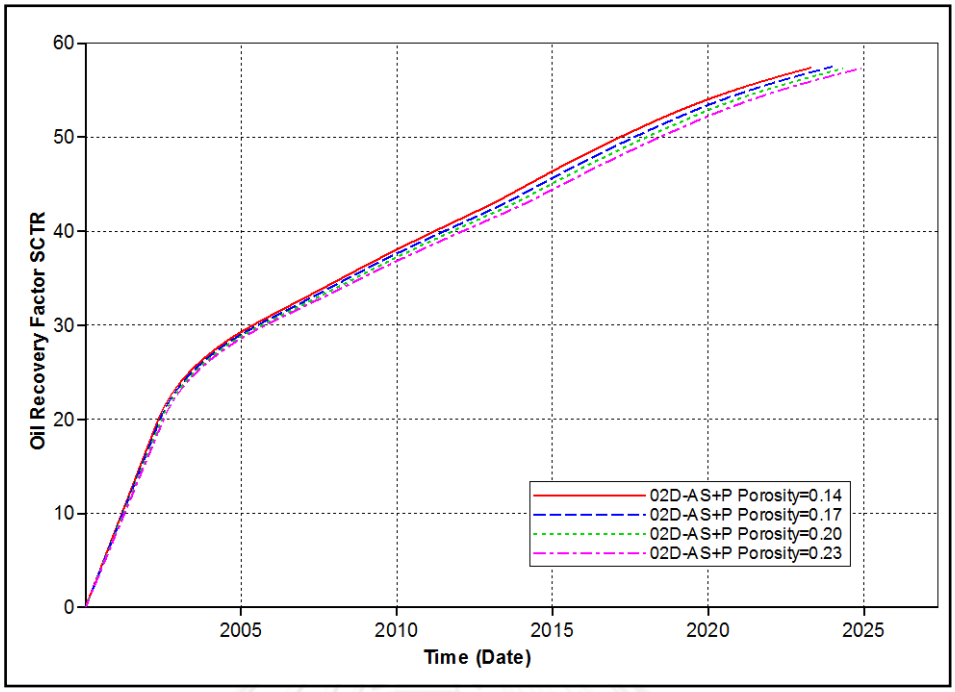

Figure 5.166 Recovery factors of various porosities in high permeability channel by AS+P flooding in model 02D as a function of time

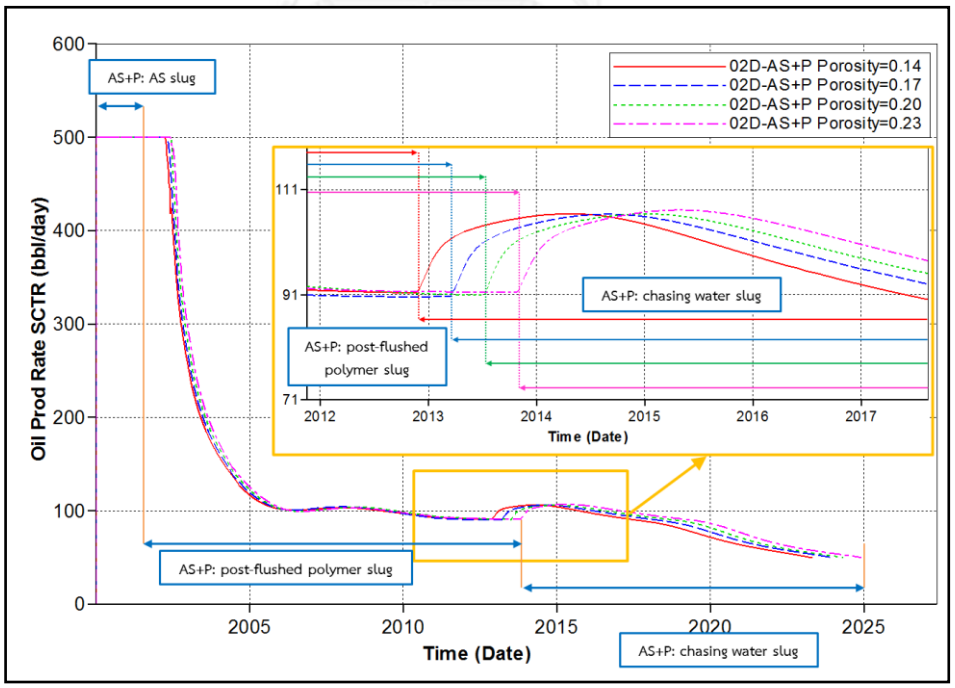

Figure 5.167 Oil production rates of various porosities in high permeability channel by AS+P flooding in model 02D as a function of time

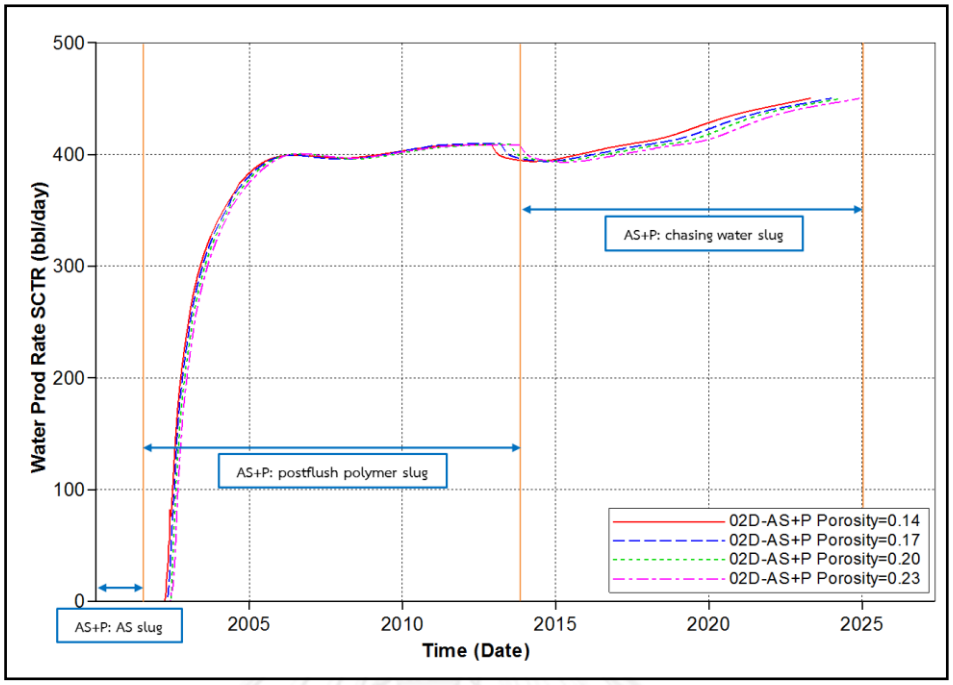

Figure 5.168 Water production rates of various porosities in high permeability channel by AS+P flooding in model 02D as a function of time

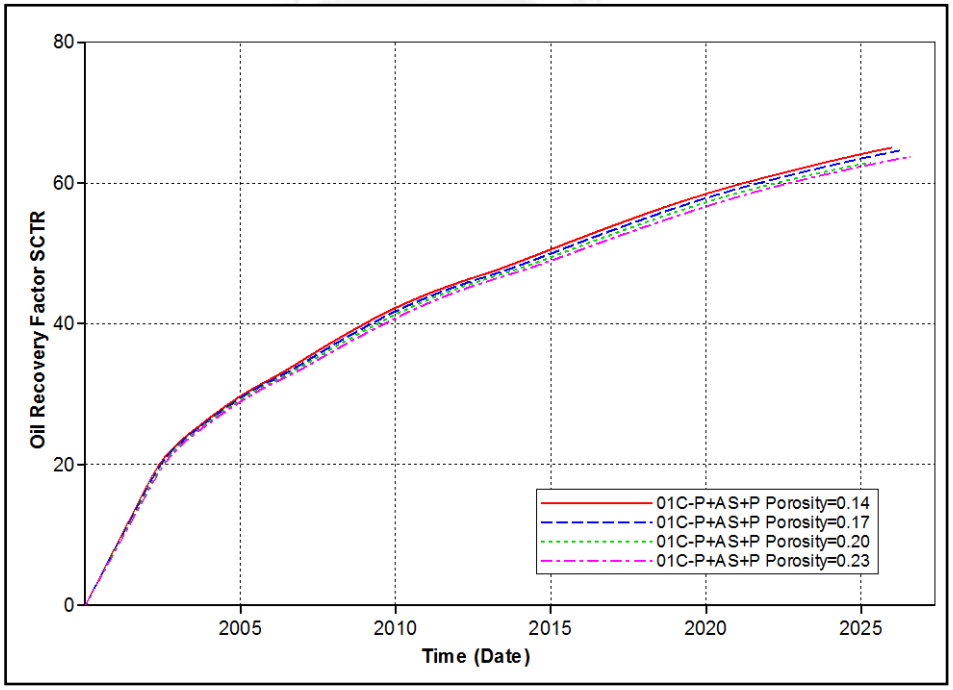

Figure 5.169 Recovery factors of various porosities in high permeability channel by P+AS+P flooding in model 01C as a function of time

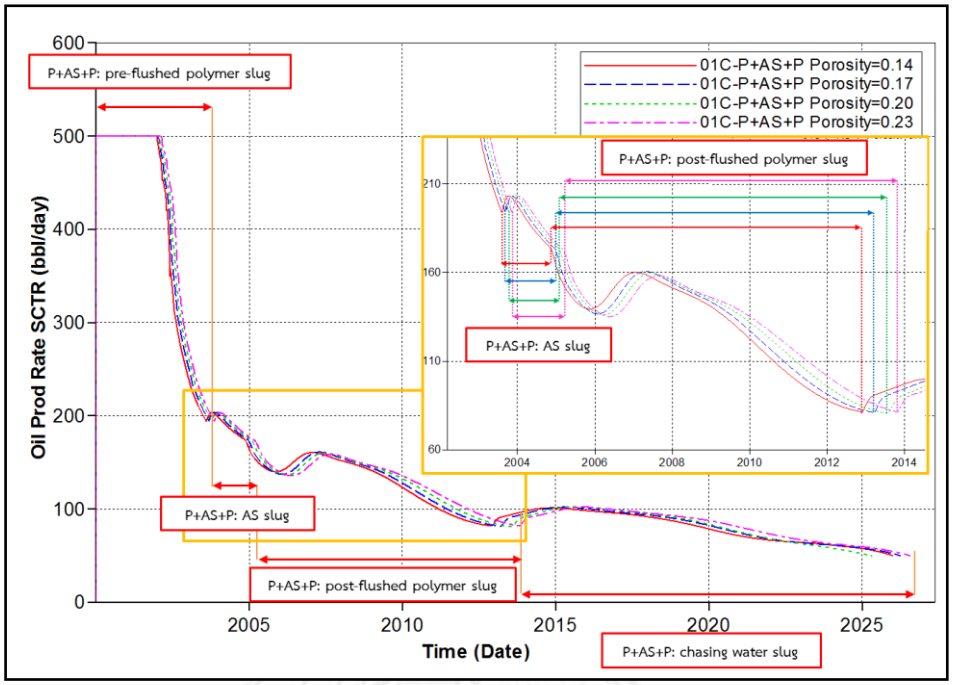

Figure 5.170 Oil production rates of various porosities in high permeability channel by P+AS+P flooding in model 01C as a function of time

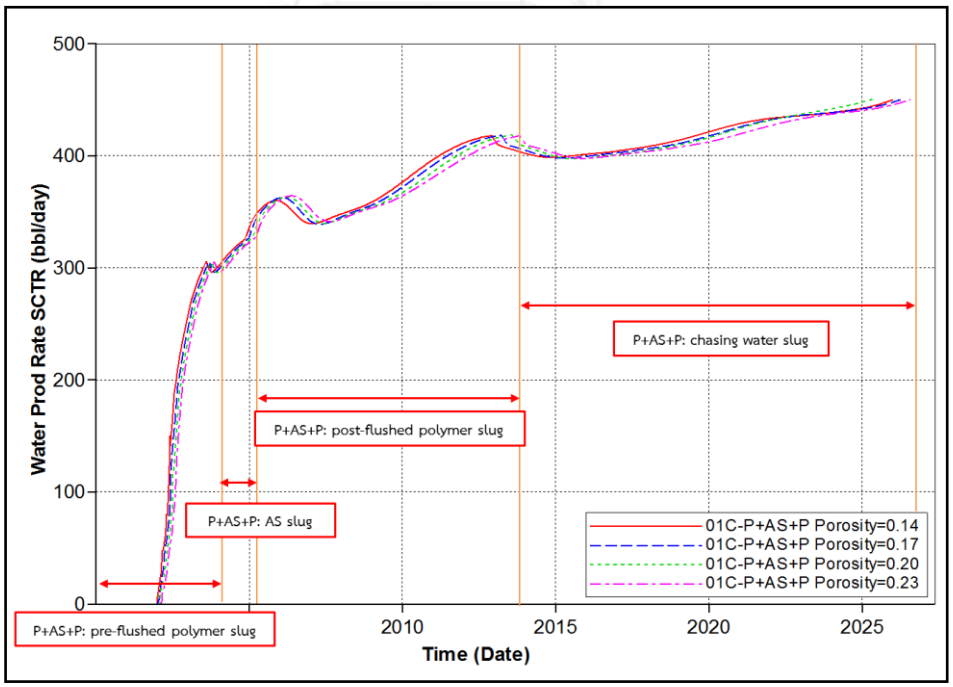

Figure 5.171 Water production rates of various porosities in high permeability channel by P+AS+P flooding in model 01C as a function of time

Table 5.20 Summary of AS+P injection period in various porosities in high permeability channel

Case	AS injection		Post-flushed polymer	
	Start	End	Start	End
Porosity=0.14	00y 01m	01y 04m	01y 04m	12y 11m
Porosity=0.17	00y 01m	01y 05m	01y 05m	13y 03m
Porosity=0.20	00y 01m	01y 05m	01y 05m	13y 07m
Porosity=0.23	00y 01m	01y 05m	01y 05m	13y 10m

Table 5.21 Summary of P+AS+P injection period in various porosities in high permeability channel

Case	Pre-flushed polymer		AS injection		Post-flushed polymer	
	Start	End	Start	End	Start	End
Porosity=0.14	00y 01m	03y 08m	03y 08m	04y 11m	04y 11m	12y 11m
Porosity=0.17	00y 01m	03y 09m	03y 09m	04y 12m	04y 12m	13y 03m
Porosity=0.20	00y 01m	03y 10m	03y 10m	05y 02m	05y 02m	13y 07m
Porosity=0.23	00y 01m	03y 11m	03y 11m	05y 03m	05y 03m	13y 10m

5.5.6 Summary of Sensitivity Analysis

In this section, recovery factors and incremental recovery factors of both AS+P and P+AS+P flooding compared to waterflooding are summarized by tornado chart format in Figures 5.172 to 5.175. Results of AS+P flooding show high sensitivity on recovery factors when Corey's exponent of rock at normal condition and wettability are changed, whereas results of P+AS+P flooding shows high sensitivity on recovery factor in Corey's exponent of ultra-low IFT condition, wettability and permeability contrast between channel and matrix. However, permeability contrast between channel and matrix directly depends on the direction of high permeability channel, therefore P+AS+P flooding (model 01C) is strongly affected from high

permeability direction more than results obtained from AS+P flooding (model 02D). It can be concluded that parameters that are closely related to flow ability of fluids are sensitive to ASP flooding. Wettability of reservoir highly affects recovery factor of both AS+P and P+AS+P methods. Improvement of recovery factor of both AS+P and P+AS+P compared to waterflooding can be assured as shown in the Figures 5.174 and 5.175. Although tornado chart of incremental of recovery factors of P+AS+P flooding compared to waterflooding indicates higher sensitivity value than AS+P flooding in all cases, high sensitivity to variation of parameters could result in negative effect of this technique.

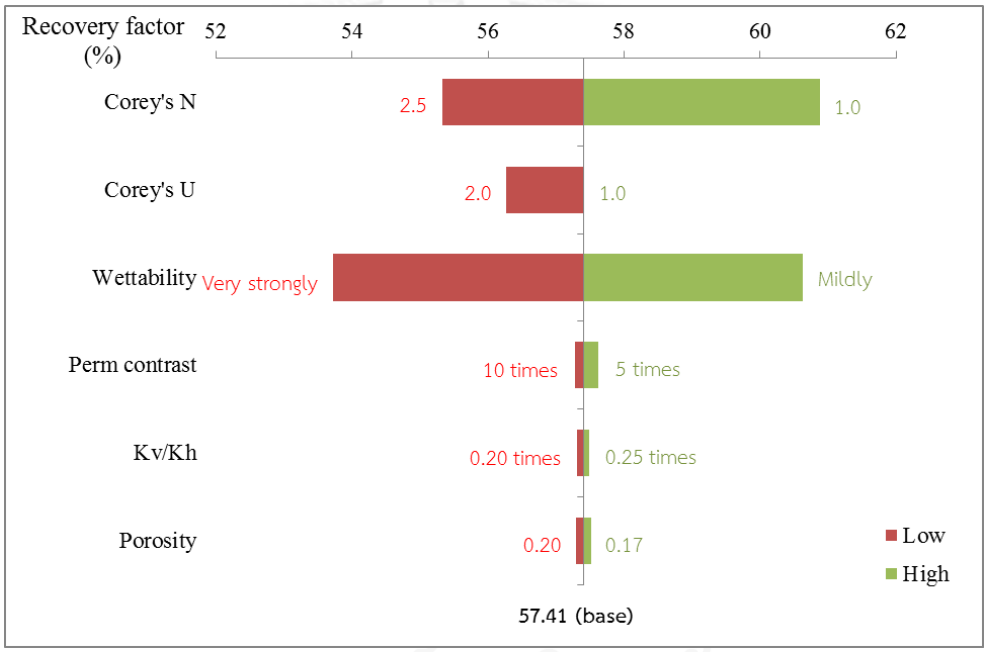

Figure 5.172 Tornado chart illustrating sensitivity of parameters on recovery factors of AS+P flooding

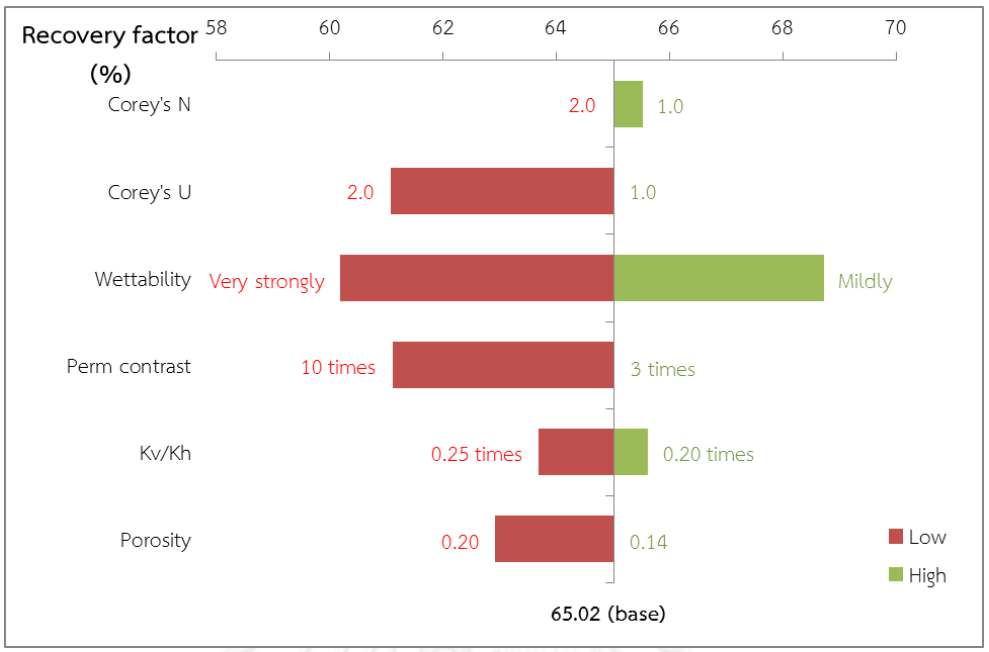

Figure 5.173 Tornado chart illustrating sensitivity of parameters on of recovery factors of P+AS+P flooding

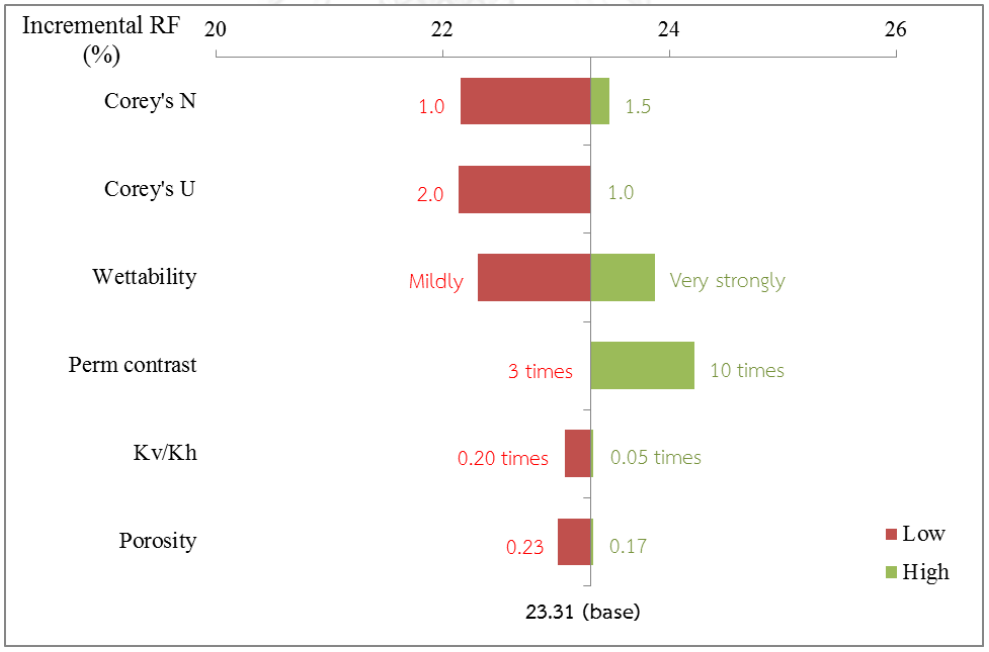

Figure 5.174 Tornado chart of sensitivity of parameters on incremental recovery factors compared to waterflooding of AS+P flooding

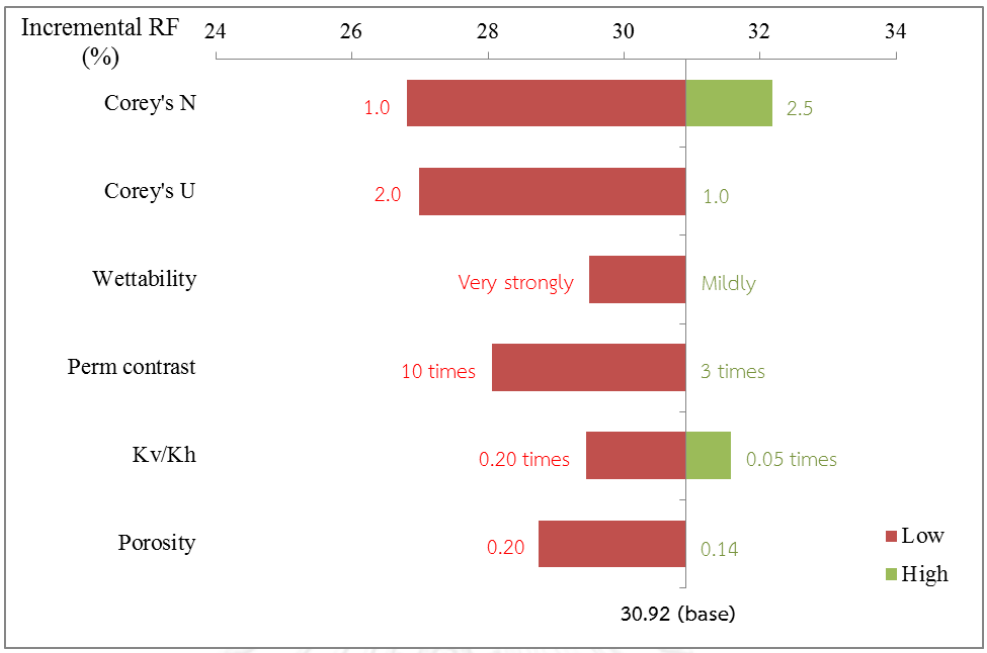

Figure 5.175 Tornado chart of sensitivity of parameters on incremental recovery factors compared to waterflooding of P+AS+P flooding

CHAPTER 6
CONCLUSION AND RECOMMENDATION

This chapter summarizes new finding from the study including effects of petrophysical properties and operational parameters on effectiveness of alkali-surfactant-polymer (ASP) flooding in oil-wet reservoir containing high permeability channel. Part of conclusions can be used as consideration for implementation of ASP flooding when certain conditions as previously mentioned are presented in the reservoir. Moreover, several recommendations are also suggested for future studying.

6.1 Conclusion

From chapter 5, it can be summarized as the following conclusions.

1. From results in Sections 5.2.1 and 5.2.4, pre-flushed water slug size should not be higher than 0.20 PV in order to yield high oil recovery factor. Amount of pre-flushed water prior to polymer injection mainly affects quantity of water in reservoir which consecutively affects ability of polymer to form oil bank from remaining oil saturation. However, this value can be increased when production constraint is changed.
2. Observation of slug size of polymer in Section 5.2.2 was found that chasing water after polymer injection enhances effectiveness of the process by improving polymer slug propagation into the reservoir. Nevertheless, too small polymer slug size can be destabilized by chasing water. Hence, optimal polymer slug size is required to identify. In this study, 0.55 PV polymer slug size is suggested as proper amount that can stabilize moving front and yield appropriate additional oil produced per mass of polymer used.

3. Resistance factor (*R*) of polymer flooding process reduces effective permeability to water by means of polymer adsorption onto rock surface. According to this, aqueous phase travels with stabilize front. In Section 5.2.3, results showed that higher resistance factor would result in high recovery factor but just in proper range: higher resistance factor reduces amount of injected polymer required to yield the same recovery factor. Proper resistance factor also depends on wetting condition of reservoir. In this study, resistance factor of 12.5 for 300 ppm polymer concentration is best for moderately oil-wet reservoir where k_{rw} at residual oil saturation is 50% of k_{ro} at irreducible water saturation.
4. Pre-flushed polymer slug in double-slug polymer flooding can stabilize travelling front in high permeability channel, acting like buffer slug to prevent alkali-surfactant (AS) breakthrough. From the study of slug size of pre-flushed polymer in Section 5.3.1, optimized value is 0.25PV.
5. Effect of AS injection in between double-slug polymer flooding is studied in Section 5.3.2, results expressed that AS slug provides both advantage and disadvantage at the same time. Increasing of AS slug size can reduce residual oil due to more injected chemical but only certain parts of reservoir especially around injector receive this benefit. Nevertheless, AS injection also increases relative permeability to water together with water saturation. Therefore, high water production rate during post-flushed polymer period occurs when size of AS slug is increased, sweeping high remaining water saturation. In this study, AS slug size of 0.10 PV of chosen chemical concentrations is suggested.
6. Incremental recovery factor of pre-flushed polymer followed by alkali-surfactant slug and chased by polymer slug (P+AS+P) compared to waterflooding shows better performance than alkali-surfactant slug chased by polymer slug (AS+P) in all heterogeneous models in Section 5.4. Width/height ratio (w/h ratio) of high permeability channel can be used to predict the incremental recovery factors based on waterflooding as well as difference between P+AS+P and AS+P flooding. Lower value of w/h ratio reflects benefit on both flooding methods. However, result is also depending on direction of high permeability channel to flow direction of injected fluid.

7. In Section 5.5.1.1, Corey's exponent of rock at normal condition affects to all waterflooding, AS+P and P+AS+P flooding. Although Corey's exponent of 1.0 provides less volumetric sweep efficiency, displacement efficiency is relatively high since flow ability is favored to reach residual oil saturation. For Corey's exponent of rock at ultra-low IFT condition in Section 5.5.1.2, higher value of Corey's exponent at ultra-low IFT condition results in higher residual oil remained during AS injection period. Hence, displacement efficiency of AS injection is strongly dependent on Corey's exponent at ultra-low IFT condition.
8. For the study of wettability condition in Section 5.5.2, stronger oil-wet condition results in less recovery factor by means of all methods. Nevertheless, improvement of oil recovery factors is obtained by means of both AS+P as well as P+AS+P in every wetting condition in this study. Effect of wetting condition occurs at low-IFT zone which is the condition between normal and ultra-low IFT conditions. Residual oil in low-IFT zone of weaker oil-wet is less compared to other stronger oil-wet wetting condition.
9. Impact of permeability contrast between channel and matrix is determined in Section 5.5.3. Effectiveness of all flooding is mainly dependent on direction of high permeability channel to flow direction of fluid. Increase of permeability contrast slightly affects recovery factor when direction of high permeability channel is normal to direction of flow between injector and producer.
10. Ratio of vertical to horizontal permeability directly affects to stability of pre-flushed polymer in P+AS+P flooding. From the observation of pre-flushed polymer concentration profiles in Section 5.5.4, higher vertical permeability favors water underrunning to the bottom of reservoir, breaking buffer pre-flushed polymer slug and reducing recovery factor by early water breakthrough.
11. Increment of porosity in high permeability channel delays all responses of injected fluids due to increase storage in high permeability channel, requiring longer period of injection as demonstrated in Section 5.5.5.
12. Although incremental recovery factor of P+AS+P flooding based on waterflooding is higher than that of AS+P flooding for all cases in Section 5.5.6, high sensitivity to variation of parameters could result in negative image of this technique.

6.2 Recommendation

The following recommendations are provided for future ASP flooding simulation.

1. Presence of clay and divalent ion can deplete make up chemicals by ion exchange and precipitation mechanism. These can decrease effectiveness of ASP flooding and hence, should be included in simulation model if possible.
2. Laboratory experiment should be conducted to provide relative permeability curves and capillary pressures in each IFT condition.
3. Study of resistance factor of polymer should be performed with the variation of petrophysical parameters such as wettability, type of polymer and relative permeability curve.

REFERENCES

1. Bo, Q., T. Zhong, and Q. Liu, *Pore Scale Network Modeling of Relative permeability in Chemical flooding*, in *SPE International Improved Oil Recovery Conference in Asia Pacific*. 2003, Society of Petroleum Engineers: Kuala Lumpur, Malaysia.
2. Han, D., et al., *The Effect of Wettability on Oil Recovery by Alkaline/Surfactant/Polymer Flooding*, in *SPE Annual Technical Conference and Exhibition*. 2006: San Antonio, Texas, USA
3. Zhang, Y., S. Huang, and M. Dong, *Determining the Most Profitable ASP Flood Strategy for Enhanced Oil Recovery* Journal of Canadian Petroleum Technology, 2005. **44**(02): p. 42-49.
4. French, T.R., *A Method For Simplifying Field Application Of ASP Flooding* in *SPE/DOE Improved Oil Recovery Symposium*. 1996, Society of Petroleum Engineers: Tulsa, Oklahoma.
5. Anderson, G.A., et al., *Optimization of Chemical Flooding in a Mixed-Wet Dolomite Reservoir* in *SPE/DOE Symposium on Improved Oil Recovery*. 2006: Tulsa, Oklahoma, USA.
6. Tabary, R., et al., *Improved Oil Recovery With Chemicals in Fractured Carbonate Formations*, in *SPE International Symposium on Oilfield Chemistry*. 2009: The Woodlands, Texas
7. Teklu, T.W., et al., *Numerical Modeling of Polymer-augmented Waterflooding in Heterogeneous Reservoirs* in *SPE Middle East Oil and Gas Show and Conference*. 2013: Manama, Bahrain
8. Zhijian, Q., et al., *A Successful ASP flooding Pilot in Gudong Oil Field* in *SPE/DOE Improved Oil Recovery Symposium*. 1998: Tulsa, Oklahoma.
9. Li, H., et al., *Performance Analysis of ASP Commercial Flooding in Central Xing2 Area of Daqing Oilfield* in *SPE Symposium on Improved Oil Recovery*. 2008: Tulsa, Oklahoma, USA.
10. Li, H., et al., *Alkline/Surfactant/Polymer (ASP) Commercial Flooding Test In Central Xing2 Area of Daqing Oilfield*, in *SPE International Improved Oil Recovery Conference in Asia Pacific*. 2003: Kuala Lumpur, Malaysia
11. Shutang, G. and G. Qiang, *Recent progress and evaluation of ASP flooding for EOR in Daqing oil field* in *SPE EOR Conference at Oil & Gas West Asia*. 2010: Muscat, Oman.
12. J.J. Taber, F.D.M.a.R.S.S., *EOR Screening Criteria Revisited - Part 1: Introduction to Screening Criteria and Enhanced Recovery Field Projects* SPE Reservoir Engineering, 1997. **12**(03): p. 189 - 198.

13.Donaldson, E.C., G.V. Chilingar, and T.F. Yen, *Enhanced oil recovery*. Developments in petroleum science. 1985, Amsterdam ; New York: Elsevier.
14.J.J. Taber, F.D.M.a.R.S.S., *EOR Screening Criteria Revisited—Part 2: Applications and Impact of Oil Prices* SPE Reservoir Engineering, 1997. **12**(03): p. 199 - 206.
15.Srisuriyachai, F., *Evaluation of Alkali Flooding Combined with Intermittent Flow in Carbonate Reservoir*, in *Department of Chemical, Mining and Environmental Engineering (DICMA), Faculty of Engineering*. 2008, University of Bologna.
16.Tiab, D. and E.C. Donaldson, *Petrophysics : theory and practice of measuring reservoir rock and fluid transport properties*. 1996, Houston, Tex.: Gulf Pub. xiv, 706 p.
17.Liu, S., *Alkaline Surfactant Polymer Enhance Oil Recovery Process*, in *Department of Chemical and Petroleum Engineering, Faculty of Engineering*. 2008, Rice University.
18.Lake, L.W., *Enhance oil recovery*. 1989: New Jersey: Prentice-Hall.
19.Craig, F.F. and Henry L. Doherty Memorial Fund of AIME., *The reservoir engineering aspects of waterflooding*. Society of Petroleum Engineers of AIME Monograph. 1971, New York,: H. L. Doherty Memorial Fund of AIME. 134 p.
20.Panthangkool, A., *Evaluation of Polymer Flooding in Multi-Layered Heterogeneous Reservoir: The Study of Viscosity and Injection Rate of Polymer Solution*, in *Department of Mining and Petroleum Engineering, Faculty of Engineering*. 2012, Chulalongkorn University.
21.Link, P.K., *Basic petroleum geology*. 1982, Tulsa: Oil & Gas Consultants International. xii, 235 p.
22.Azari, M. and M. Soliman, *Review of Reservoir Engineering Aspects of Conformance Control Technology*, in *Permian Basin Oil and Gas Recovery Conference*. 1996: Midland, Texas.
23.Rider, M.H., *The geological interpretation of well logs*. 2nd ed. 1996, Houston: Gulf Publishing. viii, 280 p.
24.McCain, W.D., *The properties of petroleum fluids*. 2nd ed. 1990, Tulsa, Okla.: PennWell Books. xxxxi, 548 p.
25.Sheng, J. and Knovel (Firm), *Modern chemical enhanced oil recovery theory and practice*. 2011, Gulf Professional Pub.,: Amsterdam ; Boston. p. 1 online resource.

APPENDICES

APPENDIX A
RESERVOIR MODEL CONSTRUCTION BY CMG SIMULATOR

CMG Builder program with a specific selection of STARS simulator are used in this study. There are six sections required for the input of reservoir information including reservoir properties, pressure-volume-temperature (PVT) properties, rock-fluid properties and well & recurrent.

Simulator Setting

Parameter	Value
Simulator	STARS
Working Units	Field
Porosity	Single porosity
Simulation start date	2000/01/01

1. Reservoir

1.1 Create Cartesian Grid

The reservoir is simply modeled by using “Create Cartesian Grid” wizard. The inputs of creating grid are demonstrated below.

Parameter	Value
Grid Type	Cartesian
K Direction	Down
Number of Grid Blocks	33, 33, 9 (I, J, K direction respectively)
Block widths (I direction)	33×30
Block widths (J direction)	33×30

1.2 Array Properties

Parameter	Whole grid
Grid top (ft) at Layer1	3200
Thickness (ft)	12
Porosity	0.14
Permeability I (mD)	500
Permeability J (mD)	500
Permeability K (mD)	50
Water Mole Fraction	1

2. Components

2.1 PVT Using Correlation

Parameter	Option	Value
Reservoir temperature (°F)		140
Generate data up to max. pressure of		3000 psi
Bubble point pressure calculation	Value provided	660 psi
Oil density at STC (14.7 psia 60°F)	Stock tank oil gravity (API)	20
Gas density at STC (14.7 psia 60°F)	Gas gravity (Air = 1)	0.70
Oil properties(Bubble point, R_s, B_o) correlation	Standing*	
Oil compressibility correlation	Glaso*	
Dead oil viscosity correlation	Ng and Egbogah*	
Live oil viscosity correlation	Beggs and Robinson*	
Gas critical properties correlation	Standing*	
Set/Update Values of Reservoir Temperature, Fluid Densities in Dataset		Available

*Refers to default of simulator

2.2 Water properties using correlation

Parameter	Value
Reservoir temperature (TRES)	140 °F
Reference pressure (REFPW)	1440 psi
Water bubble point pressure	
Water salinity (ppm)	0
Set/Update Values of Reservoir Temperature, Fluid Densities in Dataset	Available

Water bubble point pressure is left to be blank for the default value of water.

3. Rock-Fluid

The parameter in this section is illustrated only the preliminary data before using Process Wizard in Appendix B.

3.1 Rocktype Properties

Parameter	Value
Rock Wettability	Oil wet
Method for evaluating 3-phase KRO	Stone's second model

3.2 Relative Permeability Table

The rock-fluid properties are contained the water-oil relative permeability table, liquid-gas table including with capillary pressure of water.

S_w	k_{rw}	k_{row}	P_{cow}
0.15	0	0.6	0
0.175	0	0.535185185	-0.111
0.2	0	0.474074074	-0.222
0.225	0.001171875	0.416666667	-0.333
0.25	0.0046875	0.362962963	-0.444
0.275	0.010546875	0.312962963	-0.556
0.3	0.01875	0.266666667	-0.667
0.325	0.029296875	0.224074074	-0.778
0.35	0.0421875	0.185185185	-0.889
0.375	0.057421875	0.15	-1
0.4	0.075	0.118518519	-1.111

0.425	0.094921875	0.090740741	-1.222
0.45	0.1171875	0.066666667	-1.333
0.475	0.141796875	0.046296296	-1.444
0.5	0.16875	0.02962963	-1.556
0.525	0.198046875	0.016666667	-1.667
0.55	0.2296875	0.007407407	-1.778
0.575	0.263671875	0.001851852	-1.889
0.6	0.3	0	-2

S_l	k_{rg}	k_{rog}
0.4	0.6	0
0.425	0.551041667	0
0.45	0.504166667	0
0.475	0.459375	0.000619835
0.5	0.416666667	0.002479339
0.525	0.376041667	0.005578512
0.55	0.3375	0.009917355
0.575	0.301041667	0.015495868
0.6	0.266666667	0.02231405
0.625	0.234375	0.030371901
0.65	0.204166667	0.039669421
0.675	0.176041667	0.050206612
0.7	0.15	0.061983471
0.725	0.126041667	0.075
0.75	0.104166667	0.089256198
0.775	0.084375	0.104752066
0.8	0.066666667	0.121487603
0.825	0.051041667	0.13946281

0.85	0.0375	0.158677686
0.925	0.009375	0.223760331
1	0	0.3

4. Initialization

Parameter	Value
Vertical Equilibrium Calculation Methods	Depth-Average Capillary-Gravity Method
Reference Pressure (REFPRES)	1440 psi
Reference Depth (REFDEPTH)	3200 ft
Water-Oil Contact Depth (DWOC)	3308 ft

5. Numerical

Parameter	Value
First Time Step Size after Well Change (DTWELL)	0.001
Isothermal Option (ISOTHERM)	ON
Linear Solver Iterations (ITERMAX)	200

6. Wells and Recurrent

6.1 Injector Well

6.1.1 Perforations

Parameter	Value
Radius (ft)	0.51
Perforation start	1,33,1
Perforation end	1,33,9

6.1.2 Well Events

ID & Type

Name: INJECTOR

Type: INJECTOR MOBWEIGHT IMPLICIT

Constraint:

Constraint	Parameter	Limit/Mode	Value	Action
OPERATE	STW surface liquid rate	MAX	1000 bbl/day	CONT
OPERATE	BHP bottom hole pressure	MIN	2000 psi	CONT

6.2 Producer Well

6.1.1 Perforations

Parameter	Value
Radius (ft)	0.51
Perforation start	33,1,1
Perforation end	33,1,9

6.1.2 Well Events

ID & Type

Name: PRODUCER

Type: PRODUCER MOBWEIGHT IMPLICIT

Constraint:

Constraint	Parameter	Limit/Mode	Value	Action
OPERATE	STL surface liquid rate	MAX	500 bbl/day	CONT
OPERATE	BHP bottom hole pressure	MIN	200 psi	CONT
MONITOR	WCUT water-cut (fraction)		0.95	STOP
MONITOR	STO surface oil rate	MIN	50 bbl/day	STOP

6.3 Dates

Add a range of dates: 360 months (not include the first month)

APPENDIX B
CHEMICAL MODEL CONSTRUCTION BY CMG SIMULATOR

The chemical model of alkali, surfactant and polymer are constructed from the Process Wizard in Components. The inputs of data are demonstrated below.

1. Process Wizard Setting

Parameter	Value
Process	Alkaline, surfactant, foam, and/or polymer model
Model	Alkaline, surfactant and polymer flood (add 3 components)

2. Detail of ASP Setting

Parameter	Value
Use reversible partitioning of surfactant into oil	No
Use irreversible partitioning of surfactant into oil	No
Number of relative permeability sets for interpolation	3
Use adsorption for alkaline	No
Use adsorption for surfactant	Yes
Make surfactant adsorption dependent on alkaline weight	Yes
Number of alkaline weight % value	3
Alkaline weight percent #1	0
Alkaline weight percent #2	0.3
Alkaline weight percent #3	0.6

Interfacial tension is also dependent on surfactant weight %	Yes
Number of surfactant weight % value	2
Surfactant weight percent #1	0
Surfactant weight percent #2	0.005
Rock type conversion of adsorption values (gm rock to PV)	Limestone
Rock density (gm/cm3)	2.71

3. Interfacial Tension Setting

Surfactant wt %	Alkaline wt %	IFT
0	0	30
0	0.15	9.613
0	0.3	9.319
0	0.6	7.738
0	0.7	6.995
0	0.8	4.88
0	1	4.492
0	1.2	3.665
0.005	0	3
0.005	0.15	0.057
0.005	0.3	0.054
0.005	0.6	0.023
0.005	0.7	0.021
0.005	0.8	0.012
0.005	1	0.009
0.005	1.2	0.01

4. Adsorption Setting

The porosity of laboratory surfactant and polymer sample is 0.2494 in surfactant and polymer models.

Alkaline wt %	Wt% Surfactant	Surfactant adsorption (mg/100gram rock)
0	0	0
0	0.005	26.14
0.3	0	0
0.3	0.005	3
0.6	0	0
0.6	0.005	3

Weight% Polymer	Polymer adsorption (mg/100gram rock)
0	0
0.06	10

5. Component and Phase properties

Chemical	MW (lb/lbmole)
Water	18
Polymer	8000
Surfactant	348.5
Alkaline	106

6. Component adsorption

Parameter	Value
Adsorption table dependency Enter/Edit Table Concentration	0
Composition dependence	Independent of temperature

7. Rock-Fluid Interpolation set2

S_w	k_{rw}	k_{row}	P_{cow}
0.15	0	0.8	0
0.175	0	0.754292827	-0.0384375
0.186111	0	0.734268216	-0.055531774
0.2	0	0.709490897	-0.0769
0.20625	0.000567012	0.698434021	-0.086515625
0.222222	0.003801426	0.670442372	-0.111088547
0.234375	0.007313679	0.649400841	-0.129785938
0.25	0.012830006	0.622678666	-0.153825
0.2625	0.017930478	0.601572057	-0.17305625
0.275	0.023570226	0.580709468	-0.1922875
0.288889	0.030411923	0.557818346	-0.213655727
0.3	0.036288737	0.539728012	-0.23075
0.31875	0.046959372	0.509654738	-0.259596875
0.333333	0.055869956	0.486665532	-0.282032821
0.355556	0.070404757	0.452319721	-0.316222906
0.366666	0.078080461	0.435465848	-0.333315641
0.377778	0.086017908	0.418823691	-0.350411453

0.403125	0.105055047	0.381681022	-0.389407813
0.422222	0.120213275	0.354466296	-0.418788547
0.434375	0.130208333	0.3375	-0.437485938
0.444444	0.138688651	0.323654738	-0.452977094
0.459375	0.151587721	0.303483254	-0.475948438
0.475	0.165489671	0.282842712	-0.4999875
0.488889	0.178183859	0.264906736	-0.521355727
0.5	0.188561808	0.250842912	-0.53845
0.515625	0.203483381	0.23150324	-0.562489063
0.533333	0.220845889	0.210219919	-0.589732821
0.54375	0.231278846	0.198023058	-0.605759375
0.55625	0.244008054	0.183711731	-0.624990625
0.571875	0.260235971	0.166333327	-0.649029688
0.583334	0.272356575	0.153959361	-0.666659359
0.6	0.290309895	0.136541587	-0.6923
0.619444	0.311733038	0.117121827	-0.722214594
0.6375	0.332077108	0.1	-0.74999375
0.655556	0.35284544	0.083804861	-0.777772906
0.678125	0.379388385	0.064951905	-0.812495313
0.691666	0.395618979	0.054433608	-0.833328141
0.727778	0.439996049	0.029629493	-0.888886453
0.763889	0.485917216	0.010475608	-0.944443227
0.8	0.533333333	0	-1

S_l	k_{rg}	k_{rog}
0.2725	0.804141496	0
0.305568	0.749941807	0.000378356
0.338636	0.697017696	0.00691576
0.371705	0.64539914	0.01748541
0.39375	0.611731162	0.026140181
0.404773	0.595123242	0.030883445
0.427273	0.561700051	0.041348151
0.437841	0.546225196	0.046603581
0.454545	0.522061141	0.055326616
0.470909	0.498744981	0.064342668
0.484688	0.479389327	0.072278592
0.509091	0.445742935	0.08706722
0.525	0.424251505	0.097190864
0.537045	0.408217055	0.105098826
0.55	0.391202614	0.113831296
0.563636	0.373556544	0.123270381
0.575625	0.358267707	0.131773954
0.590909	0.339088347	0.142885252
0.605937	0.32057634	0.154098948
0.625	0.297597911	0.16872394
0.63625	0.284306952	0.177559988
0.65	0.26833977	0.188561808
0.675	0.240108768	0.209121444
0.702386	0.21040837	0.232442727
0.735455	0.176332479	0.261677626
0.7575	0.154757103	0.281798265
0.775	0.138311011	0.298120666

0.787812	0.12666721	0.310263286
0.809091	0.108099225	0.33078423
0.825	0.094872436	0.346410162
0.836364	0.085783006	0.357718252
0.85	0.075286978	0.371446014
0.909063	0.035538076	0.432857547
0.925	0.026617966	0.449957706
1	0	0.533333333

8. Rock-Fluid Interpolation set3

S_w	k_{rw}	k_{row}	P_{cow}
0	0	0	0
1	1	0	0

S_l	k_{rg}	k_{rog}
0	1	0
1	0	1

9. Log Capillary number for interpolation set

Interpolation	Phase	Values
Interpolation set 1	Wetting phase	-7
	Non-Wetting phase	-7
Interpolation set 2	Wetting phase	-5
	Non-Wetting phase	-5
Interpolation set 3	Wetting phase	-4
	Non-Wetting phase	-4

10. Injected fluid at INJECTOR

Injected polymer	300 ppm	500 ppm	700 ppm
Component	Mole fraction	Mole fraction	Mole fraction
WATER	0.999999325	0.999998874	0.999998424
Polymer	6.752E-07	1.12556E-06	1.5761E-06
Surfactant	0	0	0
Alkaline	0	0	0

Injected AS	0.28% Surfactant and 1.3% Alkaline
Component	Mole fraction
WATER	0.99761577
Polymer	0
Surfactant	0.000146591
Alkaline	0.002237639

VITA

Mr. Charat Thamcharoen was born on July 21st, 1985 in Bangkok, Thailand. He received his Bachelor degree in Electrical Engineering from Faculty of Engineering, Chulalongkorn University in 2007. After graduation, he started his career in automotive industry as an analysis member for three years at Keihin Auto Parts (Thailand). After that, he joined CAT Telecom Public Company Limited as a telecommunication internal auditor until 2014. He continued his study in the Master's Degree program in Petroleum Engineering at the Department of Mining and Petroleum Engineering, Faculty of Engineering, Chulalongkorn University since the academic year 2012.